INSTITUTE
FOR
AEROSPACE STUDIES

UNIVERSITY OF TORONTO

TP5927E

CRASHWORTHINESS OF LIGHT AIRCRAFT STRUCTURES

by

R. C. Tennyson, A. P. Nanyaro, H. C. Teichman and J. S. Hansen

FINAL REPORT

PREPARED FOR THE

TRANSPORTATION DEVELOPMENT CENTRE

October 31, 1982

CA1
DTC 801
82
C64
c.2

The contents of this report reflect the views of the contractor and not necessarily the official views or policies of the Transport Canada Research and Development Centre.

Library and Information Centre/
Centre de Documentation (GSLA)
CU LE
SEP 6 1983
Transport Canada / Transports Canada

REPORT DOCUMENTATION FORM

1. Transport Canada Report No.	2. TDC Project No.	3. Recipient's Catalogue No.
TP3927E	4121	

4. Title and Subtitle	5. Report Date
Crashworthiness of Light Aircraft Structures	August 1982
	6. Performing Organization Report No.

7. Author(s)	8. Transport Canada File No.
R. C. Tennyson, A. P. Nanyaro, H. C. Teichman & J. S. Hansen	D1455-106-3

9. Performing Organization Name and Address	10. DSS File No.
Institute for Aerospace Studies University of Toronto Downsview, Ontario.	09SD.T8200-9-9544
	11. DSS or Transport Canada Contract No.
	OSD79-00130

12. Sponsoring Agency Name and Address	13. Type of Report and Period Covered
Transportation Development Centre(TDC) 1000 Sherbrooke St. West Suite 2421 Montreal, Quebec. H3A 2R3	Final, March 80 - August 82
	14. Sponsoring Agency Code 4121

15. Supplementary Notes	16. TDC Project Officer
	C. Alfred Versailles

17. Abstract

A comprehensive program has been undertaken to investigate both analytically and experimentally the dynamic behaviour of aircraft fuselage structures subject to various impact conditions. Two analytical models have been used to derive the motion equations, one based on a self-consistent finite element (CFE) technique and the other on a more approximate, lumped mass-finite element approach (LMFE). Although both analyses are restricted to linear geometric considerations, they do permit the inclusion of non-linear material behaviour and dissipative effects. Extensive testing of scale model stiffened aluminum fuselage sections has been completed for a wide range of wing loads, angles of incidence and impact velocities. Both vertical drop tests and 'free-flight' impacts using a pendulum gantry have been studied. Test data have been obtained in terms of maximum structural strains, g-loads and high speed photographs of the dynamic collapse modes.

18. Key Words	19. Distribution Statement
Aircraft Crashworthiness, Fuselage Structures, Finite Element Model, Crash Facility, Model Tests.	Limited number of copies available from TDC.

20. Security Classification (of this report)	21. Security Classification (of this page)	22. No. of Pages	23. Price
Nil	Nil		Nil

FORMULE DE DOCUMENTATION POUR RAPPORT

1. N° du rapport Transports Canada	2. N° de l'étude — CDT	3. N° de catalogue du destinataire
TP3927E	4121	

4. Titre et sous-titre	5. Date du rapport
Crashworthiness of Light Aircraft Structures	août 1982
—	6. N° du rapport de l'organisme exécutant

7. Auteur(s)	8. N° de dossier Transports Canada
R. C. Tennyson, A. P. Nanyaro, H. C. Teichman and J. S. Hansen	D1455-106-3

9. Nom et adresse de l'organisme exécutant	10. N° de dossier — ASC
Institute for Aerospace Studies, University of Toronto, Downsview, Ontario.	09SD.T8200-9-9544
	11. N° de contrat — ASC ou Transports Canada OSD79-00130

12. Nom et adresse de l'organisme parrain	13. Genre de rapport et période visée
Centre de développement des transports (CDT) 1000 o., rue Sherbrooke Suite 2421 Montréal (Québec) H3A 2R3	Final, mars 80-août 82
	14. Code de l'organisme parrain 4121

15. Remarques additionnelles	16. Agent de projet — CDT
	C. Alfred Versailles

17. Résumé

Un programme complet d'étude analytique et d'expérimentations a été exécuté pour déterminer le comportement dynamique de nacelles d'avions soumises à des impacts d'intensités variables. Deux modèles analytiques ont permis d'obtenir les équations de mouvement, l'un fondé sur une méthode cohérente des éléments finis, l'autre sur une solution approchée à l'aide du programme LMFE (lumped mass-finite element). Bien que ces deux méthodes analytiques se limitent normalement aux valeurs géométriquement linéaires, leur domaine d'application a pu être étendu pour tenir compte des non linéarités des matériaux et des effets de dissipation. Des essais exhaustifs ont été faits sur des sections à l'échelle et rigides d'une nacelle en aluminium, dans des conditions de charges alaires, d'incidences et de vitesses d'impact variables. Les chercheurs ont étudié l'effet des impacts en chute verticale et, à l'aide d'un portique à pendule, celui des impacts en vol libre. Ils ont mesuré les facteurs de charge et les déformations maximales en plus de prendre des photographies haute vitesse au moment où s'effectuait la ruine des maquettes.

18. Mots-clés	19. Diffusion
Résistance à l'écrasement. Structures de nacelles. Méthode des éléments finis. Installation d'essais d'écrasement. Essais sur maquettes.	Le CDT dispose d'un nombre limité d'exemplaires.

20. Classification de sécurité (de ce rapport)	21. Classification de sécurité (de cette page)	22. Nombre de pages	23. Prix
nil	nil	70	nil

CRASHWORTHINESS OF LIGHT AIRCRAFT STRUCTURES

by

R. C. Tennyson, A. P. Nanyaro, H. C. Teichman and J. S. Hansen

FINAL REPORT

PREPARED FOR THE

TRANSPORTATION DEVELOPMENT CENTRE

October 31, 1982

Contents

		Page
	Nomenclature	
1.	INTRODUCTION	1
2.	ANALYTICAL MODELS	1
	2.1 Finite Element-Lumped Mass Model	2
	2.2 Consistent Finite Element Formulation	5
	2.3 Derivation of General Equations of Motion of an Impacting Aircraft	7
3.	DESCRIPTION OF TEST PROGRAMME	18
	3.1 Fuselage Test Model	18
	3.2 Crash Test Facility	19
	3.3 Data Acquisition System	20
4.	FREE-FLIGHT IMPACT TEST	21
5.	COMPARISON OF COMPUTER MODEL PREDICTIONS WITH TESTS	22
	5.1 Level Impacts	22
	5.2 Oblique Angle Impacts	23
	5.3 Free-Flight Impact	24
6.	CONCLUSIONS	24
	REFERENCES	
	TABLES	
	FIGURES	
	APPENDICES	

Nomenclature

$\vec{A}$	acceleration in inertial reference frame
A_s	cross-sectional area of a stringer
A_{rib}	cross-sectional area of a rib
a	x side length of element
a_{ij}	i, j = 0,..., 3, coefficients of $\omega(x, y)$ trial function
a_I	acceleration at time integration step I
b	y side length of the element
$\vec{b}$	fuselage body reference frame
$\bar{c}_i$	transformation matrix from element to body reference frames
c	transformation matrix from body to inertial reference frames
c.m.	centre of mass
c^o	continuity of displacements at element boundaries
c'	continuity of displacements and slopes at element boundaries
D	displacement coefficient matrix in $\epsilon = D\bar{\omega}$
dv	differential element of volume
d_I	nodal displacements at time interval I
$\bar{d}$	total vector of element degrees of freedom at nodes
$\bar{d}_c$, $\bar{d}_p$	nodal degrees of freedom in Cartesian and curvilinear coordinates respectively
E	Young's modulus of elasticity
$\vec{e}_i$	element i reference frame
f*	force in Cartesian coordinates including inertial forces
F	$(6n_s \times 6n_s)$ matrix relating $\bar{d}$ to Γ
$\vec{f}_i$	impact forces at node i
$\bar{F}^{sj}$	force applied by finite elements to nodal body j
$\bar{G}(\xi, \eta, \zeta)$	(3×1) matrix of element body forces

G	shear modulus
$\bar{g}$	element gyroscopic coupling matrix $(6n_j \times 6n_j)$
$\vec{H}^j$	angular momentum of nodal body j about its mass centre
h	plate thickness
I^j	inertia matrix for inertia dyadic in basis $\vec{e}$
$\vec{i}$	inertial reference frame
I_{xx}	moment of inertia about x-axis
I_{yy}	moment of inertia about y-axis
I_{zz}	moment of inertia about z-axis
K	stiffness matrix
$\bar{k}$	element stiffness matrix
K^*	as defined in Eq. 39
K^{**}	as defined in Eq. 39
$\bar{k}_o$	plastic preload element structural stiffness matrix
$\bar{k}_\Delta$	linear structural element stiffness matrix
$\bar{L}_s^s$	$(6n_s \times 1)$ matrix of forces and torques on the nodes of element s in the element basis
L_s^b, L_s	matrix of forces and torques on the nodes of element s in fuselage body reference frame
ℓ	length of element or model
M	mass matrix
$\bar{m}_s$	element s consistent mass matrix
$\bar{m}$	element consistent mass matrix
m^j	mass at j-th nodal point or nodal mass
M^*	moments in Cartesian coordinates including inertial forces
m_s	mass of element s
$\bar{M}$	total mass matrix of structure
n_s	number of nodes for finite elements
P_D	$(3 \times 6n_s)$ matrix relating $\bar{\omega}$ to Γ
$\vec{P}$	applied load vector

$\vec{P}_B(x, y)$	applied membrane or bending load vector
$\vec{p}$	position of particle with volume dV from element centre of mass
r	radius of curvature
$\vec{R}_c$	position vector of element centre of mass from fuselage centre of mass
R*	$\begin{bmatrix} 1 & 0 & 0 & \\ 0 & 1 & 0 & 0 \\ 0 & 0 & 1 & \\ \hline & & & \\ 0 & & & TR^* \\ & & & \end{bmatrix}$
R^{*T}	R* transposed
$\vec{r}^i$	nodal position of a node i from fuselage centre of mass
s	subscript for element s
$\vec{t}^j$	torque on nodal body j in fuselage body reference frame
$\vec{t}^j$	external torque on nodal body j
TR*	transformation matrix from curvilinear coordinates to Cartesian coordinates
U, U_{rib}	strain energy, strain energy of rib
U*	virtual strain energy
u	x displacement of trial function
$u_{,x}$	derivative of u with respect to x
$\vec{u}$	nodal displacement vector
u_{ij}	i, j = 1, 2 nodal displacements at node ij in x direction
v	y displacement of trial function
$v_{,y}$	derivative of v with respect to y
v_{ij}	y displacement at node ij
w	displacement in the z direction (out of plane)
$\bar{w}$	displacements u, v, w (6×1) matrix includes plastic displacement vector $\bar{p}$
W'	matrix relating $\bar{\omega}$ to $\bar{d}$, or PF^{-1}

W^*	virtual work
$\ddot{\bar{W}}$	$\bar{W}$ differential twice with time in inertial reference frame
$\bar{W}$	$\bar{W}$ in body reference frame
W'_c	W' at element centre of mass
$w_{,x}$, $w_{,y}$, $w_{,xy}$, $w_{,\theta}$	derivatives of w
x,y,z	Cartesian or curvilinear coordinate axes
$\vec{X}$	position of fuselage centre of mass in inertial reference frame
θ, x	polar coordinates

Greek Symbols

$\bar{\alpha}$	element angular acceleration stiffness matrix
$\bar{\beta}_j$	rotation of nodal body j
δ	small variation
Γ	scalar unknowns from nodal displacements
$\bar{\varepsilon}$	strain matrix
ξ, η, ζ	Cartesian coordinates for element
θ	polar coordinate
$\bar{\kappa}$	centrifugal stiffness matrix
$\bar{\rho}$	plastic deformation vector of element
$\bar{\sigma}$	stress matrix
$\bar{\sigma}'$	stress due to plasticity and nonlinearity
ς	torsional angle of deformation of a rib or stringer

ω	angular velocity
ω^e	element angular velocity about body axes
ω^b	fuselage body angular velocity about inertial axes

Operational Symbols

$( )^T$	indicates matrix transposed
$( )^{\sim}$ or $(\tilde{\ })$	indicates formation of (3x3) shear symmetric matrix from (3x1) matrix
$\frac{\vec{i}d}{dt}(\vec{V})$	time derivative of vector $\vec{V}$ in reference frame $\vec{i}$
$(\dot{\ })$	time derivative
$(\ddot{\ })$	time derivative of $(\dot{\ })$
$( )^{-1}$	matrix inverse
$\triangleq$	equality of definition
∇	$= \left\{ \frac{\partial}{\partial \xi} \frac{\partial}{\partial \eta} \frac{\partial}{\partial \xi \eta} \right\}^T$
$\Delta( )$	small change of $( )$
$( )_{,xx}$	second derivative with respect to x
$( )_{,x}$	first derivative with respect to x

1. INTRODUCTION

This report represents the last phase of a combined analytical/experimental programme investigating the crashworthiness of aircraft fuselage structures. In this study, emphasis has been given to completing the development of the consistent finite element formulation based on curved elements. This work, in its early stages, was described in our previous report to Transport Canada (Report No. TP2616, March 1980) but no results were presented at that time. Further, the free-flight crash facility had not been employed to test a fuselage model, although a "calibration" run was reported based on a refurbished rib-stiffened structure. Consequently this experimental work was continued and results are now presented on extensive testing of a modified stringer/rib construction. In summary, the objectives of this study are:

(1) Complete the curved element consistent finite element formulation and apply this model to various "crash" conditions using the fuselage test cases;

(2) Compare the predictions of (1) with the lumped mass/finite element formulation (based on flat elements) to assess the accuracy and costs of both methods;

(3) Perform a free-flight impact test to provide a basis of comparison for the above computer models.

2. ANALYTICAL MODELS

As noted earlier, two models have been completed, both of which can be used to predict the dynamic structural behaviour of aircraft fuselages under 'crash' conditions. The essential differences between the two formulations are:

(i) One method consists of a lumped mass representation of the structure whose stiffness properties are determined by a finite element description based on flat (straight) elements. Equations of motion are then formulated in terms of the associated mass/stiffness matrices.

(ii) The second method is based on a consistent finite element formulation using curved elements and dynamic equations of equilibrium.

Both models include panel buckling and plasticity in selected structural elements.

Since the hybrid (first) method has been described extensively in our previous report (TP2616), only a brief outline will be given here.

2.1 Finite Element-Lumped Mass Model

The fuselage structure was modelled by flat, straight elements. The element library consists of:

- Stringers; constant axial force member.
- Beams; 12 degrees of freedom beam element. Axial force, shear forces, and torque are uniform along the length, with a linear variation of bending moments.
- Membrane Elements; flat rectangular panels carry in-plane loads only (i.e., uniform shear and axial loads). Panels cannot resist bending.

The initial modelling consisted of:

Number of degrees of freedom	368
Number of nodes	79
Total number of elements	188
Number of rod elements	56
Number of beam elements	84
Number of membrane elements	48

However, to reduce prohibitive computer execution and memory storage costs that arise in a dynamic analysis, the 368 degrees of freedom stiffness matrix was reduced to a 138 degrees of freedom stiffness matrix by static condensation. The degrees of freedom retained in the static condensation procedure were those considered important in the prediction of the gross behaviour of the fuselage structure to crash conditions.

Figures 1 and 2 illustrate the initial and reduced models used in the numerical calculations.

Equations of motion were then assembled in a matrix format. The total system equation is partitioned and written as,

$$\left[\begin{array}{c|c} K_{II} & K_{IN} \\ \hline K_{NI} & K_{NN} \end{array}\right] \left[\begin{array}{c} X_I \\ \hline X_N \end{array}\right] + \left[\begin{array}{c|c} M_I & 0 \\ \hline 0 & 0 \end{array}\right] \left[\begin{array}{c} \ddot{X}_I \\ \hline \ddot{X}_N \end{array}\right] = \left[\begin{array}{c} F_I \\ \hline 0 \end{array}\right] \qquad (1)$$

where I is defined as the "interested" degree of freedom (i.e., the degree of freedom related to a mass), N is defined as the "non-interested" degree of freedom. Rearranging the second equation of (1), one obtains,

$$\{\bar{X}_N\} = [K_{NN}]^{-1}\left[-[K_{NI}]\{\bar{X}_I\}\right] \qquad (2)$$

One can then substitute (2) into the first equation of (1) to find,

$$[M]\{\ddot{\bar{X}}_I\} + [K^{*}_{II}]\{\bar{X}_I\} = \{\bar{F}_I\} \qquad (3)$$

where

$$[K^{*}_{II}] = [K_{II}] - [K_{IN}][K_{NN}]^{-1}[K_{NI}]$$

$\equiv$ the statically condensed stiffness matrix.

Although the order of the matrices in the system have been greatly reduced, matrix $[K_{II}]^*$ is in general fully populated, having lost the property of 'bandedness' which the total stiffness matrix possessed. In the computer, only the upper triangular part of the stiffness matrix is stored. As a result of the lumped mass assumption and static condensation procedure, the mass matrix is diagonal and positive definite, and stored as a vector. The inversion of the mass matrix then requires very little effort and needs only to be performed once. Such approximations result in considerable savings in computational requirements.

This system of equations is integrated numerically to obtain the response of the structural model. Currently, an explicit central difference algorithm with a fixed time step is implemented in the computer programme. The time step is chosen on the basis of the highest "free" vibration natural frequency of the system in order to ensure numerical stability. The integration time step used was $\Delta t = 50$ μsec.

Further details on the analytical model and solution techniques can be found in TP2616. For completeness, a procedure outline describing this numerical model (known as "CRASH") is presented in Table 1, together with flowchart descriptions of the subroutines. In summary, this software package has the following capabilities:

1. Determines the dynamic response (accelerations, velocities, and displacements) for each mass and internal member loads (stresses) and deformations for certain predefined elements at each time interval;
2. Permits initial conditions of linear and angular velocity in the vertical plane and impact into a horizontal (infinitely rigid) ground at any angle of attack.

Post-processing of stored data also permits plotting of:

1. Time histories of accelerations, velocities, and displacements;
2. Views of the deformed fuselage structure from the side and of the cross-section (computer movies can be generated for side-by-side comparison with high speed film).

2.2 Consistent Finite Element Formulation

The various elements being utilized to model the aircraft fuselage structure can be described as follows: a four node, six degrees of freedom per node, curvilinear coordinate rectangular thin shell plate or membrane (Fig. 3); a six degree per node (two nodes per element) stringer element (beam); and a curved rib element. The stiffness matrices have been found in a form that does not require numerical integration. The shell element formulation is created with all the matrix manipulations done numerically to eliminate errors. The membrane elements are used here with an in-plane stiffness matrix and membrane curvature coupling matrix. The present ribs and stringers contain tension-compression and bending stiffness while torsional and warping effects have been neglected. Such approximations have been found reasonable due to the geometry of the beam elements where these and shear effects are small. As well, the coupling between in-plane and bending with curvature is taken into consideration.

Details of the element stiffness matrix derivations were given in TP2616.

Derivation of stiffness and mass matrix is similar to that done by Bogner, et al.[2,3] In the new method of derivation the matrices are found using matrix manipulations which do not require such tables as created by Bogner. The rib and curved plate element stiffnesses lack some rigid

body motion degrees of freedom when polynomials are used to represent the displacement. The stiffness can be modified by a direct introduction of rigid body displacement as done by Cantin.[1] Thus the elements are not strained during rigid-body displacement.

Assembling of Overall Stiffness Matrix

The ribs, stringers and plates are assembled in the cylindrical shell curvilinear coordinates while the floor structure is assembled in Cartesian coordinates (Fig. 4). At the point where the floor elements and shell elements meet, a transformation is performed:

$$[\vec{d}_c] = [TR^*][\vec{d}_p]$$

where c stands for Cartesian coordinates and p for curvilinear coordinates. In the case where point 2 is the joint node,

$$\begin{Bmatrix} d_{c_1} \\ d_{c_2} \end{Bmatrix} = \begin{bmatrix} \begin{bmatrix} 1 & 0 \\ 0 & 1 \end{bmatrix} & 0 \\ 0 & [TR^*] \end{bmatrix} \begin{Bmatrix} d_{c_1} \\ d_{p_1} \end{Bmatrix} \tag{4}$$

and the new stiffness matrix is

$$U^* = R^{*T} K R^* \tag{5}$$

Using symmetry, only half of the shell is considered. When torsion in the stringers is introduced, the transformation is performed so that

$$\phi_i = W_{i,y} - \frac{v_i}{r} \tag{6}$$

2.3 Derivation of General Equations of Motion of an Impacting Aircraft

The equations of motion are derived from the principle of virtual work. In a static case (or in a case of quasi-static loading) the principle states that, for any virtual displacement, the work done by the applied forces equals the change in potential energy. The virtual displacements satisfy the boundary conditions. Thus for a virtual displacement $\delta(W)$ the virtual work done by force distribution $\bar{F}$, in the whole body, is

$$\delta W^* = \int_{\text{body}} [\delta(W)^T \cdot \bar{F}] dV \tag{7}$$

The change in potential energy after the virtual displacement due to elastic and plastic deformation is

$$\delta U^* = \int_{\text{body}} [\delta(W)^T \cdot B^T \bar{\sigma}] dv \tag{8}$$

where the strain is $\{\varepsilon\} = [B]\{W\}$ and $[B]$ can be a nonlinear operator on displacement.

In a dynamic situation where plasticity, large deflections and damping can exist, the inertial forces are added (to $\bar{F}$) in the d'Alembert sense, namely

$$-\frac{\partial^2}{\partial t^2}(\mu W). \tag{9}$$

This consists of translational and rotational forces. The large deflections are represented in the nonlinear operator $[B]$. Plasticity is introduced by representing the stress $\bar{\sigma}$ by an operator acting on strain such that

$$\{\sigma\} = [S]\{\varepsilon\}. \tag{10}$$

[S] is a nonlinear operator and the strain {ε} includes plastic strain. The damping due to viscoelastic forces in the material and friction forces in the joints is given by

$$F_d = \int \int_{-\infty}^{t} \Phi(t,\tau) w(\tau) d\tau dv \tag{11}$$

where t is actual time, τ is an instant of time and Φ is the hereditary kernal of memory function represented as[5]

$$\Phi(t) = \sum_{i=1}^{n} A_i e^{-\alpha_i t} \tag{12}$$

where A_i and α_i are material or structural constants. Thus for an equilibrium state, about which the virtual displacement of $\delta(W)$ is considered,

$$\delta W^* = \delta U^*. \tag{13}$$

The above equation can be rewritten as

$$\int_{\text{body}} [\delta(W)^T] \cdot \left\{ \bar{F} - \frac{\partial^2}{\partial t^2} (\mu\{W\}) - \int_{-\infty}^{t} \Phi(t-\tau) d\tau \cdot \{W\} - B^T \bar{\sigma} \right\} dv = 0 \tag{14}$$

The only way to satisfy this condition for arbitrary $\delta(W)$ is to conclude that

$$\bar{F} - \frac{\partial^2}{\partial t^2} (\mu\{W\}) - \left(\int_{\infty}^{t} \Phi(t-\tau) d\tau \right) \cdot \{W\} - B^T \bar{\sigma} = 0 \tag{15}$$

The impact forces are introduced by imparting momentum to the modes which come in contact with the ground. The velocity with which they rebound is

proportional to the coefficient of restitution between the body and the surface and the impart velocity.

Derivation of the Finite Element Equations of Motion

Idealization

The aircraft is idealized as a flexible body with structural elements.[4] Each element (with element number s) has n_s points of contact with neighbouring elements. Each node can have a concentrated nodal mass whose contribution in the equations of motion is derived later. This contribution can be used in a lumped mass approach. The element contribution in stiffness, masses and forces can be derived independently. The forces are summed to get the dynamic equilibrium of the whole aircraft. In this derivation the element forces are shown. Any equilibrium is intended to entail the whole body and should not be confused with equilibrium between the elements. As shown in Fig. 5, there are 3 main basic reference frames. The $\vec{i}$ reference frame is for inertial position on the ground, $\vec{b}$ is for the body (i.e., fuselage) and centred on the structure's centre of gravity, and $\vec{e}_i$ is the i-th element centred on its local centre of mass (when necessary, used to transform the nodal degrees of freedom). The centre of mass for the fuselage is assumed to remain constant as the fuselage deforms. The small changes of fuselage shape, and due to its small mass compared to the wing load, do not affect the position of the centre of mass. The element deflection consists of both elastic and plastic deformations (Fig. 6). The several vector bases are related according to the following equations (where d is the nodal displacement):

$$\left.\begin{aligned} \vec{d}_{body} &= \bar{c}_i \, \vec{d}_{element_i} \\ \vec{d}^T_{body} &= \vec{d}^T_{element_i} \, \bar{c}^T_i \\ \vec{d}_{inertial} &= c\vec{d}_{body} \end{aligned}\right\} \quad \vec{b}^T c = \vec{e}_i^T \qquad (16)$$

Finite Element Equations

Deformations of each element can be represented as polynomials with their coefficients determined from the nodal deformations. Since the variational nodal deformations d_i (i = 1...n nodes) define the fuselage displacement unknowns, the equation of motion of the fuselage ultimately consists of $6n_s$ scalar second-order differential equations. The 3 displacements, defined by $\bar{W}(\xi,\eta,\zeta)$, are expressed as,

$$\bar{W}(\xi,\eta,\zeta) = \begin{Bmatrix} u \\ v \\ w \end{Bmatrix}, \quad \bar{W} = P_b \Gamma \tag{17}$$

where Γ represents the scalar unknowns from the nodal displacements.

$$P_b = \begin{bmatrix} 1 & \xi & \eta & \xi\eta & 0 & 0 & \longrightarrow \\ 0 & 0 & 0 & 0 & 1 & \xi & \eta & \xi\eta & 0 & 0 & \longrightarrow \\ 0 & \longrightarrow & & & & & & & 1 & \xi & \eta & \xi\eta & \xi & \eta^2 \ldots \end{bmatrix}$$

The nodal displacements are,

$$\begin{aligned} &\bar{W}_i = \bar{W}(\xi_i, \eta_i) = P_b(\xi_i, \eta_i)\Gamma \\ &\bar{W} = W'\bar{d} \qquad \text{where} \qquad \bar{d}^T = \{\bar{W}_i \ \bar{\beta}_i\} \\ &\bar{\beta}_i^T = \bar{W}^T \left\{ \frac{\partial}{\partial\xi}, \frac{\partial}{\partial\xi}, \frac{\partial}{\partial\eta\partial\xi} \right\}_i = \bar{W}^T \{\Gamma\}_i^T \end{aligned} \tag{18}$$

and

$$W' = P_b F^{-1} \quad \text{where} \quad F^T = \{P_b^T\}\{1, \nabla\}_i, \quad i = i, \eta_s$$

For static equilibrium of a mechanical system, the work W^* accomplished by external forces in the course of virtual displacement equals the strain energy U^* stored in the deforming element. This equality is preserved for

non-dissipative dynamic systems in motion if one adds to the external forces an inertial force $A\mu dv$, where A is acceleration, μ density and dv the volume. Using the local element vector basis,

$$W^* = \bar{d}^{*T} \bar{L}_s + \int_s \bar{W}^T \bar{G}\, dv - \int_s \bar{W}^T A\mu dv \tag{19}$$

One can neglect the internal forces $\bar{G}$ (other than structural forces). The 'bar' quantities refer to the local basis. $\bar{L}_s$ consists of forces at the element nodes arising from external forces and moments, interaction forces and torques between it and the other elements. The strain energy, when neglecting the thermal stresses, is,

$$U^* = \int_s \frac{1}{2} \bar{\epsilon}^{*T} \bar{\sigma}\, dv = \bar{d}^{*T} \frac{1}{2} \int_s \bar{W}'^T D^T S D \bar{W}' dv \bar{d}^* + \bar{d}^* \frac{1}{2} \int_s \bar{W}'^T D^T \bar{\sigma}' dv \tag{20}$$

where the stiffness matrix $\int_s \bar{W}'^T D^T S D \bar{W}'$ is known.

The second contribution is from steady stresses such as plastic or nonlinear induced stresses. $\bar{\epsilon}$, $\bar{\sigma}$ represent stress and strain, respectively, in the element basis, and S, D relate strain and stress, and strains and displacements, respectively.

Equating U^* and W^* and differentiating with respect to the nodal displacements d^*, one can obtain $\bar{L}_s$ as

$$\bar{L}_s = \int_s \bar{W}'^T D^T S D W' dv\, \bar{d}^* + \int_s W'^T D^T \bar{\sigma}' dv + \int_s W'^T \bar{A} \mu dv \tag{21}$$

The acceleration of the element in the inertial reference frame is,

$$\vec{A} \triangleq \vec{i} \left(\frac{d^2}{dt^2} (\vec{x} + \vec{R}_c + \vec{p} + \vec{w}) \right) \tag{22}$$

where $\vec{i}$ implies inertial reference frame. $\vec{A}$ must be obtained from Eq. (22). One has to get $\bar{A}$ from this and substituted into Eq. (21) to define $\bar{L}_s$. The vectors are given in the different reference frames as

$$\vec{x} \triangleq \{\vec{i}\}^T \bar{x} \qquad \text{position of centre of mass (c.m.)}$$

$$\vec{R}_c \triangleq \{\vec{b}\}^T \bar{R}_c \qquad \text{position of element from c.m.}$$

$$\vec{p} \triangleq \{\vec{e}\}^T \bar{p} \qquad \text{position of particle in the element} \tag{23}$$

$$\vec{w} \triangleq \{\vec{c}\}^T \bar{w} = \{\vec{b}\} \bar{w}_i \qquad \text{is the deformation of the single point in the element}$$

Differentiating using the relation

$$\vec{i} \frac{d\vec{V}}{dt} = \frac{b_d}{dt} \vec{V} + \vec{\omega}^b \times {}^b\vec{V} \tag{24}$$

(for a vector $\vec{V}$ in reference frame $\vec{b}$ to be differentiated in reference $\vec{i}$, and $\vec{\omega}^b$ is the angular velocity of $\vec{b}$ with respect to $\vec{i}$). $\vec{\omega}^b$ is the angular velocity of the body with respect to the inertial reference frame and $\vec{\omega}^e$, the angular velocity of the element with respect to the body reference frame, is neglected. If $\tilde{\omega}$ is defined as

$$\tilde{\omega} \triangleq \begin{bmatrix} 0 & -\omega_3 & \omega_2 \\ \omega_3 & 0 & -\omega_1 \\ -\omega_2 & \omega_1 & 0 \end{bmatrix} \tag{25}$$

where 1, 2, 3 represent three orthogonal axes, $\vec{A}$ can be shown to be (in element basis),

$$\vec{A} = \{\vec{e}\}^T [\bar{c}\bar{c}\ddot{x} + \bar{c}[\dot{\tilde{\omega}}^b (R_c + \bar{c}^T \bar{p}) + \tilde{\omega}^b \tilde{\omega}^b (R_c + \bar{c}^T \bar{p}] + \ddot{\bar{w}} +$$

$$+ \bar{c}[2\tilde{\omega}^b \bar{c}^T \dot{\bar{w}} + (\dot{\tilde{\omega}}^b + \tilde{\omega}^b \tilde{\omega}^b) \bar{c}^T \bar{w}]) \tag{26}$$

Note $\omega^e = \omega^b + \bar{c}\,\dot{\bar{c}}^T$ and $\dot{\bar{c}}$ is neglected. One can express $\bar{W}$ in terms of $\bar{d}$, and $\bar{L}$ can be expressed in terms of $\vec{A}$ as

$$\begin{aligned}\bar{L}_s = &\int_s \bar{W}'^T D^T S D W' dv\ \bar{d} + \int_s W'^T D^T \bar{\sigma}' dv + \int_s W'^T \bar{c}\, c\, \ddot{x}\, \mu dv \\ &+ \int_s W'^T \bar{c}[(\tilde{\dot{\omega}}^b + \tilde{\omega}^b \tilde{\omega}^b)(R_c - \bar{c}^T \bar{p})]\mu dv + \int_s W'^T W' \mu dv\ \ddot{\bar{d}} \\ &+ \int_s W'^T \bar{c}\, 2\tilde{\omega}^b \bar{c}^T W' \mu dv\ \dot{\bar{d}} + \int_s W'^T \bar{c}(\tilde{\dot{\omega}}^b + \tilde{\omega}^b \tilde{\omega}^b)\bar{c}^T W' \mu dv\ \bar{d}\end{aligned} \qquad (27)$$

The coefficients of $\ddot{\bar{d}}$, $\dot{\bar{d}}$, $\bar{d}$ are identified as,

$\bar{m} \triangleq \int_s W'^T W' \mu dv$ or element consistent mass matrix

$\bar{g} \triangleq 2\int_s W'^T \bar{c}\, \tilde{\omega}^b \bar{c}^T W' \mu dv$ or element gyroscopic coupling matrix

$\bar{k} \triangleq \int_s W'^T D^T S D W' dv$ the element stiffness matrix (structural) (28)

$\bar{\alpha} = \int_s W'^T \bar{c}\, \tilde{\dot{\omega}}^b \bar{c}^T W' \mu dv$ the element angular acceleration stiffness matrix

$\bar{k} = \bar{k}_o + \bar{k}_\Delta$ geometric or plastic preload stiffness matrix and linear deformation stiffness matrix

$\kappa = \int_s W'^T \bar{c}\, \tilde{\omega}^b \tilde{\omega}^b \bar{c}^T W' \mu dv$ the element centrifugal stiffness matrix

Using $\int_s W' \mu dv = m_c^* W'_c$, where c implies centre of element and m is the mass,

$$\bar{L}_s = \bar{m}^s \ddot{\bar{d}}^s + \bar{g}^s \dot{\bar{d}}^s + (\bar{k}_o^s + \bar{k}_\Delta^s + \bar{\kappa}^s + \bar{\alpha}^s)\bar{d}$$

$$+ \int_s w'^T \bar{c}(\tilde{\dot{\omega}}^b + \tilde{\omega}^b \tilde{\omega}^b)\bar{c}^T \bar{\rho}\mu dv$$

$$+ w_c'^T m_c[\bar{c}^s \ddot{\bar{x}} + \bar{c}^s(\tilde{\dot{\omega}}^b + \tilde{\omega}^b \tilde{\omega}^b)\bar{R}_c] \qquad (29)$$

Note that s implies element 's'. One can sum for all elements assuming no nodal masses to obtain f_i impact forces. For dynamic equilibrium of the whole body,

$$0 = \Sigma\, \bar{c}^{sT} \dot{\bar{L}}_s - \bar{f}_i \quad \text{and} \quad s \in \text{all elements} \qquad (30)$$

where rotational and shear effects are neglected.

Derivation of Nodal Mass Equations

Given that the acceleration of nodal bodies $\vec{A}$ is

$$\vec{A} \triangleq \vec{i} \frac{d^2}{dt^2}(\bar{x} + \bar{r}^j + \bar{u}^j) \qquad (31)$$

where $\bar{r}$ is the nodal position from the c.m. and $\bar{u}^j$ is the nodal deformation of the j-th mode. One can differentiate $\vec{A}$ with respect to time in the inertial reference frame to get the sum of forces,

$$0 = \Sigma c\, \vec{f}^j - \bar{c}^{sT} \bar{F}_j^s(m^j[\ddot{\bar{x}} + [(\tilde{\dot{\omega}}^b + \tilde{\omega}^b \tilde{\omega}^b)(\bar{r}^j + \bar{u}^j)] + 2\tilde{\omega}^b \dot{\bar{u}}^j + \ddot{\bar{u}}^j)\} \qquad (32)$$

where $\vec{f}$ and $\vec{F}_j$ represent external forces and forces due to other nodal sources, respectively.

Equations of rotation of the j-th nodal body are derived from

$$\vec{T}^j = \dot{\vec{H}}^j = \bar{I}^j \dot{\bar{\omega}}^j + \tilde{\bar{\omega}}^j + \bar{I}^j \bar{\omega}^j \text{ for } \bar{I}^j = \text{constants} \tag{33}$$

where $\vec{T}$ = torque and $\vec{H}$ is the angular momentum

$\bar{I}^j$ is the inertia dyadic of the nodal body

Dot ≡ differentiation in inertial reference frame.

The equation obtained when $\dot{\beta}$ are nodal rotations, when $\{\vec{b}\}^T \bar{T}^j$ are summed, is

$$0 = \{\vec{b}\}^T [\bar{c}\bar{T}^j - \Sigma \bar{c}^{sT} \bar{T}^s] \tag{34}$$

where

$$\bar{T}^s = \bar{I}^j \dot{\bar{\omega}}^b + \tilde{\bar{\omega}}^b \bar{I}^j \bar{\omega}^b + \bar{I}^j \ddot{\bar{\beta}}^j + \left[\tilde{\bar{\omega}}^b \bar{I}^j - (\bar{I}^j \omega^b)\tilde{} + \right.$$

$$\left. + \bar{I}^j \tilde{\bar{\omega}}^b\right] \dot{\bar{\beta}}^j + \bar{I}^j \tilde{\dot{\bar{\omega}}}^b + (\bar{I}^j \dot{\omega}^b)\tilde{} + \tilde{\bar{\omega}}^b \bar{I}^j \tilde{\bar{\omega}}^b + \tilde{\bar{\omega}}^b (\bar{I}^j \bar{\omega}^b)] \tilde{\bar{\beta}}^j \tag{35}$$

This combination is then added to the rest of the equations.

Linearized Equations of Motion

The finite element equations of motion can be linearized by assuming that $\tilde{\bar{d}}$, $\bar{d}$, $\bar{d}$, $\bar{\omega}$ and $\dot{\bar{\omega}}$ are small so that only first order terms are retained. Thus one finds

$$\bar{L}_s = \bar{c}^T \int_s W'^T D^T S D W' dv \bar{c} \ddot{\bar{d}}^s + \int_s c^T W'^T \bar{c} \ddot{\bar{x}} \mu dv$$

$$+ \int_s W'^T \bar{c} (\tilde{\dot{\omega}}) (R_c + \bar{c}^T \bar{p}) \mu dv$$

$$+ \bar{c}^T \int_s W' W' \mu dv \bar{c} \ddot{\bar{d}}^s \tag{36}$$

where $\bar{d}^s$ is in the body coordinate system. The second and third integrals are simplified and expressed in terms of m_s (or mass of the element) at the centre of the element (W_c' used). The remaining equations can be linearized in the same manner. Equations in the body coordinate system are of most interest since the transducers are usually placed on the aircraft.

Level Impact Case

In the case where the fuselage axis is parallel to the ground during the entire crash, $\tilde{\omega}^b$ is zero,

$$\tilde{L}_s^b = \bar{c}^T \bar{k} \bar{c} \bar{d}^s + c^T m_s W_{c_s}^T \tilde{c}\ddot{\bar{x}} + \bar{c}^T \bar{m} \bar{c} \ddot{\bar{d}}^s \tag{37}$$

where $\bar{d}$'s are in the body reference frame $\bar{k}$ and $\bar{m}$ are the stiffness and consistent mass matrices, respectively. The consistent matrix and inertial mass are calculated for every element and summed. Nodal mass equations are also found.

Integration with Time

Integration with time is done using the Newmark-β method such that,[6]

$$\begin{aligned}
\bar{d}_{I+1} &= \bar{d}_I + \Delta t\, \bar{V}_I + \Delta t^2 \left[\left(\tfrac{1}{2} - \beta\right) \bar{a}_I + \beta \bar{a}_{I+1}\right] \\
\bar{V}_{I+1} &= \bar{V}_I + \tfrac{1}{2} \Delta t (\bar{a}_I + \bar{a}_{I+1}) \\
\bar{a}_{I+1} &= 4/\Delta t^2 \left(\Delta \bar{d}_{I+1} - \Delta t\, \bar{V}_I - \tfrac{1}{4} \Delta t^2\, \bar{a}_I\right)
\end{aligned} \tag{38}$$

where $\bar{d}$, $\bar{V}$ and $\bar{a}$ are displacement, velocity and acceleration, respectively. I implies step 'I' in integration and Δt is the time change between steps. Using the tangential stiffness matrix K, allowing for linear and nonlinear analyses (i.e., follow nonlinear curve assuming linear steps), one can then solve

$$
\begin{aligned}
K^{**}\,\Delta\bar{d} &= P^{**} \\
K^{**} &= \bar{M} + \beta\Delta t^2 K^{*} \\
P^{*} &= M\left[\Delta t V_I + \left(\frac{1}{2} - \beta\right)\Delta t^2 a_I\right] + \beta\Delta t^2\left[F_{I+1} - f_I\right] \\
f_I &= K_I^{*}\, d_I^{*}
\end{aligned}
\tag{39}
$$

where β is a variable introduced by the integration method. $\beta = 1/4$ is currently being used.

This implicit integration method has advantages of unconditional stability and accuracy when solving nonlinear structural dynamics problems.[7,10] The 'Frontal Solver' is used while integrating with time.[8,9] The special relationship shown in Eq. (39) is a characteristic of the Newmark-β method which is usable with the 'Frontal Solver'. In this method Gaussian elimination is done as soon as all the contributions to a degree of freedom have been made. If the K^{*} [e.g., (39)] does not change with time, no more inversions are needed. Thus the computer memory required is small compared to methods where all the global matrices are assembled first and sometimes inverted at every time step in some integration schemes. This method of approach provides a considerable advantage for a system with a large number of degrees of freedom. In addition, it is to be noted that the implicit method used here is superior to explicit methods due to the previously mentioned stability characteristics since

the computer storage required is comparable in both methods. As well, large systems can give a lot of detail which is not available when using the lumped or 'Hybrid' methods. If $\beta = 1/2$ unconditional stability is guaranteed. No static condensation is required.

3. DESCRIPTION OF TEST PROGRAMME

3.1 Fuselage Test Model

An experimental model having a geometric scale factor of about 1/3 was found suitable for characterizing a large number of typical general-transport aircraft structures, ranging in weight from a 6,000 lb aircraft up to about 48,000 lbs, such as the DHC Dash 7. To ensure that the test model possessed a certain degree of dynamic similarity with actual aircraft structures, a nondimensional analysis was performed.

Using this scale factor, a high-wing fuselage configuration was selected. All test models were fabricated from 0.012 inch thick 2024-T3 aluminum skin stiffened with twelve light-rib frames and two solid cross-section heavy main frames (bulkheads) to pick up the wing load. A skeleton aluminum floor structure was added for completeness. Longitudinal stringers were added to this test phase which involved "free-flight" impact (for details see Fig. 7). The fuselage models were 36 inches in diameter, 91 inches long, and weighed approximately 36 pounds. Figures 8 and 9 show two photographs of this new test model.

The wing load was simulated by attaching "dead" weights to a rigid mounting fixture which was bolted to both of the interior main frames. Note that in contrast to all of the previous models (refer to TP2616), this structure contained two longitudinal stiff beams with end weights. From our calibration test run (using a refurbished fuselage), it was found that

complete pitchover occurred after first impact. This was due to a high c.g. position and an unacceptably low value of the pitch moment of inertia. Analysis of the appropriate parameters led to the design of the wing mass system shown in the photographs.

3.2 Crash Test Facility

To provide the fuselage model with a forward velocity component as well as a vertical velocity component at impact, a pendulum gantry was constructed over a large 40 ft x 12 ft reinforced concrete pad. This facility used to simulate a free-flight crash test condition is depicted in the schematic, Fig. 10. The fuselage specimen was suspended from the gantry top pivot point by a rigid swing arm and drawn back above the impact surface by a pullback cable. The fuselage mounting fixture was attached to the rigid swing arm by a pyrotechnic bolt tension separator. The test sequence was initiated when the fuselage was released from the pullback cable, permitting the model to swing pendulum style onto the impact surface. The fuselage mounting fixture was then separated from the swing arm by the pyrotechnic device just above the impact surface, freeing the model from restraint. The umbilical cable remained attached to the fuselage for data acquisition throughout the duration of the test. The separation point occurred when the rigid swing arm was 90° from the impact surface, blocking off a beam of light from a laser. The casting of a shadow on the photoelectric cell resulted in an instantaneous firing of the pyrotechnic device. Should the pyrotechnic device not fire, the fuselage would continue to swing through, and then back and forth in a pendulum style motion over the impact surface.

The height of the fuselage above the impact surface at release determined the vertical impact velocity which can be varied for subsequent tests.

The firing of the pyrotechnic device imparts no velocity of its own on the fuselage at separation. The horizontal velocity was determined by the amount of fuselage pullback required to raise the model's centre of mass above its centre of mass separation point. The maximum forward velocity that currently can be achieved in this facility is approximately 26 ft/sec (18 mph). The desired pitch angle at separation was set by the adjustment of the four cables which connect the mounting fixture to a point on the rigid swing arm just below the separation point. A consequence of this pendulum style swing technique is the creation of a large upward pitch rate about the model's centre of mass at separation which must be taken into consideration before testing to obtain the desired pitch angle at surface impact. A barrier was also constructed and placed at the end of the pad to prevent damage to cameras and other surrounding apparatus.

3.3 Data Acquisition System

Data acquisition from the crash tests was accomplished with photographic coverage using low and high speed cameras, and with onboard strain gauges and accelerometers. The strain gauges were bonded to the inner edge of the main load carrying frames, the locations of which are shown in Fig. 11. Strain gauge type miniature accelerometers were positioned in the fuselage to measure accelerations both in the normal and longitudinal directions to the fuselage axis. The major locations of interest included the wing mass, to measure the g loads applied to the main frames, and on the floor (vertical and horizontal) frame at mid-length to assess the g loads transmitted to the seat structure. The accelerometer locations are shown in Figs. 12, 13 and 14 for the various impact tests.

The accelerometer and strain gauge signals were sent through a SE Bridge Conditioning Unit and a SE Galvo Conditioning Unit before being

output on a Honeywell visicorder oscillograph (Model 1508). The accelerometer signals were also passed through a 200 Hz low pass filter and input to a Bruel and Kjaer 7003 FM-tape recorder. The analog data on the FM-tape were then digitized at 3000 samples per second and stored on a magnetic computer tape for additional processing. This data could then be filtered further or integrated once to yield velocities and twice to yield displacements. Figure 15 depicts the data acquisition system.

The recorder contained type M200-350 (electro-magnetic damped) miniature galvanometers having a resistance of 350Ω and a flat frequency response (± 5%) from 0 to 180 Hz. The strain gauges were 350Ω steel foil type gauges (Micro Measurement) having excellent frequency response characteristics. The accelerometers used were the damped and undamped strain-gauge miniature type (Entran EGBL-125) having low impedances. Other specifications of the accelerometers include a range of DC to ± 30g at 0-300 Hz and ± 100g at 0-1000 Hz extending to ± 150g and ± 500g, respectively, and a sensitivity of 2.5 mV/g. In addition, high speed 16 mm Hycam cameras were employed to record the dynamic behaviour for comparison with computer model predictions.

4. FREE-FLIGHT IMPACT TEST

Using the rib/stringer stiffened fuselage of Fig. 8, a free-flight test was conducted using a wing load of 537 lbs. The initial release parameters were:

Angle of incidence ≅ 3°

Nose-up pitch rage ≅ 1.18 rad/sec

Horizontal velocity ≅ 259 in/sec

With a preset release height of 6.75", the vertical initial impact velocity (including angular rotation effects) was predicted to be ≈ 34.6 in/sec. At initial impact, the remaining parameters changed to:

Angle of incidence ≅ 10.6°

Nose-up pitch rate ≅ 1.43 rad/sec

Horizontal velocity ≅ 233 in/sec

High speed photographs in Fig. 16 (∿ 400 pps) show the free-flight impact test through to final failure of the forward end. These far-field views permit one to compare the vehicle dynamics with predictions. Another series of high speed photographs (∿ 300 pps) are presented in Fig. 17 in which more accurate measurements can be made of structural deformation after initial impact. However, final failure and the second impact are not discernible due to the closeness of the camera.

Post-crash views of the deformed fuselage are given in Figs. 18-19. Note the collapsed state of the forward end, particularly the symmetry in the floor failure mode (Fig. 19) with some local fracture. This can be seen in more detail in Fig. 19(b), including the interior rib failures. It should be noted that no failure of the main load frames occurred.

5. COMPARISON OF COMPUTER MODEL PREDICTIONS WITH TESTS

Prior to the free-flight test, several calibration cases were studied to provide a check on the instrumentation but, more importantly, to provide data for comparison with both computer models.

5.1 Level Impacts

With the strain gauges and accelerometers mounted on the structure as shown in Figs. 11 and 12, respectively, two level impact tests were conducted. The wing load was maintained at 537 lbs and the two impact velocities were 34.4 in/sec and 52.5 in/sec. Summaries of the test data for both cases are given in Tables 2 and 3. Typical output traces for the second test are shown in Figs. 20-23.

At this point it is necessary to distinguish between the two analytical models. Let us refer to the Lumped Mass-Finite Element hybrid method by the abbreviation LMFE and similarly, for the consistent Finite Element model, by the symbols, CFE.

Tables 4 and 5 present the predicted response at selected nodes (see Fig. 2) for the LMFE analysis. Corresponding graphical output of the dynamic displacement, acceleration and strain curves are presented in Appendix A.

This analysis was repeated again for the two cases using the CFE model, the results of which are given in Tables 6 and 7. Selected graphical displays are also provided in Appendix B.

5.2 Oblique Angle Impacts

Two oblique angle tests were conducted at 1.92°, 34.7 in/sec and at 3.00°, 26.0 in/sec with a wing load of 537 lbs. Locations of the strain gauges and accelerometers are given in Figs. 11 and 13, respectively. Tables 8 and 9 present the test data obtained at these selected locations, while Figs. 24-31 illustrate the response curves obtained during impact.

Using the LMFE analysis, extensive predictions of dynamic displacements, accelerations and strains were made for both impact configurations, the results of which are contained in Appendix C. Computer graphics are also provided to illustrate the transient deformation and fuselage motion that occur for the varying impact conditions. Tables 10 and 11 summarize the relevant predicted g-load and strains for the elements which can be compared with test results (Tables 8 and 9).

5.3 Free-Flight Impact

During the free-flight test, two impacts of interest occur -- first impact as the aft end rotates downwards to contact the concrete pad and then rebounds -- second impact due to a nose-down pitching motion that leads to partial structural collapse (see Figs. 18 and 19). These conditions can be seen quite clearly in the accelerator response curves shown in Figs. 32-37.

Summaries of the test data (refer to Figs. 11 and 14 for instrumentation location) are given in Tables 12 and 13.

Appendix D contains the LMFE predictions of dynamic deformations, g-loads and strains, together with computer graphics illustrating the fuselage behaviour during the free-flight test.

6. CONCLUSIONS

A detailed outline of a consistent finite element (CFE) formulation capable of describing the impact behaviour of complex fuselage structures has been presented. In addition, a pendulum gantry crash facility has been designed and constructed capable of simulating various 'controlled' crash conditions on large scale model aircraft structures (about 1/4 $\sim$ 1/3 scale factor). Earlier work on the development of a lumped mass-finite element representation has been reviewed and comparative predic tions provided. Experimental results are also included in terms of dynamic g-loads, strains and transient failure modes (based on high speed photography) for level and oblique angle impacts, as well as for a 'free-flight' crash. Although it is premature to claim success in the analytical modelling, it is expected that reasonable correlation with the test data will result. Work is continuing on the refinement and application of the CFE model to these test cases. Finally, an all-composite fuselage model of similar geometry to the aluminum configuration used in this investigation is currently being manufactured. This structure consists of a Kevlar/

epoxy skin in combination with graphite/epoxy frames and ribs. The purpose here is to provide a comparative basis for all-metal construction for assessing the 'crash' behaviour of future composite fuselage aircraft that are presently being considered.

REFERENCES

1. Cantin, G., "Rigid-Body Motions and Equilibrium in Finite Element", Finite Elements for Thin Shells and Curved Members, John Wiley and Sons, 1976.

2. Bogner, F. K., Fox, R. L., Schmit, L. A., "The Generation of Inter-element Compatible Stiffness and Mass Matrices by the Use of Interpolation Formulas", Proc. Conference Matrix Methods in Structural Mech., Air Force Flight Dynamics Laboratory, Air Force Institute of Technology, AFFDL TR 66-80, p. 403.

3. Bogner, F. K. et al, "A Cylindrical Shell Discrete Element", AIAA Journal, April 1967.

4. Likins, Peter W., "Finite Element Appendage Equations for Hybrid Coordinates - Dynamic Analysis", NASA TR-32-1525.

5. Bert, C. W., "Material Damping", Journal of Sound and Vibration, Vol. 29, 1973.

6. Newmark, M. Nathan, "A Method of Computation for Structural Dynamics", J. Engng. Mech. Div., ASCE, 85, 1959.

7. Belytschko, T., and Schoeberle, D. F., "On the Unconditional Stability of an Implicit Algorithm for Nonlinear Structural Dynamics", Journal of Applied Mechanics, Dec. 1975.

8. Iron, M. Bruce, "A Frontal Solution Program for Finite Element Analysis", Int. Jour. for Numerical Methods in Engineering, Vol. 2, 1970.

9. Hinton, E., and Owen, D. R., "Finite Element Programming", Academic Press, 1977.

10. Hughes, T. J. R., "A Note on the Stability of Newmark's Algorithm in Nonlinear Structural Dynamics", Int. Journal of Numerical Methods in Engineering, Vol. 11, No. 2, 1972.

TABLE 1: PROCEDURE OUTLINE FOR DEVELOPING A MATHEMATICAL MODEL USING PROGRAM "CRASH"

PROCEDURE	GENERAL DESCRIPTION
1. Model Vehicle using Finite-Elements	Nodes, rods, beams, membrane elements; Assemble Stiffness Matrix.
2. Identification of Critical Structure	General nonlinear load-deflection characteristics.
3. Lumped-Mass Model Layout	Mass nodes, elements.
4. "Static" Condensation of Stiffness Matrix	Eliminate the "mass-less" degrees of freedom.
5. Form Mass Matrix	Estimate of Mass and Mass moments of Inertia Properties.
6. Definition of Crash Environment	Initial conditions.
7. Establish Nonlinear Characteristics	Material nonlinear beam curve, Panel buckling stresses.
8. Initial Computer run (set max. time = o)	Review model input data
9. Revise Input Data, if required	Based on results of preliminary run.
10. Select Integration Interval	Based on the natural free vibration frequencies of system.
11. Select Data Requirements	Choose print/plot intervals.
12. Limited Computer Run (set max. time $\leq$ 0.010 sec)	Check validity and stability of model.
13. Revise Model (if required)	Based on results of computer run.
14. Extend Runs and Review Beam and Panel Data.	Determine if yields and/or buckling are consistent.
15. Revise Model as Required.	Revise nonlinearities, etc.
16. Finalize Model.	Determine run time and data to be obtained.

GENERAL FLOW CHART OF PROGRAM "CRASH"

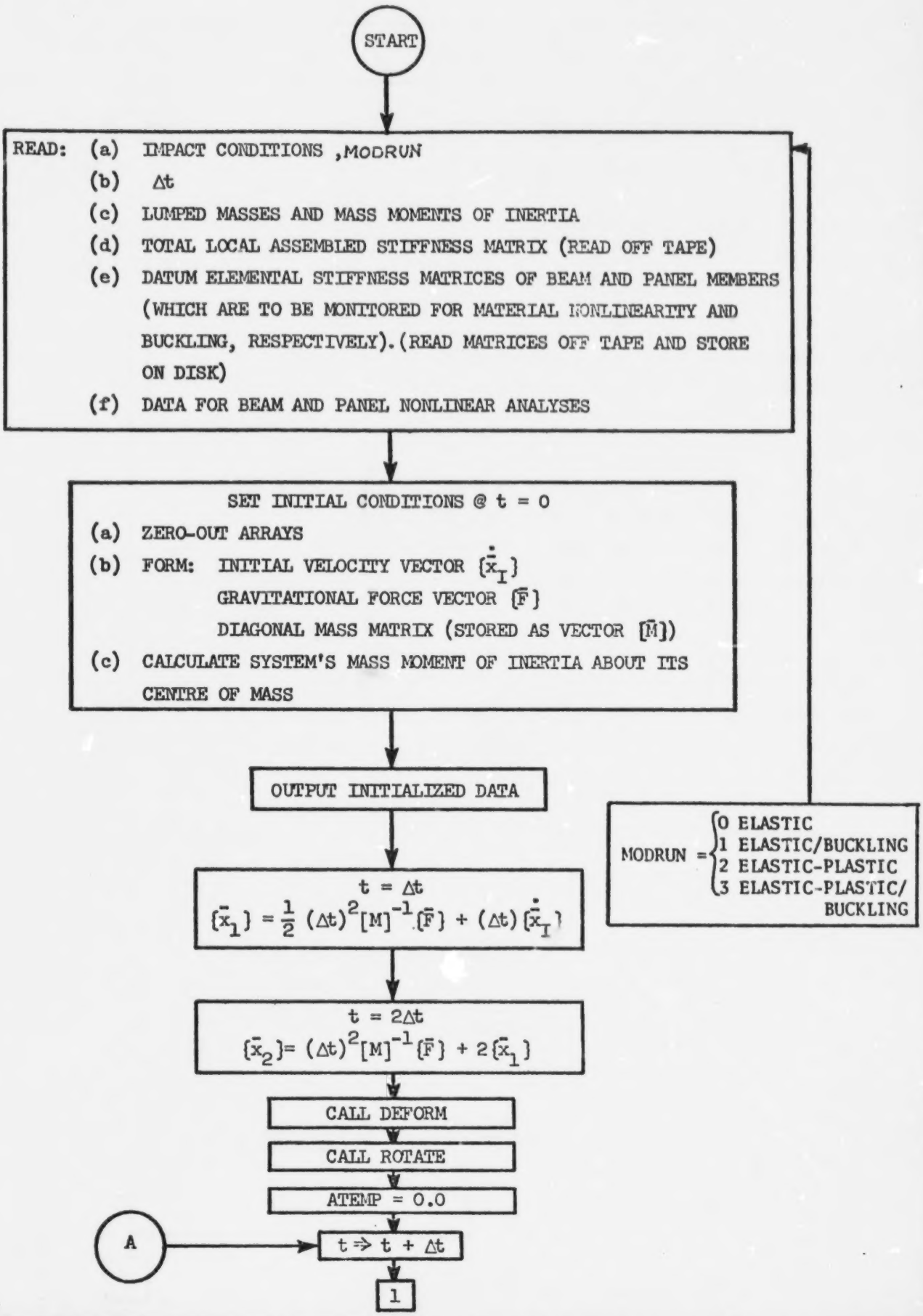
START
READ: (a) IMPACT CONDITIONS ,MODRUN
(b) Δt
(c) LUMPED MASSES AND MASS MOMENTS OF INERTIA
(d) TOTAL LOCAL ASSEMBLED STIFFNESS MATRIX (READ OFF TAPE)
(e) DATUM ELEMENTAL STIFFNESS MATRICES OF BEAM AND PANEL MEMBERS (WHICH ARE TO BE MONITORED FOR MATERIAL NONLINEARITY AND BUCKLING, RESPECTIVELY).(READ MATRICES OFF TAPE AND STORE ON DISK)
(f) DATA FOR BEAM AND PANEL NONLINEAR ANALYSES
SET INITIAL CONDITIONS @ t = 0
(a) ZERO-OUT ARRAYS
(b) FORM: INITIAL VELOCITY VECTOR $\{\dot{\bar{x}}_I\}$
GRAVITATIONAL FORCE VECTOR $\{\bar{F}\}$
DIAGONAL MASS MATRIX (STORED AS VECTOR $[\bar{M}]$)
(c) CALCULATE SYSTEM'S MASS MOMENT OF INERTIA ABOUT ITS CENTRE OF MASS
OUTPUT INITIALIZED DATA
MODRUN = 0 ELASTIC
1 ELASTIC/BUCKLING
2 ELASTIC-PLASTIC
3 ELASTIC-PLASTIC/BUCKLING
t = Δt
$\{\bar{x}_1\} = \frac{1}{2}(\Delta t)^2[M]^{-1}\{\bar{F}\} + (\Delta t)\{\dot{\bar{x}}_I\}$
t = 2Δt
$\{\bar{x}_2\} = (\Delta t)^2[M]^{-1}\{\bar{F}\} + 2\{\bar{x}_1\}$
CALL DEFORM
CALL ROTATE
ATEMP = 0.0
A
t ⇒ t + Δt
1

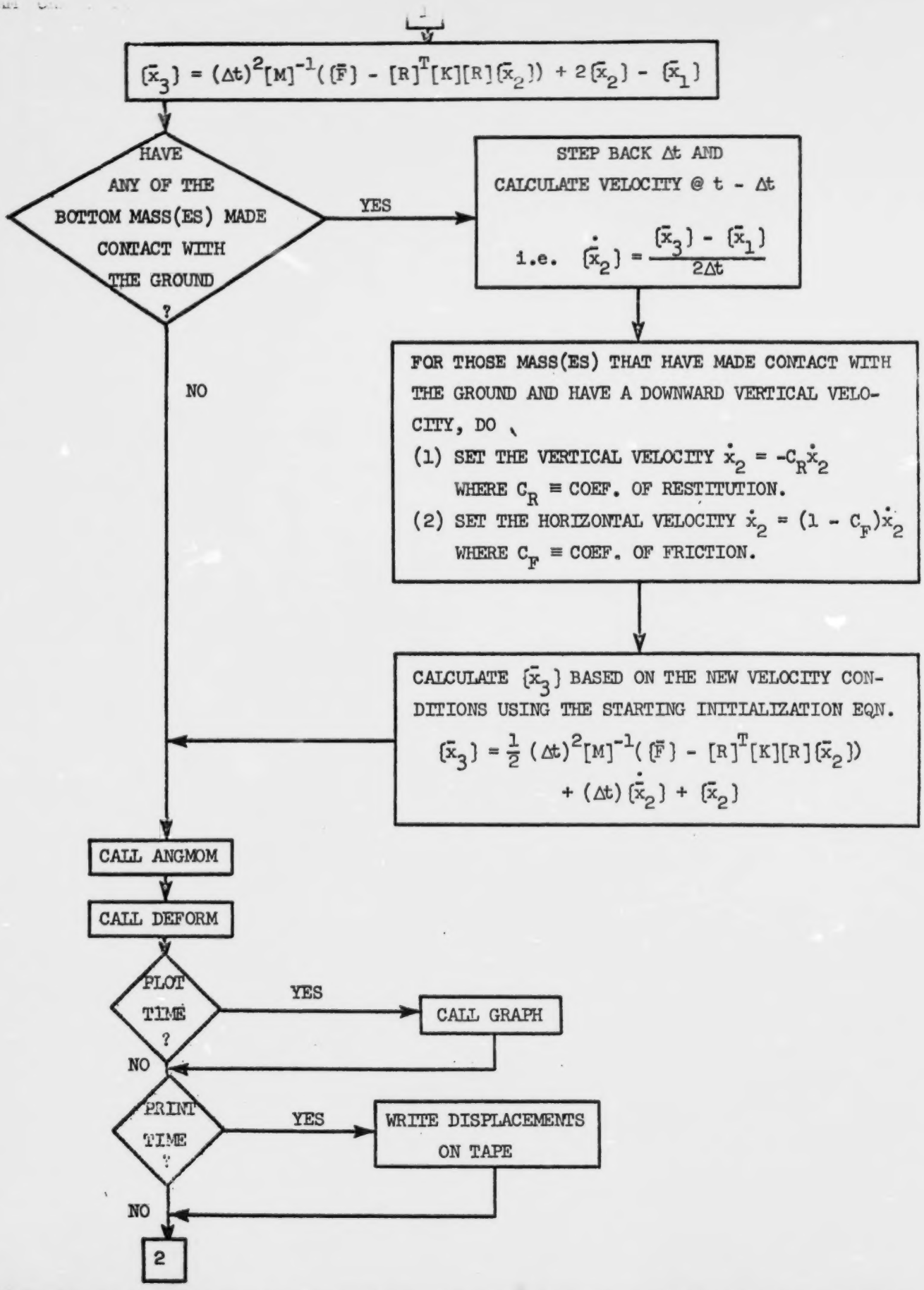
1
$\{\bar{x}_3\} = (\Delta t)^2[M]^{-1}(\{\bar{F}\} - [R]^T[K][R]\{\bar{x}_2\}) + 2\{\bar{x}_2\} - \{\bar{x}_1\}$
HAVE ANY OF THE BOTTOM MASS(ES) MADE CONTACT WITH THE GROUND ?
YES
STEP BACK Δt AND CALCULATE VELOCITY @ t - Δt
i.e. $\{\dot{\bar{x}}_2\} = \frac{\{\bar{x}_3\} - \{\bar{x}_1\}}{2\Delta t}$
NO
FOR THOSE MASS(ES) THAT HAVE MADE CONTACT WITH THE GROUND AND HAVE A DOWNWARD VERTICAL VELOCITY, DO
(1) SET THE VERTICAL VELOCITY $\dot{x}_2 = -C_R\dot{x}_2$ WHERE $C_R \equiv$ COEF. OF RESTITUTION.
(2) SET THE HORIZONTAL VELOCITY $\dot{x}_2 = (1 - C_F)\dot{x}_2$ WHERE $C_F \equiv$ COEF. OF FRICTION.
CALCULATE $\{\bar{x}_3\}$ BASED ON THE NEW VELOCITY CONDITIONS USING THE STARTING INITIALIZATION EQN.
$\{\bar{x}_3\} = \frac{1}{2}(\Delta t)^2[M]^{-1}(\{\bar{F}\} - [R]^T[K][R]\{\bar{x}_2\}) + (\Delta t)\{\dot{\bar{x}}_2\} + \{\bar{x}_2\}$
CALL ANGMOM
CALL DEFORM
PLOT TIME ?
YES
CALL GRAPH
NO
PRINT TIME ?
YES
WRITE DISPLACEMENTS ON TAPE
NO
2

PROGRAM "CRASH" CONTD.

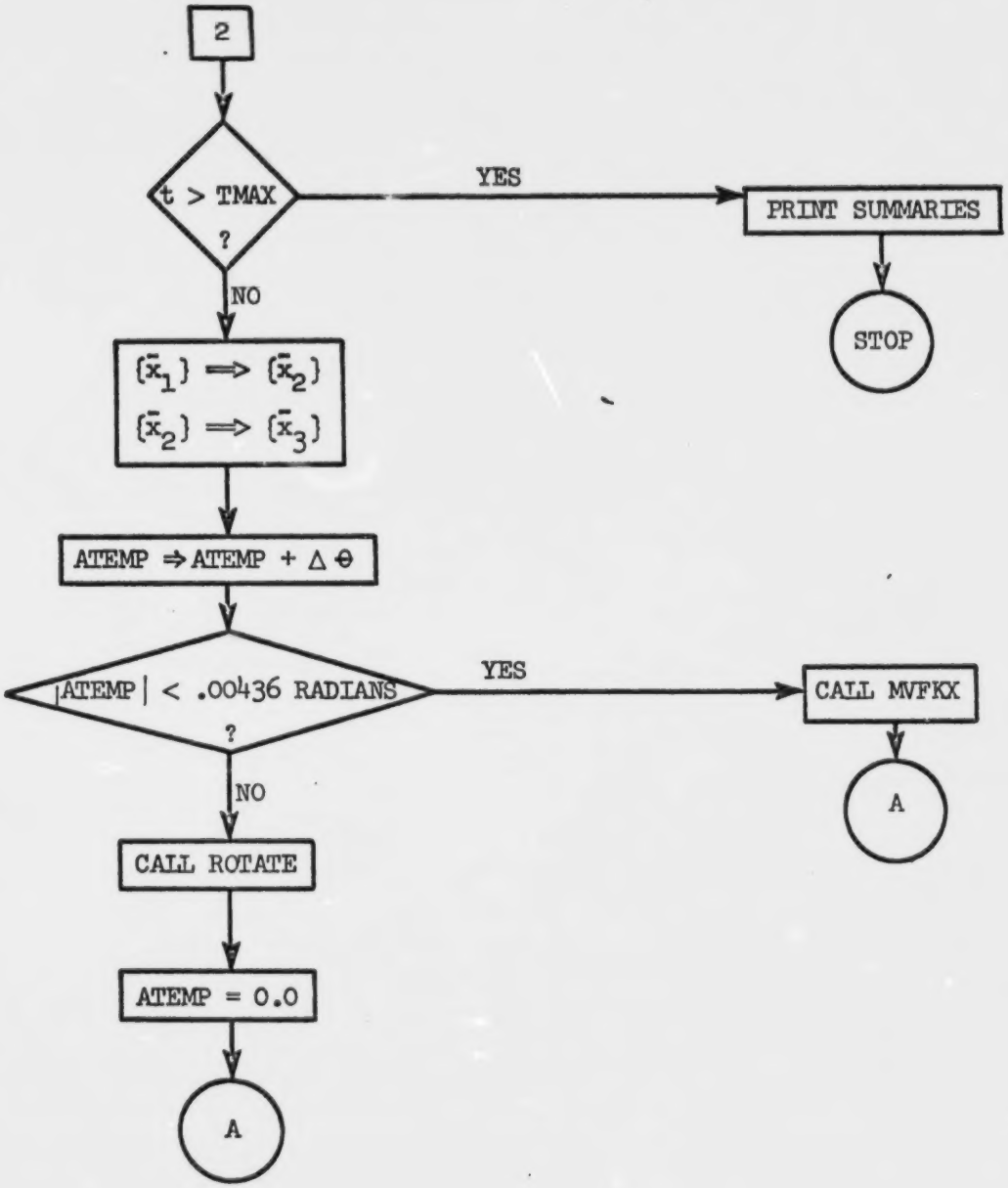

- GENERAL FLOW CHART OF SUBPROGRAM "DEFORM"

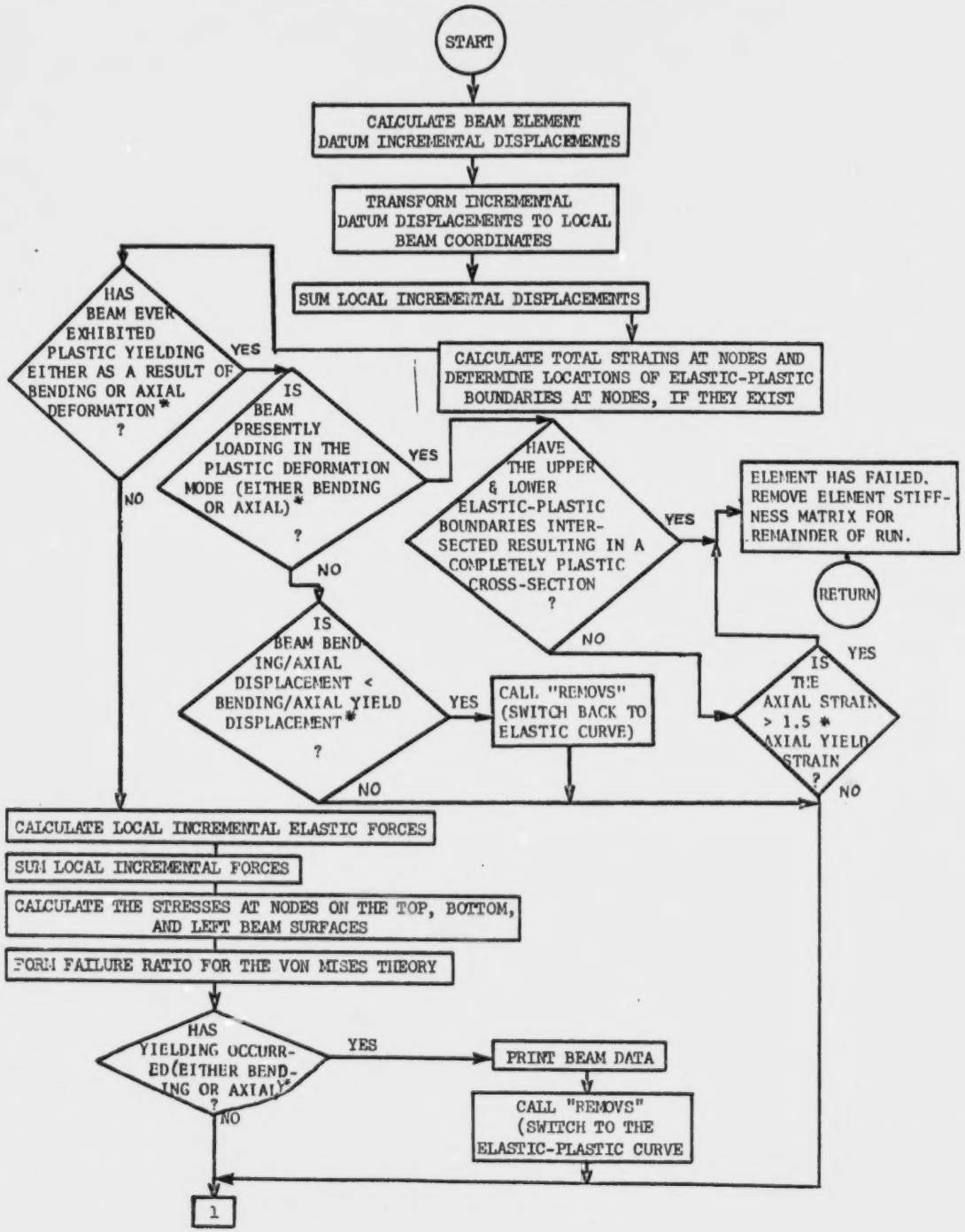
START
CALCULATE BEAM ELEMENT DATUM INCREMENTAL DISPLACEMENTS
TRANSFORM INCREMENTAL DATUM DISPLACEMENTS TO LOCAL BEAM COORDINATES
SUM LOCAL INCREMENTAL DISPLACEMENTS
CALCULATE TOTAL STRAINS AT NODES AND DETERMINE LOCATIONS OF ELASTIC-PLASTIC BOUNDARIES AT NODES, IF THEY EXIST
HAS BEAM EVER EXHIBITED PLASTIC YIELDING EITHER AS A RESULT OF BENDING OR AXIAL DEFORMATION* ?
YES
NO
IS BEAM PRESENTLY LOADING IN THE PLASTIC DEFORMATION MODE (EITHER BENDING OR AXIAL)* ?
YES
NO
HAVE THE UPPER & LOWER ELASTIC-PLASTIC BOUNDARIES INTER-SECTED RESULTING IN A COMPLETELY PLASTIC CROSS-SECTION ?
YES
NO
ELEMENT HAS FAILED. REMOVE ELEMENT STIFF-NESS MATRIX FOR REMAINDER OF RUN.
RETURN
IS BEAM BEND ING/AXIAL DISPLACEMENT < BENDING/AXIAL YIELD DISPLACEMENT* ?
YES
NO
CALL "REMOVS" (SWITCH BACK TO ELASTIC CURVE)
IS THE AXIAL STRAIN > 1.5 * AXIAL YIELD STRAIN ?
YES
NO
CALCULATE LOCAL INCREMENTAL ELASTIC FORCES
SUM LOCAL INCREMENTAL FORCES
CALCULATE THE STRESSES AT NODES ON THE TOP, BOTTOM, AND LEFT BEAM SURFACES
FORM FAILURE RATIO FOR THE VON MISES THEORY
HAS YIELDING OCCURR-ED(EITHER BEND-ING OR AXIAL)* ?
YES
NO
PRINT BEAM DATA
CALL "REMOVS" (SWITCH TO THE ELASTIC-PLASTIC CURVE
1

SUBPROGRAM "DEFORM" CONTD.

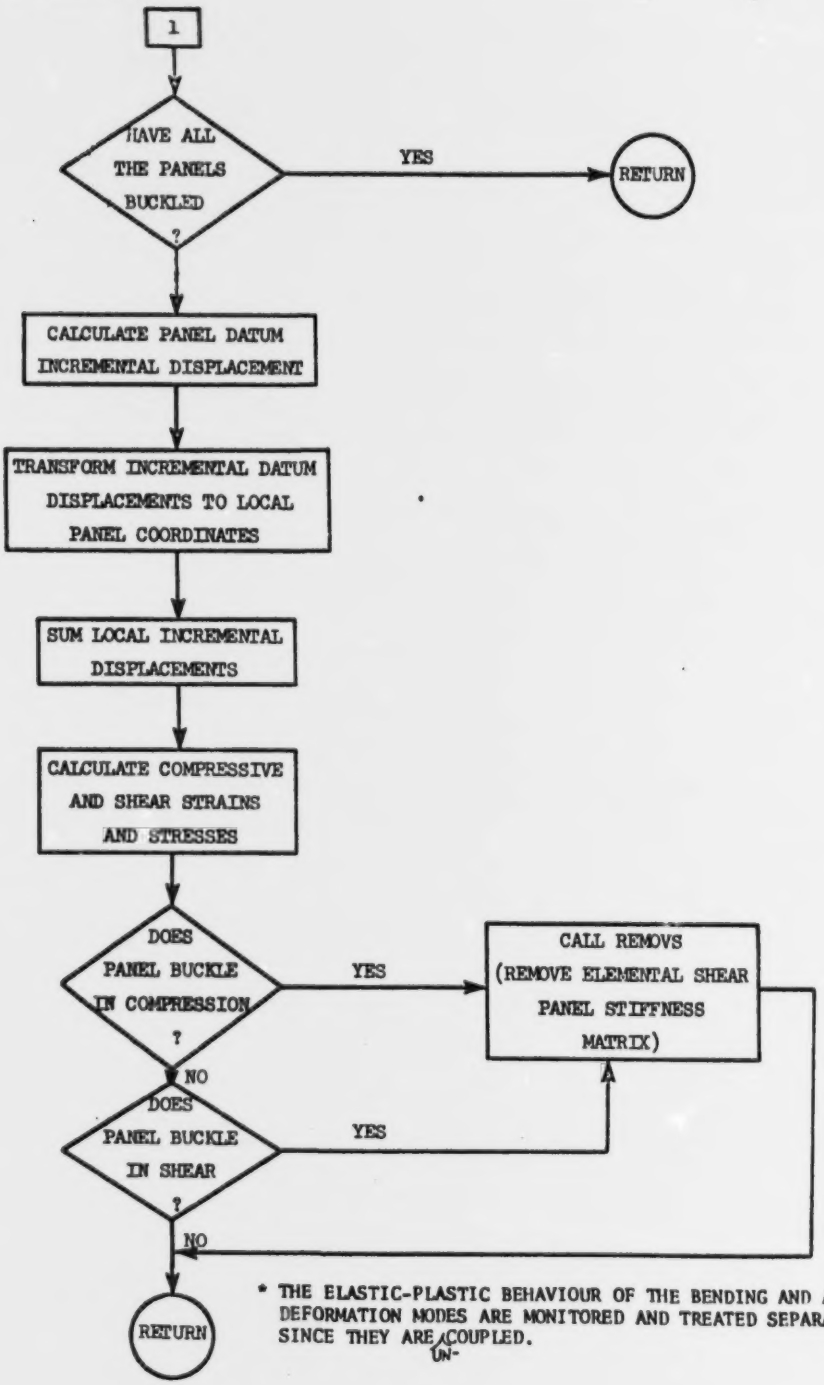

* THE ELASTIC-PLASTIC BEHAVIOUR OF THE BENDING AND AXIAL DEFORMATION MODES ARE MONITORED AND TREATED SEPARATELY, SINCE THEY ARE UNCOUPLED.

GENERAL FLOW CHART OF SUBPROGRAM "REMOVS"

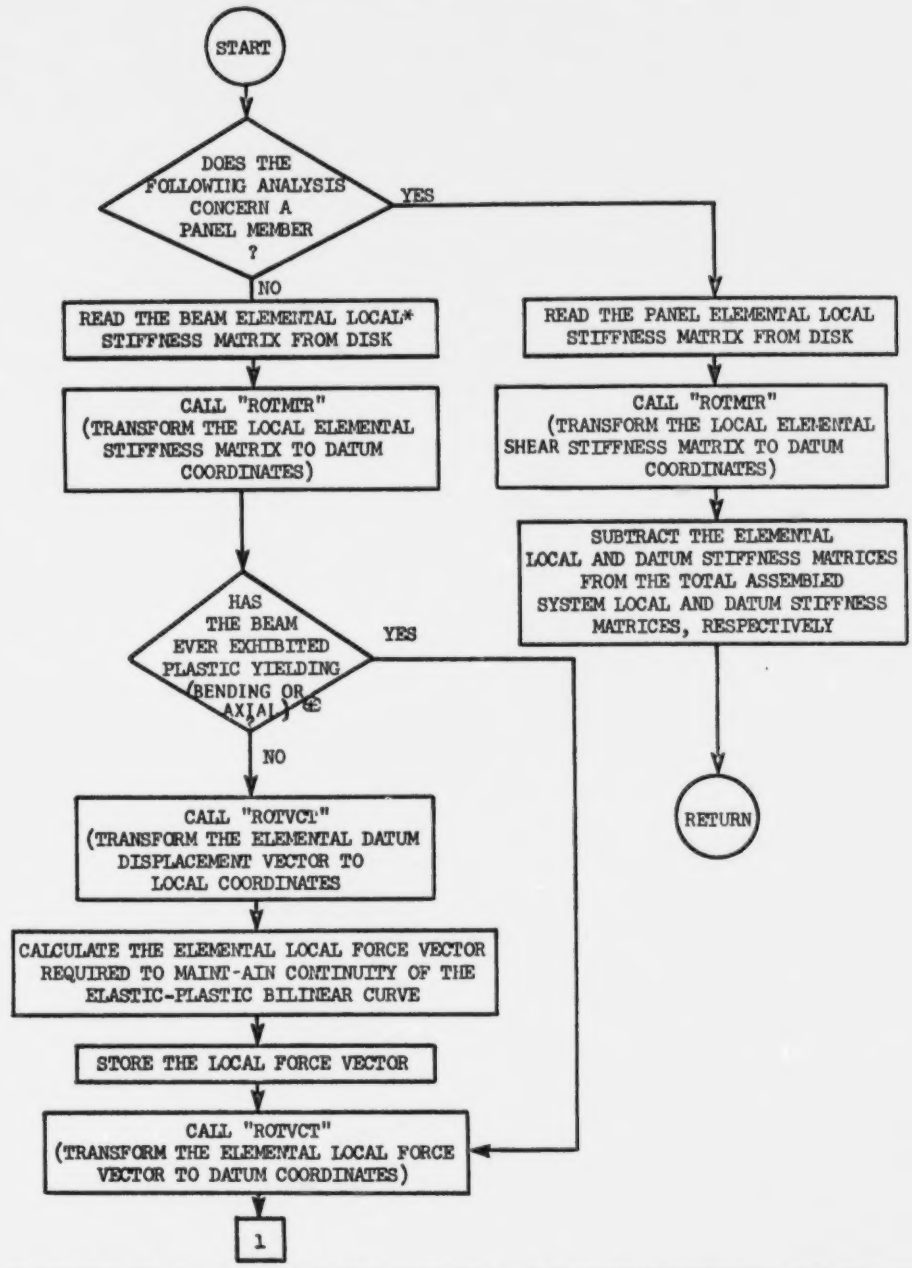
START
DOES THE FOLLOWING ANALYSIS CONCERN A PANEL MEMBER ?
YES
NO
READ THE BEAM ELEMENTAL LOCAL* STIFFNESS MATRIX FROM DISK
CALL "ROTMTR" (TRANSFORM THE LOCAL ELEMENTAL STIFFNESS MATRIX TO DATUM COORDINATES)
READ THE PANEL ELEMENTAL LOCAL STIFFNESS MATRIX FROM DISK
CALL "ROTMTR" (TRANSFORM THE LOCAL ELEMENTAL SHEAR STIFFNESS MATRIX TO DATUM COORDINATES)
SUBTRACT THE ELEMENTAL LOCAL AND DATUM STIFFNESS MATRICES FROM THE TOTAL ASSEMBLED SYSTEM LOCAL AND DATUM STIFFNESS MATRICES, RESPECTIVELY
HAS THE BEAM EVER EXHIBITED PLASTIC YIELDING (BENDING OR AXIAL) @
YES
NO
RETURN
CALL "ROTVCT" (TRANSFORM THE ELEMENTAL DATUM DISPLACEMENT VECTOR TO LOCAL COORDINATES
CALCULATE THE ELEMENTAL LOCAL FORCE VECTOR REQUIRED TO MAINT-AIN CONTINUITY OF THE ELASTIC-PLASTIC BILINEAR CURVE
STORE THE LOCAL FORCE VECTOR
CALL "ROTVCT" (TRANSFORM THE ELEMENTAL LOCAL FORCE VECTOR TO DATUM COORDINATES)
1

*NOTE: IN THIS SUBROUTINE THE WORD "LOCAL" REFERS TO THE INITIAL GLOBAL FUSELAGE COORDINATES (I.E., PITCH ANGLE = 0 DEGREES).

@NOTE: THE ELASTIC-PLASTIC BEHAVIOUR OF THE BENDING AND AXIAL DEFORMATION MODES ARE TREATED SEPARATELY.

---- SUBPROGRAM "REMOVS" CONTD.

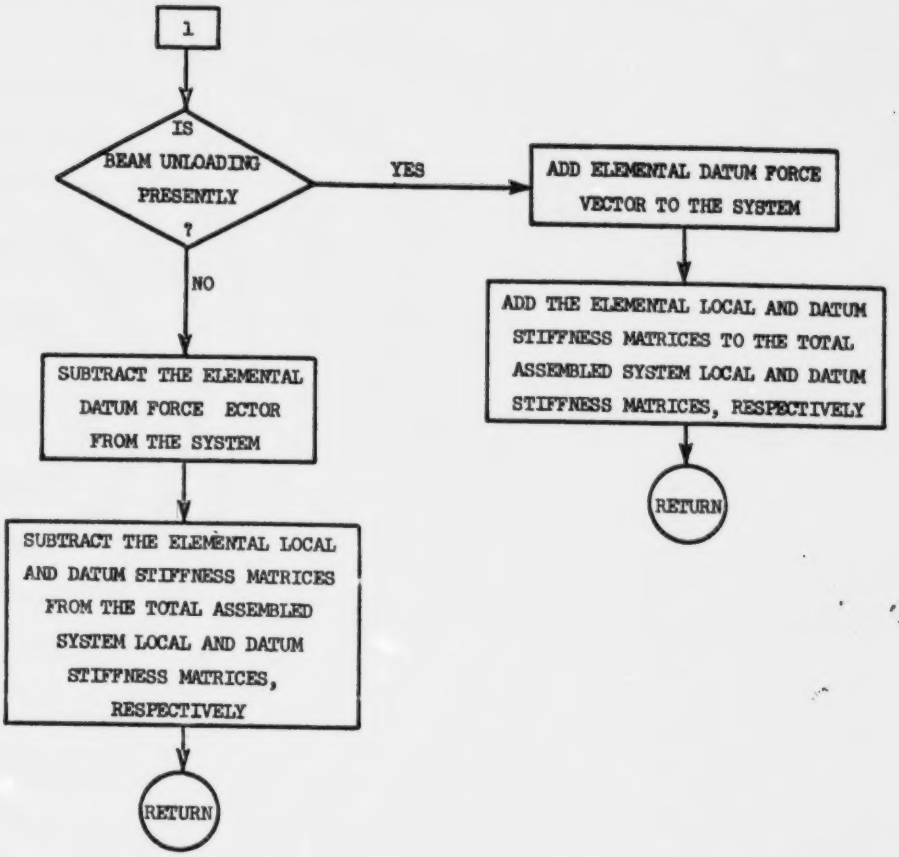
1
IS BEAM UNLOADING PRESENTLY ?
YES
NO
ADD ELEMENTAL DATUM FORCE VECTOR TO THE SYSTEM
ADD THE ELEMENTAL LOCAL AND DATUM STIFFNESS MATRICES TO THE TOTAL ASSEMBLED SYSTEM LOCAL AND DATUM STIFFNESS MATRICES, RESPECTIVELY
RETURN
SUBTRACT THE ELEMENTAL DATUM FORCE ECTOR FROM THE SYSTEM
SUBTRACT THE ELEMENTAL LOCAL AND DATUM STIFFNESS MATRICES FROM THE TOTAL ASSEMBLED SYSTEM LOCAL AND DATUM STIFFNESS MATRICES, RESPECTIVELY
RETURN

GENERAL FLOW CHART OF PROGRAM

"STIFF"

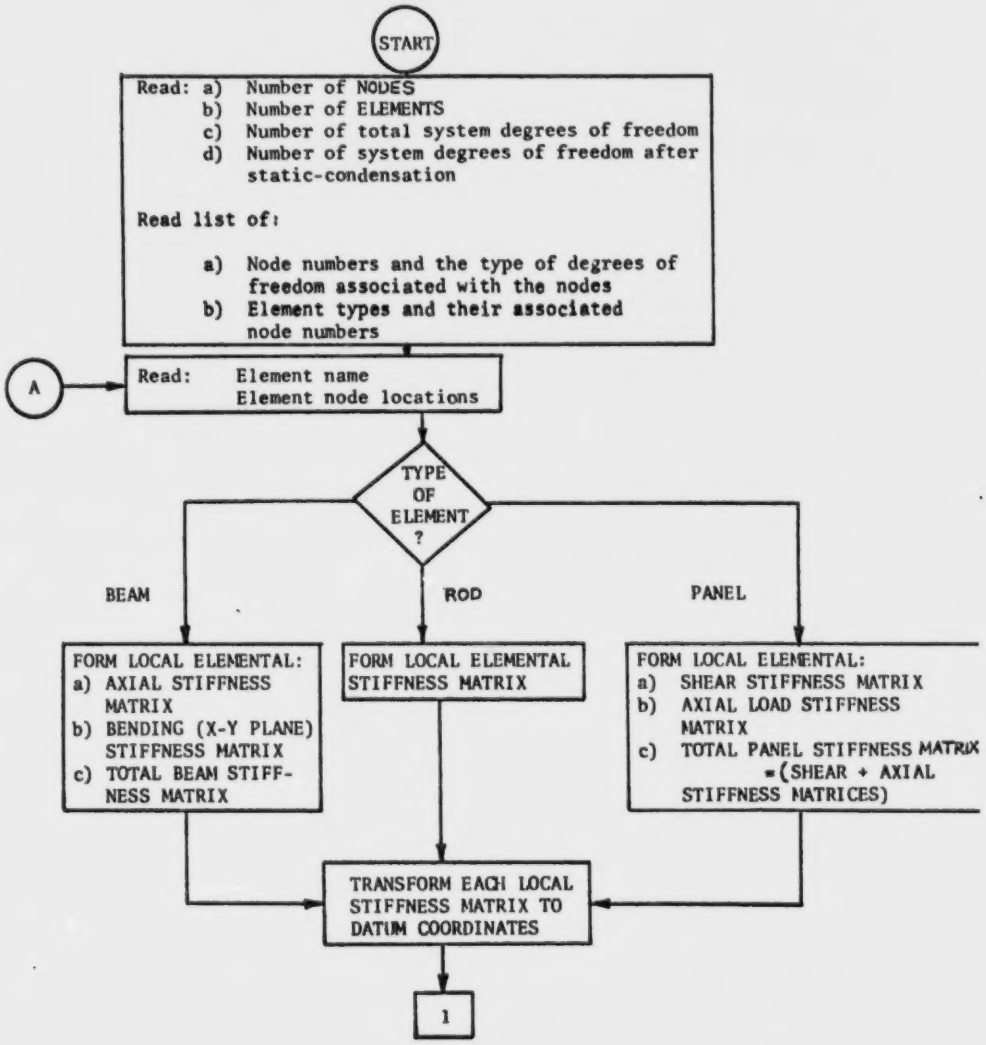
START
Read: a) Number of NODES
b) Number of ELEMENTS
c) Number of total system degrees of freedom
d) Number of system degrees of freedom after static-condensation
Read list of:
a) Node numbers and the type of degrees of freedom associated with the nodes
b) Element types and their associated node numbers
A
Read: Element name
Element node locations
TYPE OF ELEMENT ?
BEAM
ROD
PANEL
FORM LOCAL ELEMENTAL:
a) AXIAL STIFFNESS MATRIX
b) BENDING (X-Y PLANE) STIFFNESS MATRIX
c) TOTAL BEAM STIFFNESS MATRIX
FORM LOCAL ELEMENTAL STIFFNESS MATRIX
FORM LOCAL ELEMENTAL:
a) SHEAR STIFFNESS MATRIX
b) AXIAL LOAD STIFFNESS MATRIX
c) TOTAL PANEL STIFFNESS MATRIX =(SHEAR + AXIAL STIFFNESS MATRICES)
TRANSFORM EACH LOCAL STIFFNESS MATRIX TO DATUM COORDINATES
1

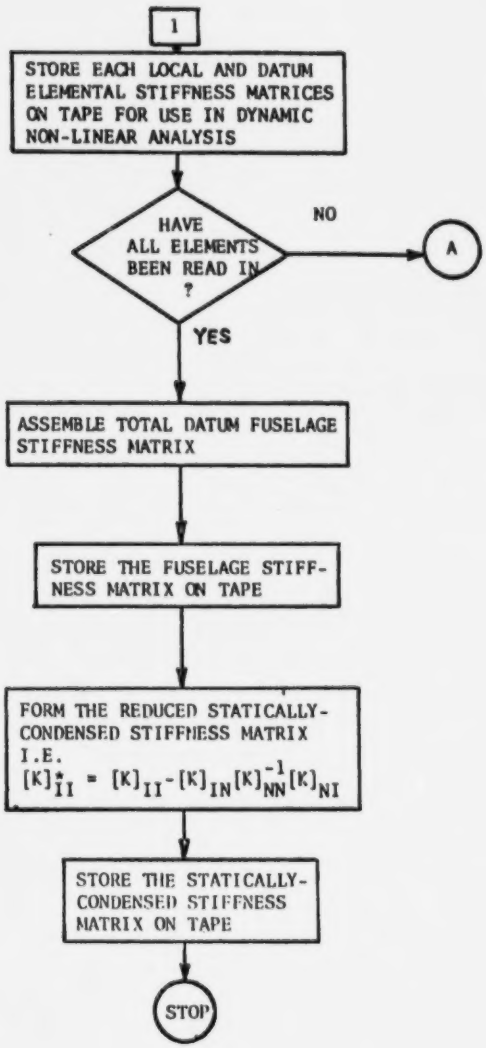
1
STORE EACH LOCAL AND DATUM ELEMENTAL STIFFNESS MATRICES ON TAPE FOR USE IN DYNAMIC NON-LINEAR ANALYSIS
HAVE ALL ELEMENTS BEEN READ IN ?
NO
A
YES
ASSEMBLE TOTAL DATUM FUSELAGE STIFFNESS MATRIX
STORE THE FUSELAGE STIFFNESS MATRIX ON TAPE
FORM THE REDUCED STATICALLY-CONDENSED STIFFNESS MATRIX I.E.
$[K]^{*}_{II} = [K]_{II} - [K]_{IN}[K]^{-1}_{NN}[K]_{NI}$
STORE THE STATICALLY-CONDENSED STIFFNESS MATRIX ON TAPE
STOP

TABLE 2 - SUMMARY OF PEAK MEASURED g-LOADS

(AND TIME OF OCCURRENCE-SEC.) FOR LEVEL IMPACT

CASES

IMPACT CASE	LOCATION OF ACCELEROMETERS (SEE FIG. 12)					
	#1 (27)	#3 (21)	#2 (43)	#4 (46)	#5 (43) HORIZ.	#6 (46)
LEVEL	+ 8.5	+ 8.6	+ 13.5	+ 9.7	+ 4.3	+ 11.1
V_o = 34.7 IN/SEC	(.017)	(.020)	(.003)	(.010)	(.04)	(.0007)
WING LOAD = 537 LBS.	- 1.5	- 2.0	- 40.0	- 4.6	- 3.1	- 14.2
	(.044)	(.048)	(.005)	(.018)	(.045)	(.01)
2ND IMPACT	+ 5.5	+ 4.3	+ 4.9	+ 7.0	+ 1.5	+ 6.2
	(.202)	(.207)	(.237)	(.191)	(.175)	(.191)
		- 0.6	- 15.4	- 5.7	- 2.2	- 6.2
		(.18)	(.224)	(.192)	(.178)	(.192)
LEVEL	+ 11/-1.3	+ 10.9/-		+ 9.2/-14.5		+ 20.0/-10.5
V_o = 52.5 IN/SEC	(.017, .043)	(.019)		(.019, .016)		(.016, .019)
WING LOAD = 537 LBS.						
2ND IMPACT	+ 8.5/-0.5	+ 7.4/-1.4		+ 5.5/-3.1		+ 4.9/-3.4
	(.277, .291)	(.273, .293)		(.293, .294)		(.293, .294)

* VERTICAL UNLESS OTHERWISE NOTED

TABLE 3 - SUMMARY OF MAIN FRAME INNER SURFACE MAXIMUM DYNAMIC STRAINS FOR LEVEL IMPACT TESTS (TIMES OF OCCURRENCE-SEC.)

IMPACT CASE	LOCATION OF STRAIN GAUGES (SEE FIG. 11) (STRAINS x 10^{-6})			
	SR6,1 (INSIDE GAUGE) $\theta = 0^o$	SR9,1 $\theta = 0$	SR9,14 $\theta = 52.3^o$	SR9,13 $\theta = 72.3^o$
LEVEL V_o = 44.7 IN/SEC WING LOAD = 537 LBS.	5500 (.025)	2100 (.023)	-4900 (.021)	-3900 (.021)
LEVEL V_o = 52.5 IN/SEC WING LOAD = 537 LBS.	7440 (.023)	4300 (.023)	-7150 (.022)	-5450 (.022)

TABLE 4 - PREDICTED PEAK VERTICAL g-LOADS (TIMES OF OCCURRENCE-SEC.) USING LMFE ANALYSIS - LEVEL IMPACT CASES

IMPACT CASE	MASS NODE NO. (SEE FIG. 2) C.G.	12	27	35	43	44
LEVEL V_o = 34.4 IN/SEC WING LOAD = 537 LBS.	+ 4 (.03) 2ND IMPACT @ 0.15 SEC.	+ 6/-2 .01 & .16	+ 6/-1.4 .01 & .17	+ 6/-3 .01 & .16	+ 8/-3 0 & .16	+ 6/-2 04 & .14
LEVEL V_o = 52.5 IN/SEC WING LOAD = 537 LBS.	+ 5 (.030)	+ 8/-4 .010 & .130	+ 7/-3 .015 & .135	+ 8/-4 .010 & .130	+ 9/-5 .06 & .130	+ 9/-3 .035 & .110

TABLE 5 - PREDICTIONS OF MAXIMUM DYNAMIC STRAINS (TIMES OF OCCURRENCE-SEC.) FOR SELECTED ELEMENTS USING LMFE ANALYSIS - LEVEL IMPACT CASES

IMPACT CASE	STRUCTURAL ELEMENT NO. (SEE FIG. 2) (STRAINS x 10^{-6})					
	BEAMS* 19 & 31	BEAMS 20 & 32	BEAMS 21 & 33	BEAMS 22 & 34	ROD** 151	ROD 152
LEVEL	+ 2739	+ 1300	+ 1389	+ 3292	+ 401	-160
V_o = 34.4 IN/SEC	- 3147 (.0075)	-1242 (.015)	- 1288 (.015)	- 3665 (030)	(.010)	(.010)
WING LOAD = 537 LBS.						

* MAX. OUTER SURFACE BENDING (INCL. MEMBRANE)

** AXIAL STRAIN

	19 & 31	20 & 32	21 & 33	22 & 34	ROD 152
LEVEL	+ 1900	+ 700	+ 1100	+ 2100	- 224
V_o = 52.5 IN/SEC	- 2359	- 716	- 1382	- 2233	(005 TO .008)
WING LOAD	(.010)	(015)	(.0075)	(015)	
= 537 LBS.					

TABLE 6 - PREDICTED PEAK VERTICAL g-LOADS (TIMES OF OCCURRENCE-SEC.)

USING CFE ANALYSIS - LEVEL IMPACT

IMPACT CASE	NODE NUMBER (SEE FIGURE 3) 211	215	214	61*	136*	137*
LEVEL	8.6	8.6	11.0	11.0	11.0	8.6
V_o = 34.7 IN/SEC.	(0.019)	(0.019)	(0.021)	(.019)	(.019)	(.019)
WING LOAD			- 0.8	- 8.2	- 8.2	- 5.4
= 537 LBS.			(.007)	(.01)	(.01)	(.01)
LEVEL	19.4	19.4	20.4	14.4	14.0	14.2
V_o = 525 IN/SEC.	(.02)	(.02)	(.02)	(.018)	(.016)	(.018)
WING LOAD	-.8	-.8		-7.2	7.2	-5.6
= 537 LBS.	(.001)	(.001)		(.008)	(.006)	(.01)

* FILTERED USING A FIFTH-ORDER CHEBYSHEV LOW-PASS FILTER WITH A PASSBAND OF 62.5 HZ AND STOPBAND EDGE OF 125 HZ

TABLE 7 - PREDICTIONS OF MAXIMUM DYNANIC STRAINS (TIMES OF OCCURRENCE-SEC.)

FOR SELECTED NODAL POINTS USING CFE ANALYSIS -

LEVEL IMPACT CASES

IMPACT CASE	STRUCTURAL NODE NUMBER (SEE FIGURE 3) STRAIN GAUGE POSITION (SEE FIGURE 11) (STRAINS x 1.0^{-6})		
	SR6,1 (INSIDE GAUGE) 78 (BENDING)	SR9,1 123 (AXIAL STRAIN)	SR9,14 125 (BENDING)
Level V_o = 44.7 in/sec Wing Load = 537 lbs.	6000 (.028)	500 (.028)	-100 (.019)
Level V_o = 52.5 in/sec Wing Load = 537 lbs.	10000 (.021)	800 (.021)	-15 (.020)

TABLE 8. SUMMARY OF PEAK MEASUREMENT G-LOADS (AND TIME OF OCCURRENCE-SEC) FOR OBLIQUE IMPACT CASES

IMPACT CASE	LOCATION OF ACCELEROMETERS (SEE FIGURE 13) #1	#2	#3	#4	#5*FORWARD	#6
OBLIQUE V_o = 26.0 IN/SEC FIRST IMPACT ANGLE = 3.1° WING LOAD= 537 LBS	4.1 (.070) -2.1 (.130)	14.1 (.115) -9.8 (.088) -2.7 (.115)	5.8 (.082) -6.5 (.066)	13.8 (.072) -6.5 (.066)	5.5 (.091) -6.8 (.063)	18.2 (.089) -5.6 (.064)
SECOND IMPACT	2.2 (.407) -1.6 (.373)	25.2 (.371) -5.8 (.378)	5.8 (.39) -.86(.43)	12.3 (.408) -5.8 (.375)	4.3 (.404) -3.7 (.402)	14.2 (.406) -4.5 (.414)
OBLIQUE FIRST IMPACT V_o = 34.7 IN/SEC ANGLE = 2.0° WING LOAD= 537 LBS.	2.8 (.037) -0.70 (.107) -2.5 (.165)	23.5 (.016) 23.3 (.074) -27.8 (.034)	7.9 (.049) -2.0 (.075)	8.0 (.079) 13.8 (.159) -17.8 (.037) -27.8 (.158)	5.2 (.036) -5.1 (.034)	20.6 (.028) -5.5 (.079)
SECOND IMPACT	1.1 (.345) -2.1 (.32)	16.3 (.323) -3.2 (.306)	5.1 (.322) -.9 (.38)	4.6 (.31) -11.4 (.304)	1.5 (.316) -1.5 (.319)	12.6 (.356) -4.6 (.351)

* ALL VERTICAL ACCELERATIONS UNLESS NOTED

TABLE 9. SUMMARY OF MAIN FRAME INNER SURFACE AND STRINGER MAXIMUM STRAINS FOR OBLIQUE IMPACT CASES

(TIME OF OCCURRENCE-SEC)*

LOCATION OF STRAIN GAUGES (SEE FIGURE 11) (STRAINS x 10^{-6})

IMPACT CASE	POSITION	SR6,1	SR6,1 INSIDE GAUGE	SR9,1	SR9,13	SR9,14	SR13,4
OBLIQUE V_o = 26.0 IN/SEC ANGLE = 3.1°	FIRST IMPACT	800. (.091)	8.5×10^3 (.089)	980.0 (.102)	-620. (.124)	-190. (.124)	0. (.135)
		90.0 (.134)	880.0 (.147)	90.0 (.124)	-1.8×10^3 (.097)	-2.30×10^3 (.099)	-80 (.093)
WING LOAD = 537 LBS	SECOND IMPACT	370. (.408)	7.30×10^3 (.395)	1.20×10^3 (.386)	80. (.423)	190. (.423)	0. (.423)
		60. (.383)	1.1×10^3 (.477)	0.0 (.421)	-2.0×10^3 (.386)	-2.8×10^3 (.386)	-130 (.381)
OBLIQUE V_o = 34.7 IN/SEC ANGLE = 2.0°	FIRST IMPACT	920. (.051)	10.4×10^3 (.035)	1.1×10^3 (.054)	150.(.105)	190. (.085)	-80. (.076)
		120. (.075)	-1.7×10^3 (.012)	0.0 (.072)	-2.7×10^3 (.05)	-3.6×10^3 (.05)	-170. (.049)
WING LOAD = 537 LBS.	SECOND IMPACT	490. (.351)	-1.1×10^3 (.34)	1.8×10^3 (.33)	80. (.373)	190. (.455)	0.0 (.348)
		180 (.383)	-1.7×10^3 (.383)	0.0 (.362)	-2.7×10^3 (.33)	-3.9×10^3 (.329)	-80.(.324)

* 0 SEC = FIRST IMPACT START POINT

TABLE 10 - PREDICTED PEAK g-LOADS* (TIMES OF OCCURRENCE -SEC.) FOR OBLIQUE ANGLE IMPACT CASES USING LMFE ANALYSIS

IMPACT CASE	MASS NODE NO. (SEE FIG. 2)							
	C.G.	12	35	27	43	44	45	46
	HORIZ.			HORIZ.				HORIZ.
ANGLE = 1.92°	+ 0.4	+ 4 ∿ + 5	+ 9	+ .6	+ 5	+ 4	+ 8	+ 5
V_o = 34.7 IN/SEC	(.01)	(.07 ∿ .11)	(.005)	(.02)	(.065)	(.09)	(.07)	(.08 ∿ .10)
WING LOAD	- 0.4	- 2	-6	- 1.0	- 3		-2	-4
= 537 LBS.	(.05)	(.145)	(.145)	(.05) + 2 (.115)	(.15)		(.11)	(.08 ∿ .10)
	VERT.			VERT.				VERT.
	+ 4.0			+ 4				+ 10
	(.07)			(.05)				(.005)
				- 2				- 7
				(.14)				(.15)
	PITCH							
	25 rads/ sec^2							
	(.06)							

* VERTICAL UNLESS OTHERWISE NOTED.

TABLE 11 - PREDICTED MAXIMUM DYNAMIC STRAINS (TIMES OF OCCURRENCE-SEC.) FOR OBLIQUE ANGLE IMPACTS FOR SELECTED ELEMENTS USING LMFE ANALYSIS

IMPACT CASE	STRUCTURAL ELEMENT NO. (SEE FIG. 2) (STRAINS x 10^{-6})									
	BEAMS* 19 & 31	BEAMS 20 & 32	BEAMS 21 & 33	BEAMS 22 & 34	ROD** 150	ROD 151	ROD 152	ROD 168	ROD 169	ROD 170
ANGLE ∿ 1.92^{0}	+ 4941	+ 1926	+ 1956	+ 3347	+ 529	+ 55	+ 59	+ 8208	+ 8777	+ 9291
V_0=34.7 IN/SEC	- 5572	- 2361	- 2329	- 3800	(.04 ∿ .03)	(.04)	(.04)	(.035)	(.035)	(035)
WING LOAD = 537 LBS	(.05)	(.04)	(.04)	(.04)	-200	-200	-200	-1500	-1500	-2200
					(.12 ∿ .16)	(.12 ∿ .16)	(.12 ∿ .16)	(.12 ∿ .16)	(.12 ∿ .16)	(.12 ∿ .16)
ANGLE ∿ 3.00^{0}	+ 2300 ∿ +2800	+ 1000 ∿ 900	+ 900	+ 2000	- 2900	-2900	-3100	+ 9500 ∿ 10000	+ 8500	+ 10000
V_0 = 26.0 IN/SEC.	- 3000 ∿ 3300	- 1500 ∿ 2000	- 1500 ∿ 2300	- 2800 ∿ 3500						
WING LOAD = 537 LBS	(.08 ∿ .10)	(.07 ∿ .09)	(.08 ∿ .10)	(.07 ∿ .10)	(.12 ∿ ON)	(.12+)	(.12+)	(.06)	(06)	(06)

* See Page 2

** Stringers, See p. 2

TABLE 12 - SUMMARY OF PEAK MEASUREMENT g-LOADS (AND TIME OF OCCURRENCE-SEC.)

FOR 'FREE FLIGHT' CRASH TEST

METHOD OF DATA ACQUISITION		LOCATION OF ACCELEROMETER (SEE FIG. 14)†					
		#1 HORIZONTAL	#2	#3	#4	#5 HORIZONTAL	#6
F.M.* TAPE RECORDER	FIRST IMPACT	.76 (.056) -.60 (.049)	8.3 (.073) -4.3 (.013)	3.70(.057) -.70 (.017)	8.1 (.077) 5.2 (.026) -9.4 (.057)	2.8 (.017) -5.7 (.023)	2.0 (.029) -6.1 (.006) - 5.7 (.020
	SECOND IMPACT	.6 (.145) -.87 (.152)	32.1 (.123) -17.5 (.127)	7.3 (.146) -1.2 (.207)	-29.2 (.126) 22.0 (.120)	5.1 (.151) -13.7 (.121)	18 (.128) -14.1 (.119)
VISICORDER OSCILLO-GRAPH	FIRST IMPACT	0.4 (.049) -1.3 (.059)	5.7 (.031,.077) -7.1 (.075)	1.1 (.05) -2.2 (.01)	7.08 (.03) -9.2 (.061)	3.4 (.025) -3.1 (.016)	4.0 (.022) -2.8 (.032)
	SECOND IMPACT	.88 (.16) -2.70 (.13)	18.6 (.146) -31.7 (.143)	2.8 (.203) -4.6 (.137)	-	11.4 (.132) -6.5 (.153)	16.0 (.122) -20.9 (.129)

* SAMPLING RATE WAS 8000 PER SECOND FOR 2 CHANNELS

† VERTICAL UNLESS NOTED.

TABLE 13 - SUMMARY OF MAIN FRAME INNER SURFACE MAXIMUM STRAINS

FOR 'FREE FLIGHT' TEST (TIMES OF OCCURRENCE-SEC.)

LOCATIONS OF STRAIN GAUGES (SEE FIGURE 11)

(STRAINS x 10^{-6})

POSITION	SR6,1 (INSIDE GAUGE)	SR6,2	SR6,5	SS6,4	SS9,4
FIRST IMPACT	110 (.067)	300 (.067)	50 (.067)	240 (.047)	100 (.067)
SECOND IMPACT	9400 (.133) (FRACTURE OCCURRED)	2300 (.158) - 300 (.120)	1200 (.159) - 590 (.123)	440 (.126) - 590 (.174)	200 (.110) - 550 (.150)

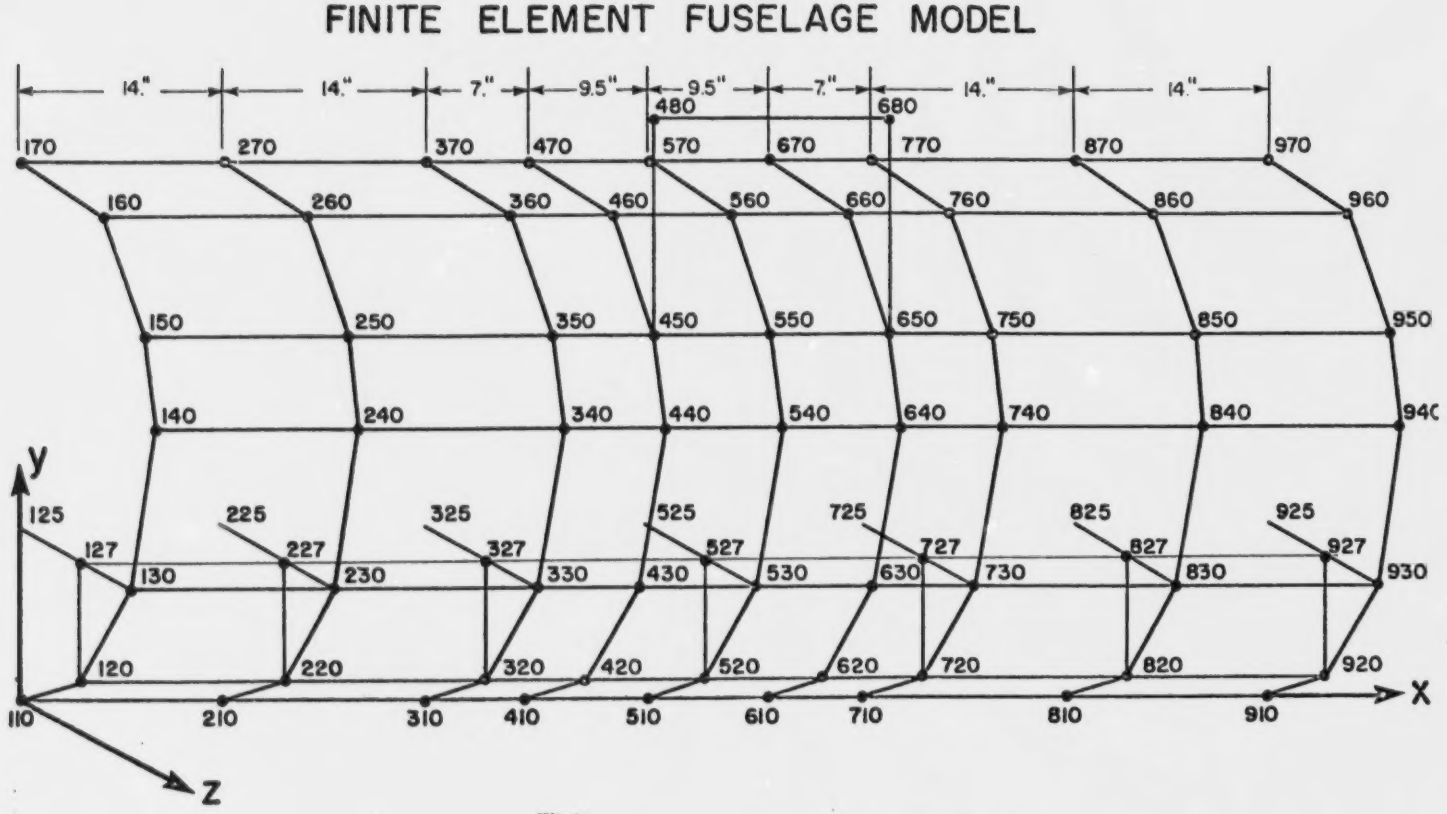

FIG. 1 FINITE ELEMENT FUSELAGE MODEL.

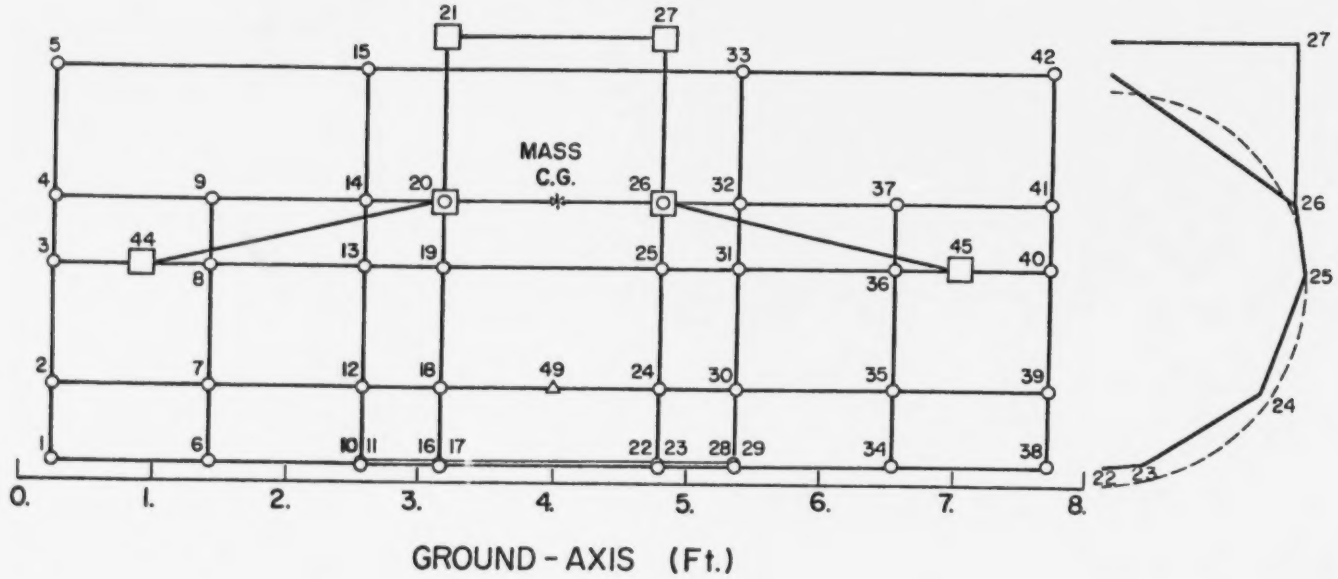

FIG. 2 REFERENCE FIGURE FOR ELEMENT NODE NUMBERS.

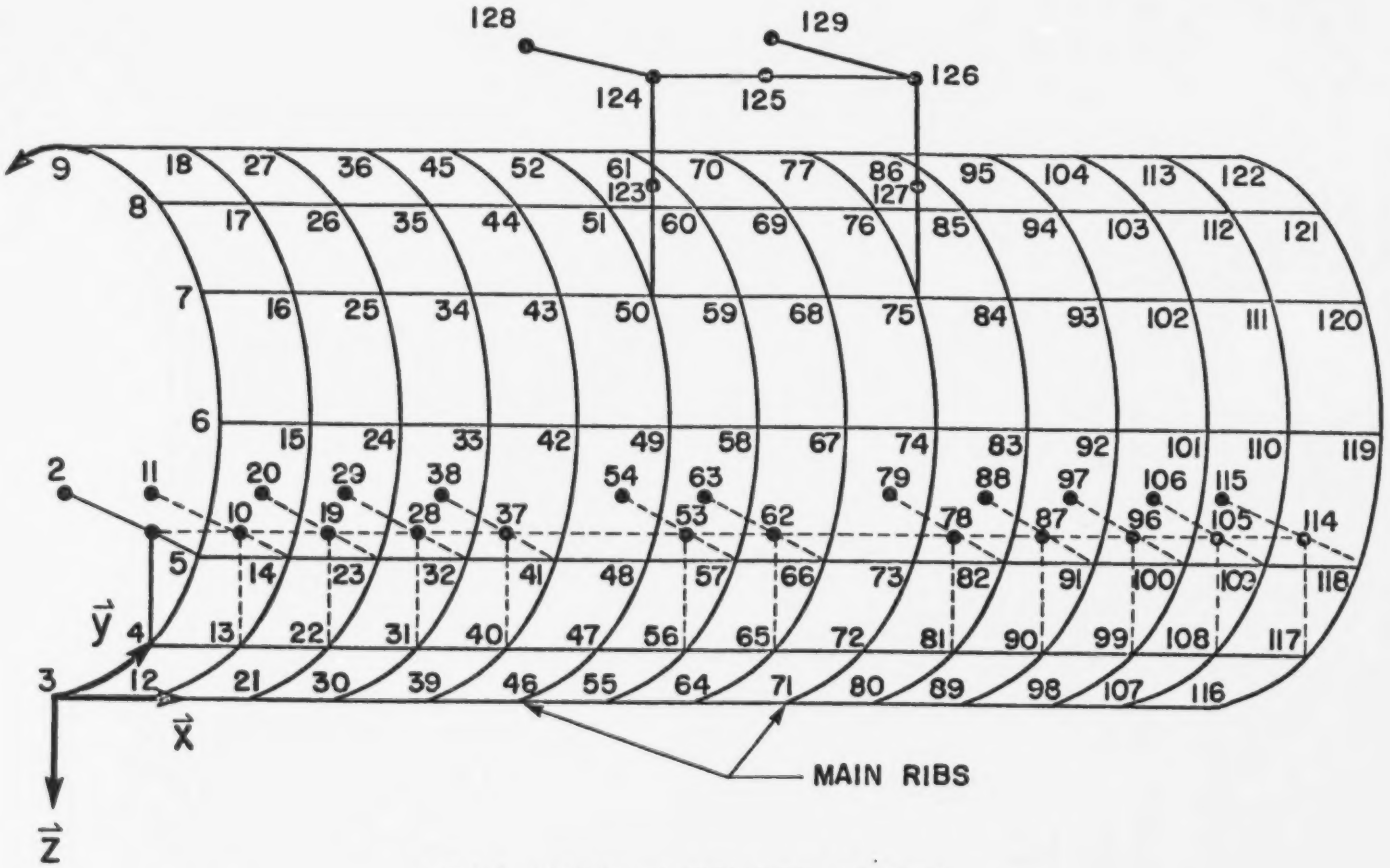

3(a) HALF FUSELAGE NODES

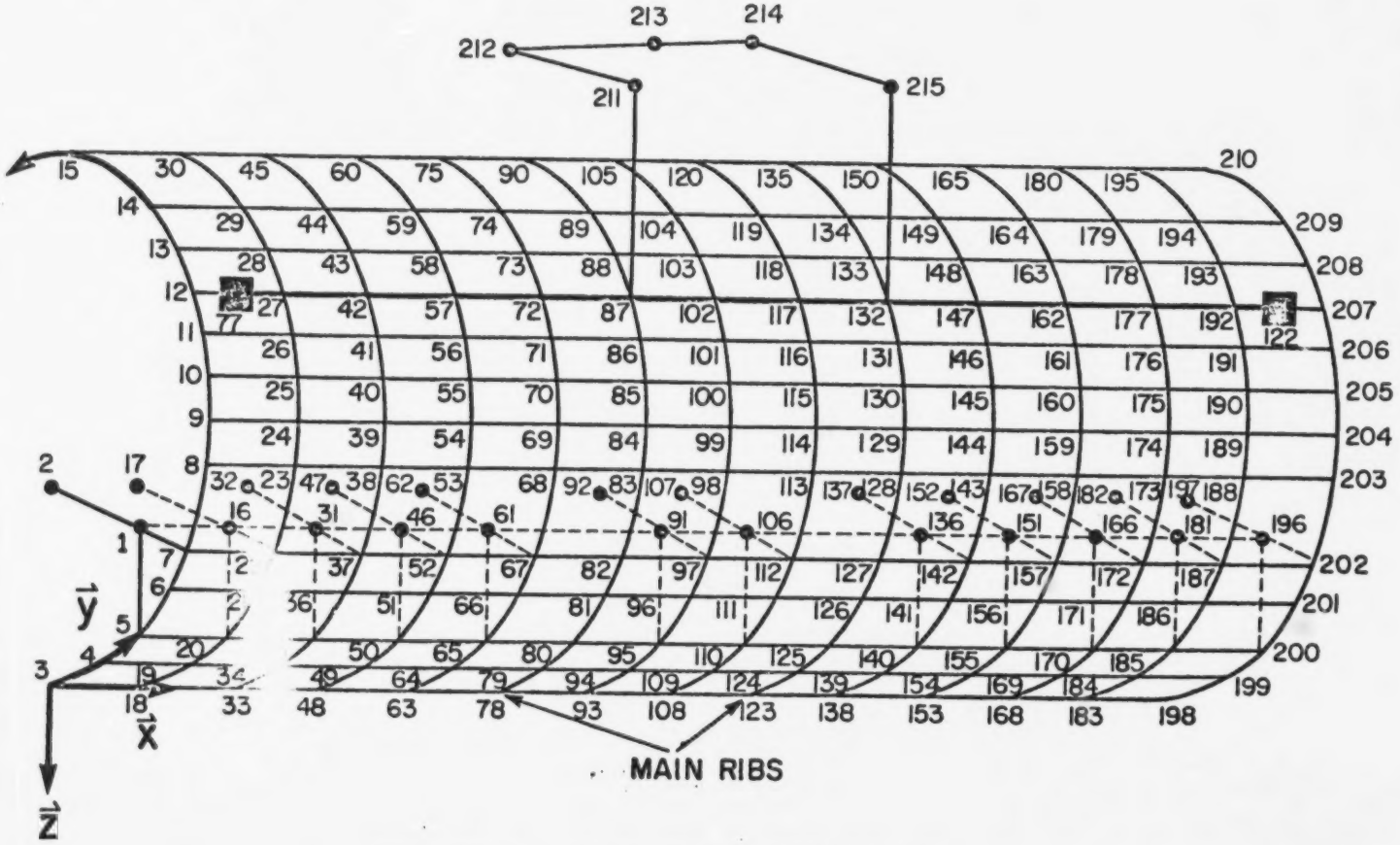

Fig. 3(b) HALF FUSELAGE NODES

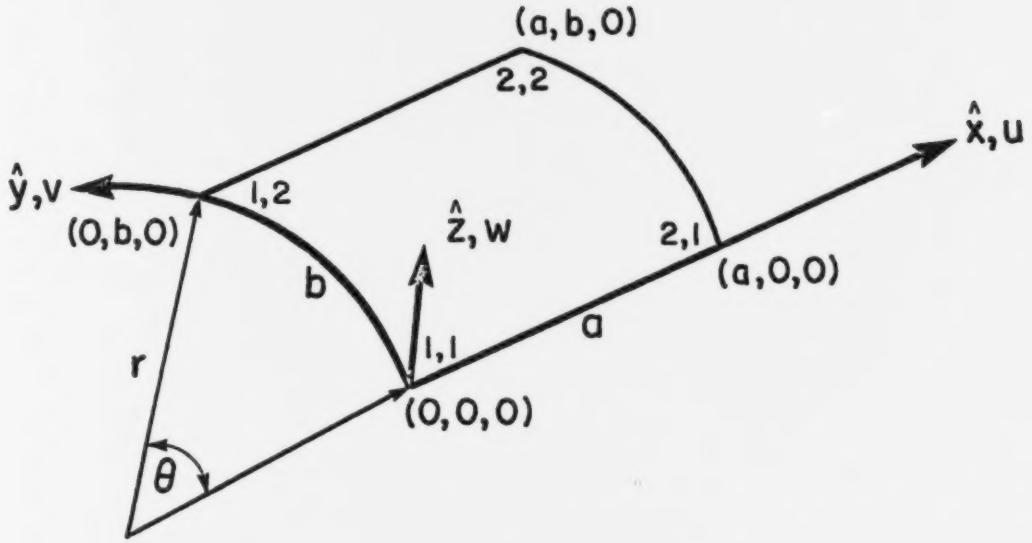

Fig. 4 CURVILINEAR ELEMENT

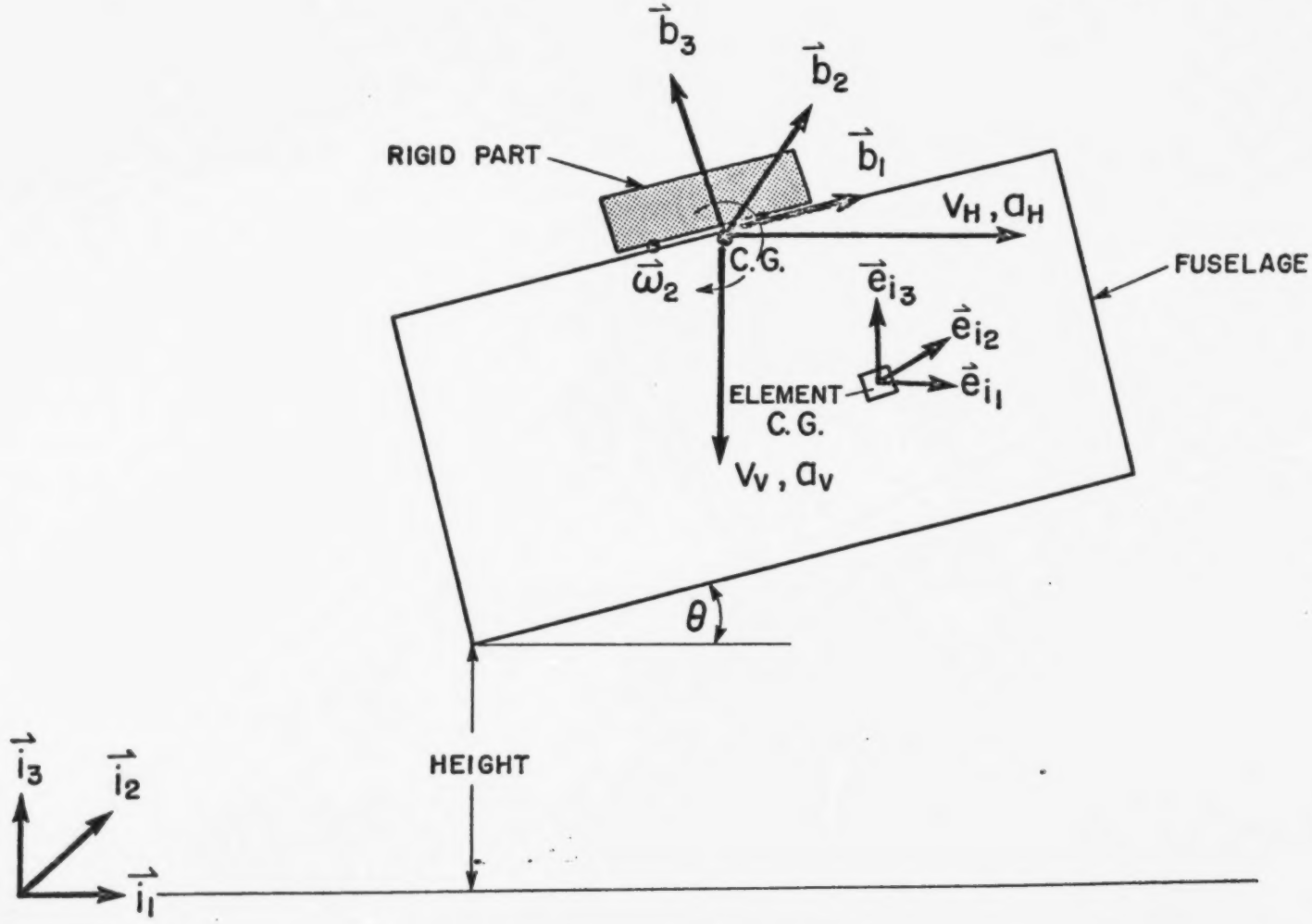

Fig. 5 REFERENCE FRAMES

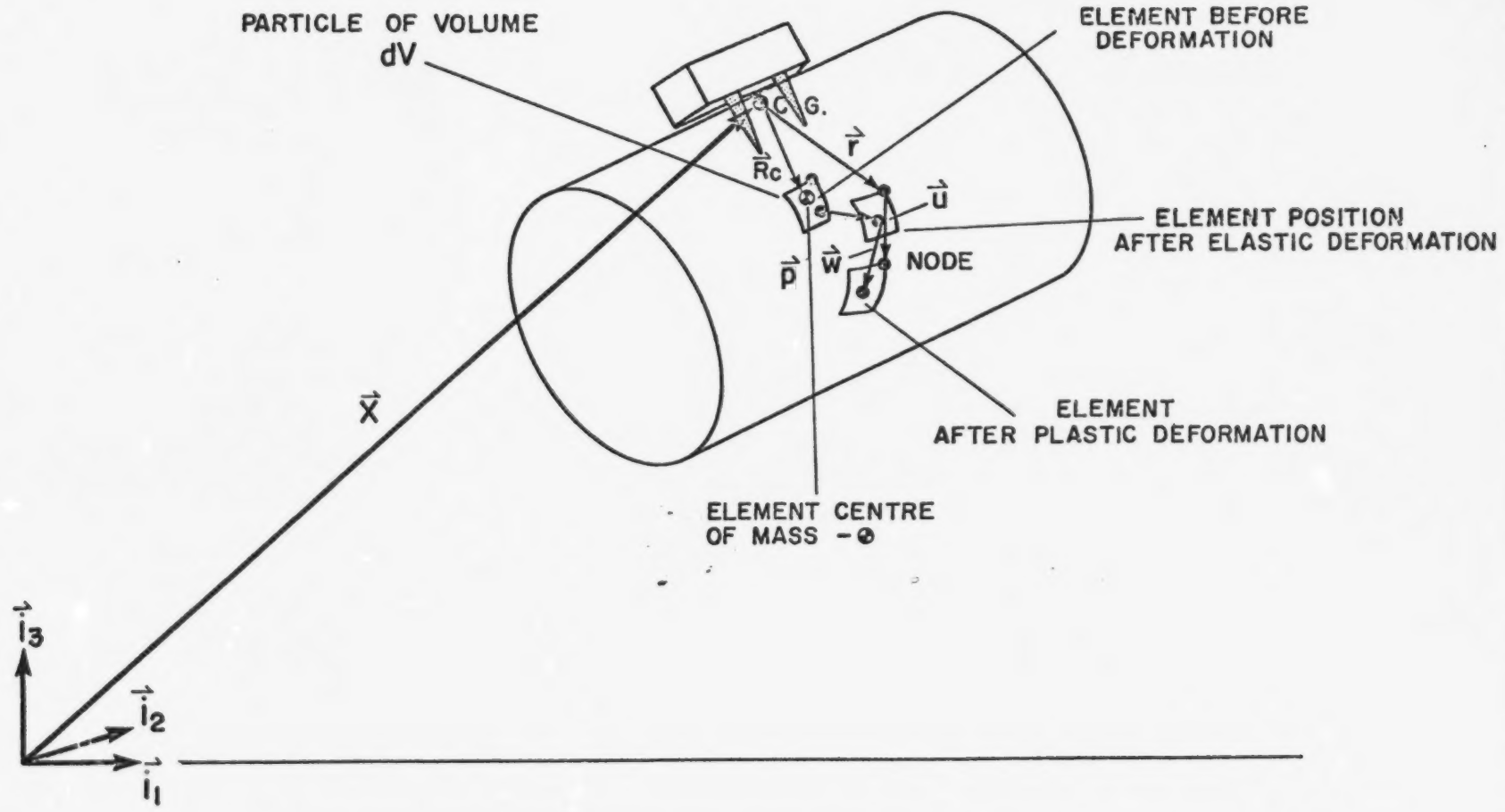

Fig. 6 VECTOR POSITION OF THE PARTICLE dV

DE HAVILLAND AIRCRAFT OF CANADA
ZEE - CS No. 360

T = .032 in
R = .8 in
$\bar{X}$ = 0.299 in
$\bar{Y}$ = 0.193 in

AREA = 0.042 in^2
I_{xx} = 1.76 10^{-3} in^4
I_{yy} = 1.61 10^{-3} in^4

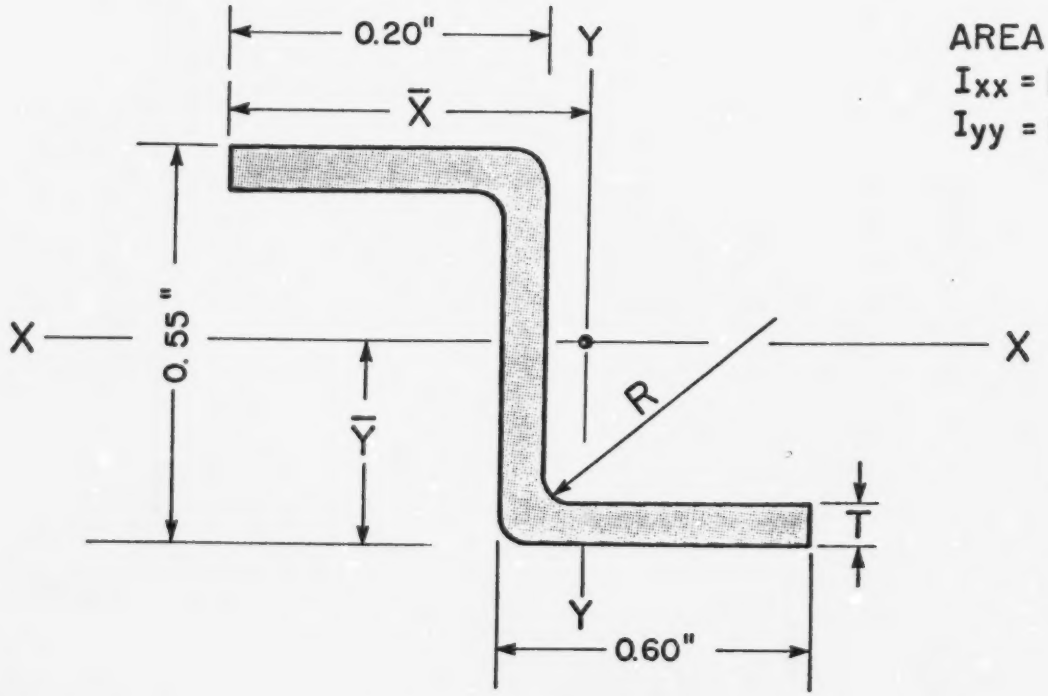

FIG. 7 STRINGER DETAILS.

APPENDIX A

PREDICTED LEVEL IMPACT

RESPONSE BASED ON LMFE

ANALYSIS

CASE 1: V_o = 34.4 in/sec

Wing Load = 537 lbs.

CASE 2: V_o = 52.5 in/sec

Wing Load = 537 lbs.

DISPLACEMENTS, ACCELERATIONS

AND STRAIN

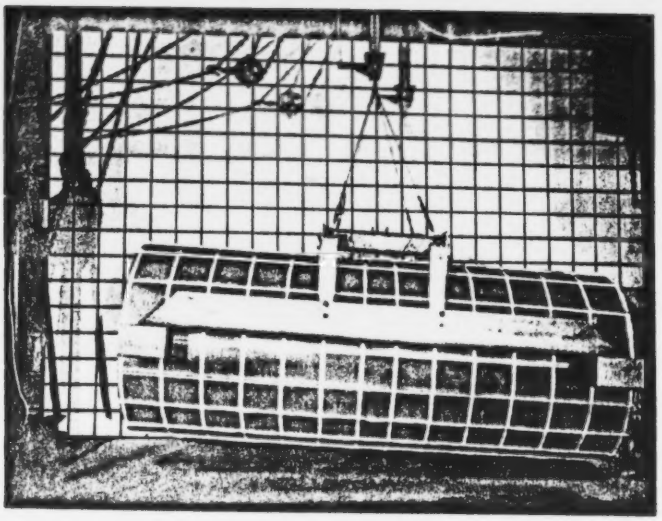

FIG. 8 PRE-CRASH SIDE VIEW OF THE FUSELAGE.

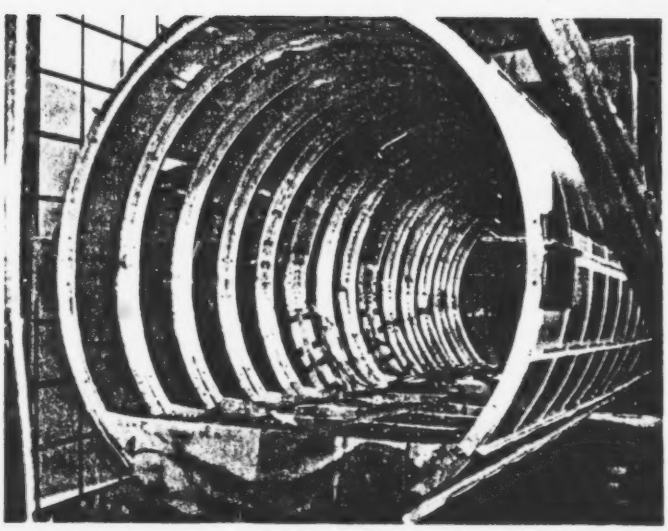

FIG. 9 PRE-CRASH INSIDE VIEW OF THE FUSELAGE.

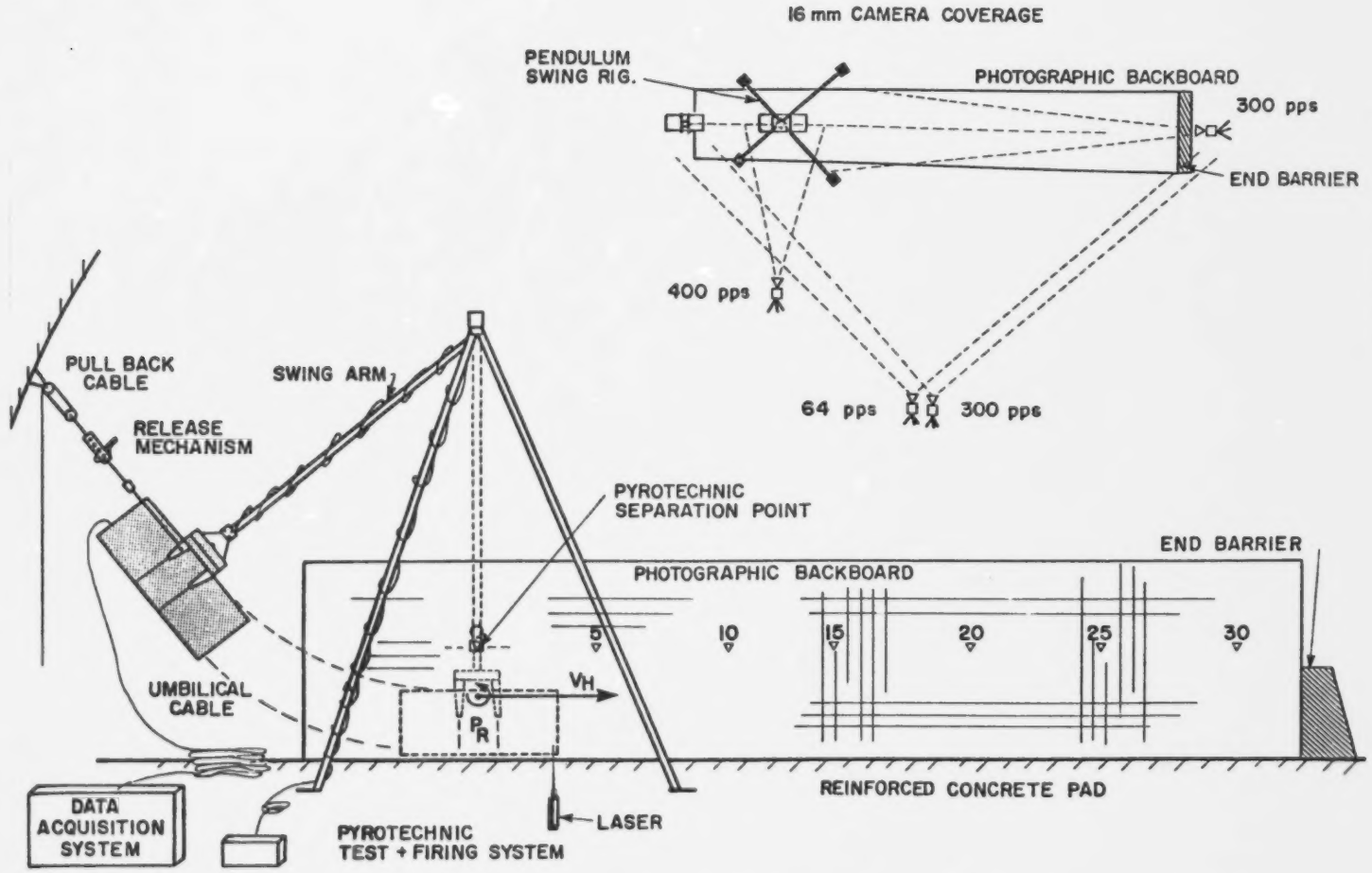

Fig. 10 SCHEMATIC OF PENDULUM GANTRY FOR FREE FLIGHT TESTS

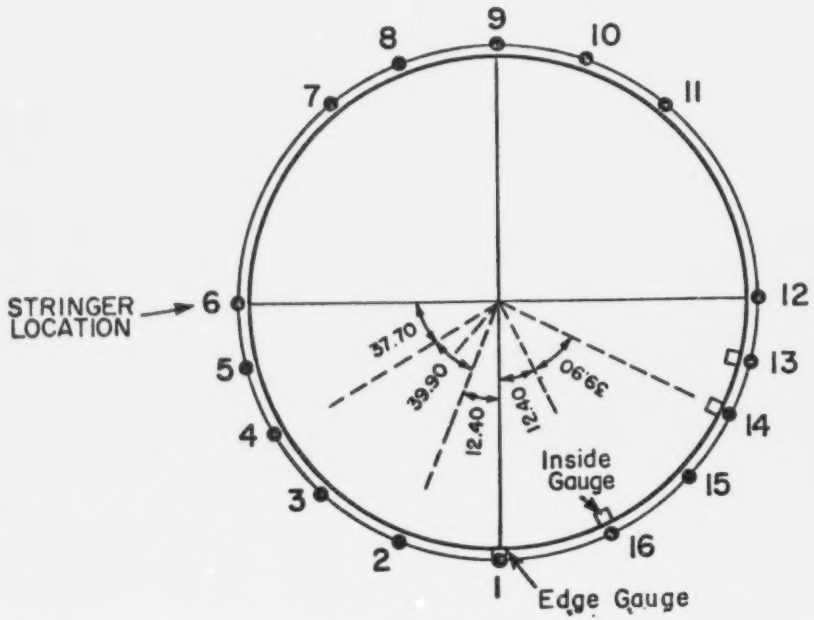

Gauges on Main Frames 6, 9

NOTATION

ssij ≡ Strain Gauge on Stringer at rib i, Stringer j

SRij ≡ Strain Gauge on rib at i, Stringer j

FIG. 11 LOCATION OF STRAIN GAUGES.

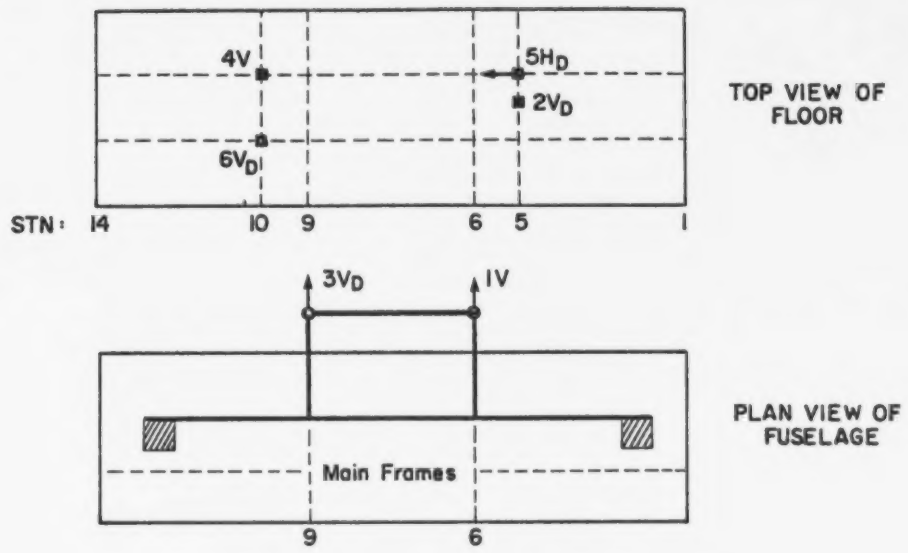

FIG. 12 ACCELEROMETER LOCATIONS FOR LEVEL TESTS

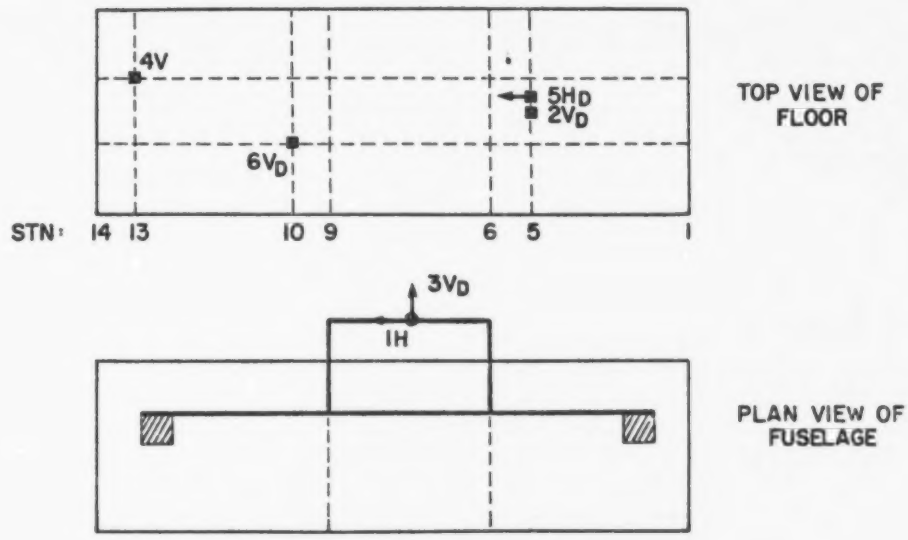

FIG. 13 ACCELEROMETER LOCATIONS FOR OBLIQUE ANGLE TESTS

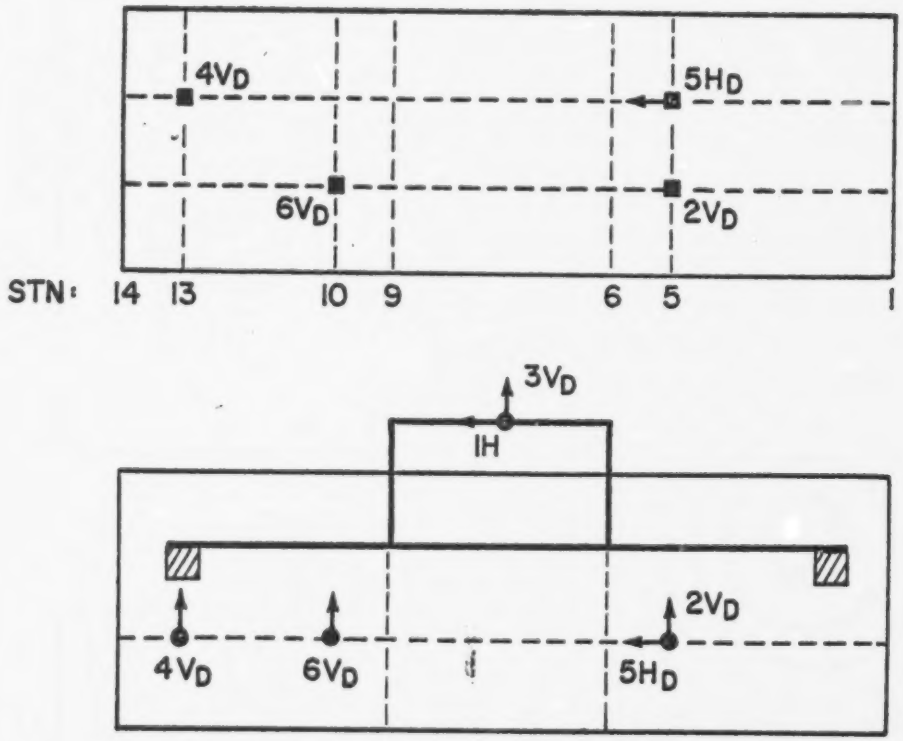

FIG. 14 ACCELEROMETER LOCATIONS FOR FREE-FLIGHT IMPACT TEST.

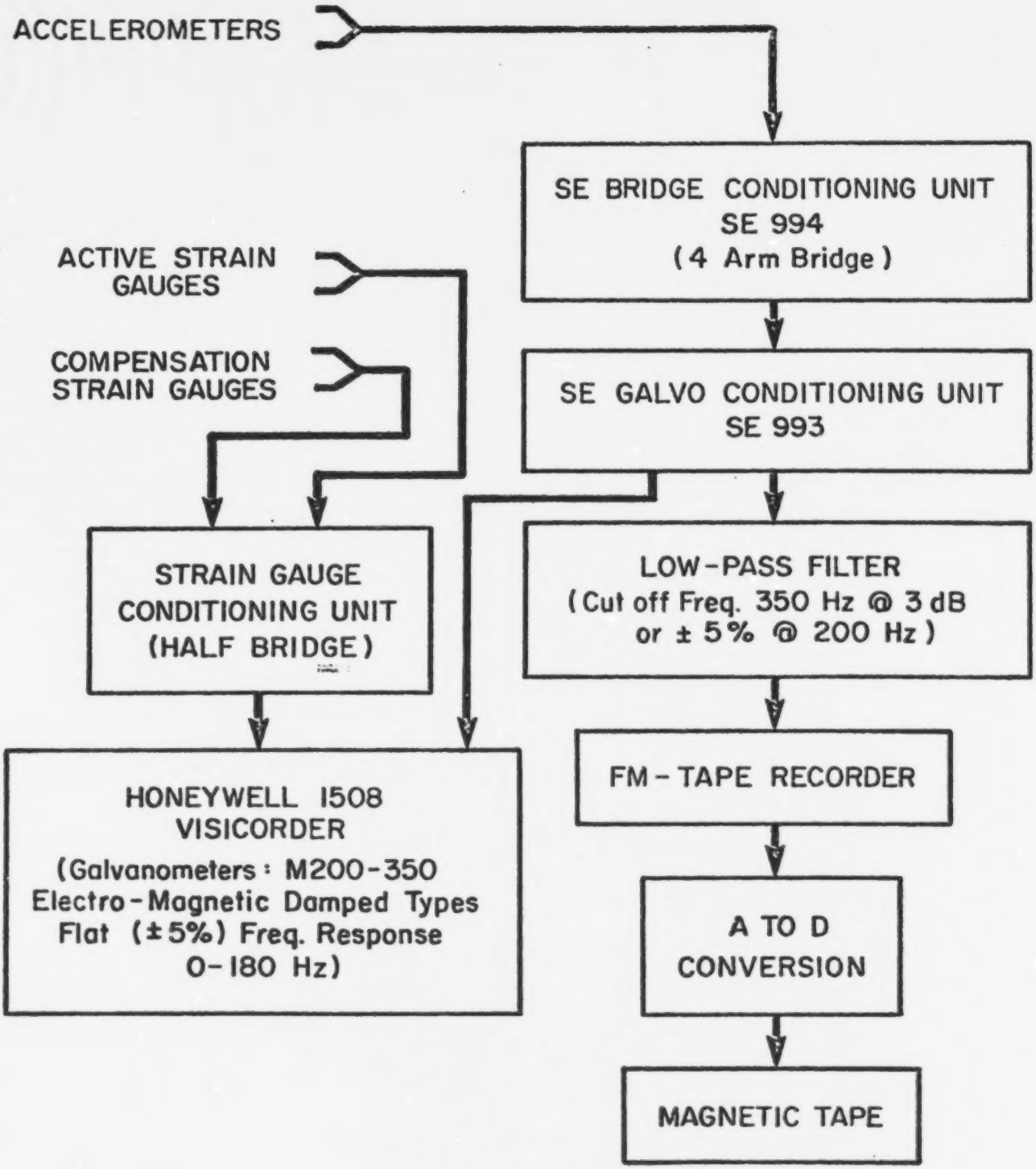

Fig. 15 DATA ACQUISITION SYSTEM

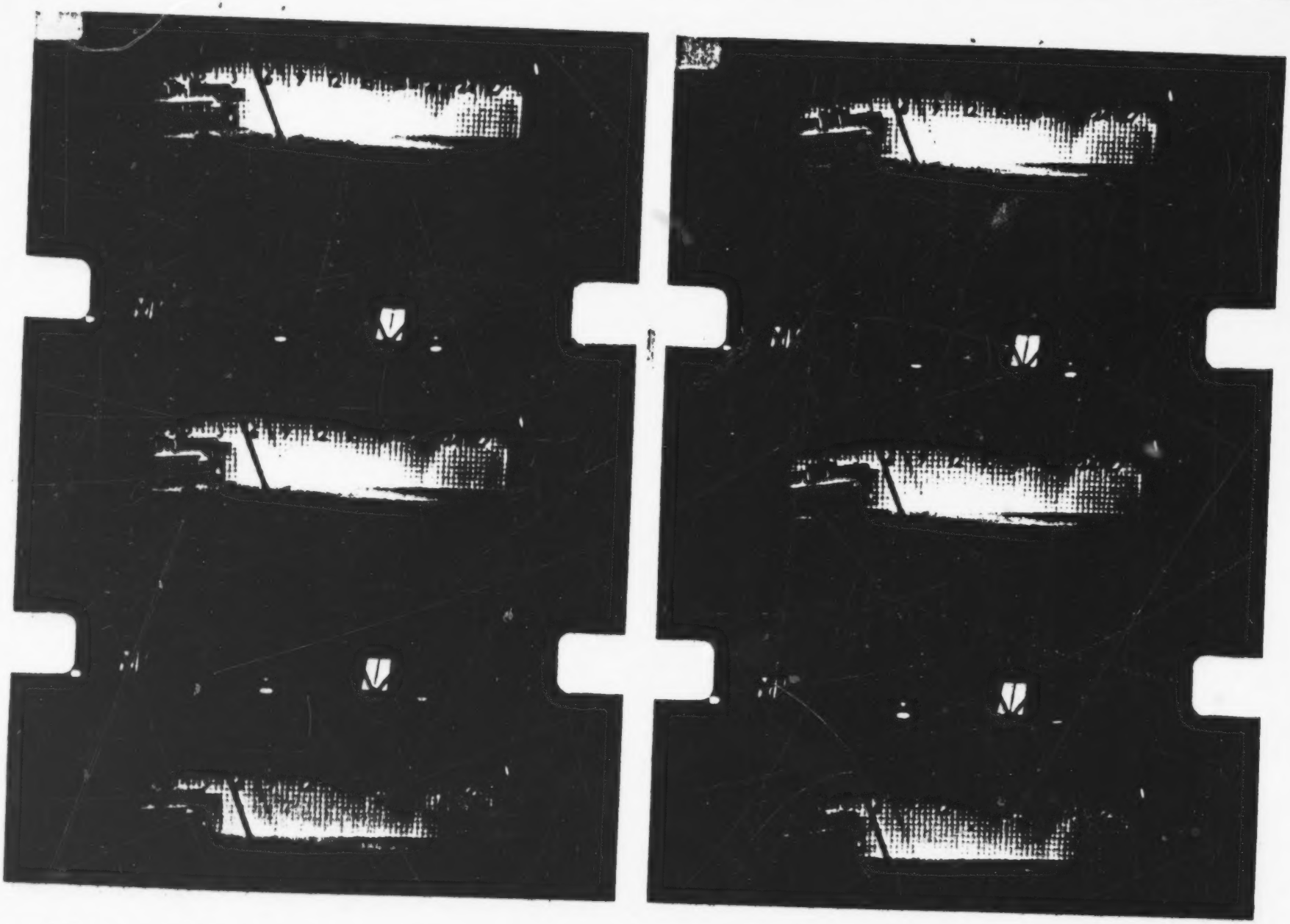

FIG. 16 HIGH-SPEED PHOTOGRAPHS OF 'FREE FLIGHT' TEST (400 PPS).

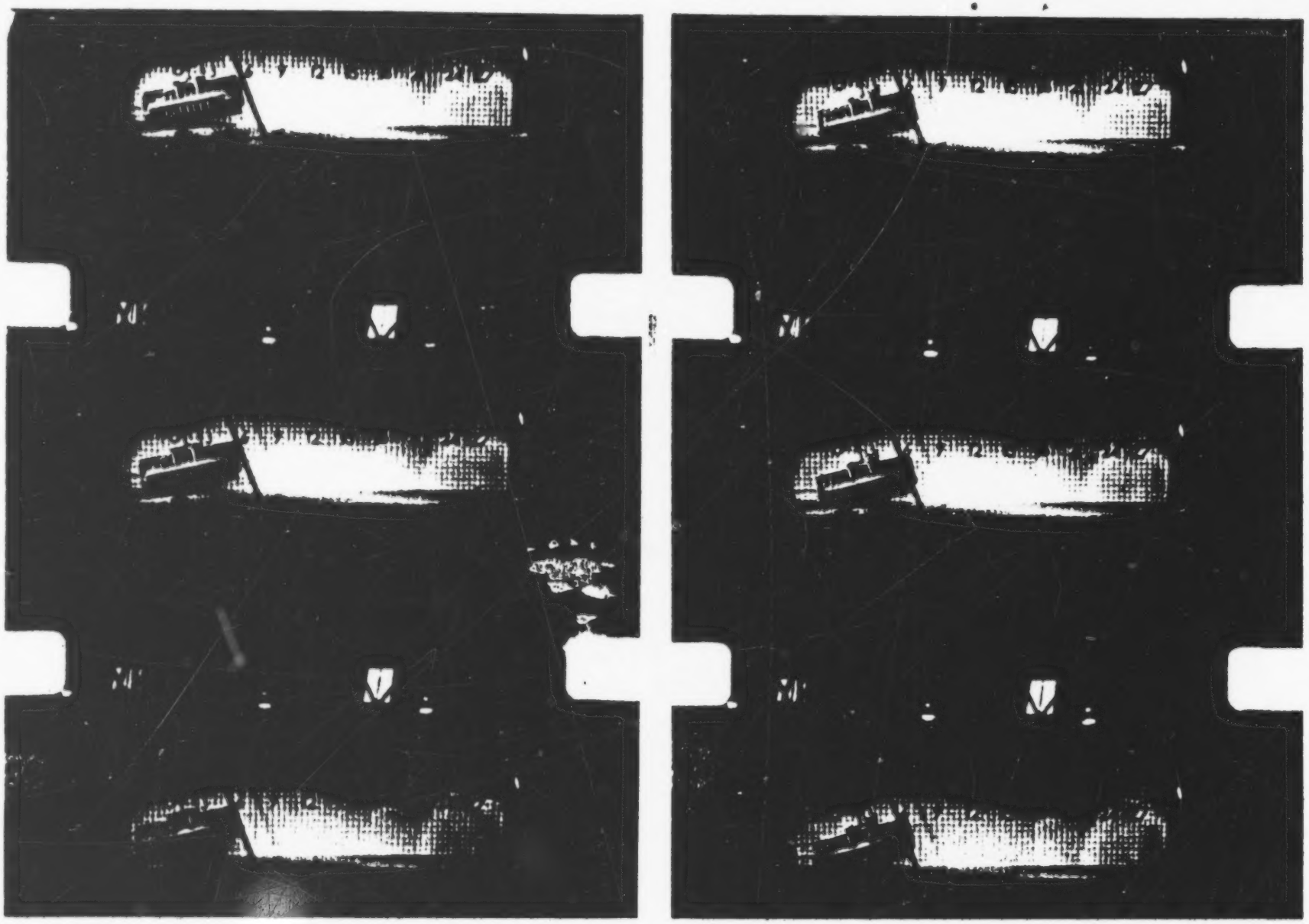

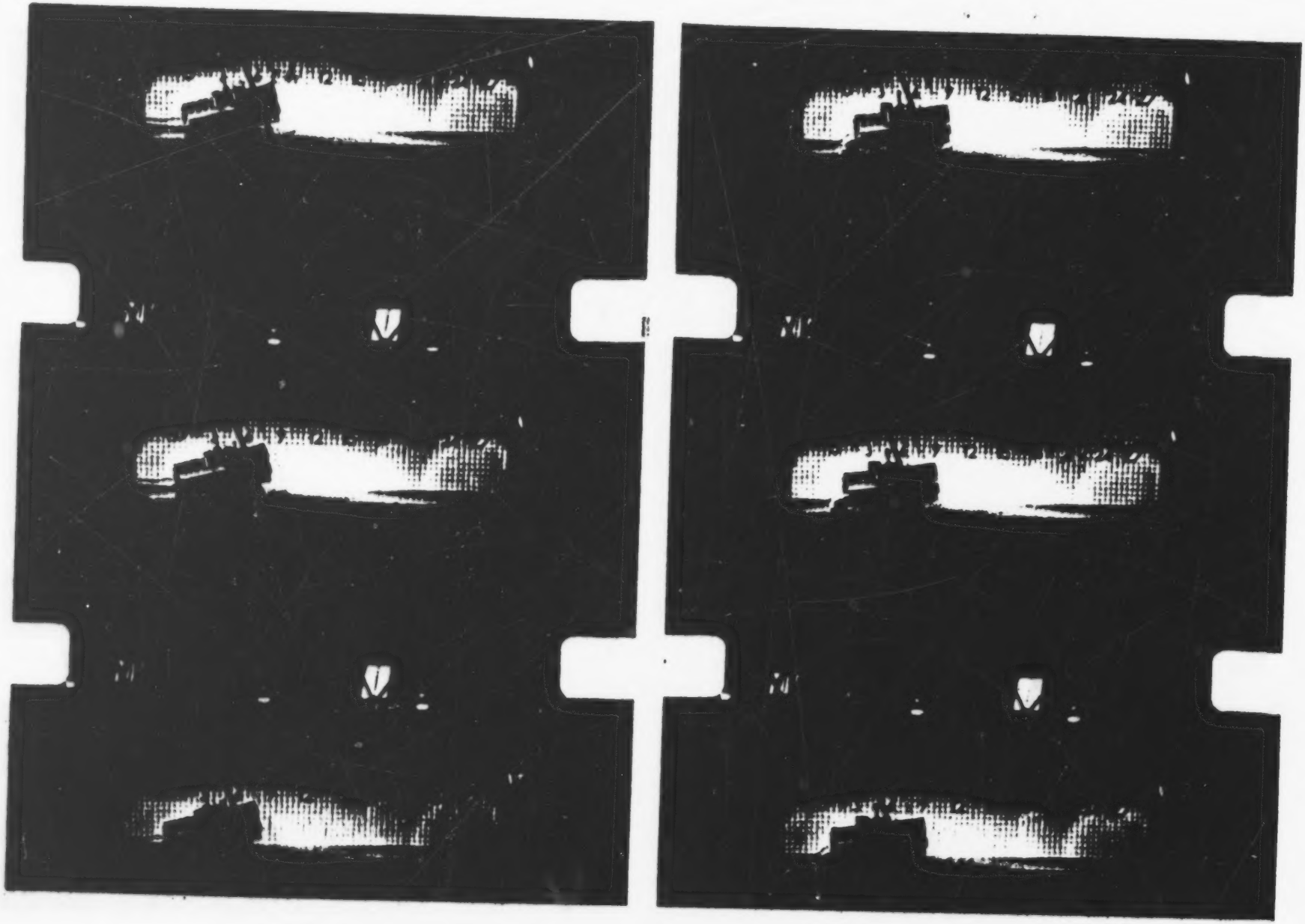

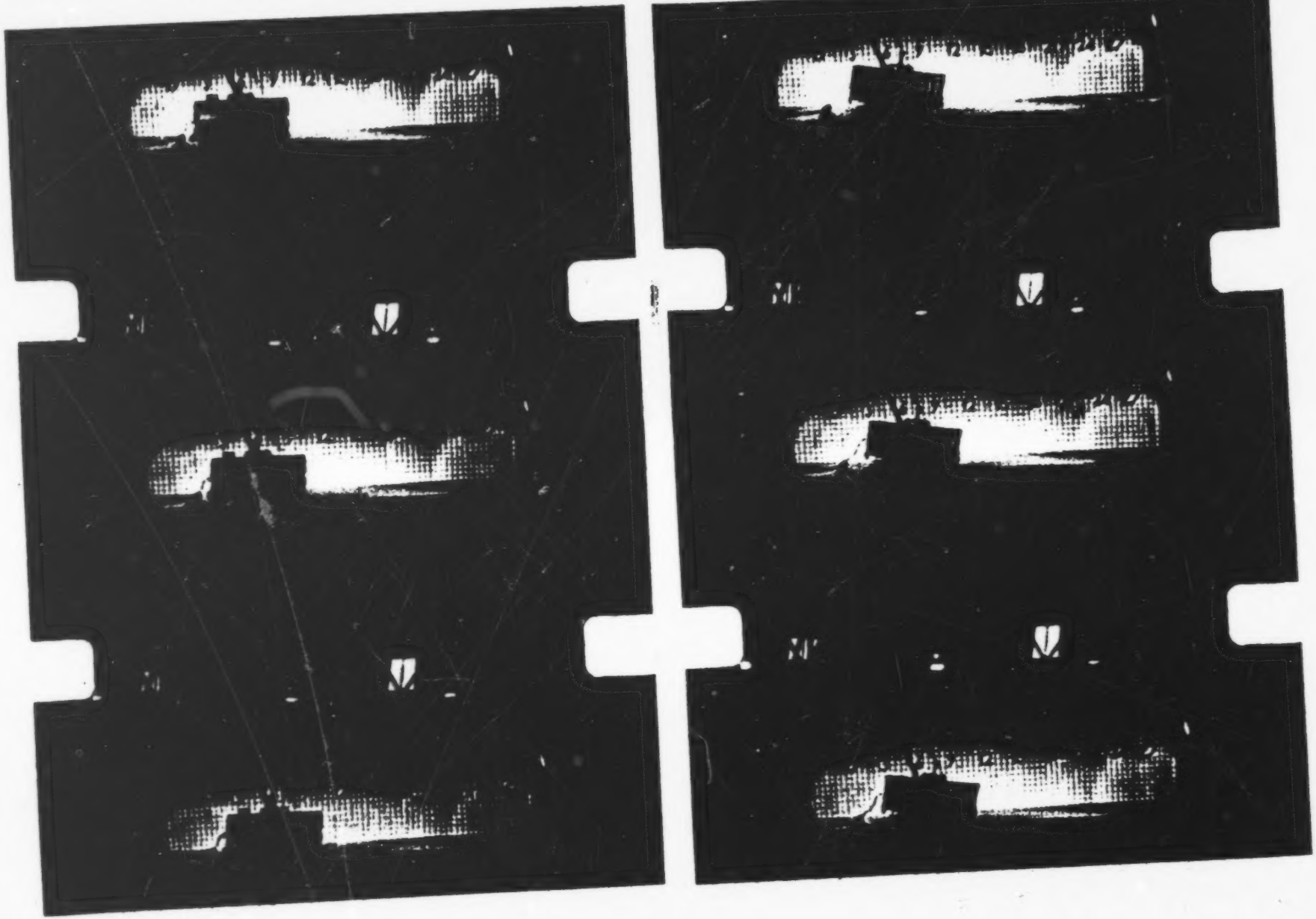

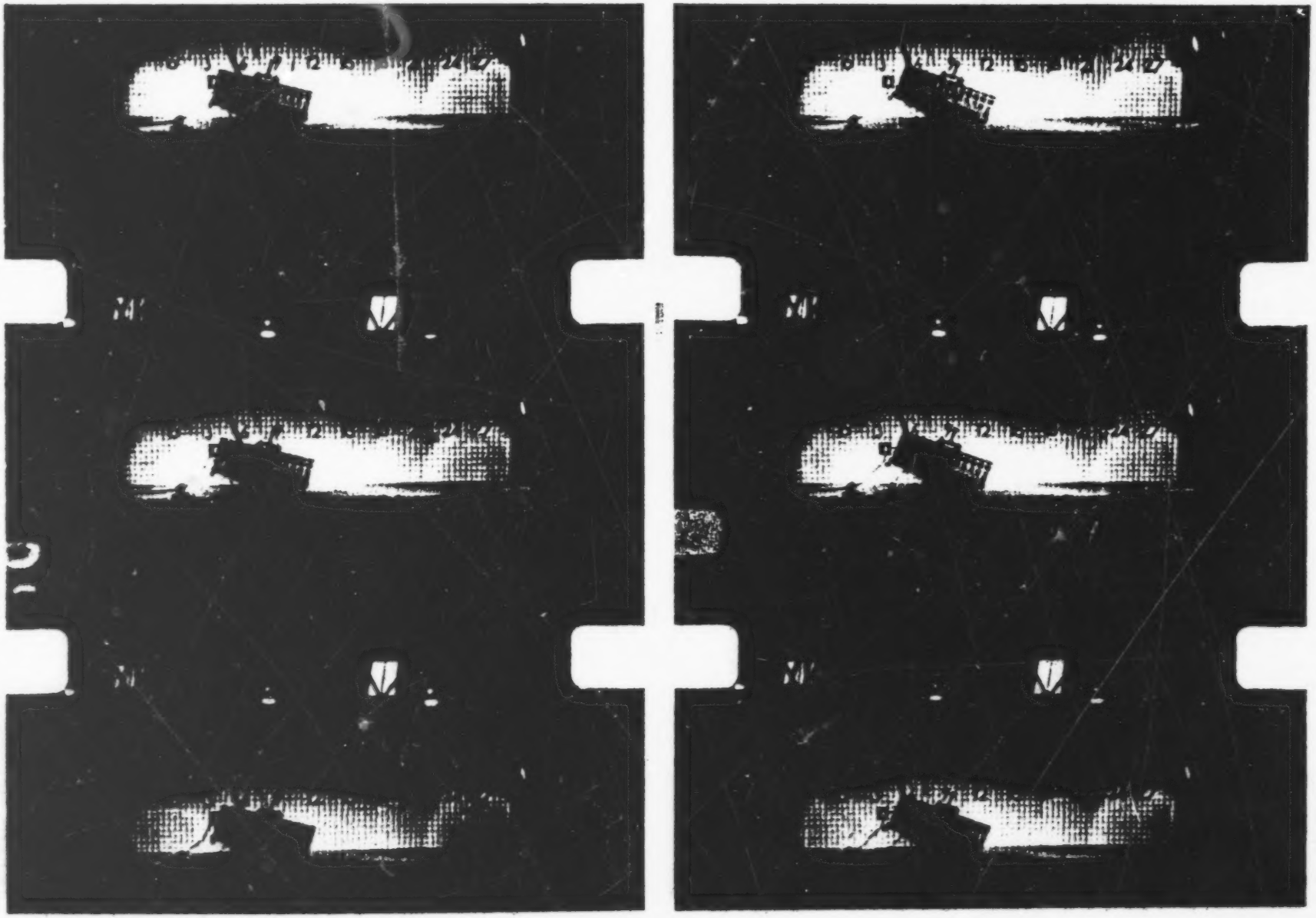

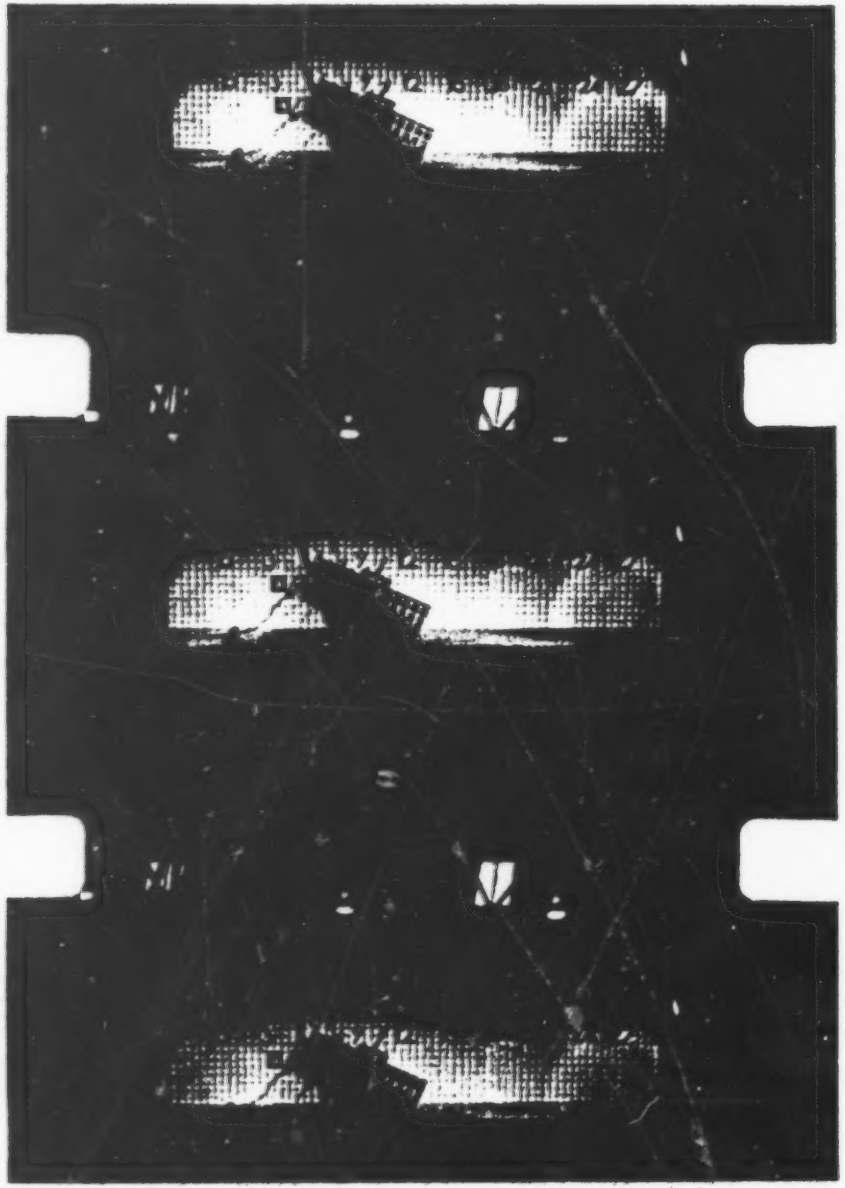

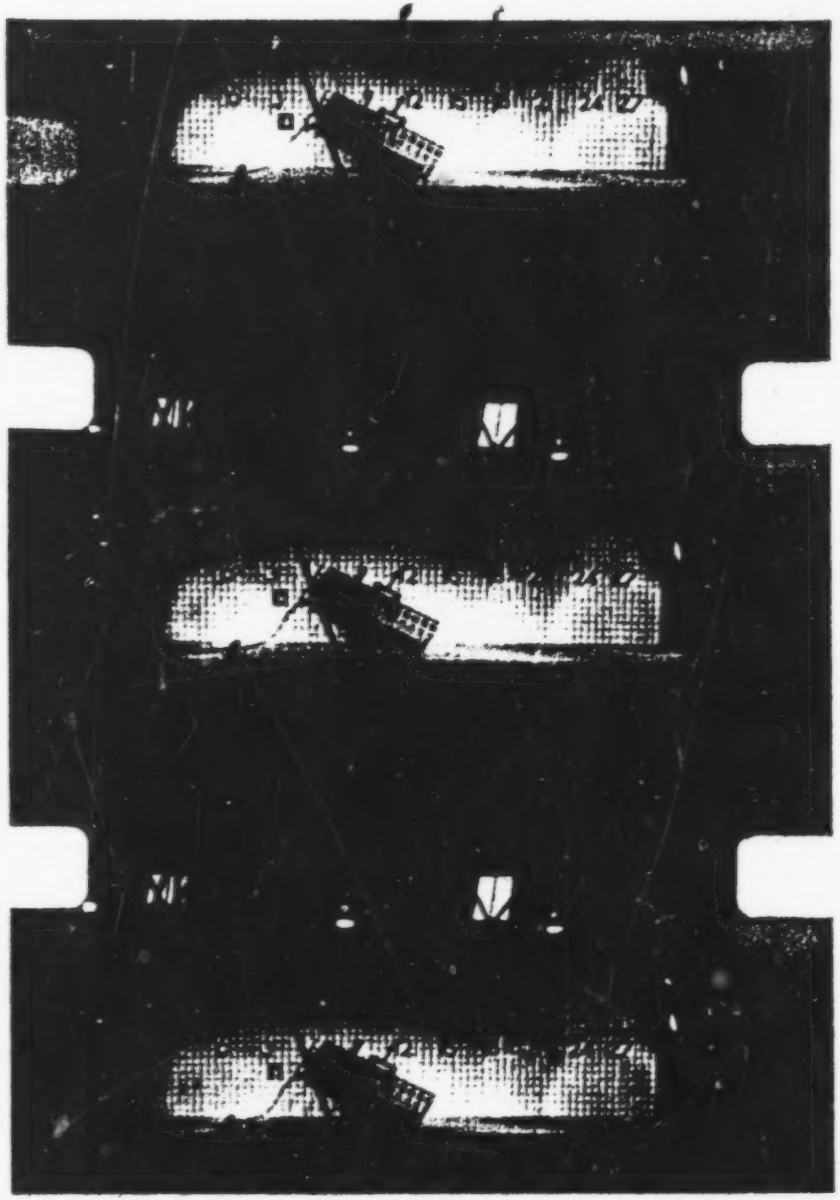

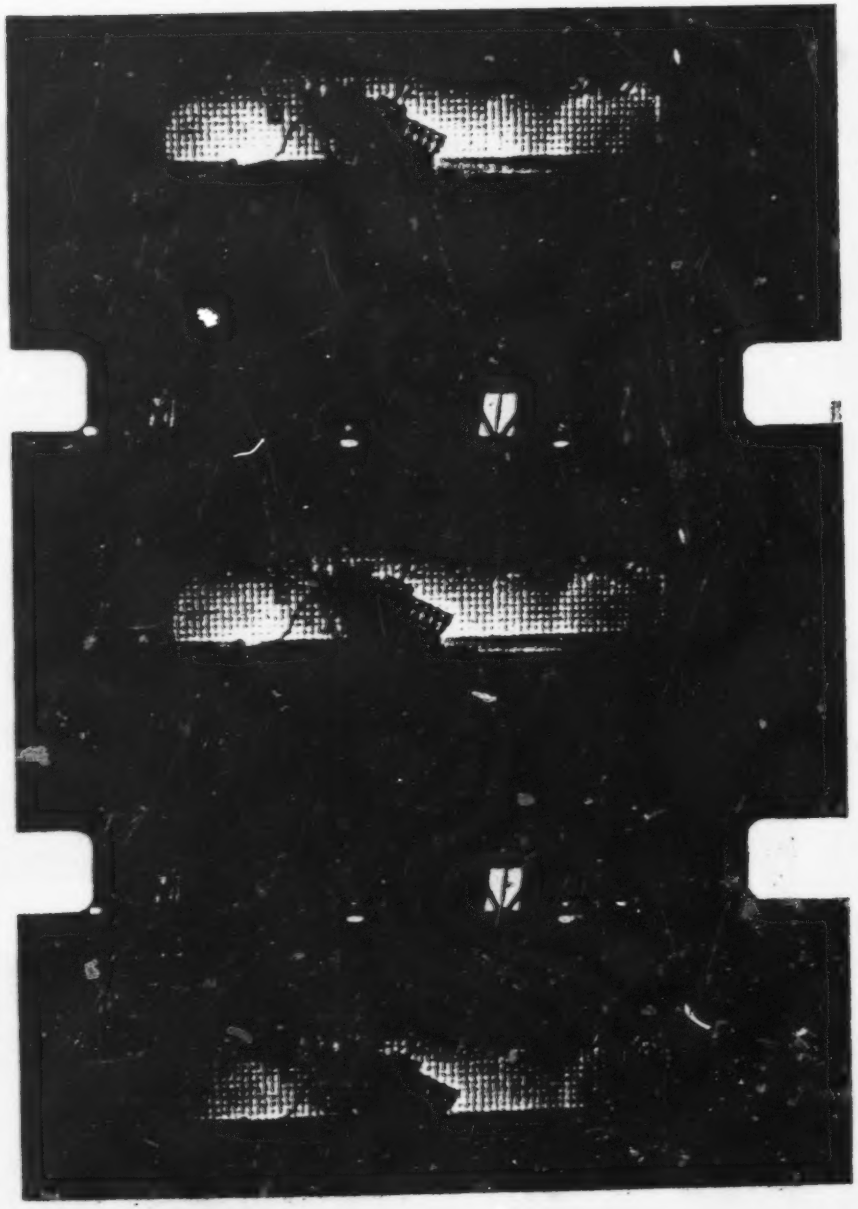

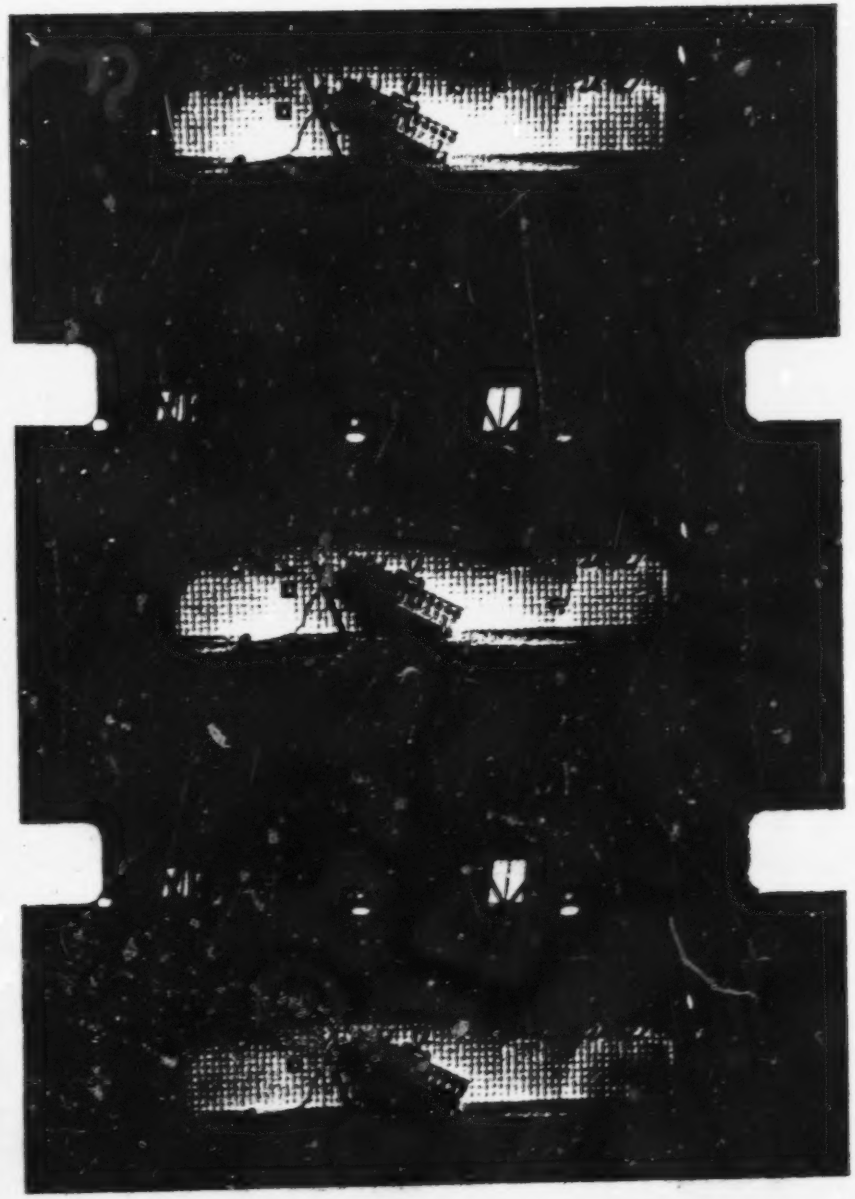

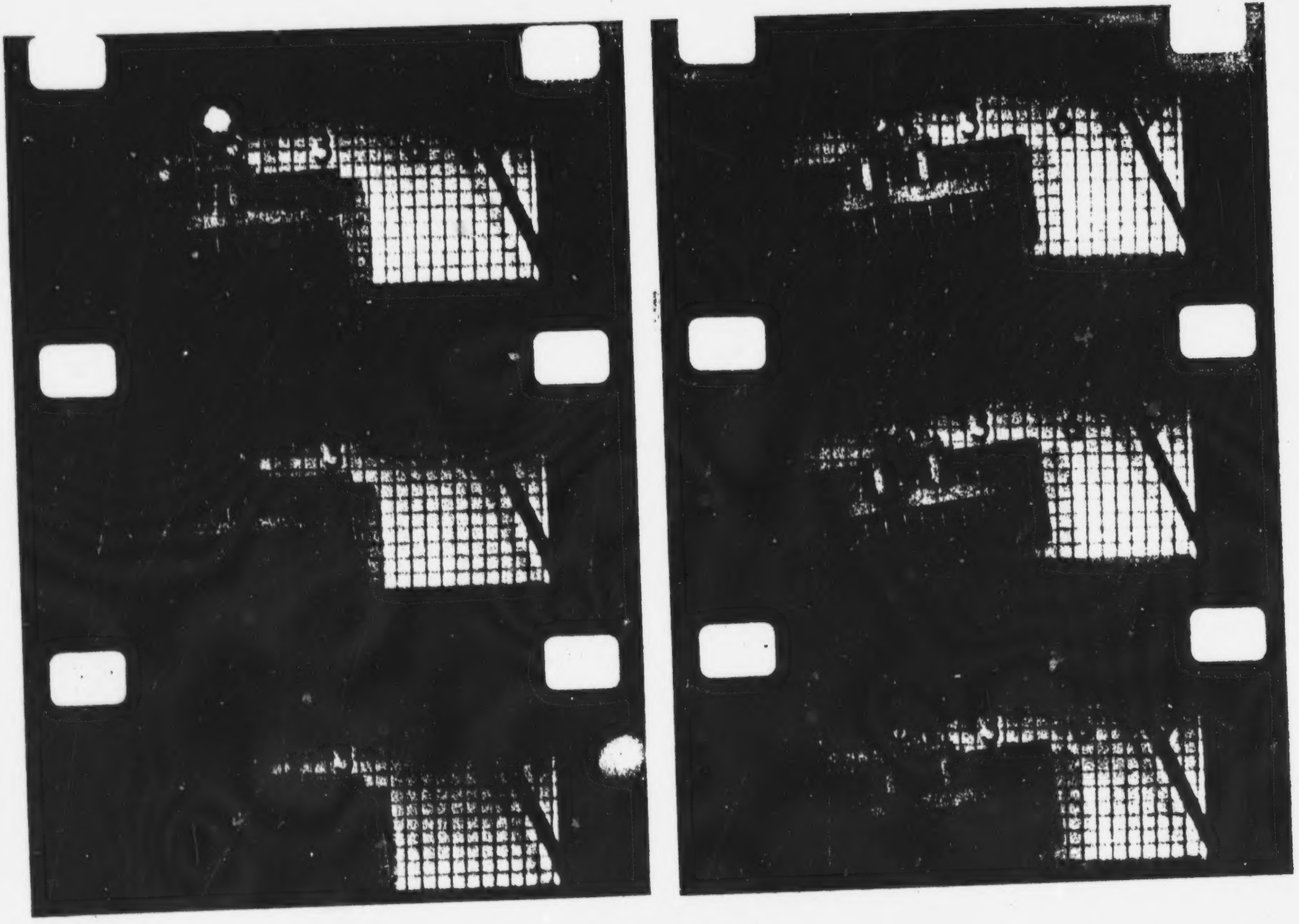

FIG. 17 HIGH-SPEED PHOTOGRAPHS OF 'FREE FLIGHT' TEST (300 PPS).

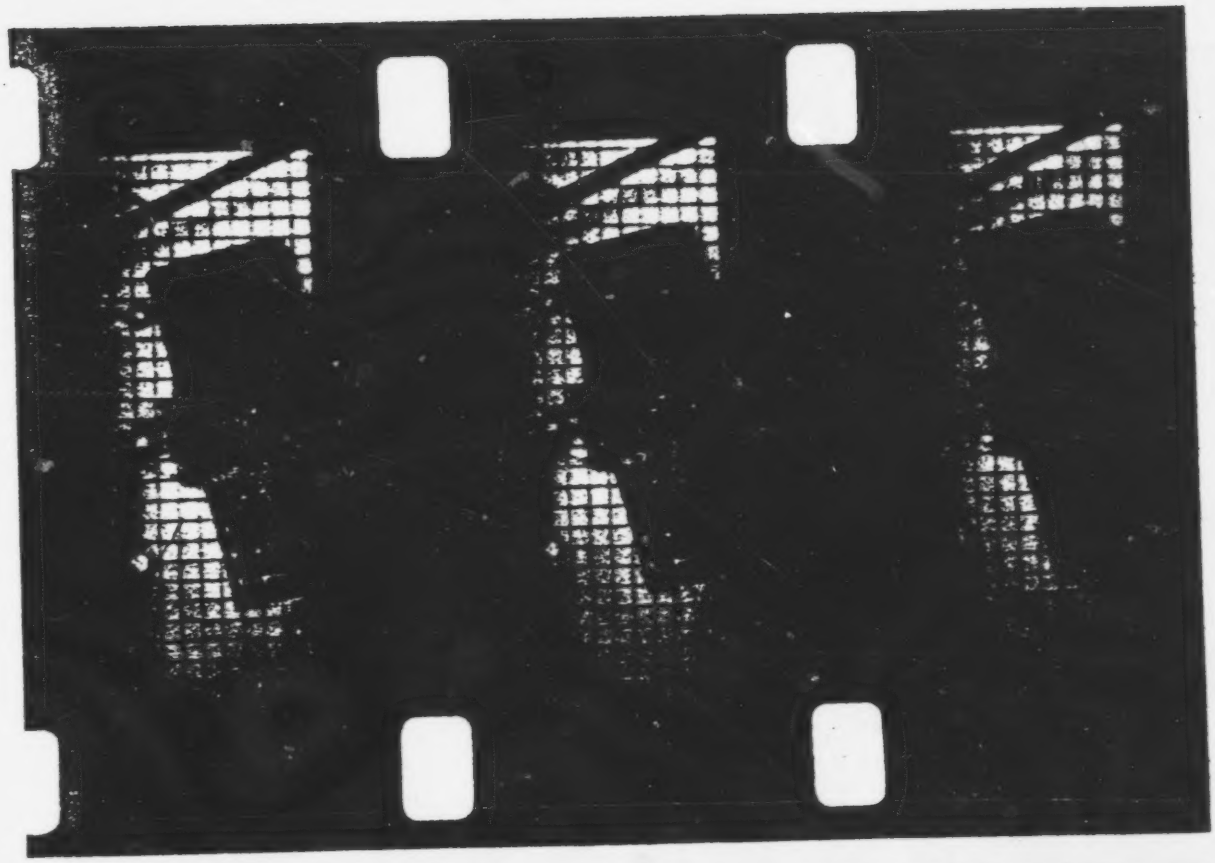

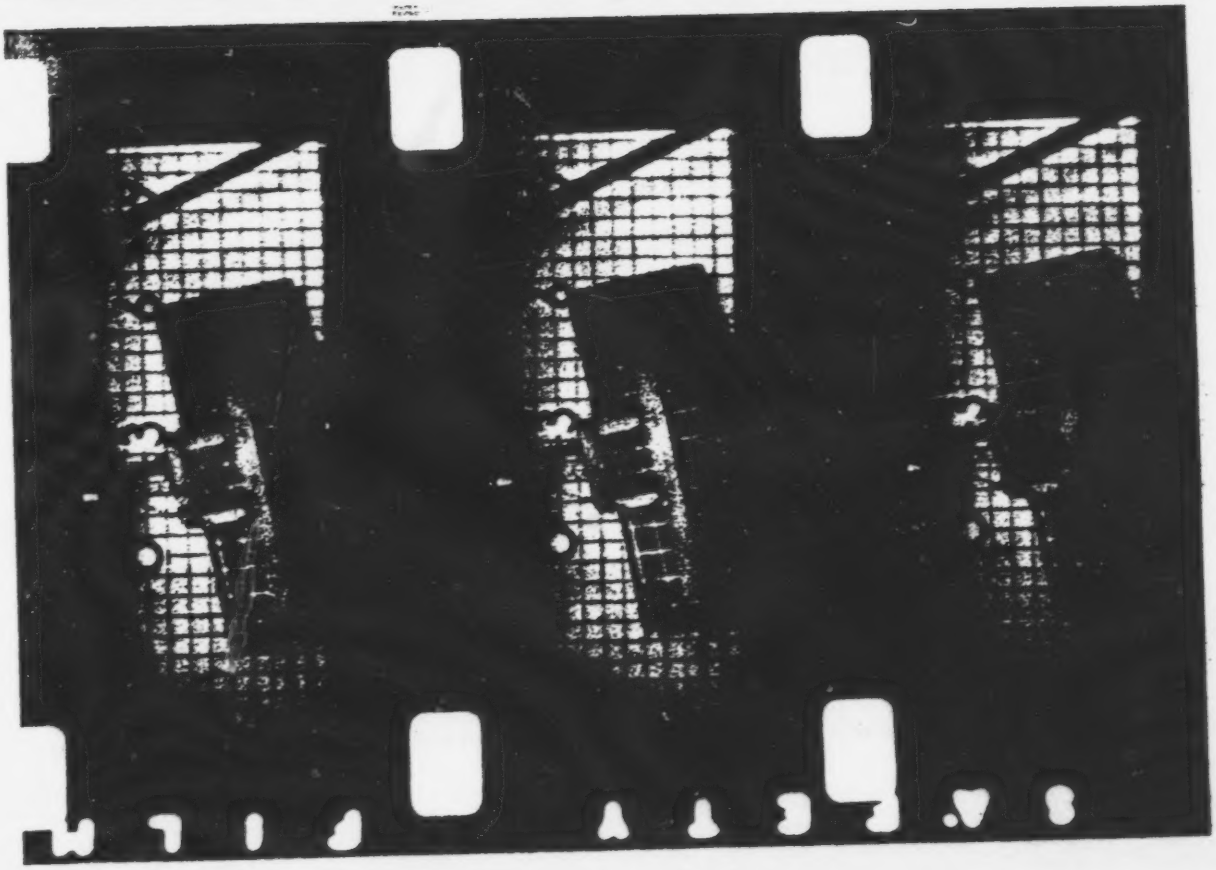

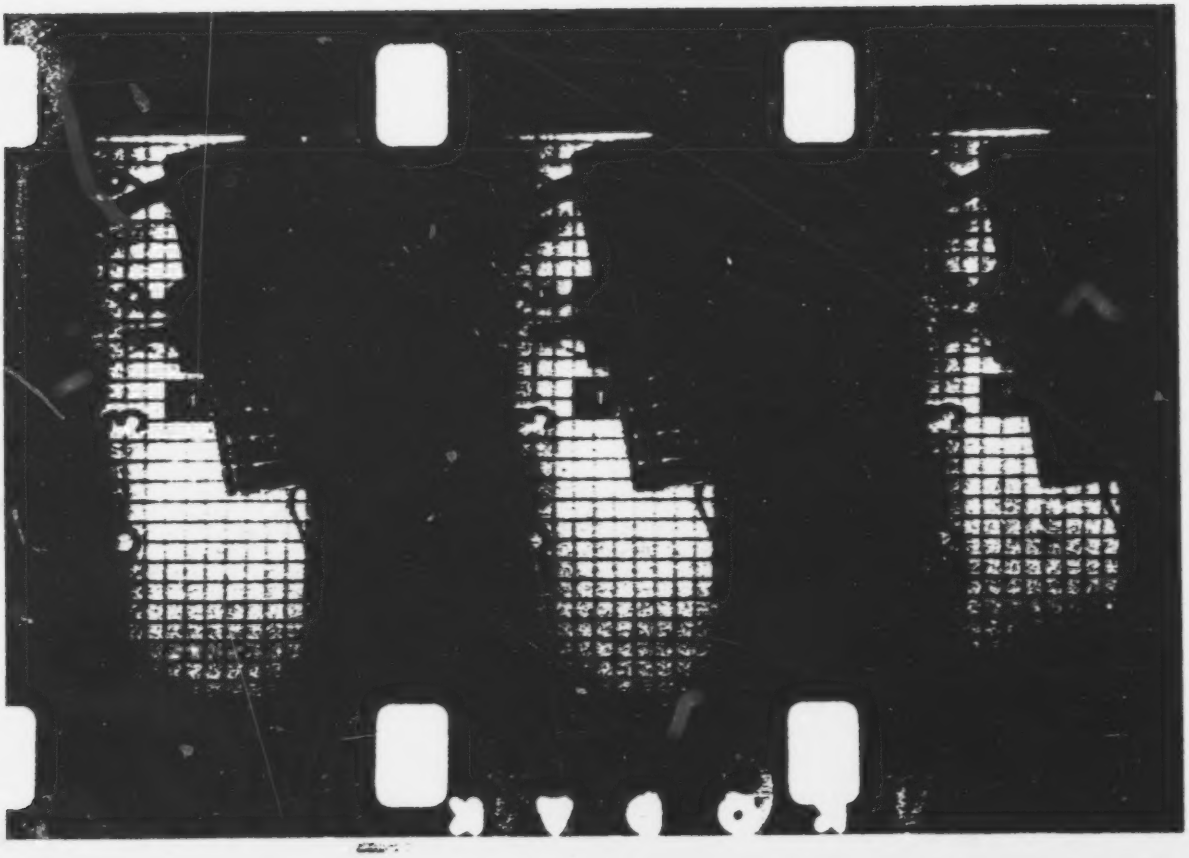

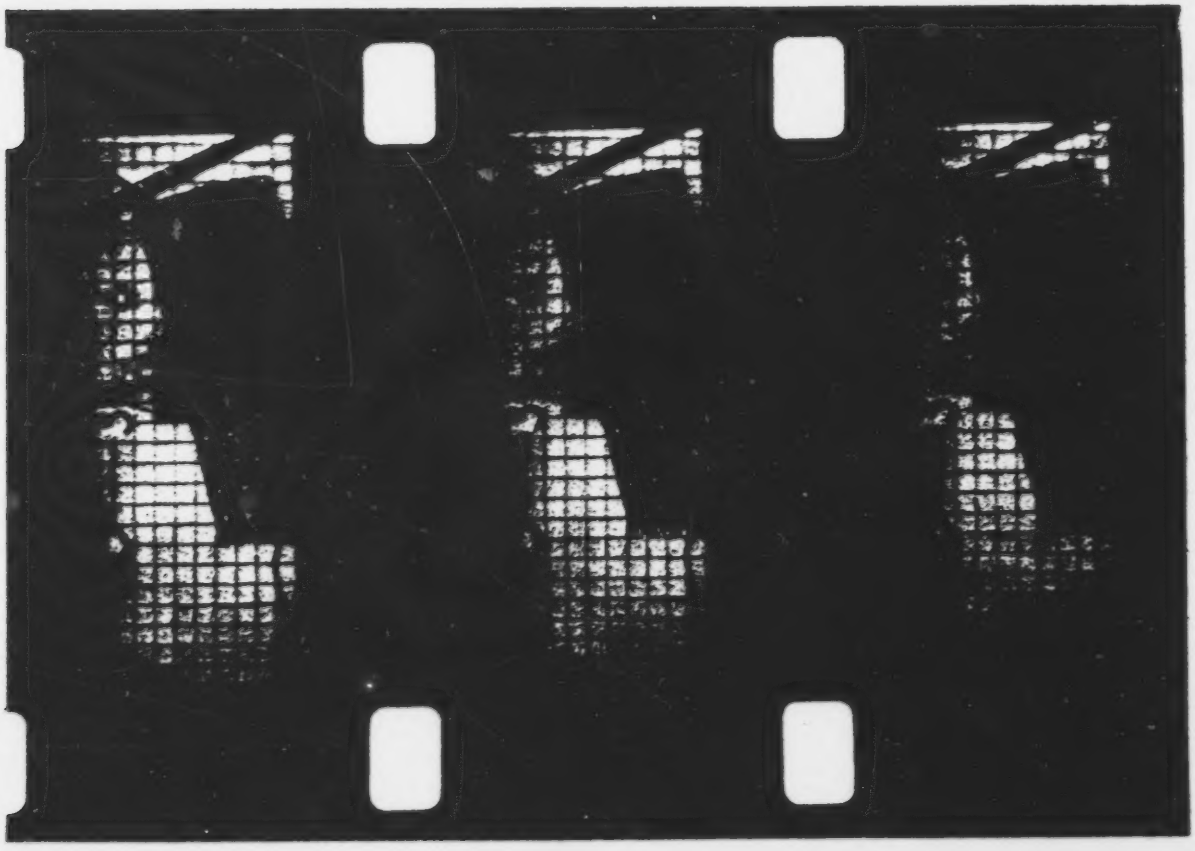

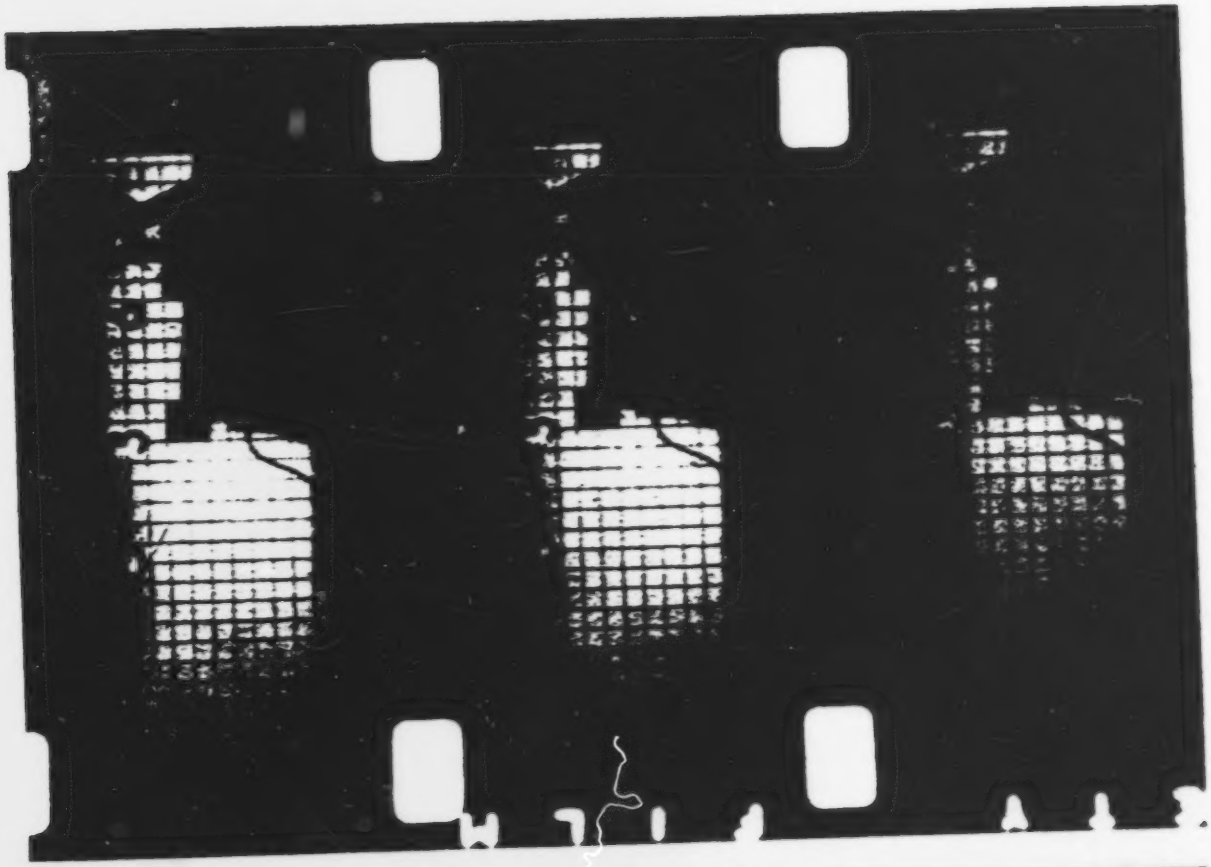

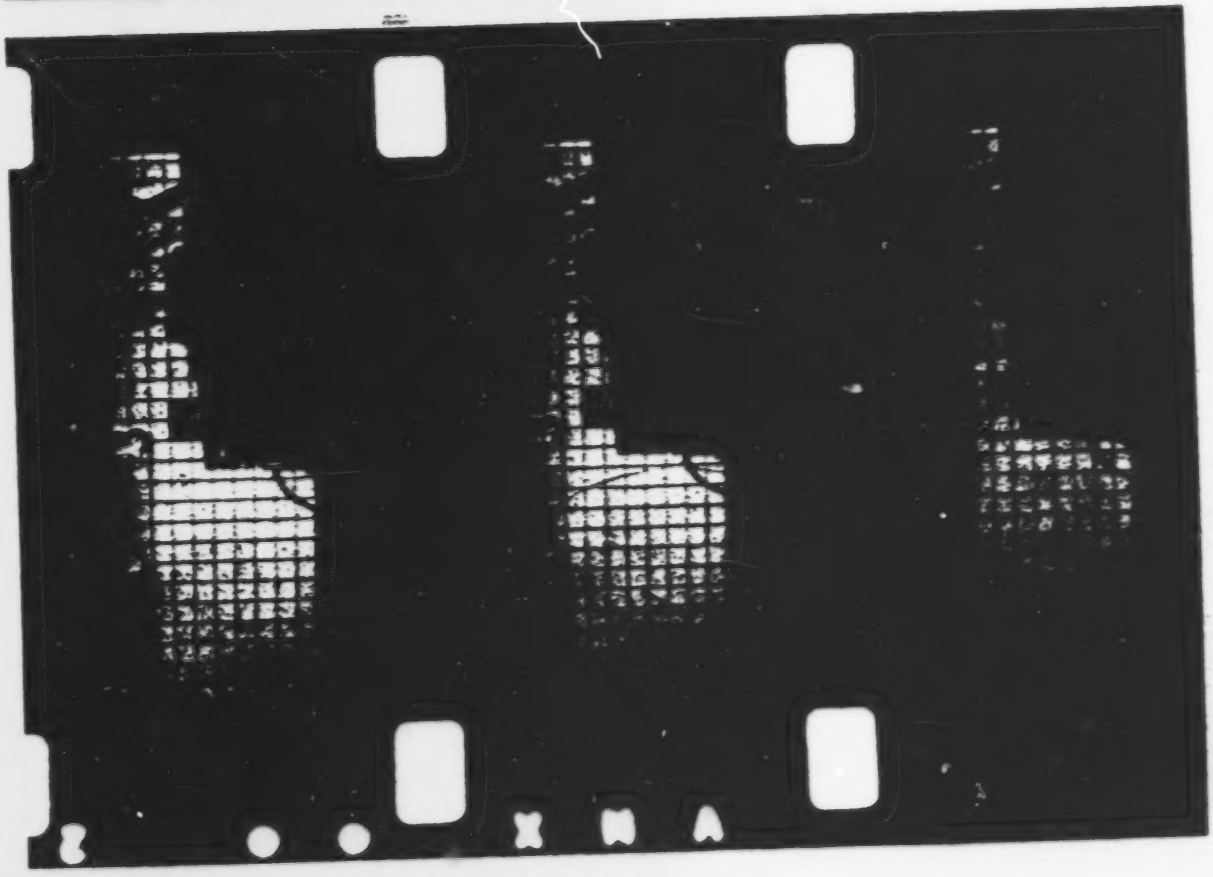

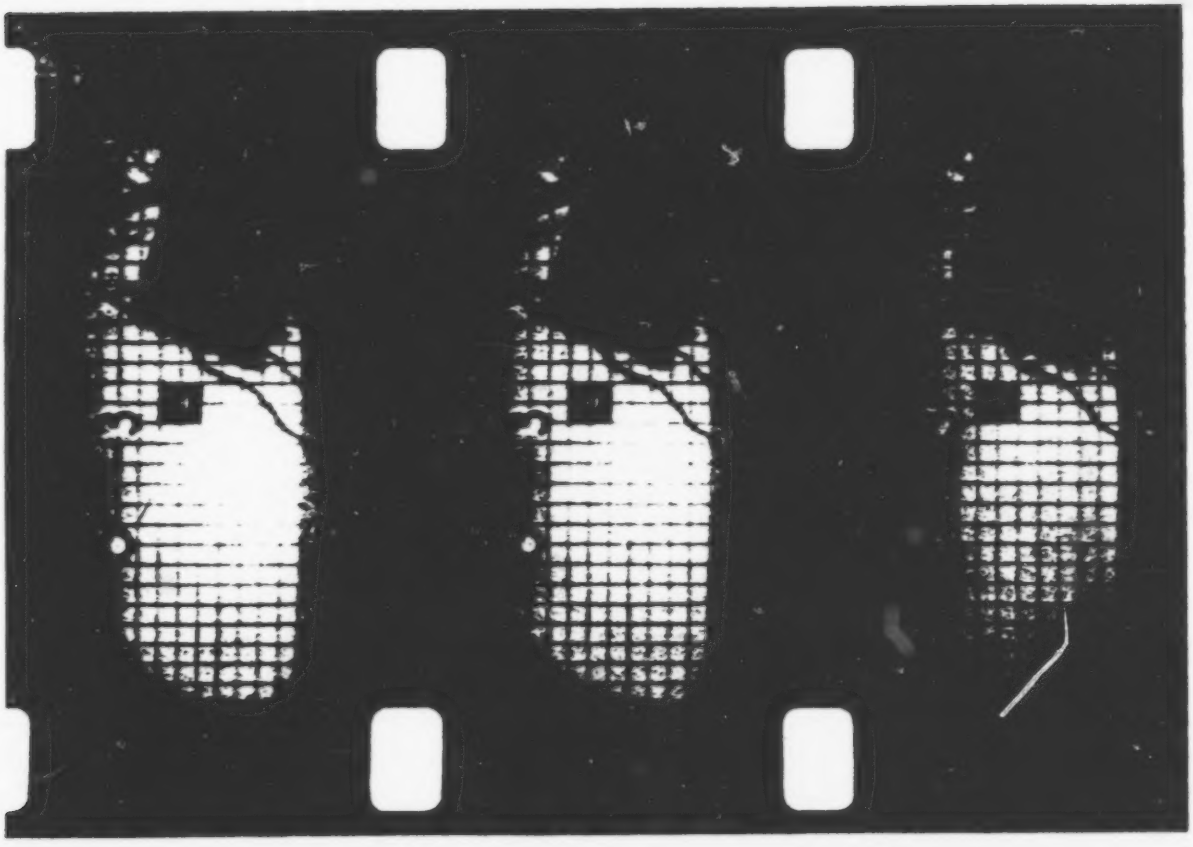

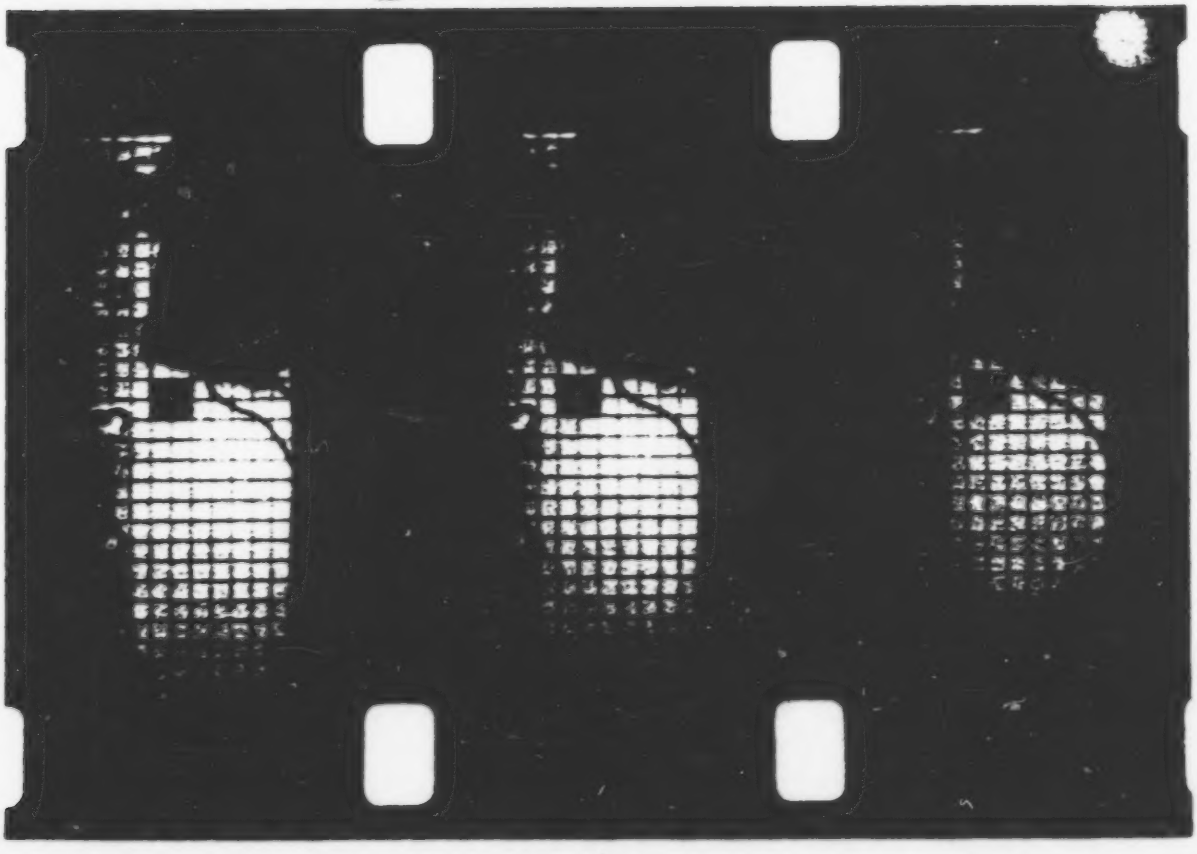

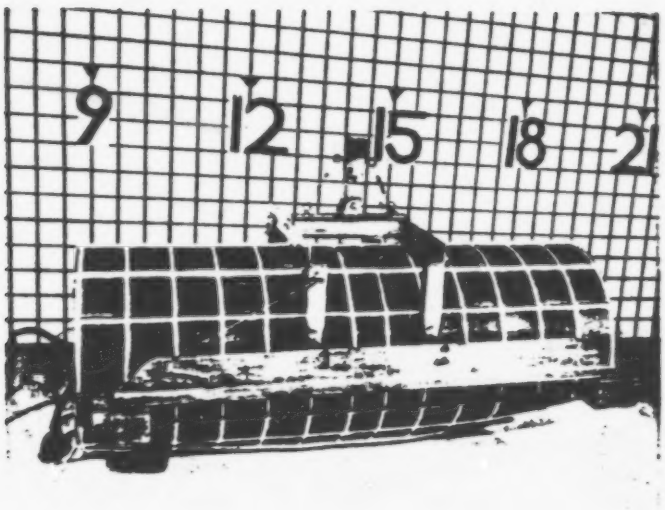

FIG. 18 POST-CRASH SIDE VIEW OF RIB/STRINGER 'FREE-FLIGHT' FUSELAGE.

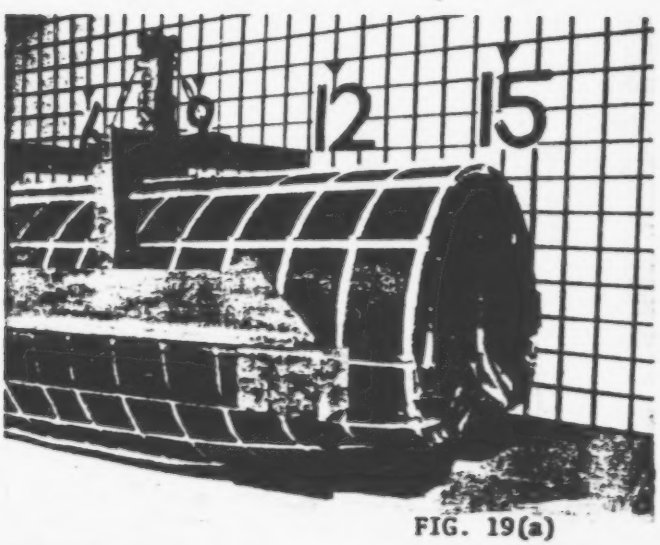

FIG. 19(a)

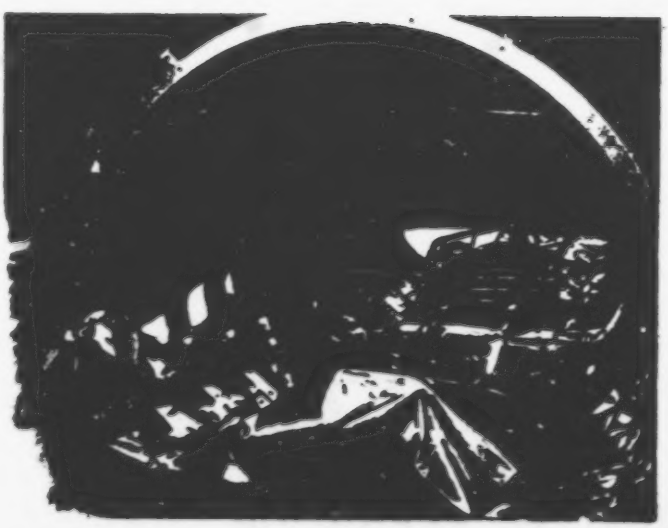

FIG. 19(b)

FIG. 19 POST-CRASH FRONT VIEW OF RIB/STRINGER 'FREE-FLIGHT' FUSELAGE.

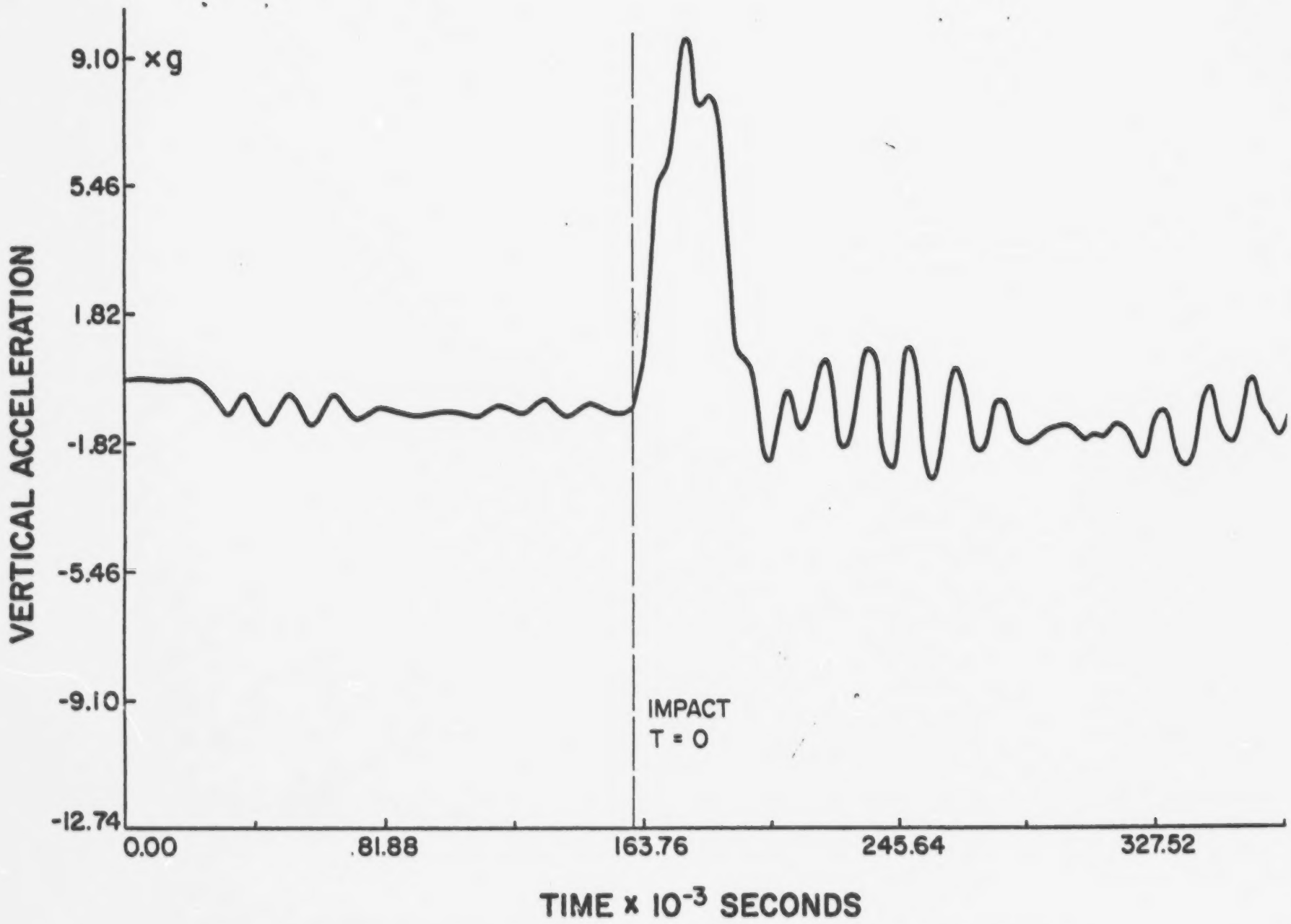

FIG. 20 ACCELERATION-TIME HISTORY OF WING LOAD (LEVEL IMPACT, V_o = 52.5 IN/SEC).

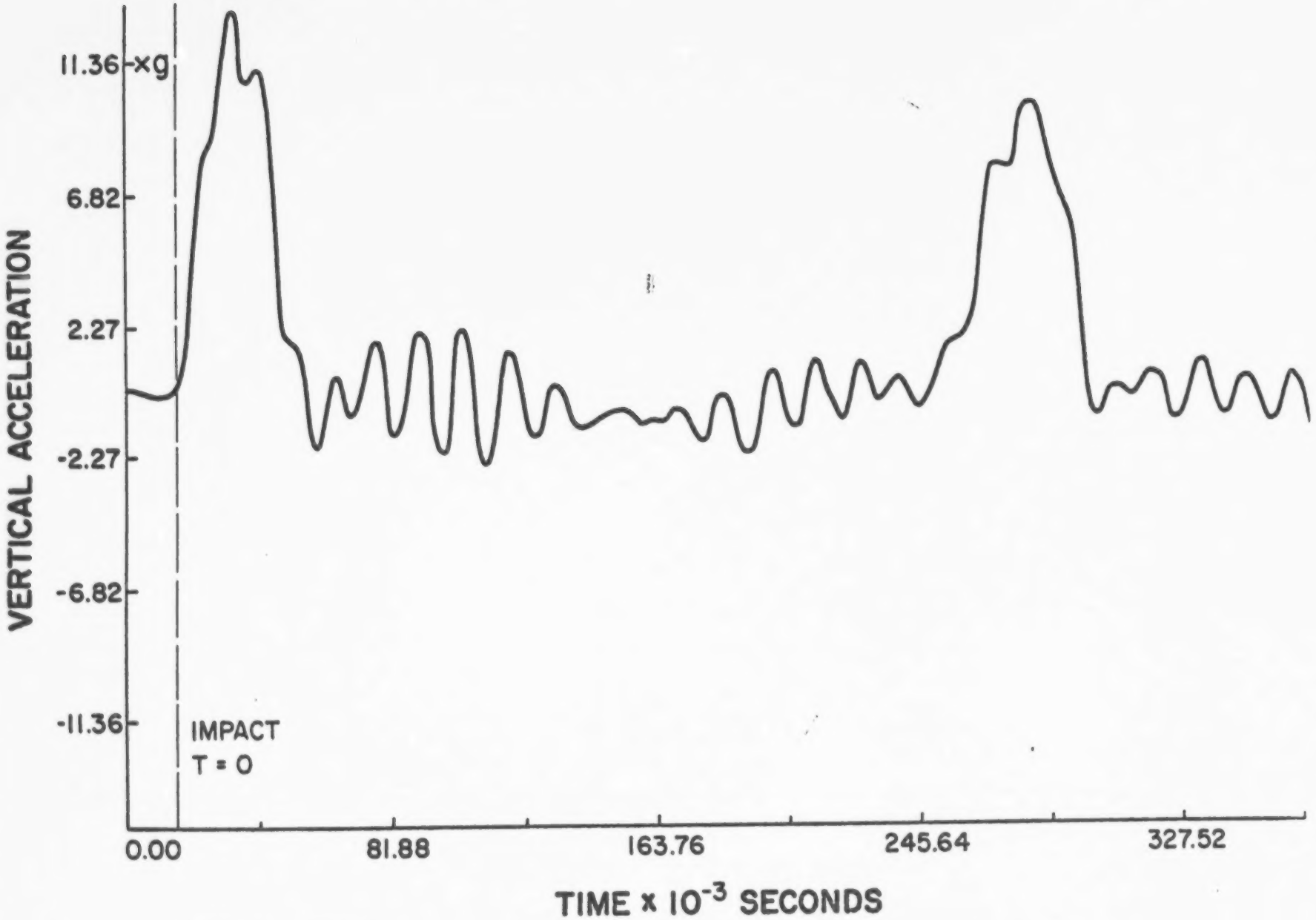

FIG. 21 ACCELERATION-TIME HISTORY OF WING LOAD (LEVEL IMPACT, V_o = 52.5 IN/SEC).

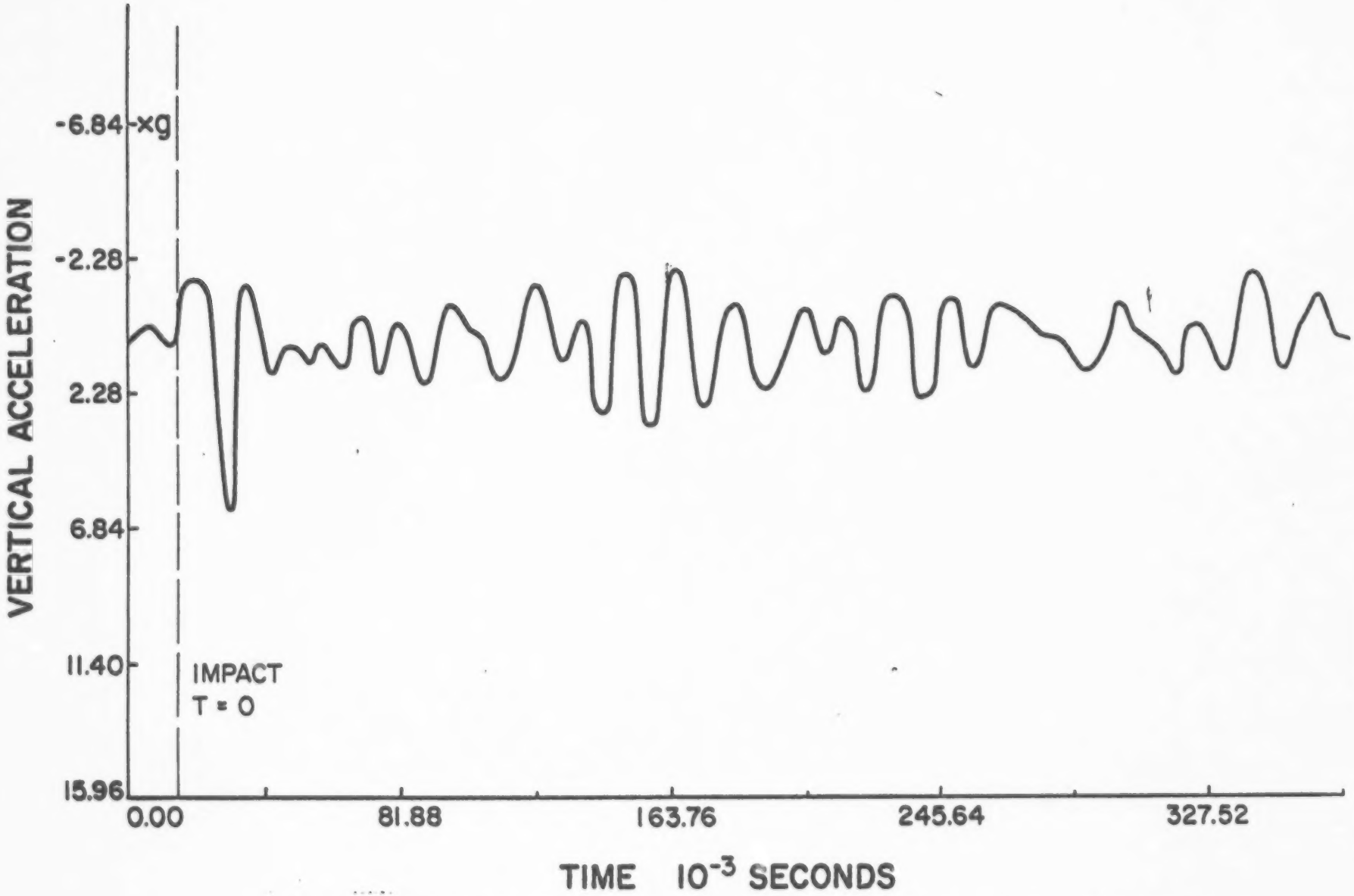

FIG. 22 ACCELERATION-TIME HISTORY @ FLOOR RIB #10 FLOOR (LEVEL IMPACT, V_o = 52.5 IN/SEC).

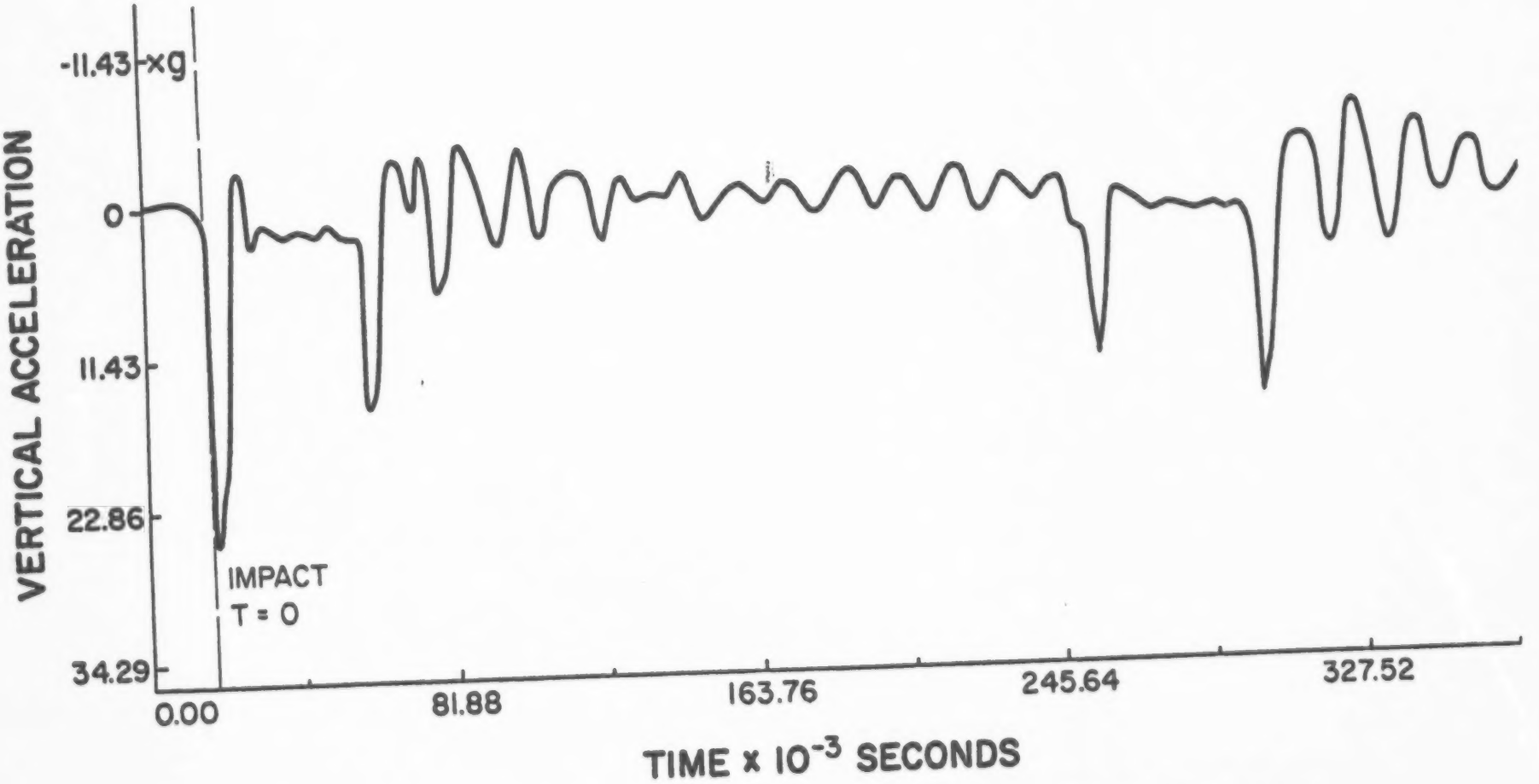

FIG. 23 ACCELERATION-TIME HISTORY @ RIB #5 FLOOR (LEVEL IMPACT, V_o = 52.5 IN/SEC).

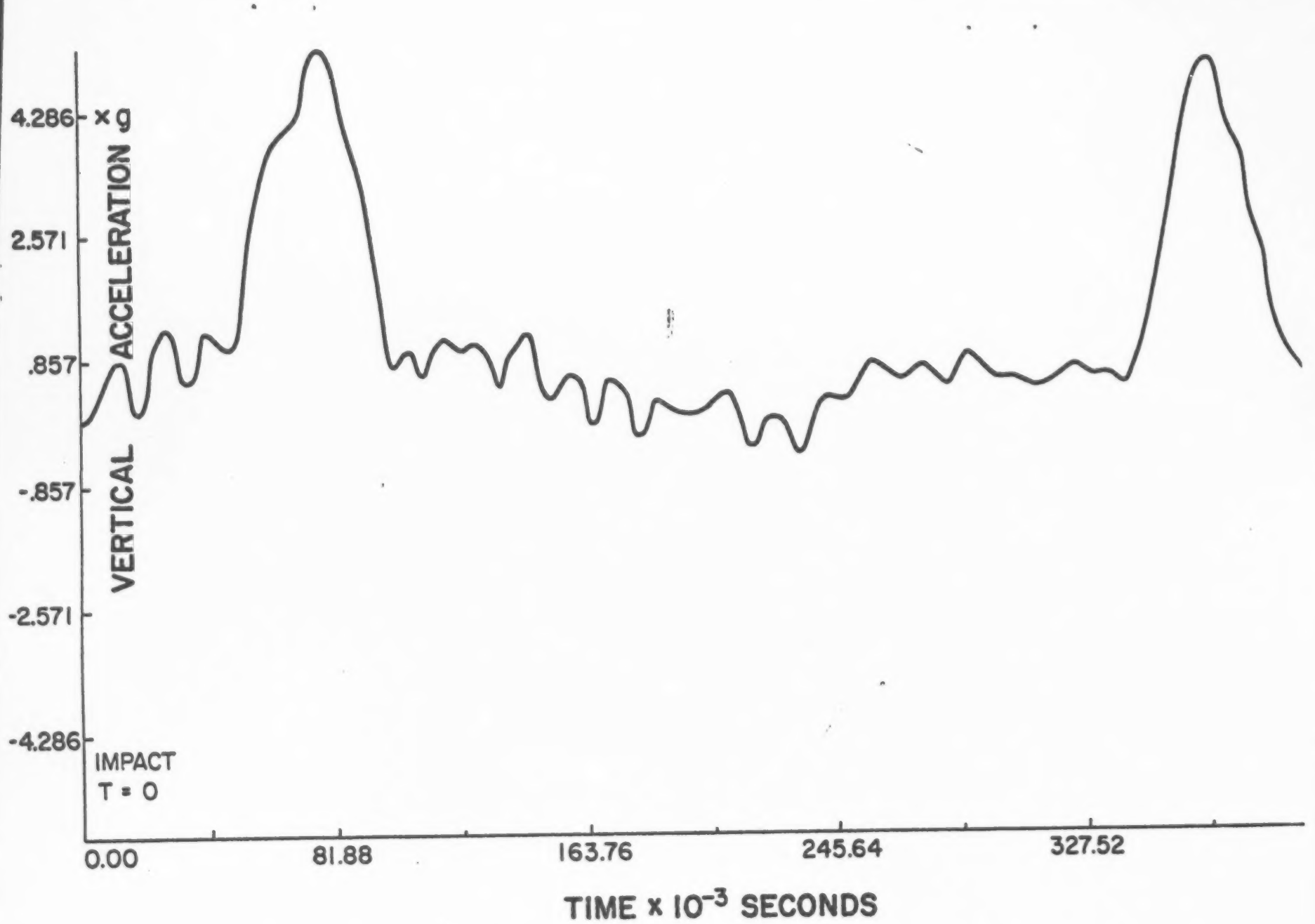

FIG. 24 ACCELERATION-TIME HISTORY OF WING LOAD (OBLIQUE, $\alpha = 3°$, $V_o = 26$ IN/SEC).

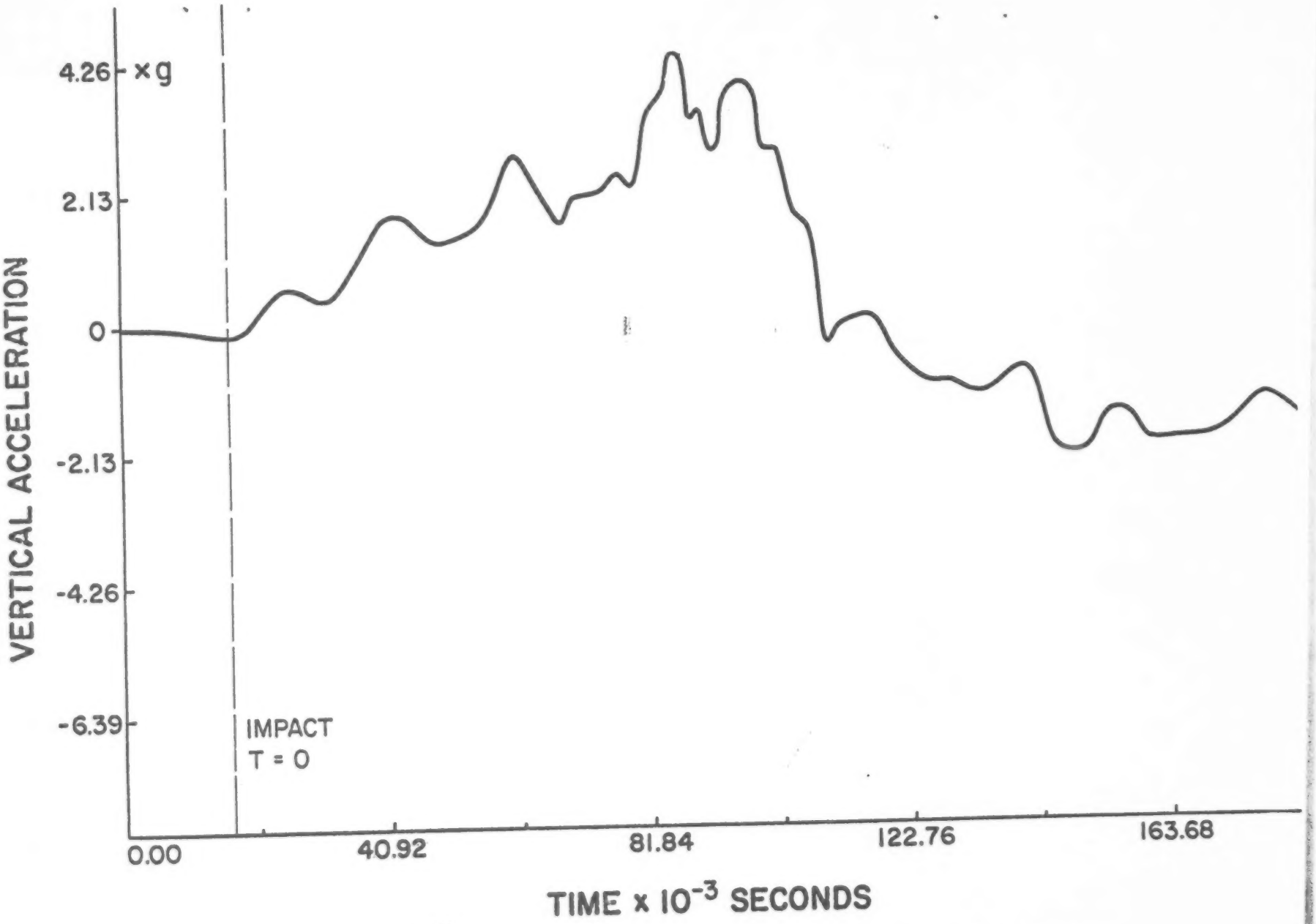

FIG. 25 ACCELERATION-TIME HISTORY OF WING LOAD (OBLIQUE, $\alpha = 3°$, $V_o = 26$ IN/SEC).

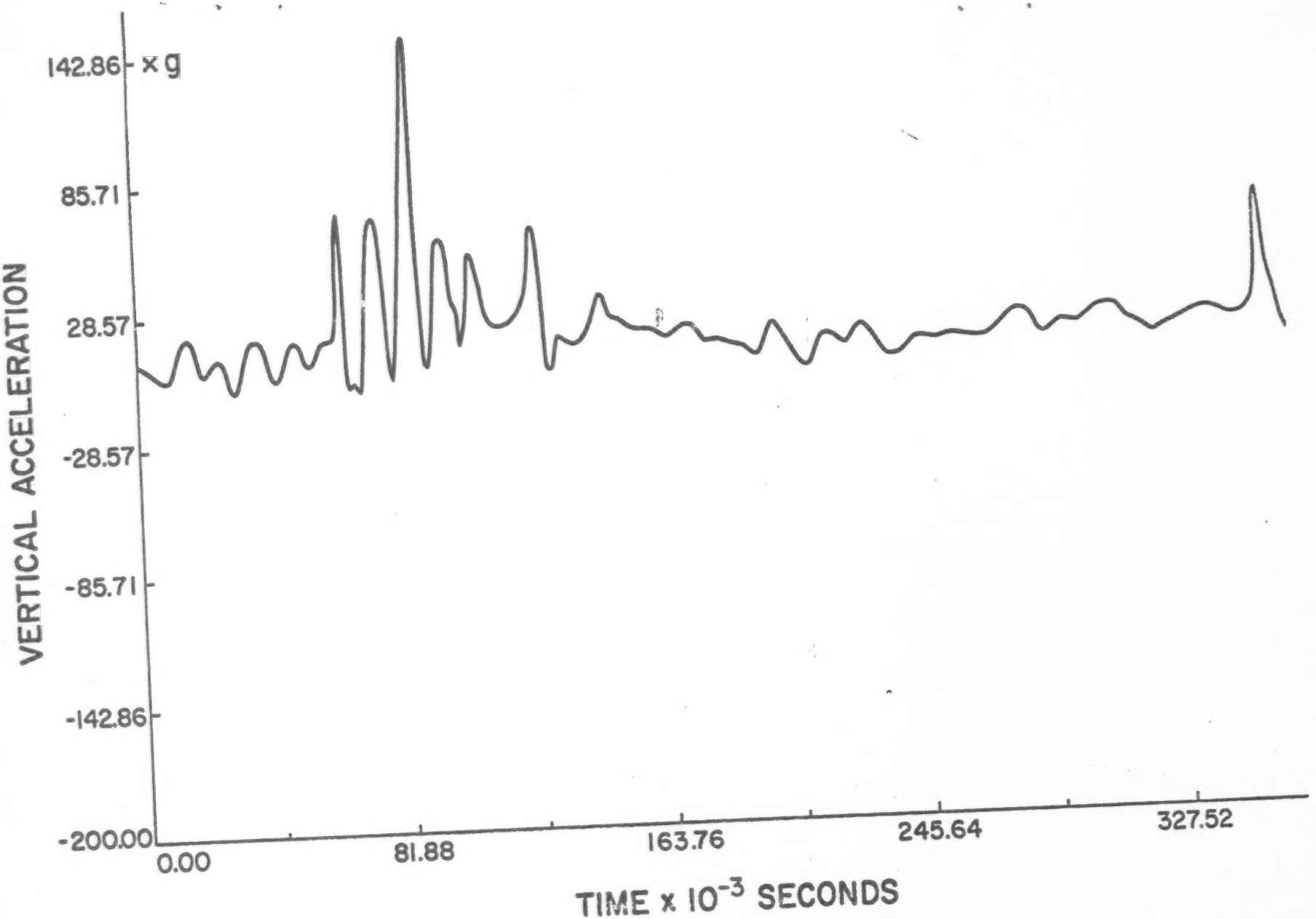

FIG. 26 ACCELERATION-TIME HISTORY @ FLOOR, RIB #10 (OBLIQUE, $\alpha = 3°$, $V_o = 26$ IN/SEC).

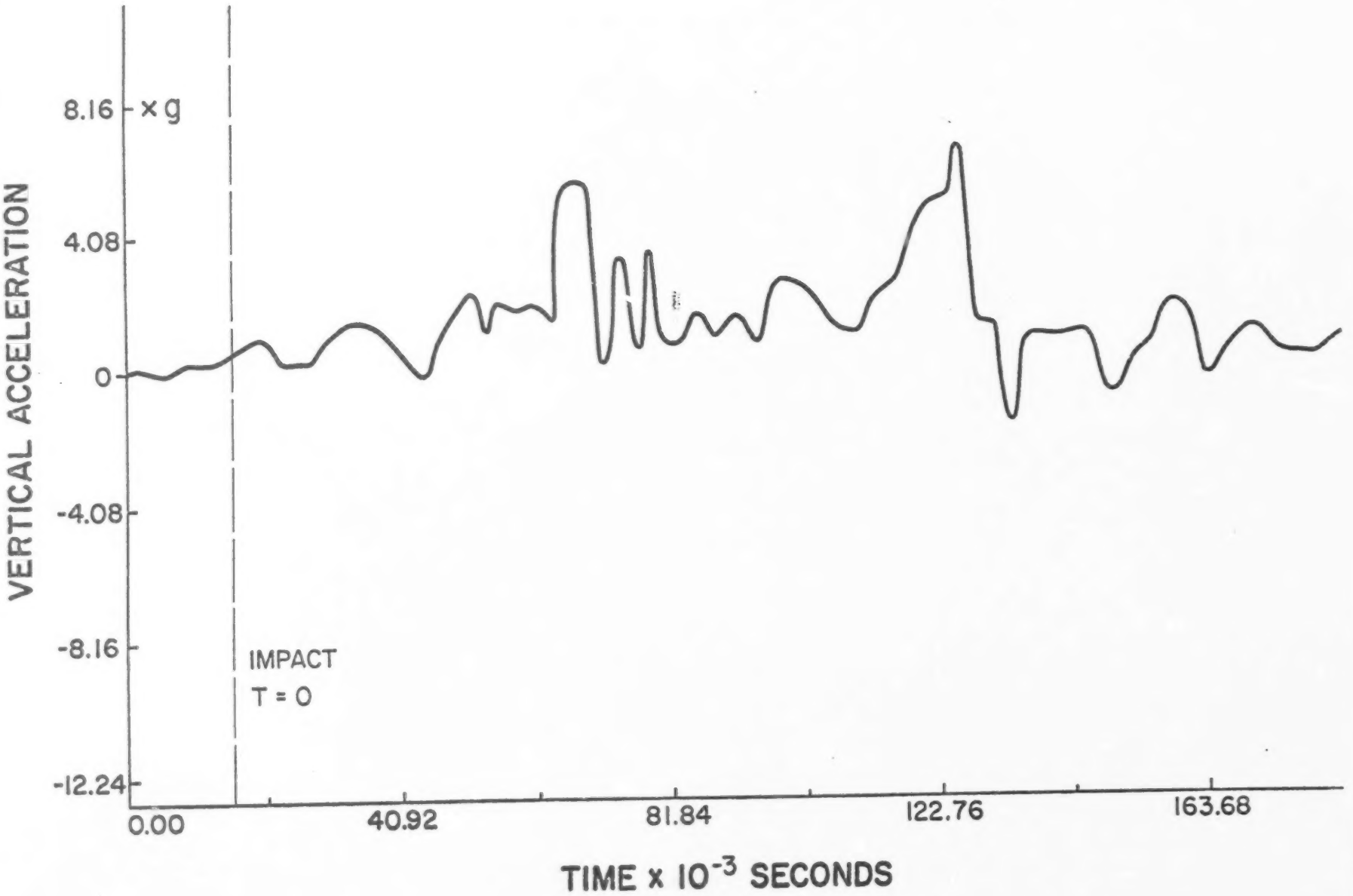

FIG. 27 ACCELERATION-TIME HISTORY @ FLOOR, RIB #5 (OBLIQUE, $\alpha = 3°$, $V_o = 26$ IN/SEC).

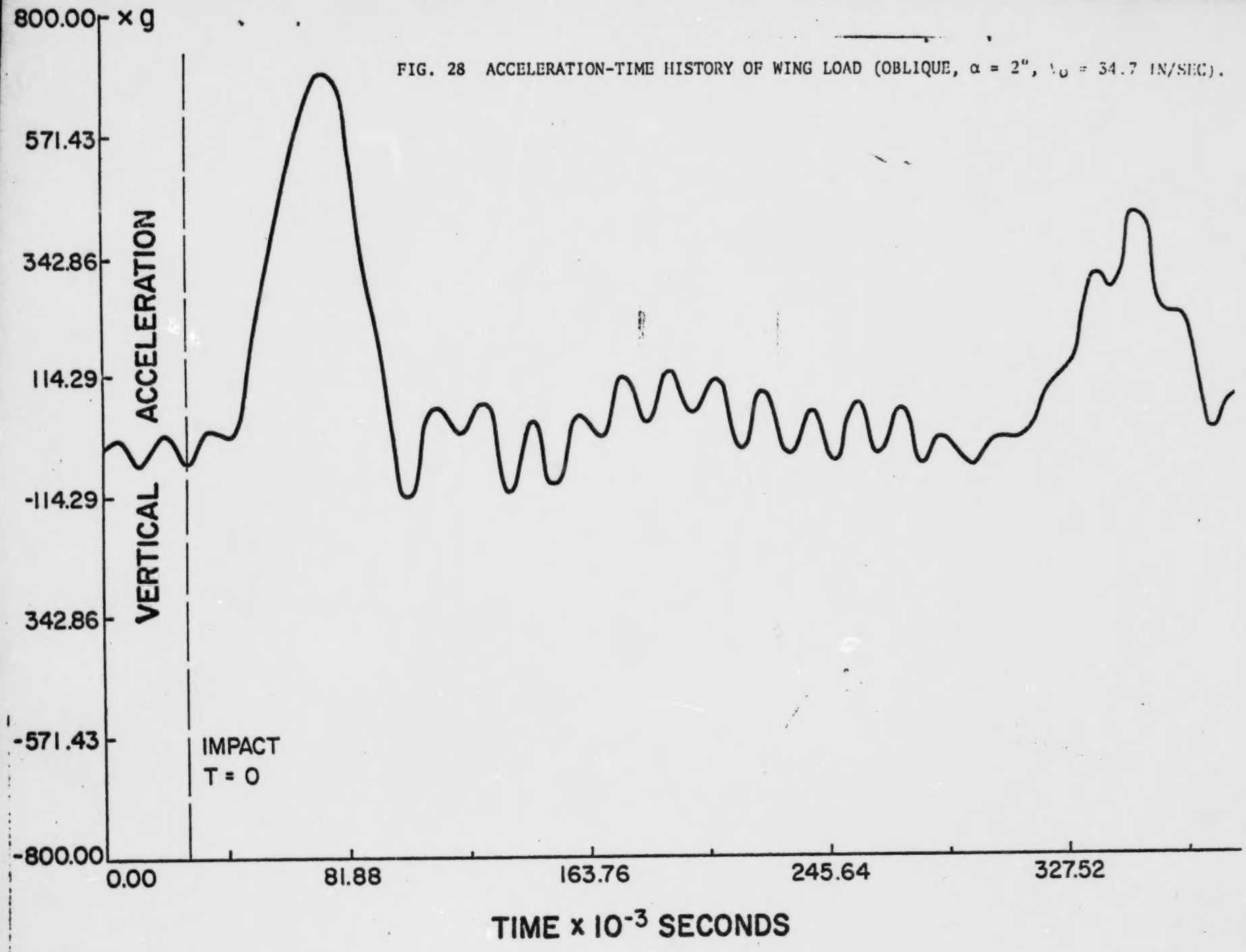

FIG. 28 ACCELERATION-TIME HISTORY OF WING LOAD (OBLIQUE, α = 2°, V_0 = 34.7 IN/SEC).

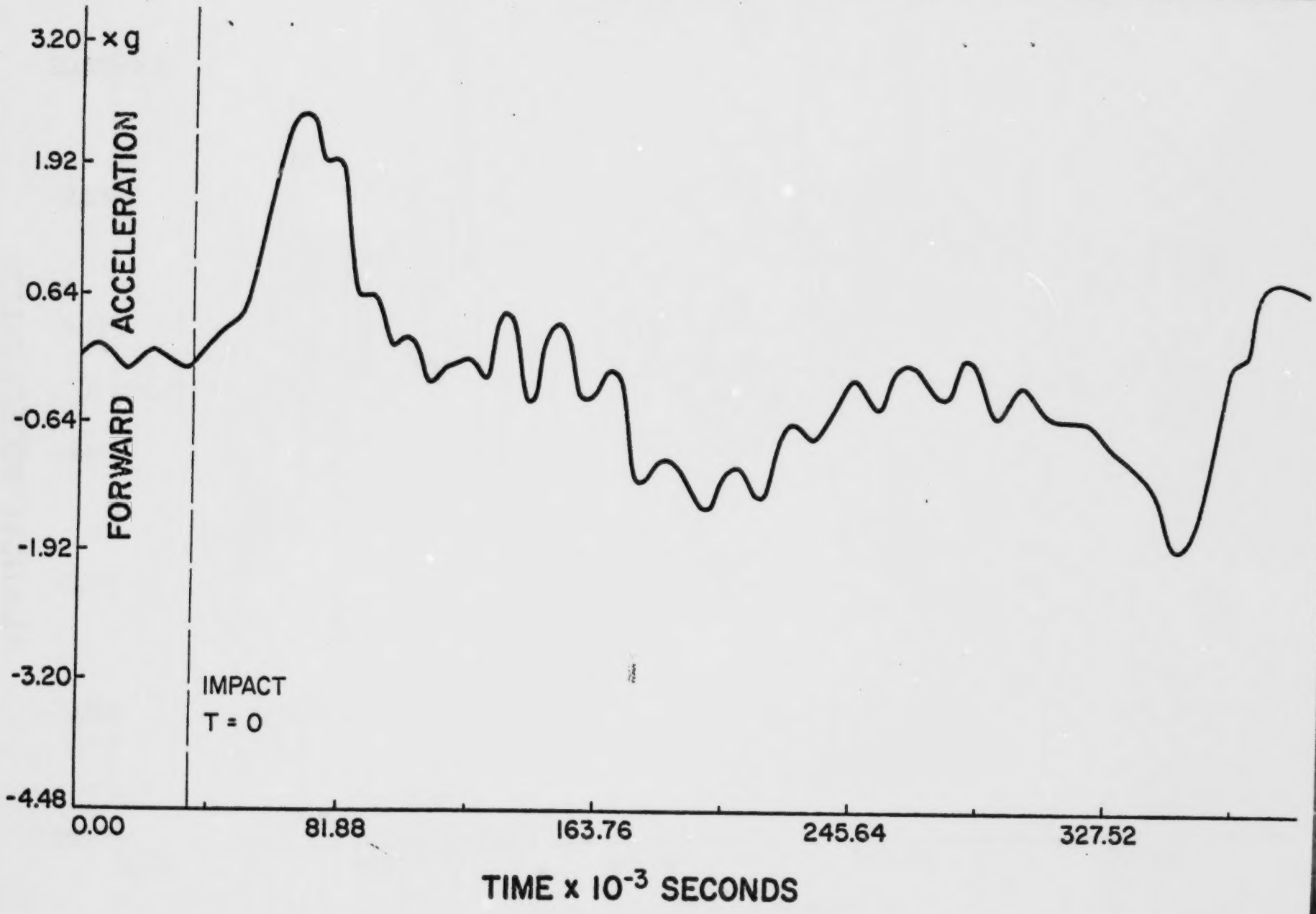

FIG. 29 ACCELERATION-TIME HISTORY @ FLOOR, RIB #5 (OBLIQUE, $\alpha = 2°$, $V_0 = 34.7$ IN/SEC).

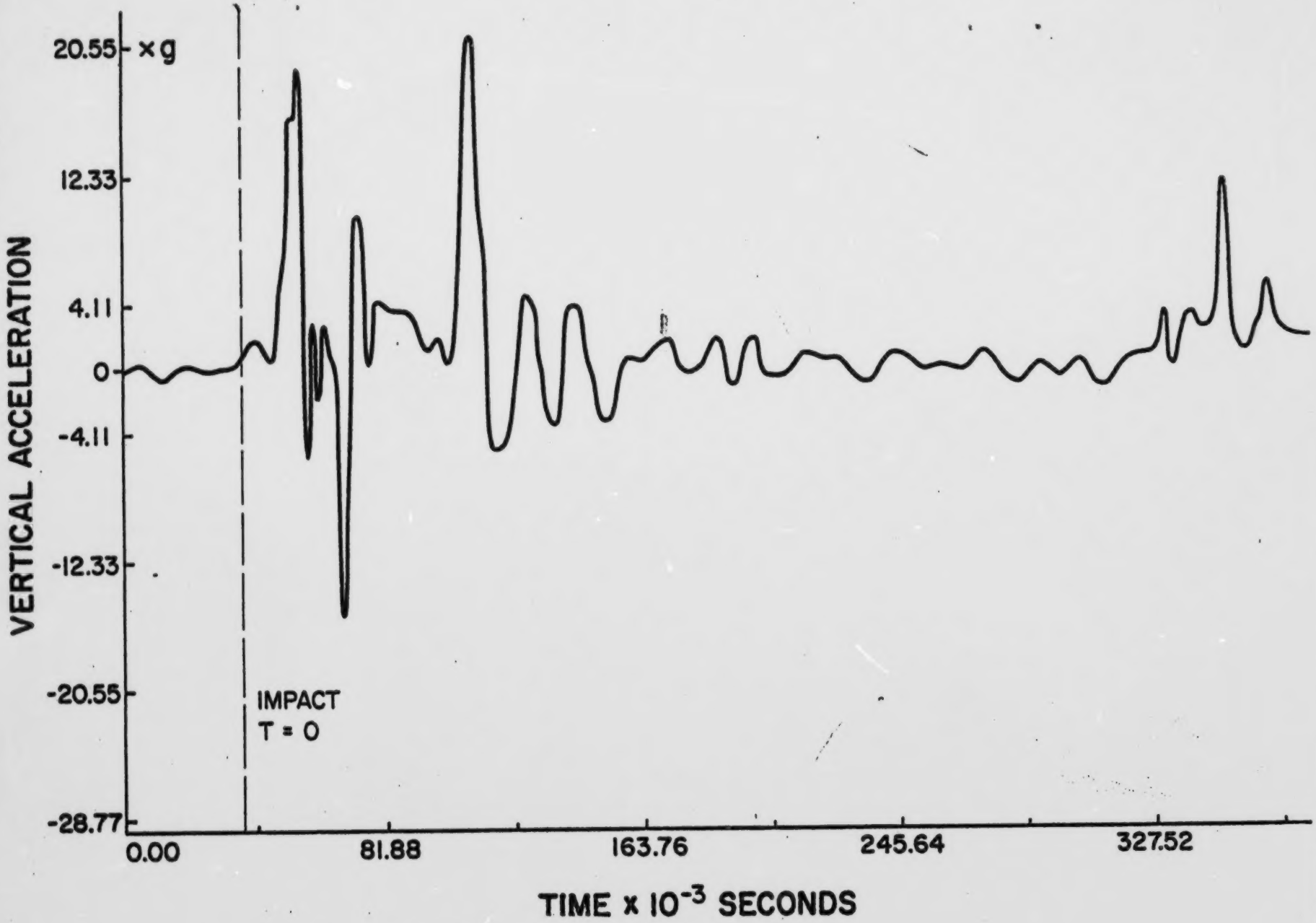

FIG. 30 ACCELERATION-TIME HISTORY @ FLOOR, RIB #5 (OBLIQUE, $\alpha = 2°$, $V_o = 34.7$ IN/SEC).

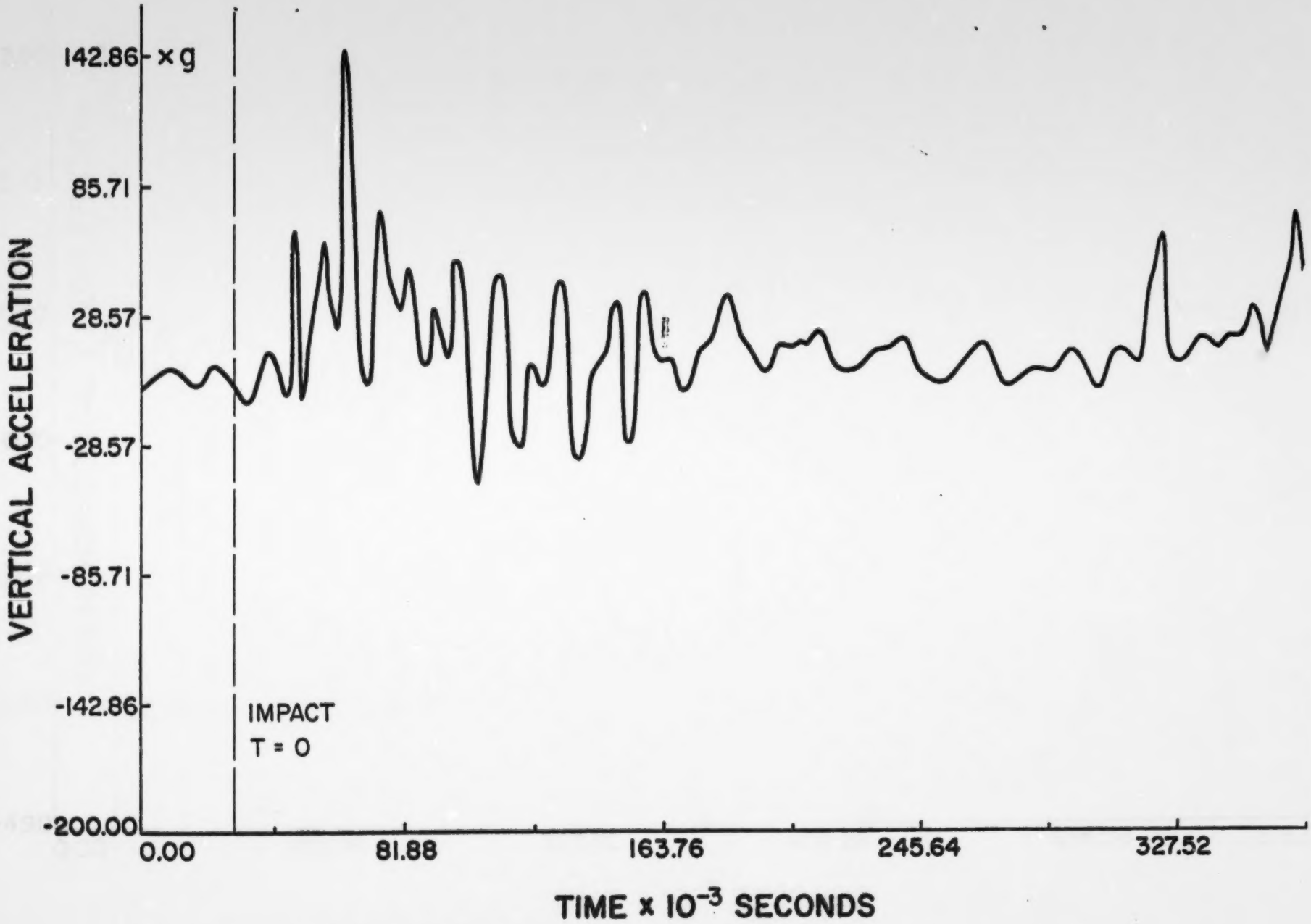

FIG. 31 ACCELERATION-TIME HISTORY @ FLOOR, RIB #10 (OBLIQUE, $\alpha = 2°$, $V_o = 34.7$ IN/SEC).

FIG. 32 ACCELERATION TIME HISTORY (WING LOAD); FREE FLIGHT

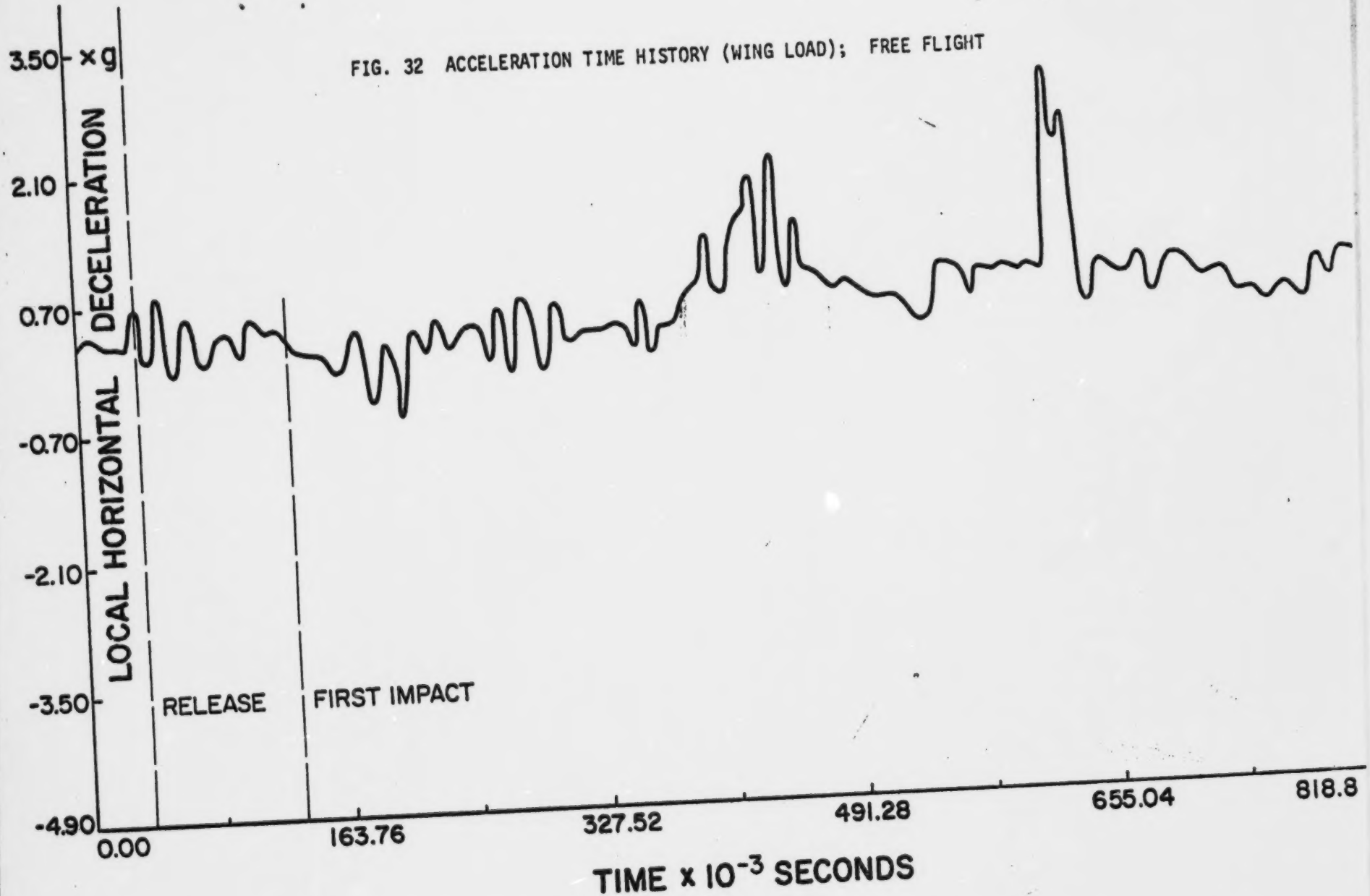

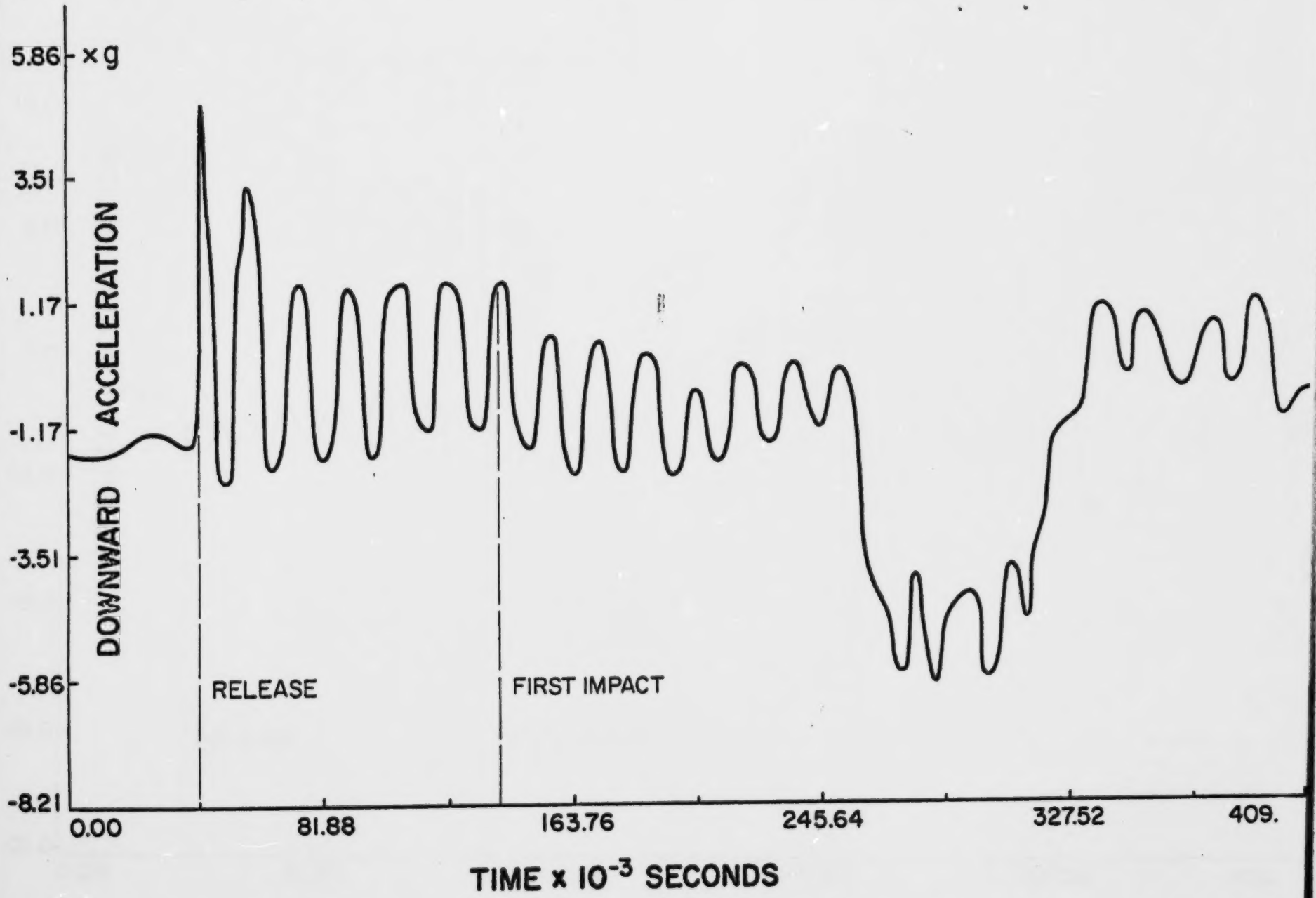

FIG. 33 ACCELERATION-TIME HISTORY (WING LOAD): FREE FLIGHT.

FIG. 34 ACCELERATION-TIME HISTORY (ONE FRAME IN FRONT OF THE FORWARD MAIN FRAME @ FLOOR LEVEL), FREE FLIGHT.

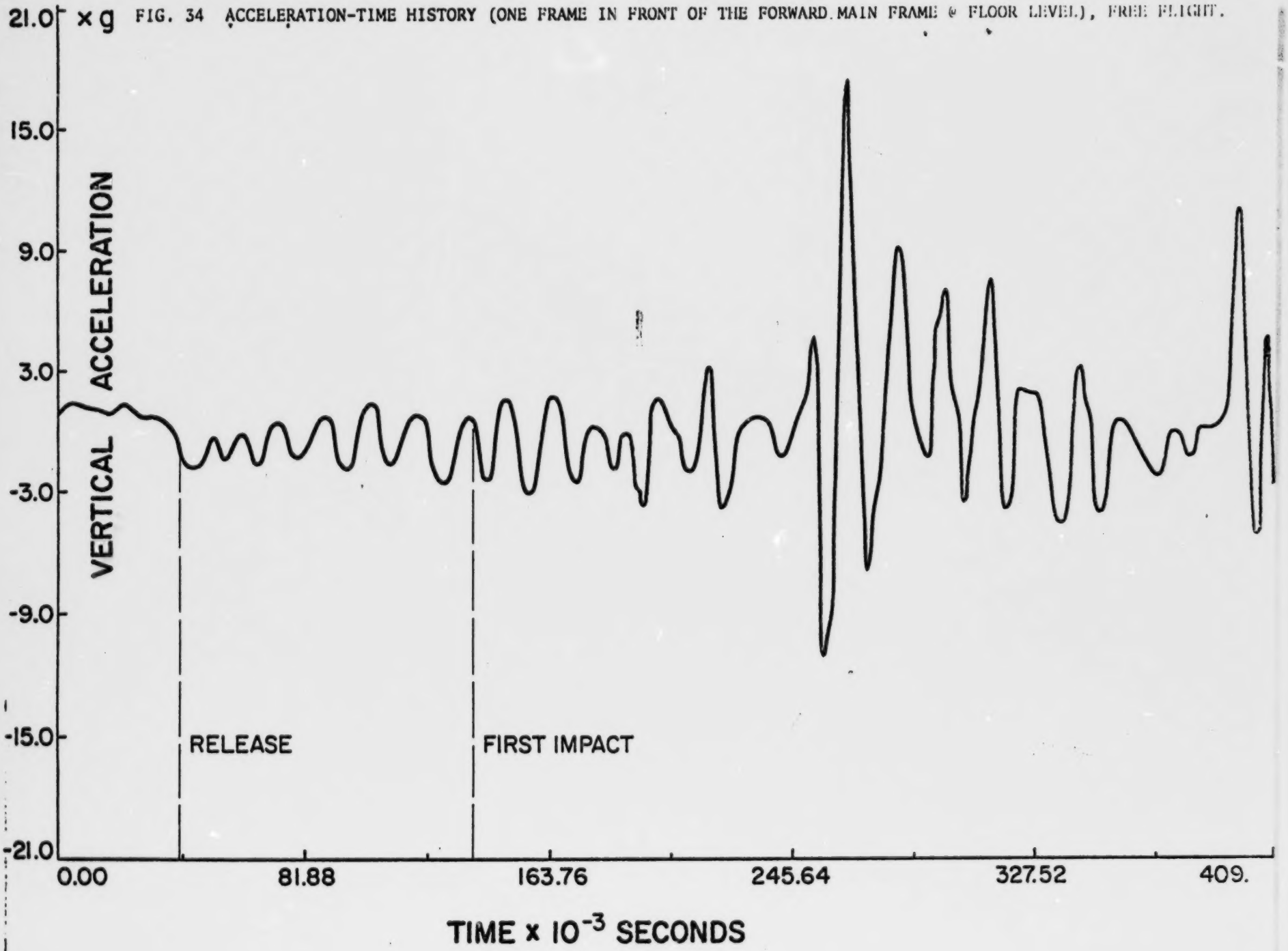

FIG. 35 ACCELERATION TIME HISTORY (1 FRAME BEHIND AFT MAIN FRAME @ FLOOR LEVEL)

FREE FLIGHT

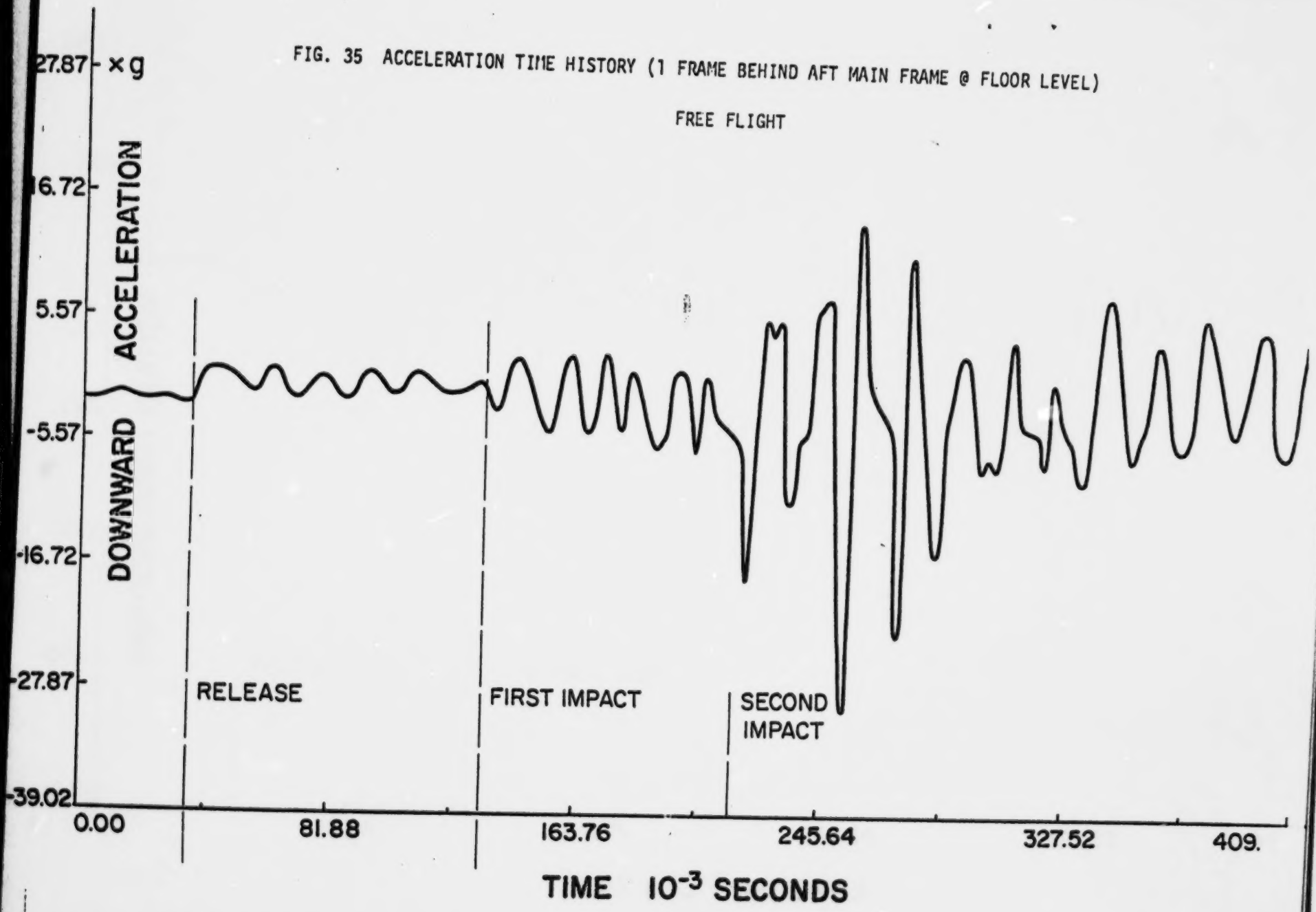

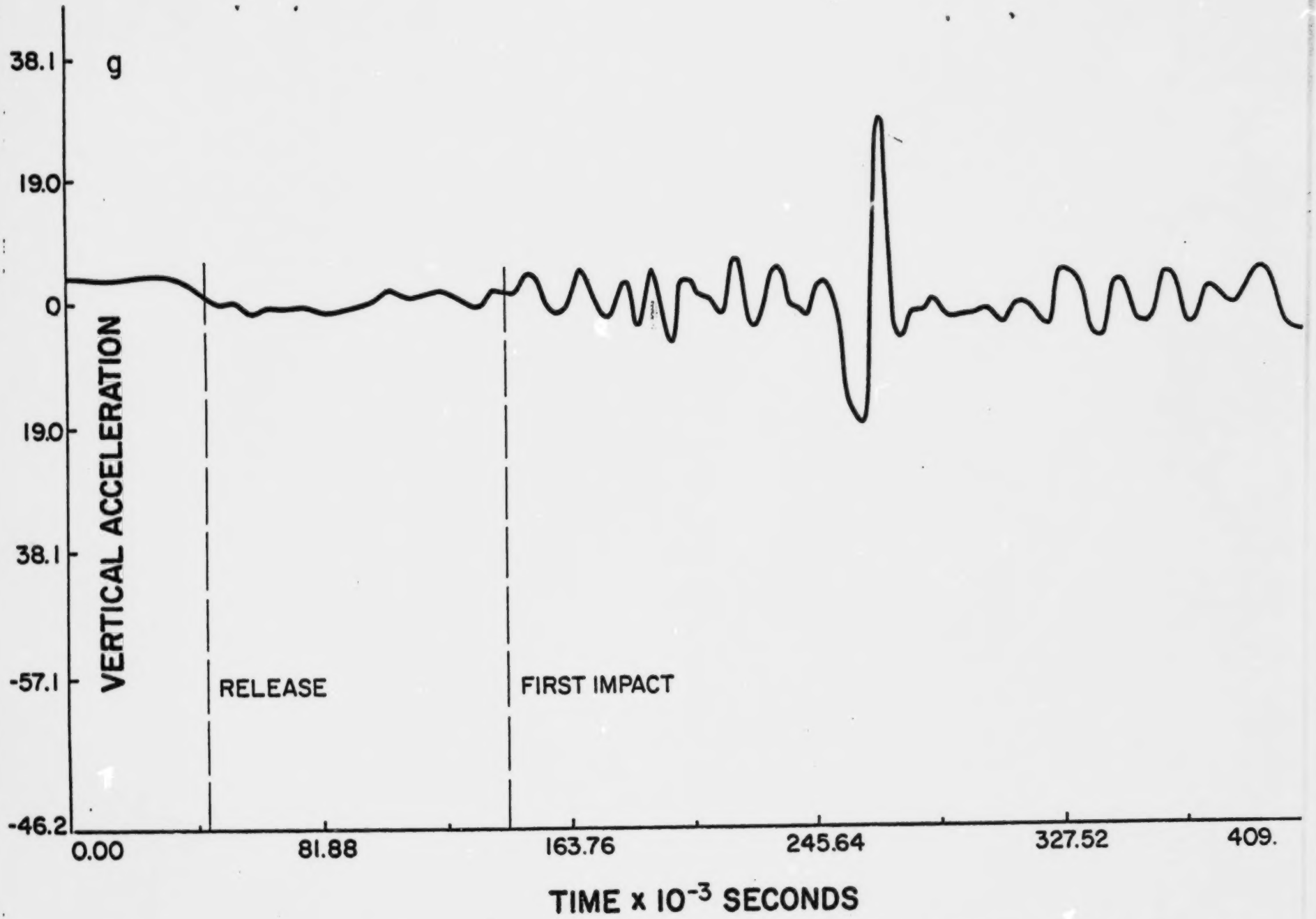

FIG. 36 ACCELERATION-TIME HISTORY (FOURTH FRAME IN FRONT OF FORWARD MAIN FRAME @ FLOOR LEVEL), FREE FLIGHT.

FIG. 37 ACCELERATION TIME HISTORY (ONE FRAME BEFORE AFT MAIN FRAME (FLOOR))

FREE FLIGHT

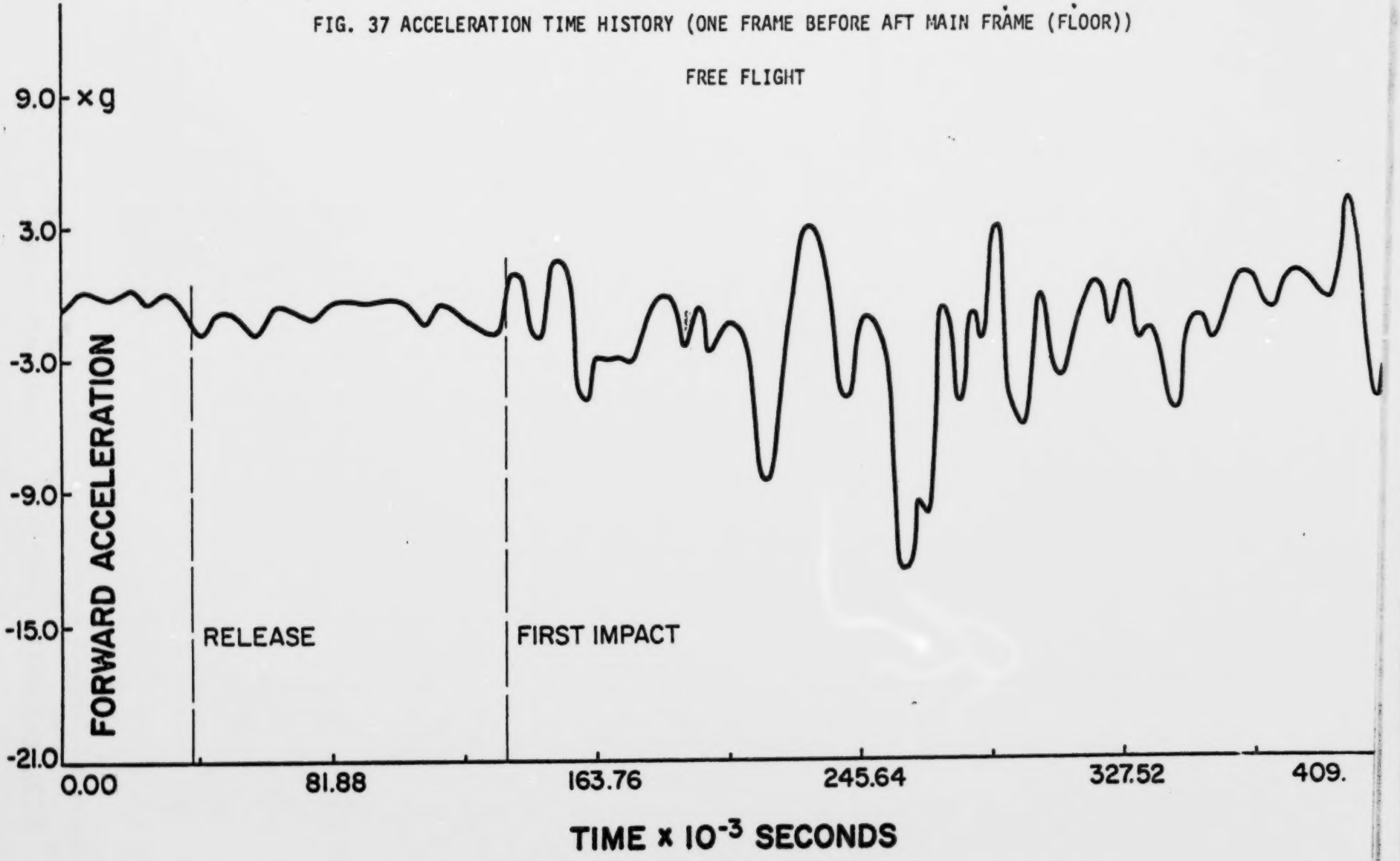

DISPLACEMENT HISTORY OF CENTRE OF MASS

DEGREE OF FREEDOM NUMBER VERT.

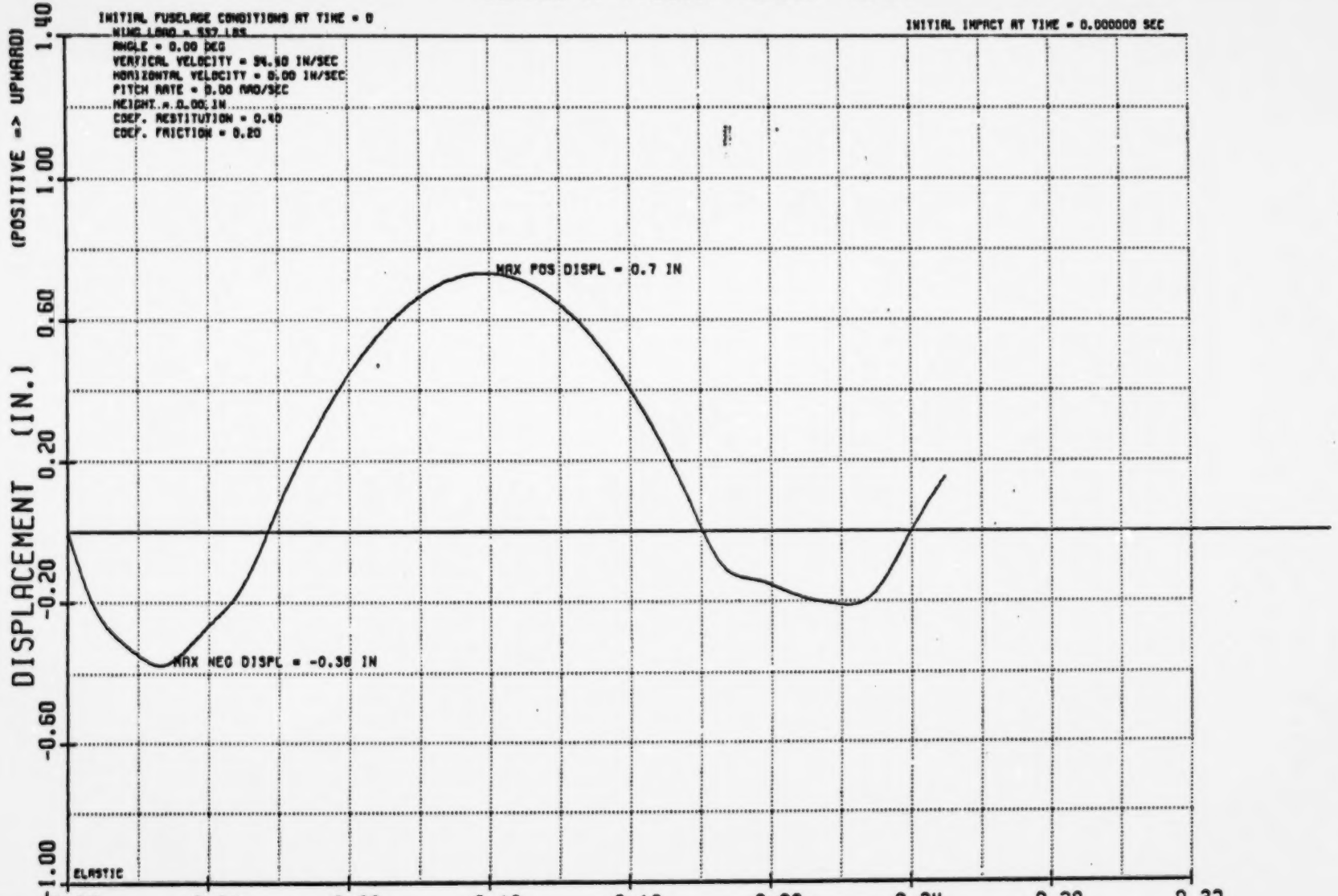

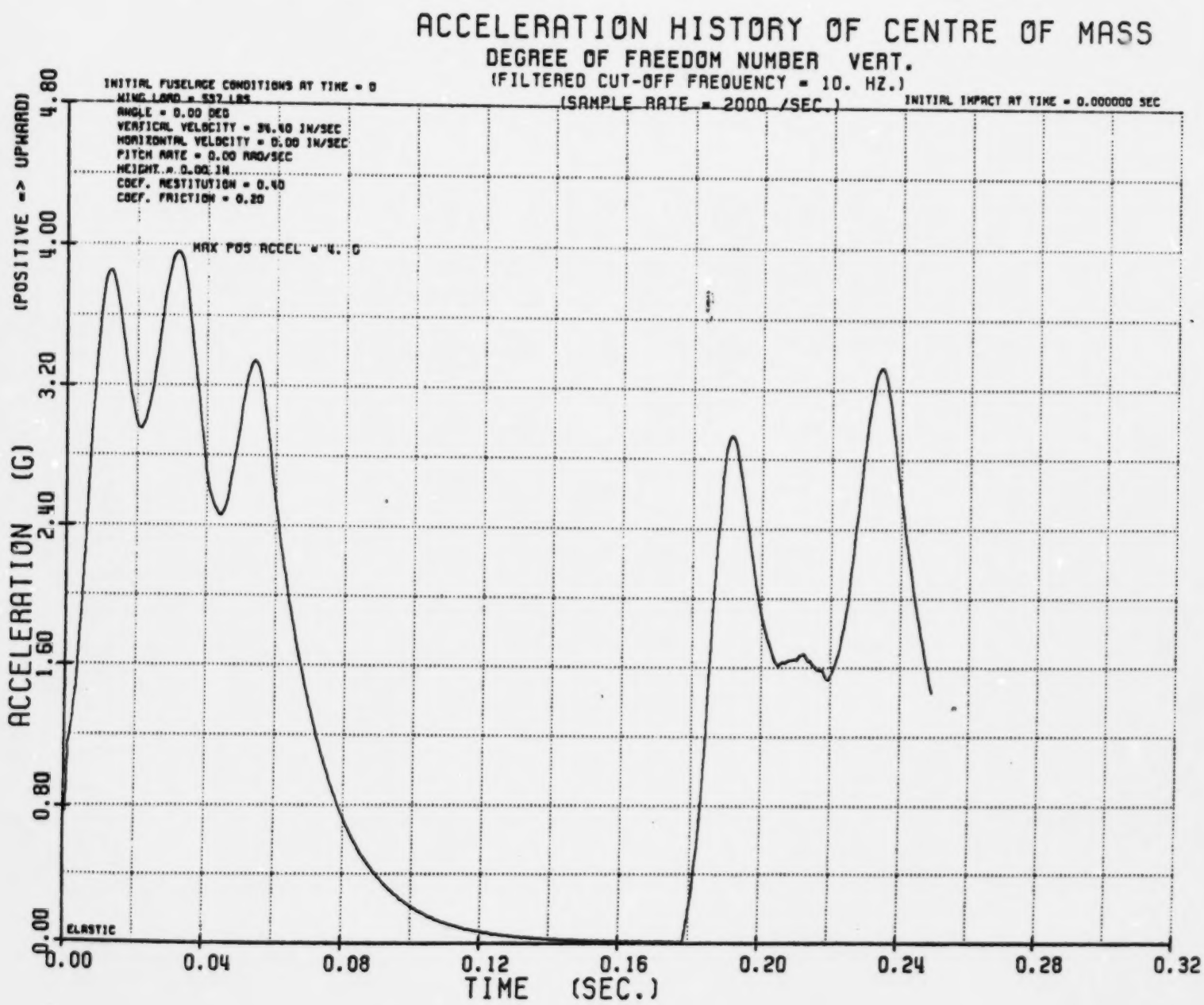
ACCELERATION HISTORY OF CENTRE OF MASS
DEGREE OF FREEDOM NUMBER VERT.
(FILTERED CUT-OFF FREQUENCY = 10. HZ.)
(SAMPLE RATE = 2000 /SEC.)
INITIAL FUSELAGE CONDITIONS AT TIME = 0
WING LOAD = 537 LBS
ANGLE = 0.00 DEG
VERTICAL VELOCITY = 36.40 IN/SEC
HORIZONTAL VELOCITY = 0.00 IN/SEC
PITCH RATE = 0.00 RAD/SEC
HEIGHT = 0.00 IN
COEF. RESTITUTION = 0.40
COEF. FRICTION = 0.20
INITIAL IMPACT AT TIME = 0.000000 SEC
MAX POS ACCEL = 4. G
ELASTIC
ACCELERATION (G) (POSITIVE => UPWARD)
0.00
0.80
1.60
2.40
3.20
4.00
4.80
0.00
0.04
0.08
0.12
0.16
0.20
0.24
0.28
0.32
TIME (SEC.)

DISPLACEMENT HISTORY OF MASS 12

DEGREE OF FREEDOM NUMBER 23 VERT.

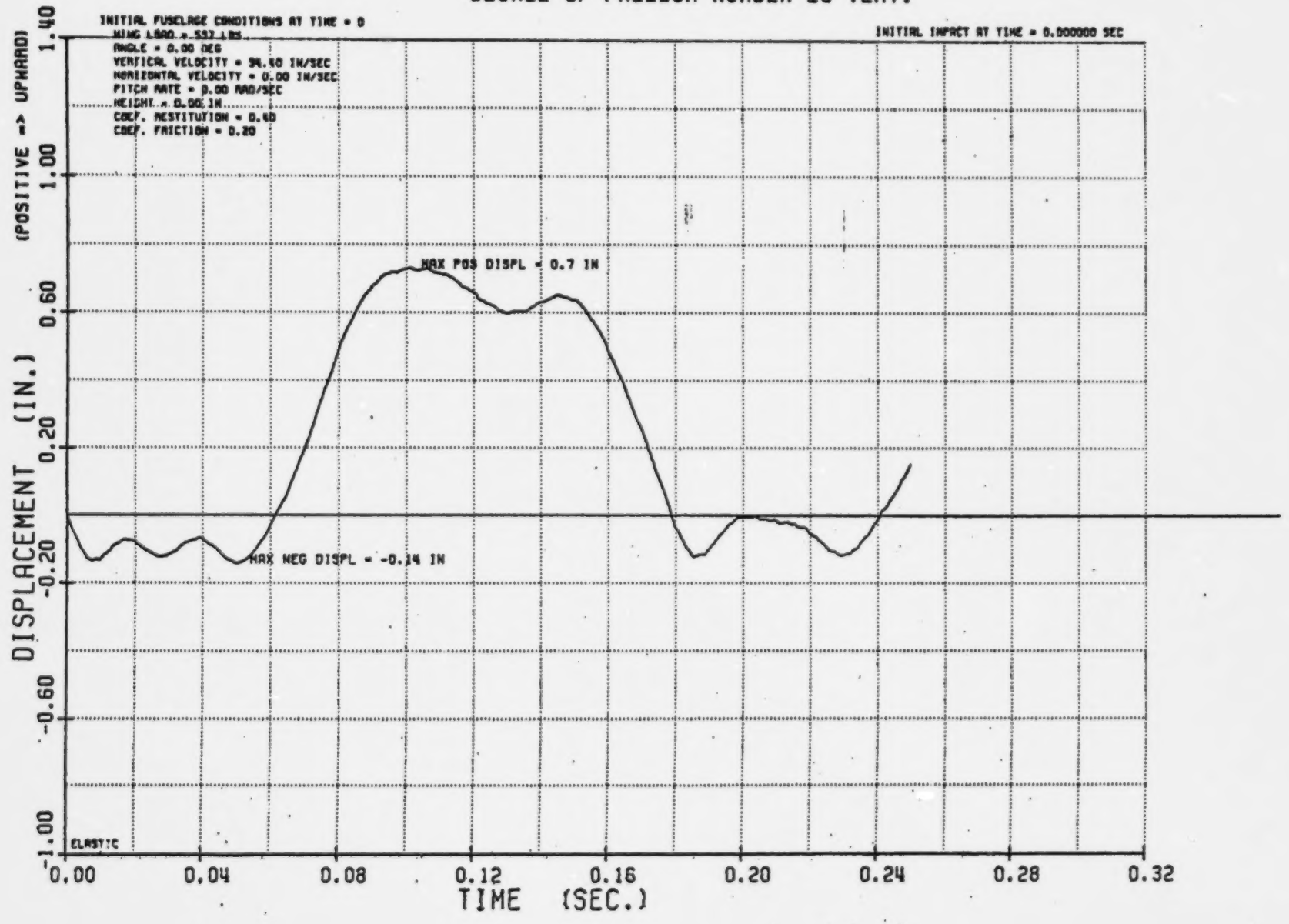

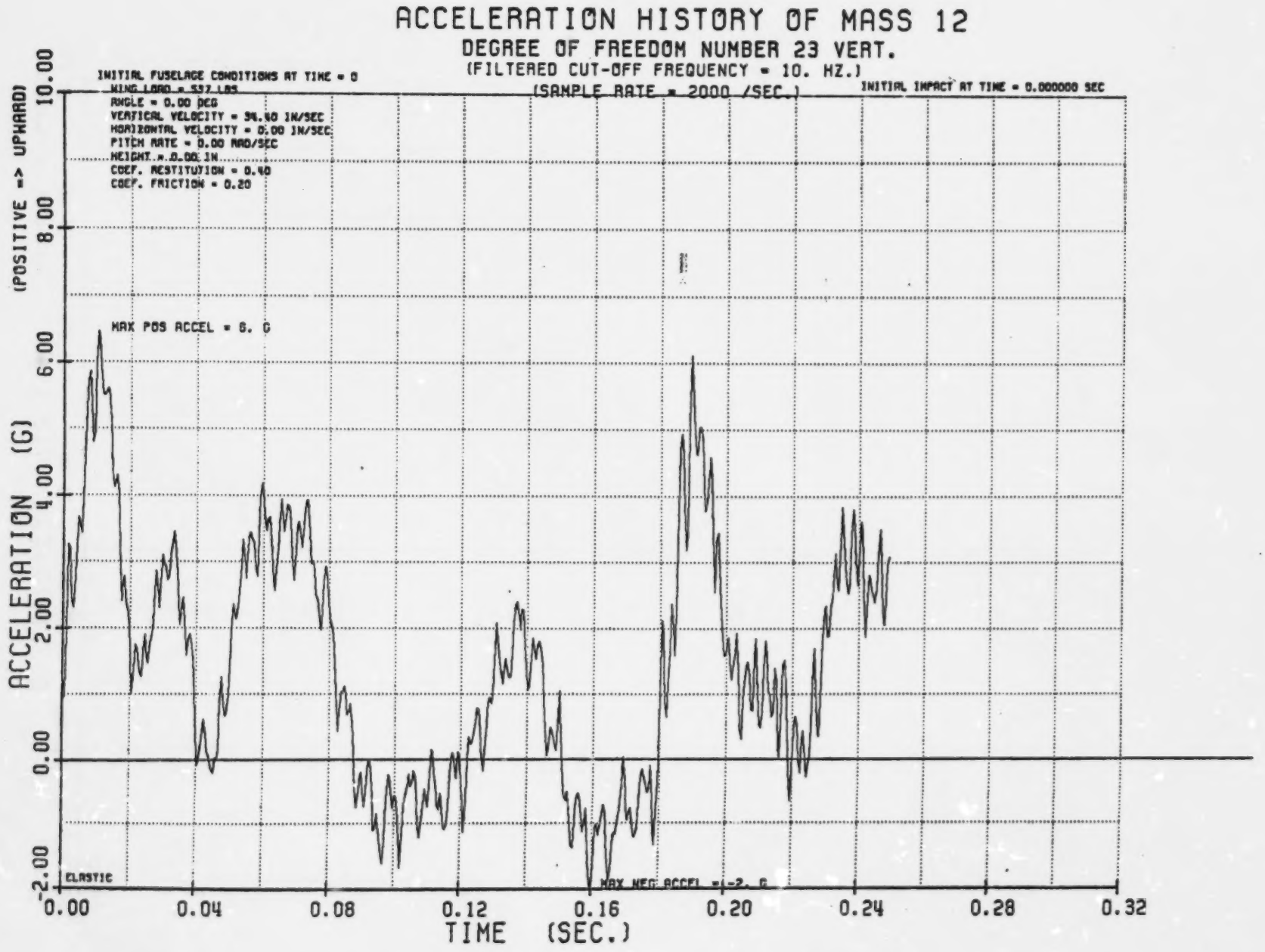
ACCELERATION HISTORY OF MASS 12
DEGREE OF FREEDOM NUMBER 23 VERT.
(FILTERED CUT-OFF FREQUENCY = 10. HZ.)
(SAMPLE RATE = 2000 /SEC.)
INITIAL FUSELAGE CONDITIONS AT TIME = 0
WING LOAD = 537 LBS
ANGLE = 0.00 DEG
VERTICAL VELOCITY = 36.60 IN/SEC
HORIZONTAL VELOCITY = 0.00 IN/SEC
PITCH RATE = 0.00 RAD/SEC
HEIGHT = 0.00 IN
COEF. RESTITUTION = 0.40
COEF. FRICTION = 0.20
INITIAL IMPACT AT TIME = 0.000000 SEC
MAX POS ACCEL = 6. G
MAX NEG ACCEL = -2. G
ELASTIC
ACCELERATION (G)
(POSITIVE => UPWARD)
10.00
8.00
6.00
4.00
2.00
0.00
-2.00
0.00
0.04
0.08
0.12
0.16
0.20
0.24
0.28
0.32
TIME (SEC.)

DISPLACEMENT HISTORY OF MASS 27

DEGREE OF FREEDOM NUMBER 130 VERT.

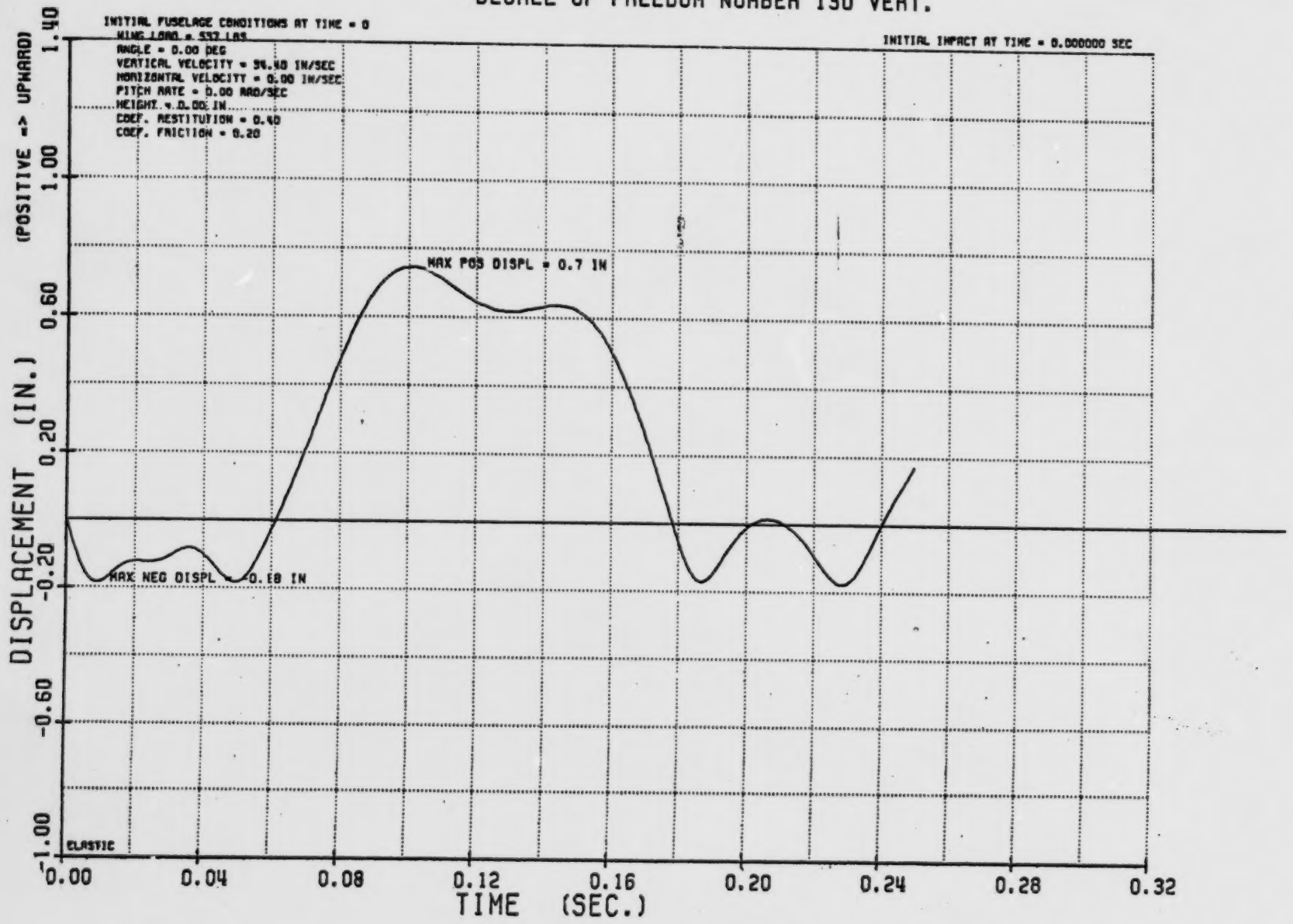

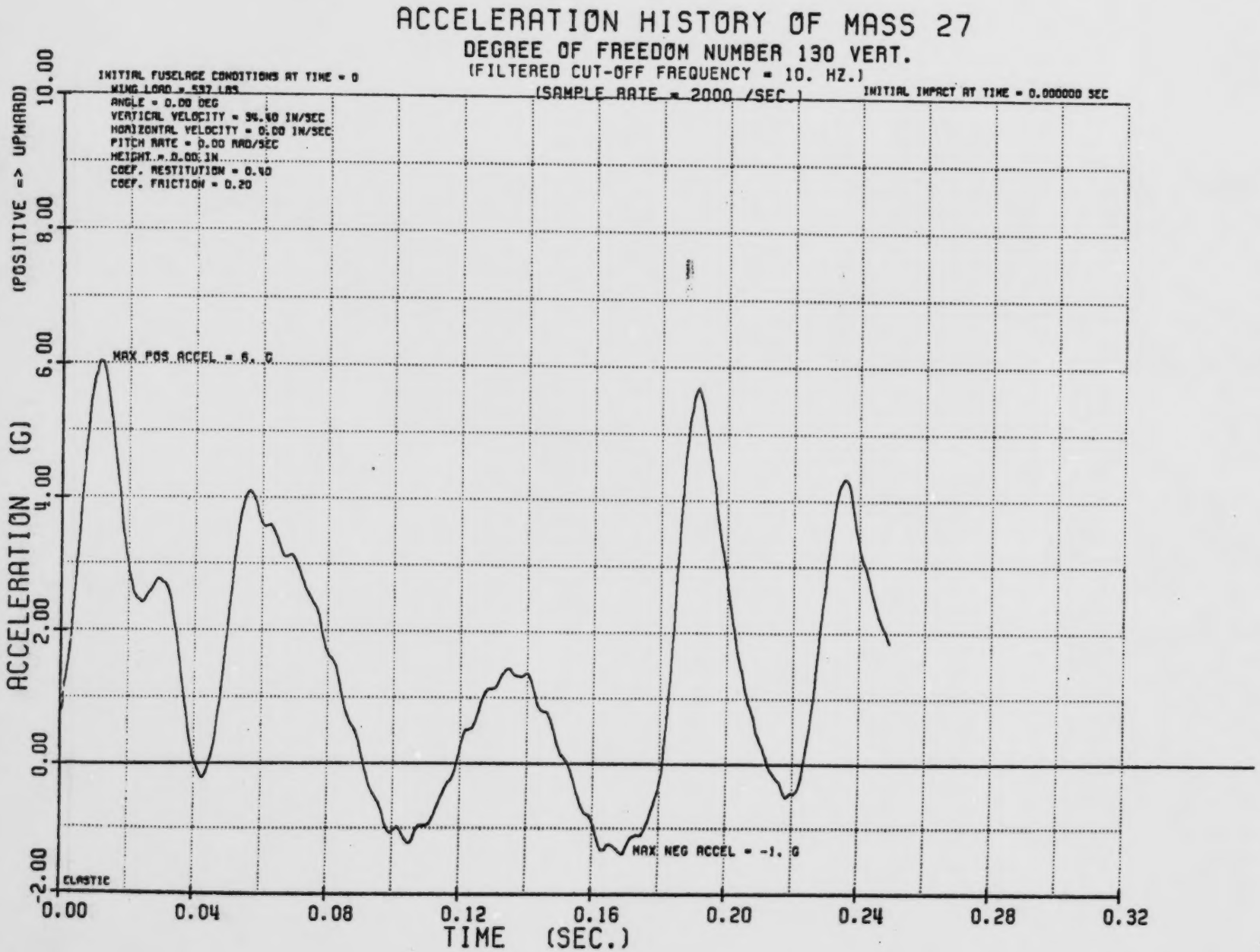
ACCELERATION HISTORY OF MASS 27
DEGREE OF FREEDOM NUMBER 130 VERT.
(FILTERED CUT-OFF FREQUENCY = 10. HZ.)
(SAMPLE RATE = 2000 /SEC.)
INITIAL FUSELAGE CONDITIONS AT TIME = 0
WING LOAD = 537 LBS
ANGLE = 0.00 DEG
VERTICAL VELOCITY = 96.40 IN/SEC
HORIZONTAL VELOCITY = 0.00 IN/SEC
PITCH RATE = 0.00 RAD/SEC
HEIGHT = 0.00 IN
COEF. RESTITUTION = 0.40
COEF. FRICTION = 0.20
INITIAL IMPACT AT TIME = 0.000000 SEC
MAX POS ACCEL = 6. G
MAX NEG ACCEL = -1. G
ELASTIC
ACCELERATION (G) (POSITIVE => UPWARD)
10.00
8.00
6.00
4.00
2.00
0.00
-2.00
0.00
0.04
0.08
0.12
0.16
0.20
0.24
0.28
0.32
TIME (SEC.)

DISPLACEMENT HISTORY OF MASS 35
DEGREE OF FREEDOM NUMBER 92 VERT.

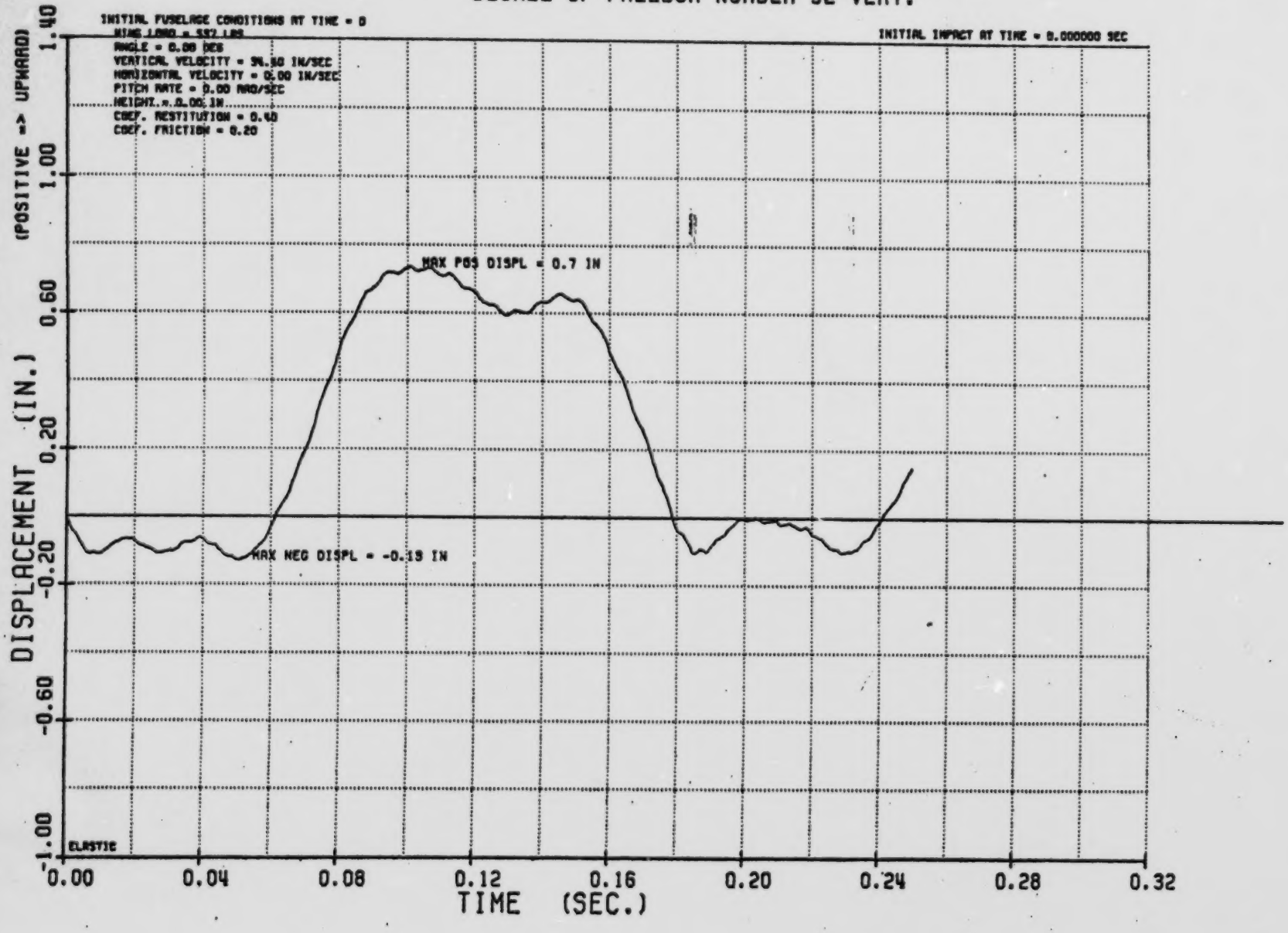

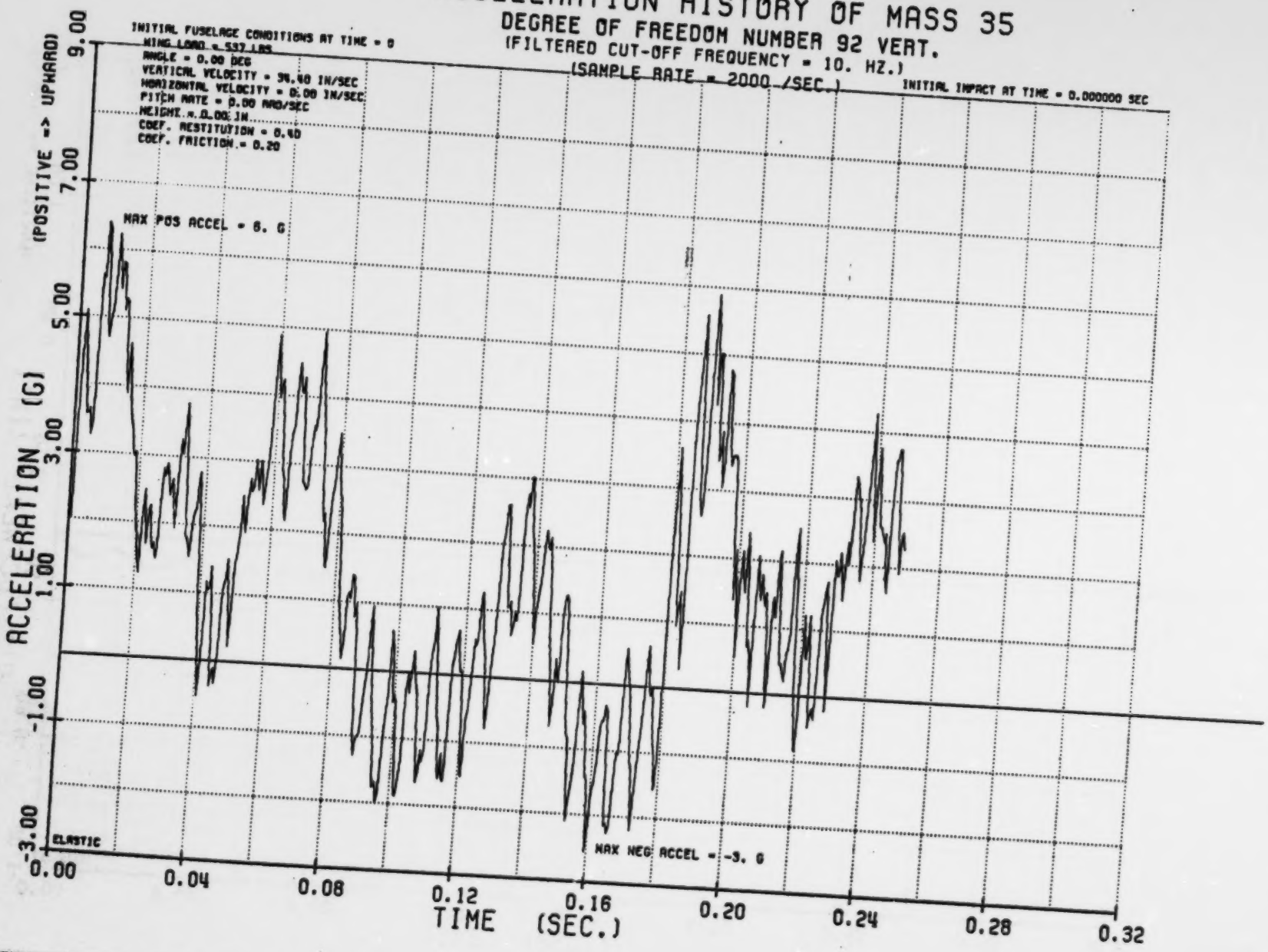
ACCELERATION HISTORY OF MASS 35
DEGREE OF FREEDOM NUMBER 92 VERT.
(FILTERED CUT-OFF FREQUENCY = 10. HZ.)
(SAMPLE RATE = 2000 /SEC.)
INITIAL FUSELAGE CONDITIONS AT TIME = 0
WING LOAD = 537 LBS
ANGLE = 0.00 DEG
VERTICAL VELOCITY = 36.60 IN/SEC
HORIZONTAL VELOCITY = 0.00 IN/SEC
PITCH RATE = 0.00 RAD/SEC
HEIGHT = 0.00 IN
COEF. RESTITUTION = 0.60
COEF. FRICTION = 0.20
INITIAL IMPACT AT TIME = 0.000000 SEC
MAX POS ACCEL = 6. G
MAX NEG ACCEL = -3. G
ELASTIC
ACCELERATION (G)
(POSITIVE => UPWARD)
9.00
7.00
5.00
3.00
1.00
-1.00
-3.00
0.00
0.04
0.08
0.12
0.16
0.20
0.24
0.28
0.32
TIME (SEC.)

DISPLACEMENT HISTORY OF MASS 43

DEGREE OF FREEDOM NUMBER 128 VERT.

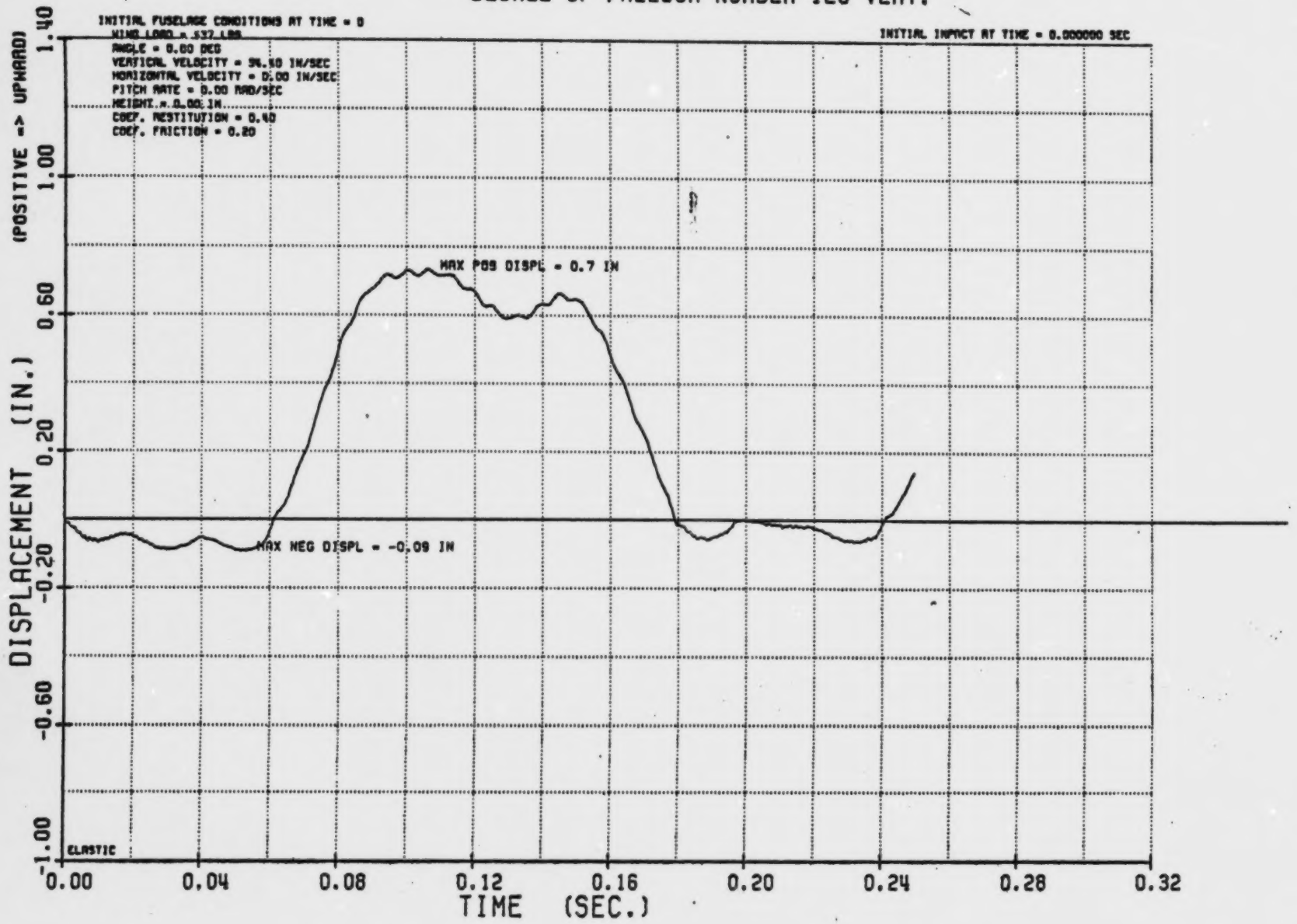

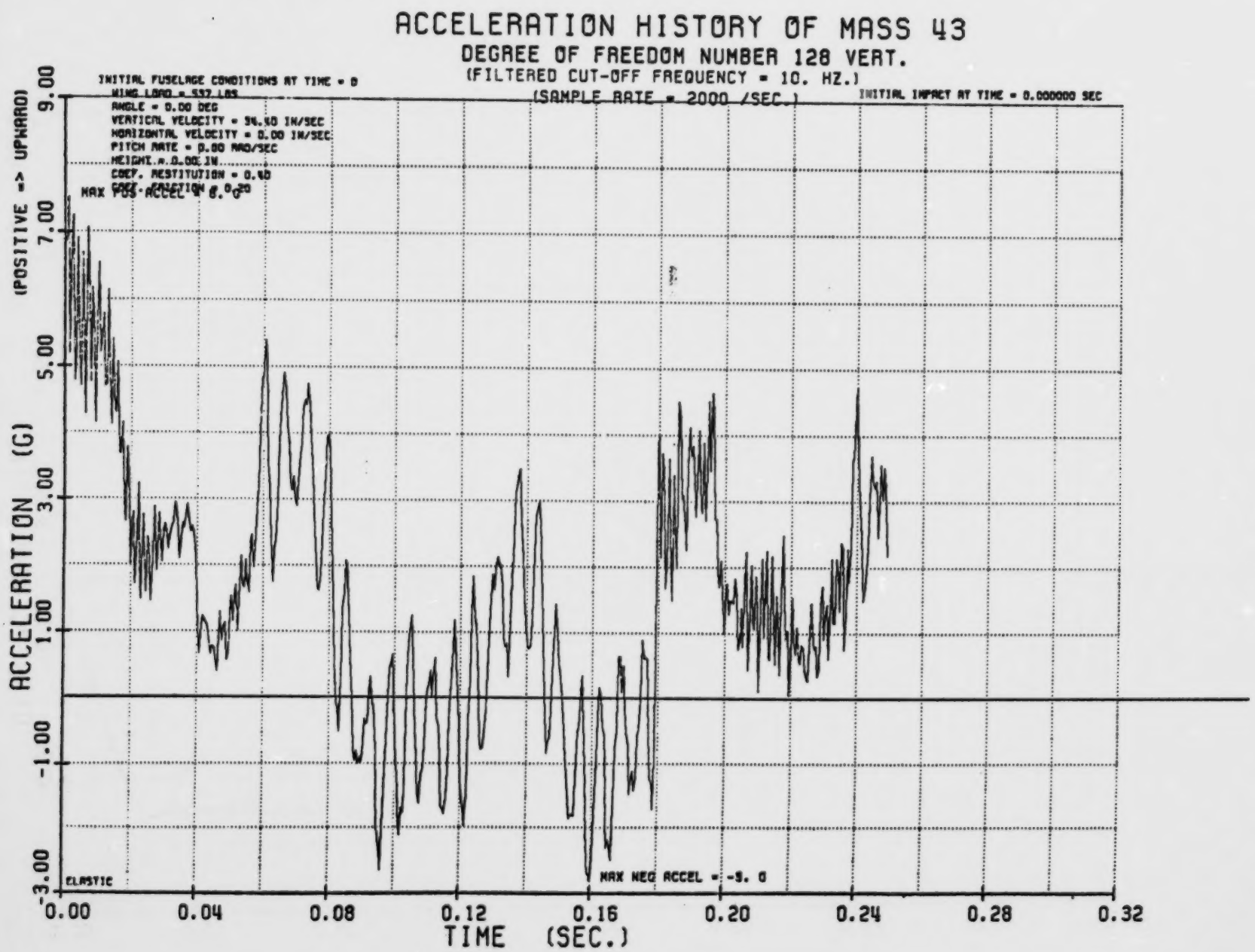
ACCELERATION HISTORY OF MASS 43
DEGREE OF FREEDOM NUMBER 128 VERT.
(FILTERED CUT-OFF FREQUENCY = 10. HZ.)
(SAMPLE RATE = 2000 /SEC.)
INITIAL FUSELAGE CONDITIONS AT TIME = 0
WING LOAD = 557 LBS
ANGLE = 0.00 DEG
VERTICAL VELOCITY = 94.50 IN/SEC
HORIZONTAL VELOCITY = 0.00 IN/SEC
PITCH RATE = 0.00 RAD/SEC
HEIGHT = 0.00 IN
COEF. RESTITUTION = 0.40
INITIAL IMPACT AT TIME = 0.000000 SEC
MAX POS ACCEL = 8.020
MAX NEG ACCEL = -3. 0
ELASTIC
ACCELERATION (G)
(POSITIVE => UPWARD)
9.00
7.00
5.00
3.00
1.00
-1.00
-3.00
0.00
0.04
0.08
0.12
0.16
0.20
0.24
0.28
0.32
TIME (SEC.)

DISPLACEMENT HISTORY OF MASS 44

DEGREE OF FREEDOM NUMBER 142 VERT.

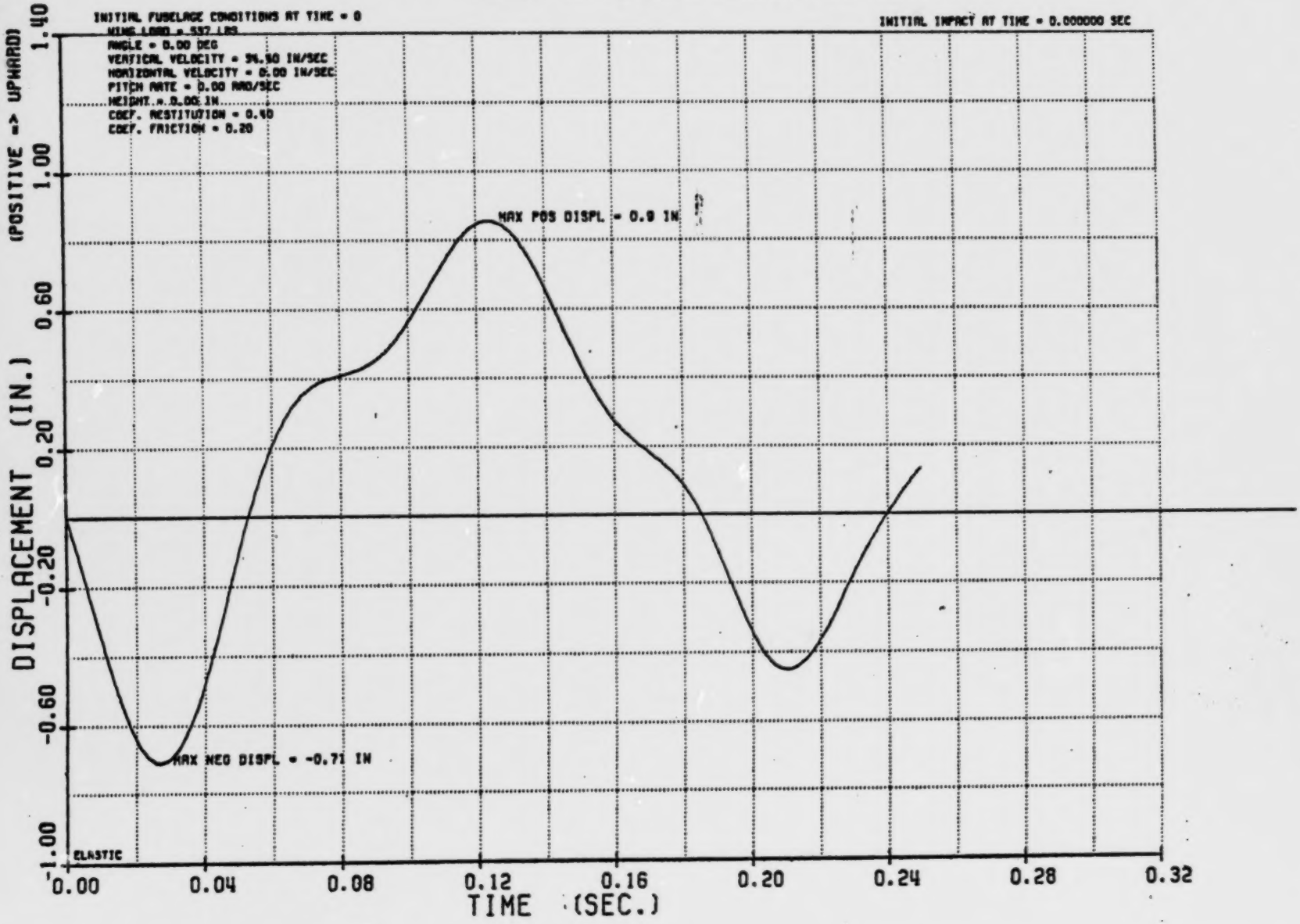

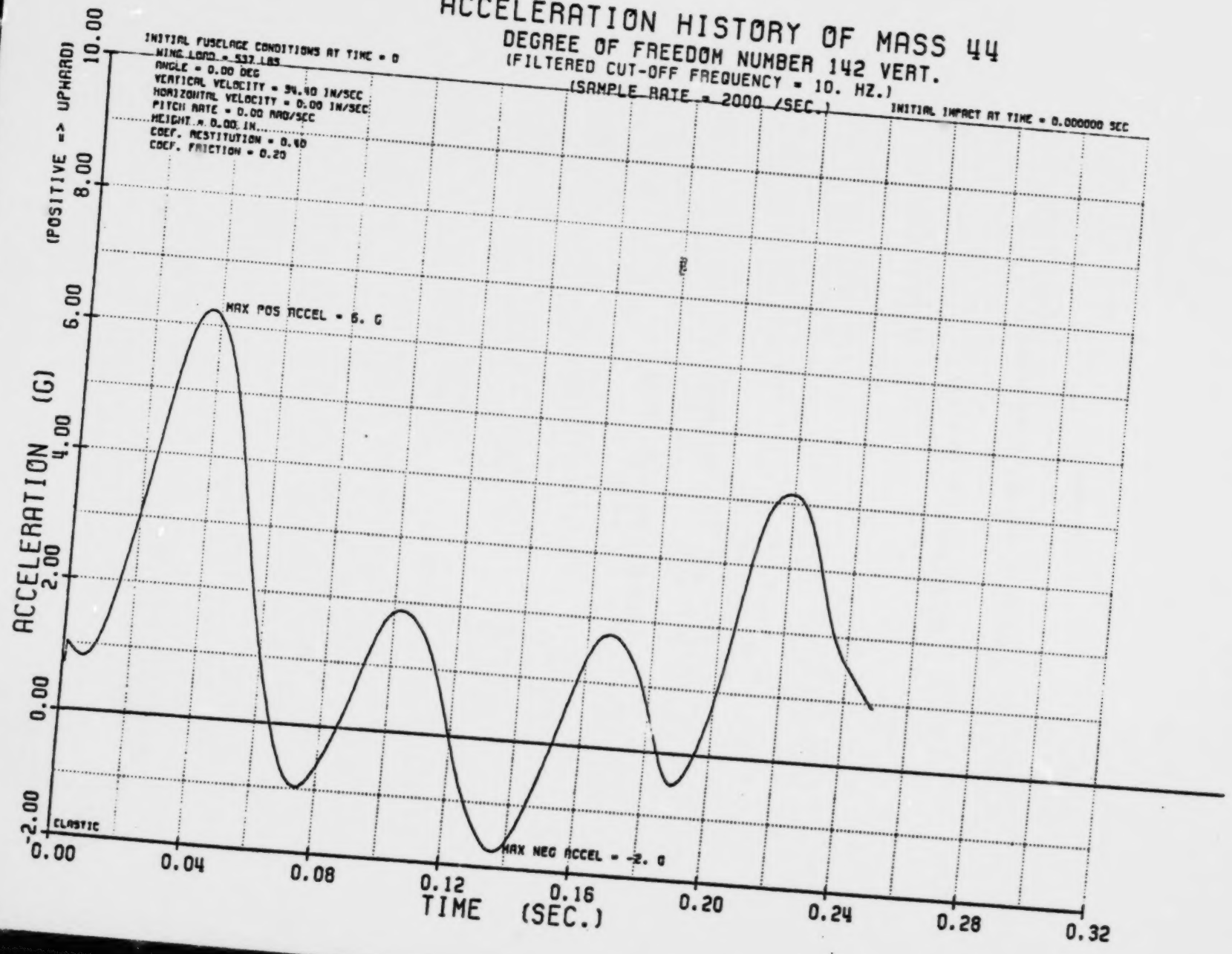
ACCELERATION HISTORY OF MASS 44
DEGREE OF FREEDOM NUMBER 142 VERT.
(FILTERED CUT-OFF FREQUENCY = 10. HZ.)
(SAMPLE RATE = 2000 /SEC.)
INITIAL IMPACT AT TIME = 0.000000 SEC
INITIAL FUSELAGE CONDITIONS AT TIME = 0
WING LOAD = 537 LBS
ANGLE = 0.00 DEG
VERTICAL VELOCITY = 36.40 IN/SEC
HORIZONTAL VELOCITY = 0.00 IN/SEC
PITCH RATE = 0.00 RAD/SEC
HEIGHT = 0.00 IN.
COEF. RESTITUTION = 0.40
COEF. FRICTION = 0.20
MAX POS ACCEL = 6. G
MAX NEG ACCEL = -2. G
ELASTIC
ACCELERATION (G)
(POSITIVE => UPWARD)
10.00
8.00
6.00
4.00
2.00
0.00
-2.00
0.00
0.04
0.08
0.12
0.16
0.20
0.24
0.28
0.32
TIME (SEC.)

APPENDIX B

PREDICTED LEVEL IMPACT RESPONSE*

BASED ON CFE FORMULATION

CASE 1: V_o = -24.7 in/sec

Wing Load = 537 lbs.

CASE 2: V_o = 52.5 in/sec

Wing Load = 537 lbs.

DISPLACEMENTS, ACCELERATIONS,

STRAINS AND GRAPHICS

(REFER TO FIG. 3 FOR ELEMENT NODE NOS.)

*Accelerations of nodes 61, 136, 137 are filtered using a fifth-order Chebyshev low-pass filter with a passband of 62.5 Hz and stopband edge of 125 Hz.

INITIAL IMPACT CONDITIONS AT T = 0.0
WING LOAD SIMULATION: 537 LBS
VERTICAL VELOCITY = -2.89 FT PER SECOND
HORIZONTAL VELOCITY = 0.00 FT PER SECOND
ANGLE = 0.00 DEG. PITCH RATE = 0.00 RAD/SECOND

TIME IS 0.0000 SECONDS
TIME STEP = 0.00100 SECONDS

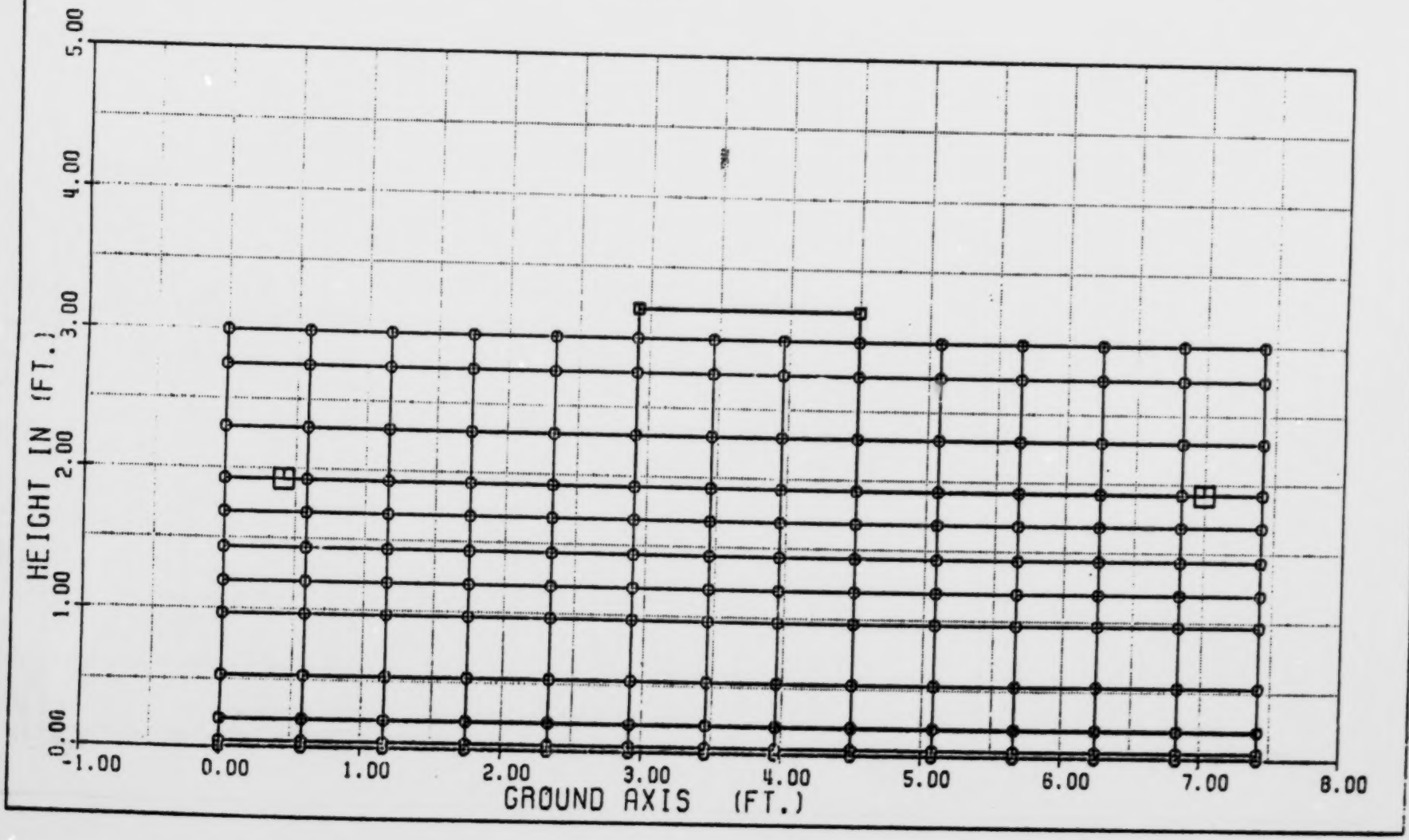

INITIAL IMPACT CONDITIONS AT T = 0.0
WING LOAD SIMULATION: 537 IBS
VERTICAL VELOCITY = -2.89 FT PER SECOND
HORIZONTAL VELOCITY = 0.00 FT PER SECOND
ANGLE = 0.00 DEG. PITCH RATE = 0.00 RAD/SECOND

TIME IS 0.0100 SECONDS
TIME STEP = 0.00100 SECONDS

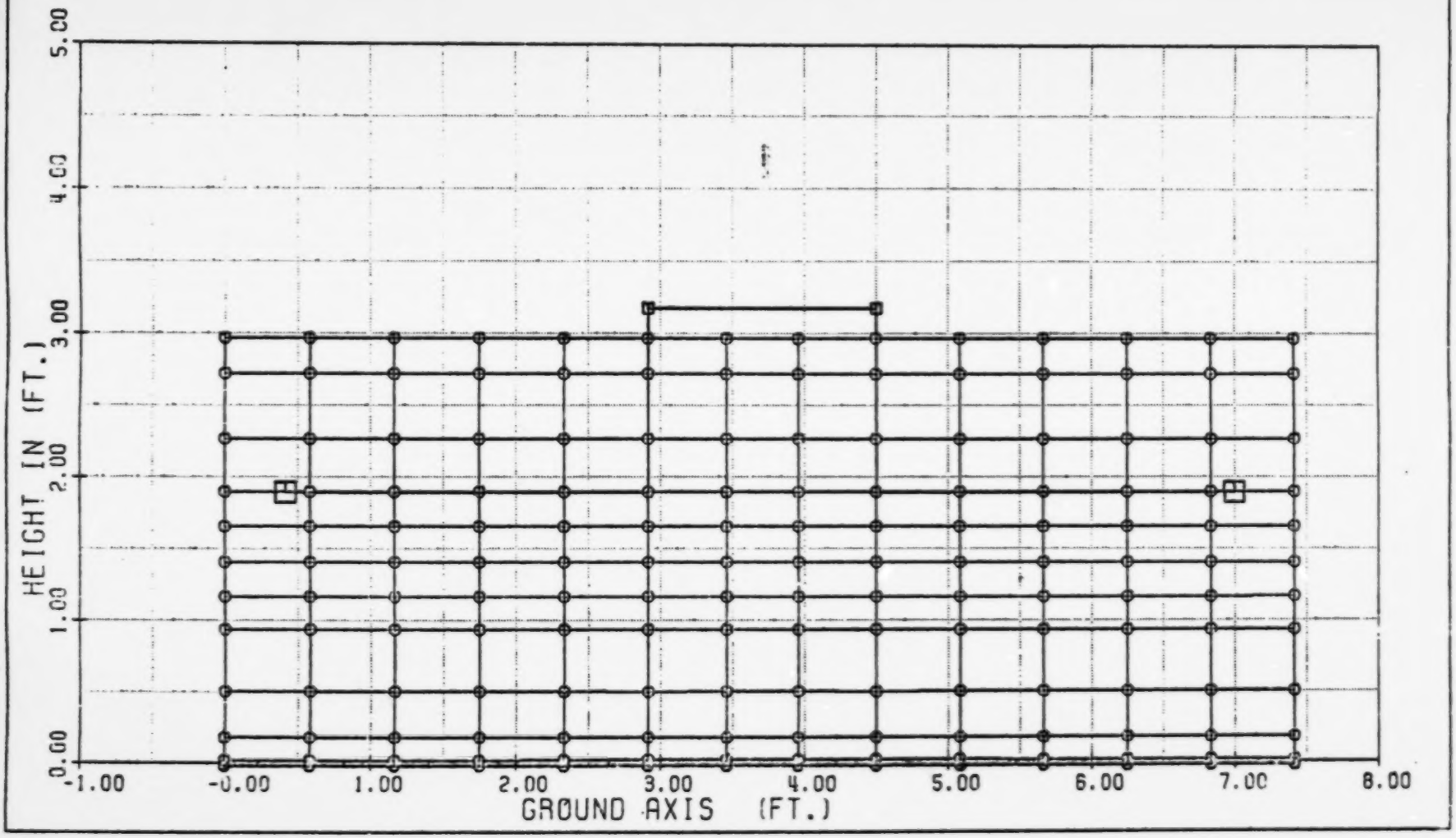

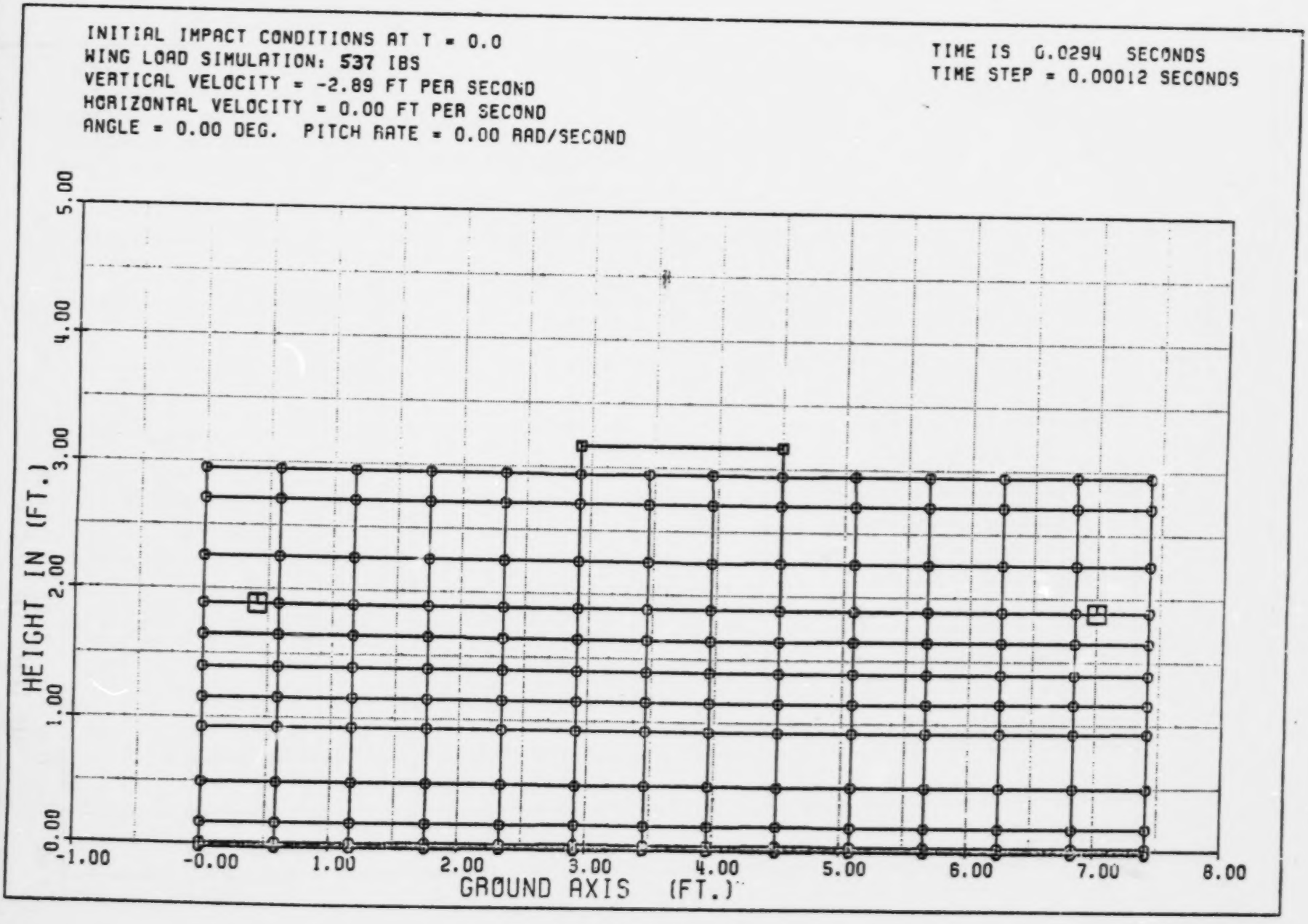
INITIAL IMPACT CONDITIONS AT T = 0.0
WING LOAD SIMULATION: 537 IBS
VERTICAL VELOCITY = -2.89 FT PER SECOND
HORIZONTAL VELOCITY = 0.00 FT PER SECOND
ANGLE = 0.00 DEG. PITCH RATE = 0.00 RAD/SECOND
TIME IS 0.0294 SECONDS
TIME STEP = 0.00012 SECONDS
HEIGHT IN (FT.)
5.00
4.00
3.00
2.00
1.00
0.00
-1.00
-0.00
1.00
2.00
3.00
4.00
5.00
6.00
7.00
8.00
GROUND AXIS (FT.)

INITIAL IMPACT CONDITIONS AT T = 0.0
WING LOAD SIMULATION: 537 IBS
VERTICAL VELOCITY = -2.89 FT PER SECOND
HORIZONTAL VELOCITY = 0.00 FT PER SECOND
ANGLE = 0.00 DEG. PITCH RATE = 0.00 RAD/SECOND

TIME IS 0.0307 SECONDS
TIME STEP = 0.00012 SECONDS

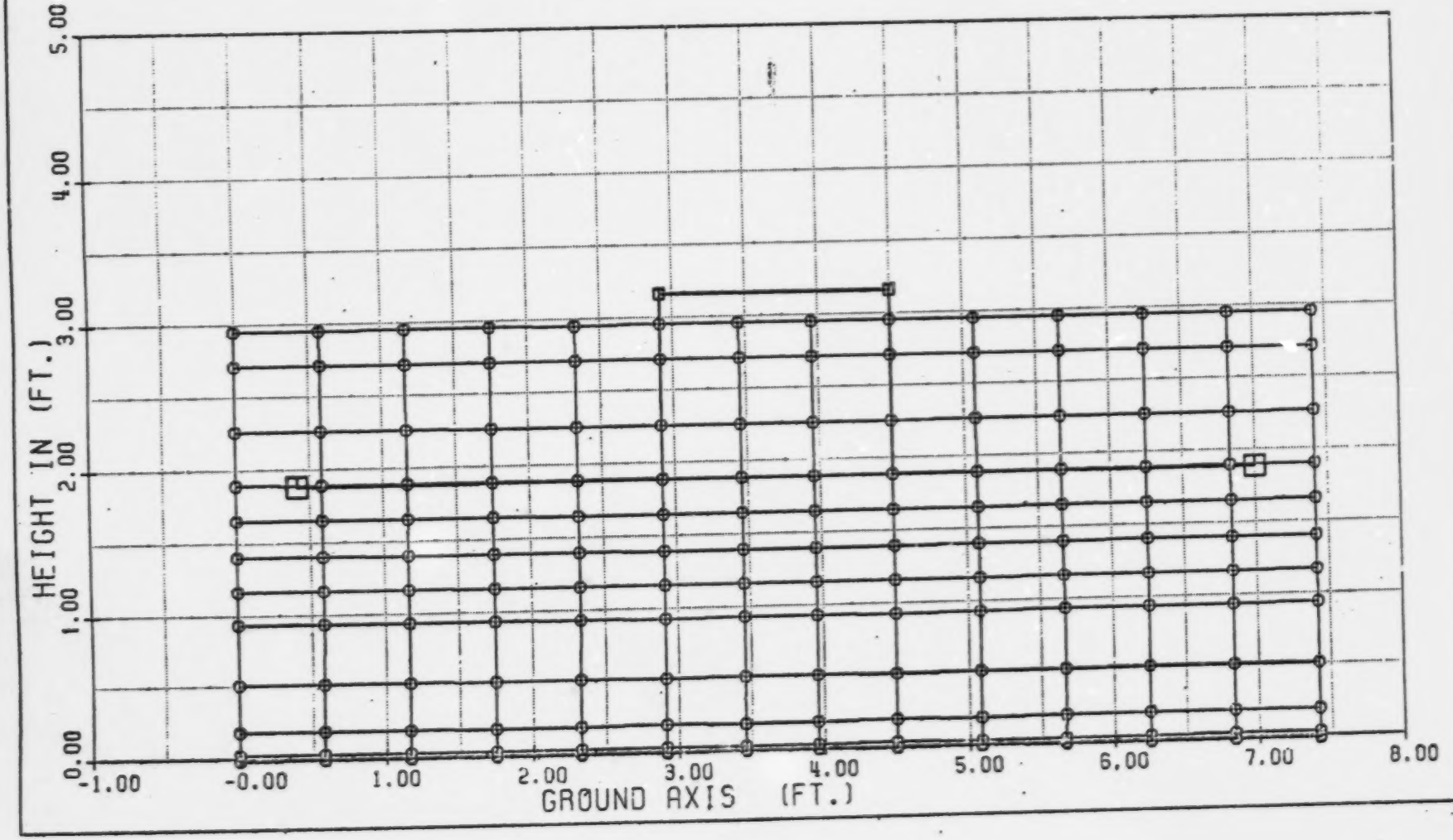

INITIAL IMPACT CONDITIONS AT T = 0.0
WING LOAD SIMULATION: 537 IBS
VERTICAL VELOCITY = -2.89 FT PER SECOND
HORIZONTAL VELOCITY = 0.00 FT PER SECOND
ANGLE = 0.00 DEG. PITCH RATE = 0.00 RAD/SECOND

TIME IS 0.0321 SECONDS
TIME STEP = 0.00012 SECONDS

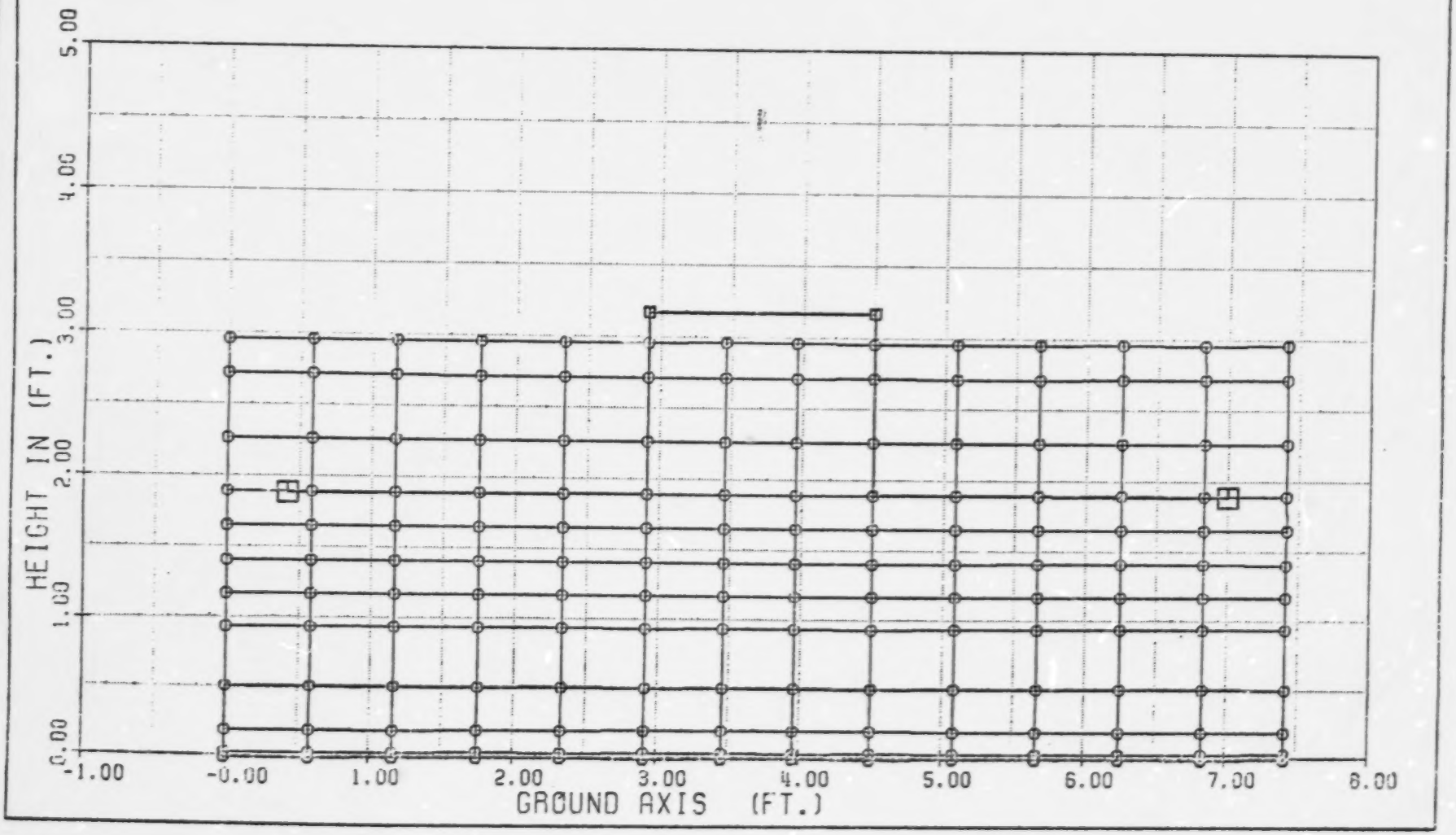

VERTICAL ACCELERATION OF NODE 211 .
UNITS: (G)

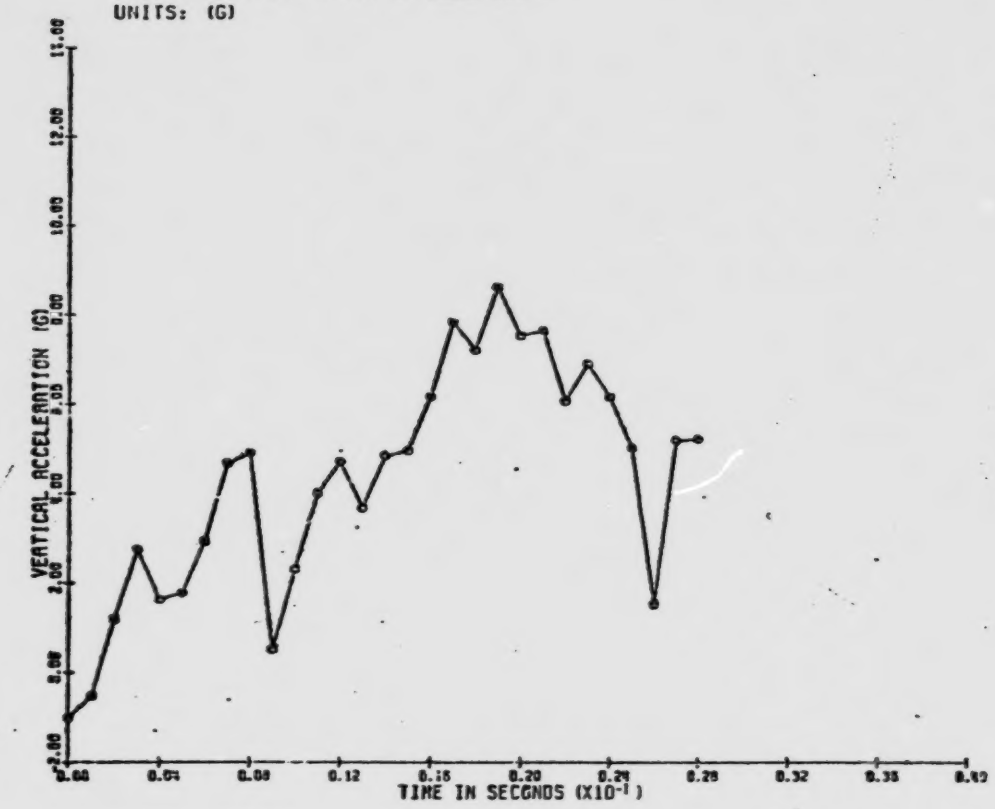

VERTICAL ACCELERATION OF NODE 214
UNITS: (G)

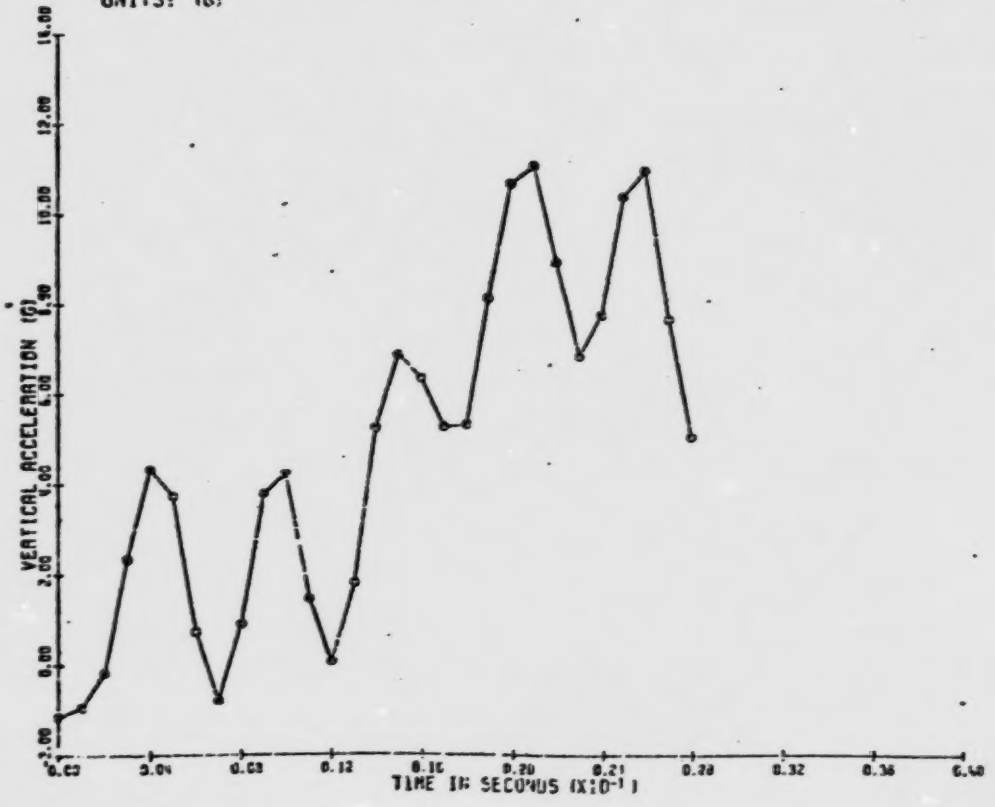

VERTICAL ACCELERATION OF NODE 61
UNITS: (G)

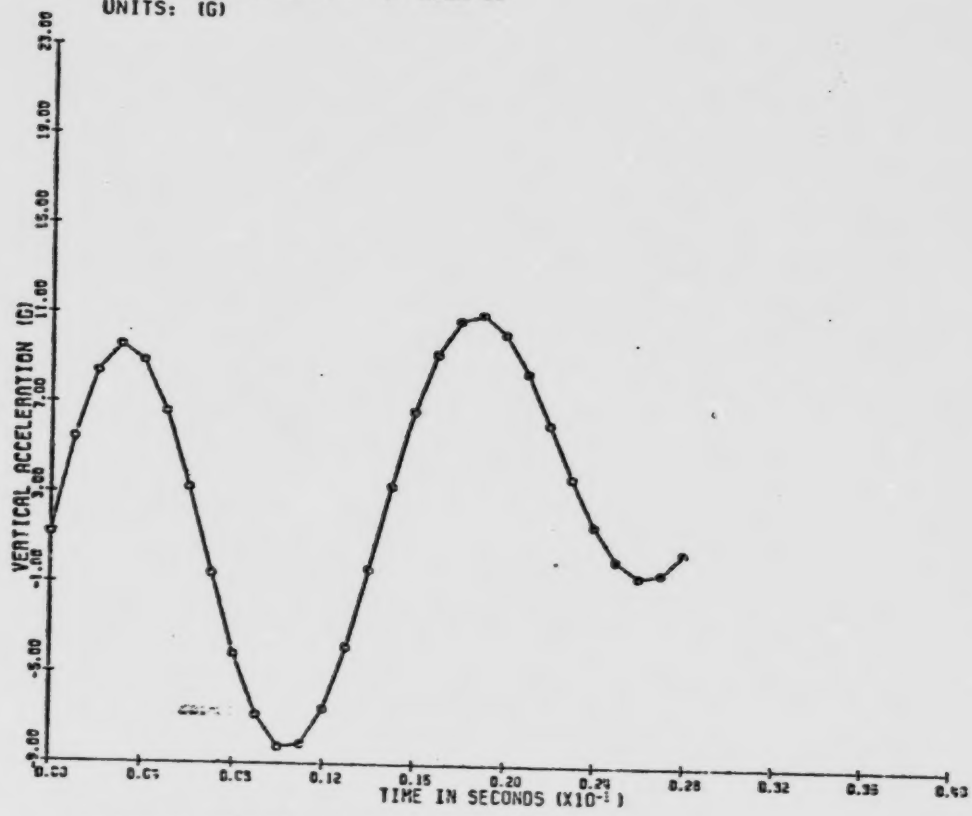

VERTICAL ACCELERATION OF NODE 137
UNITS: (G)

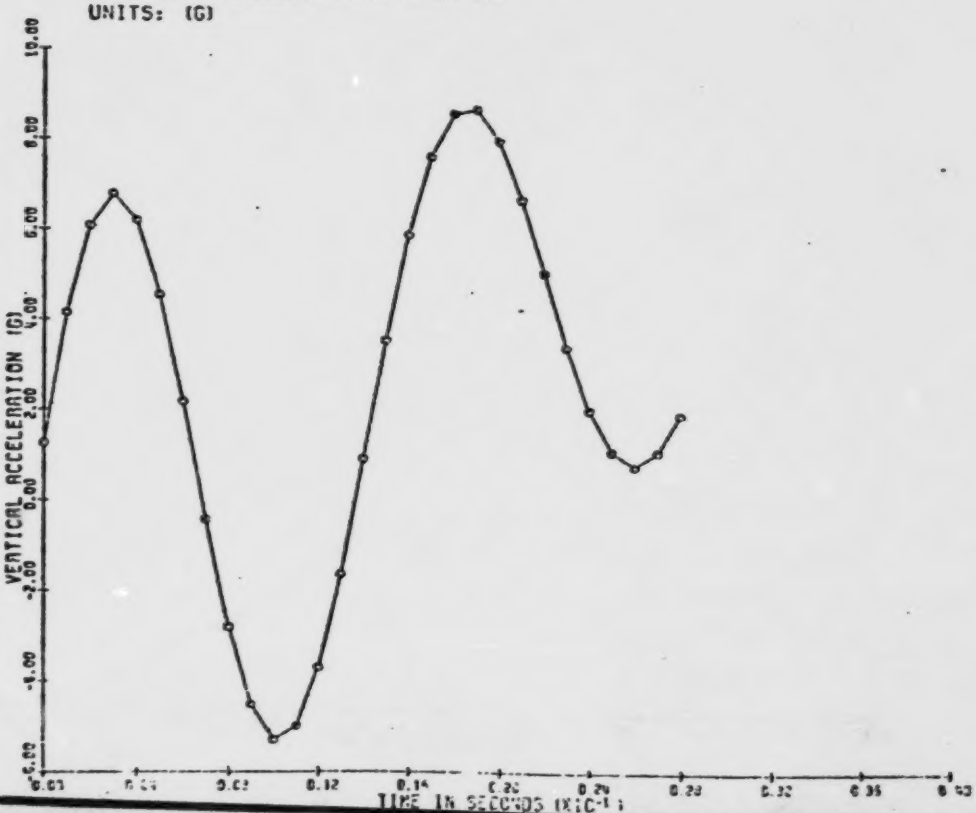

VERTICAL DISPLACEMENT OF NODE 211
UNITS:. INCHES

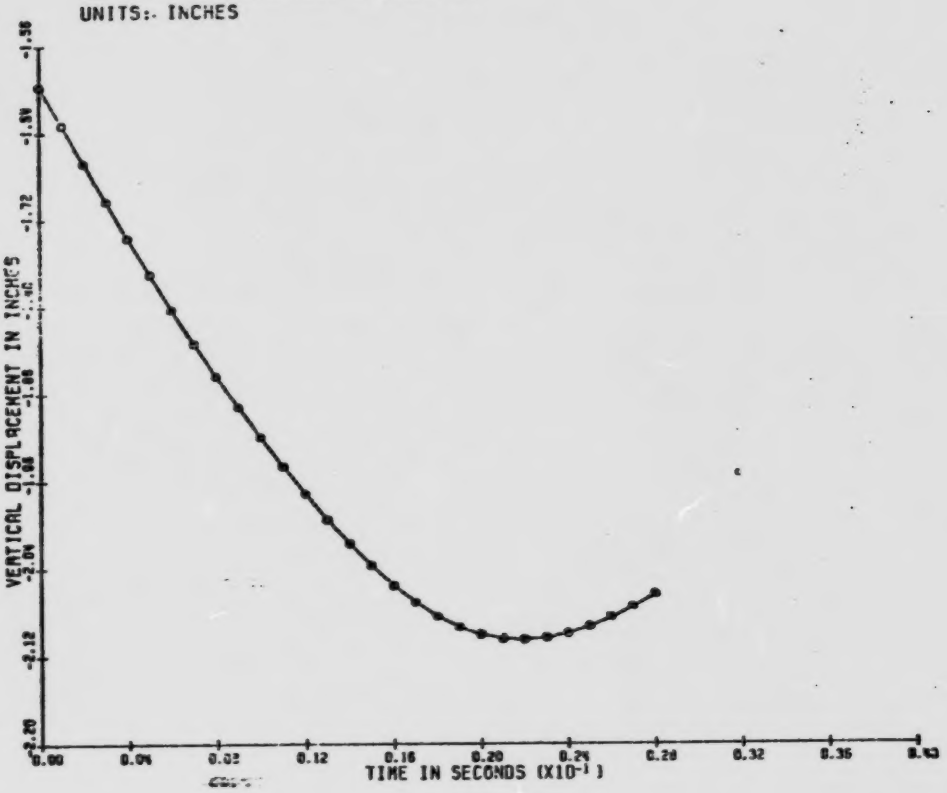

VERTICAL VELOCITY OF NODE 211
UNITS: FEET PER SECOND

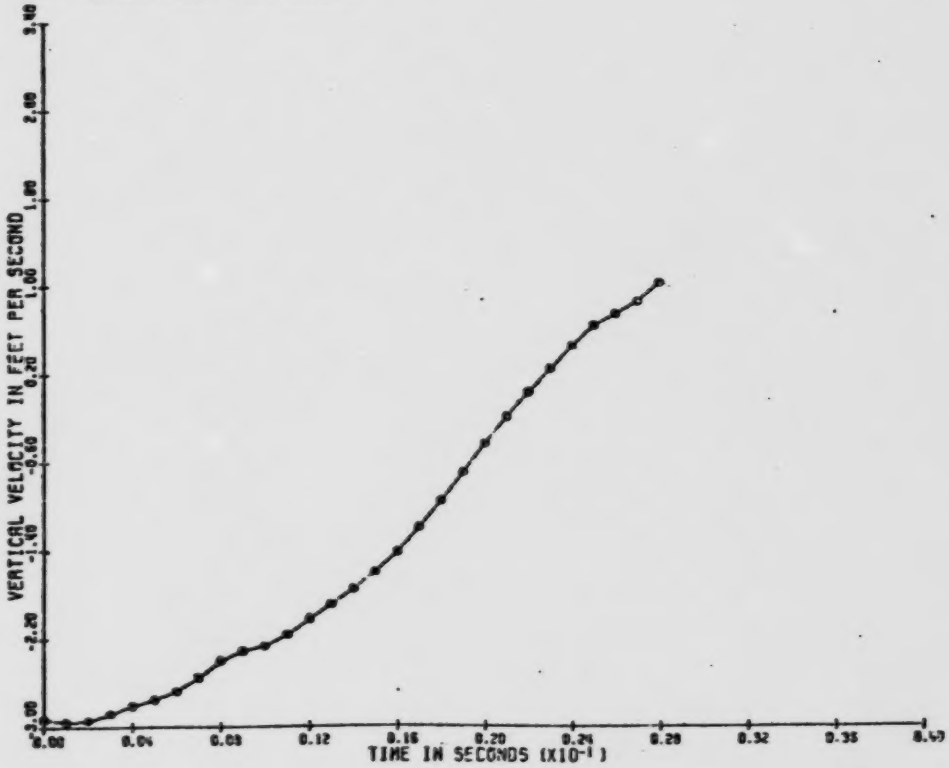

VERTICAL DISPLACEMENT OF NODE 214
UNITS: INCHES

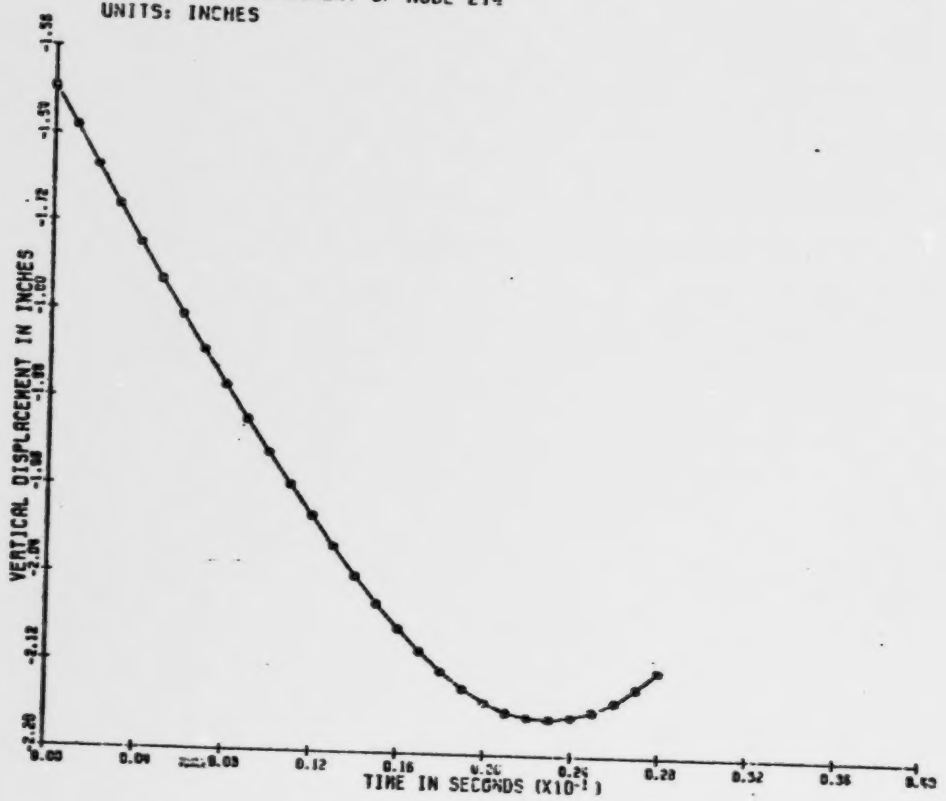

VERTICAL VELOCITY OF NODE 214
UNITS: FEET PER SECOND

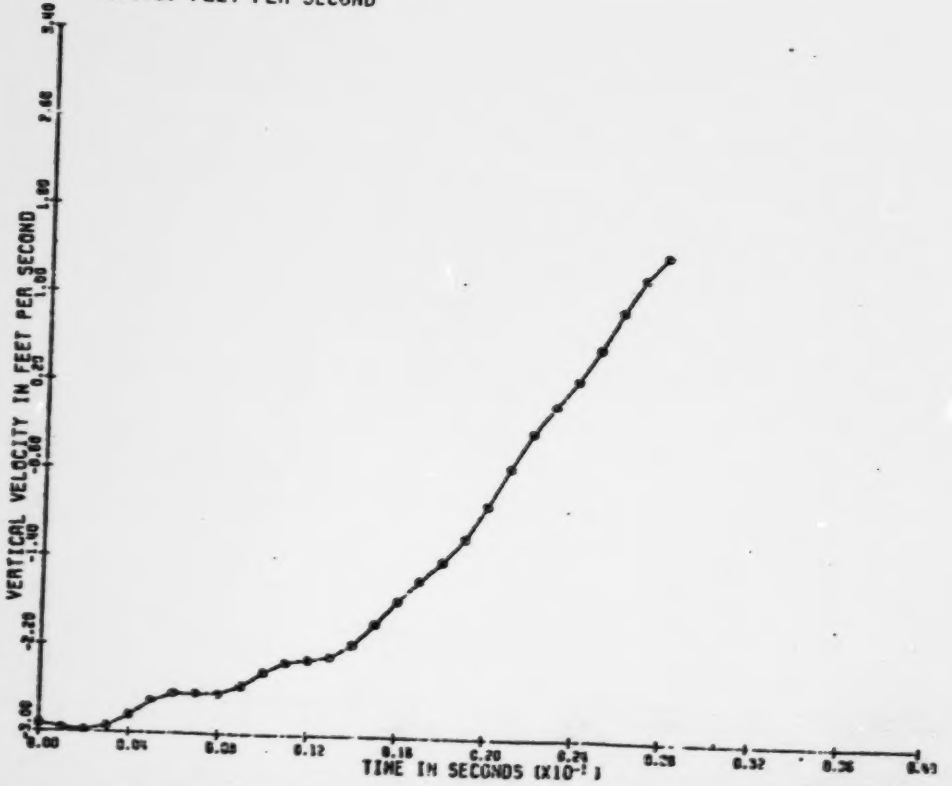

VERTICAL DISPLACEMENT OF NODE 61
UNITS: INCHES

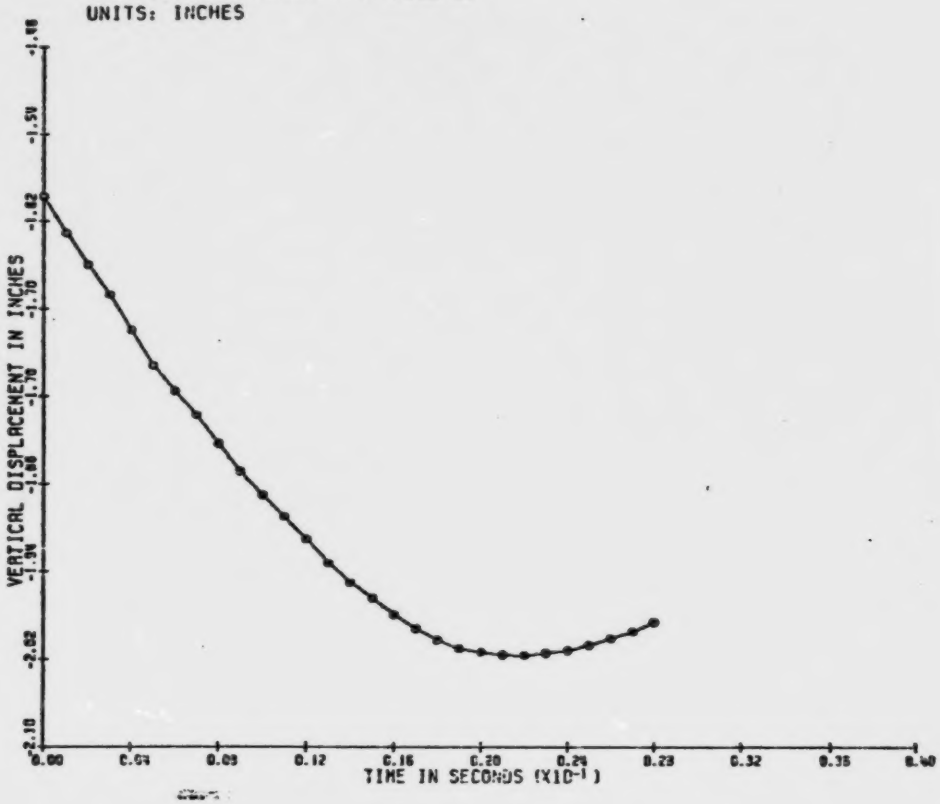

VERTICAL VELOCITY OF NODE 61
UNITS: FEET PER SECOND

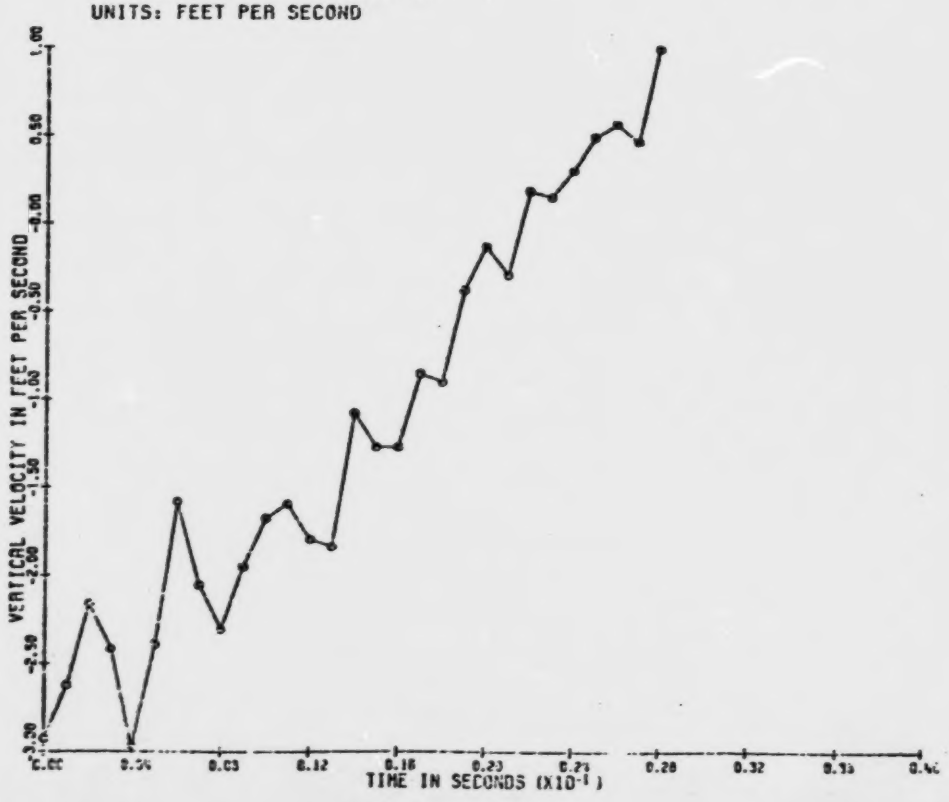

VERTICAL DISPLACEMENT OF NODE 136
UNITS: INCHES

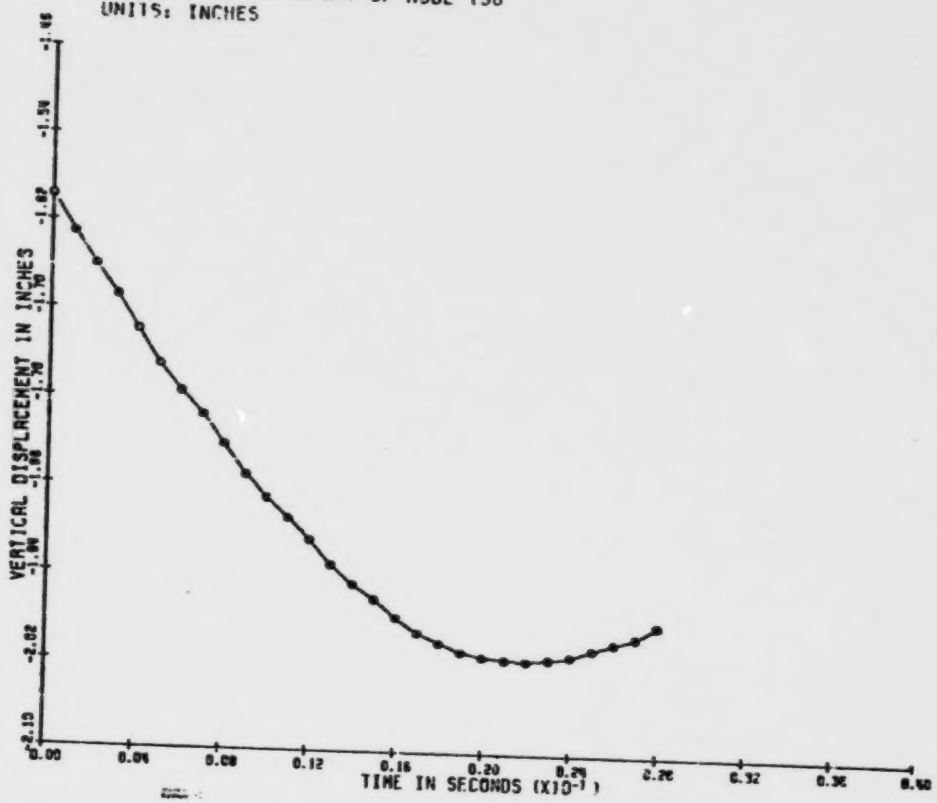

VERTICAL VELOCITY OF NODE 136
UNITS: FEET PER SECOND

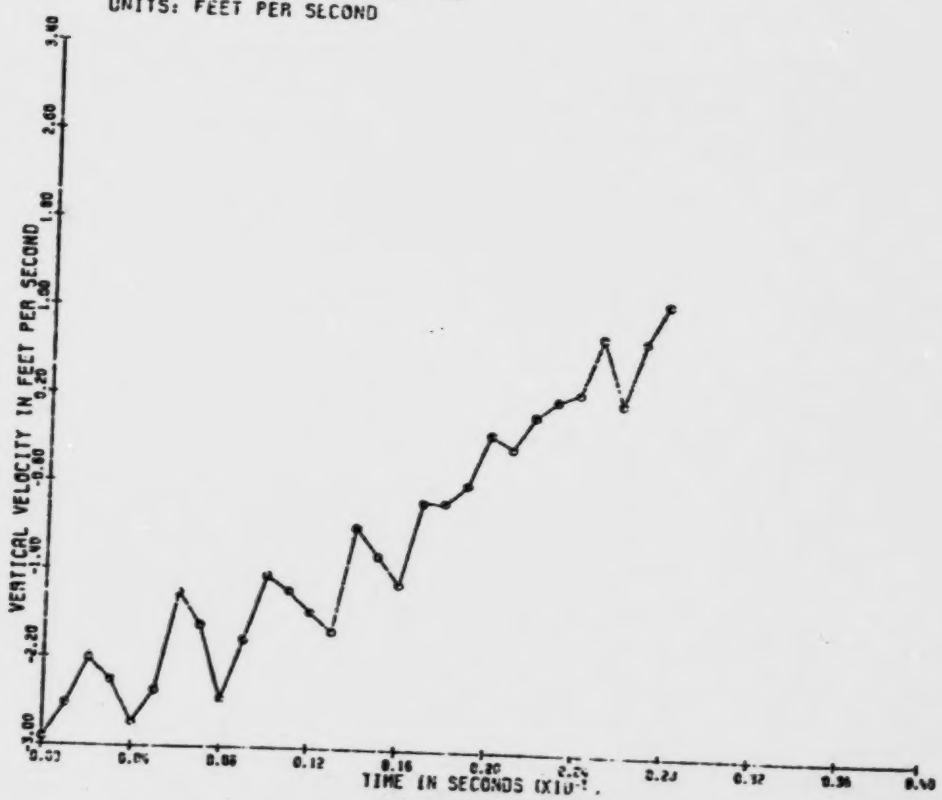

VERTICAL DISPLACEMENT OF NODE 137
UNITS: INCHES

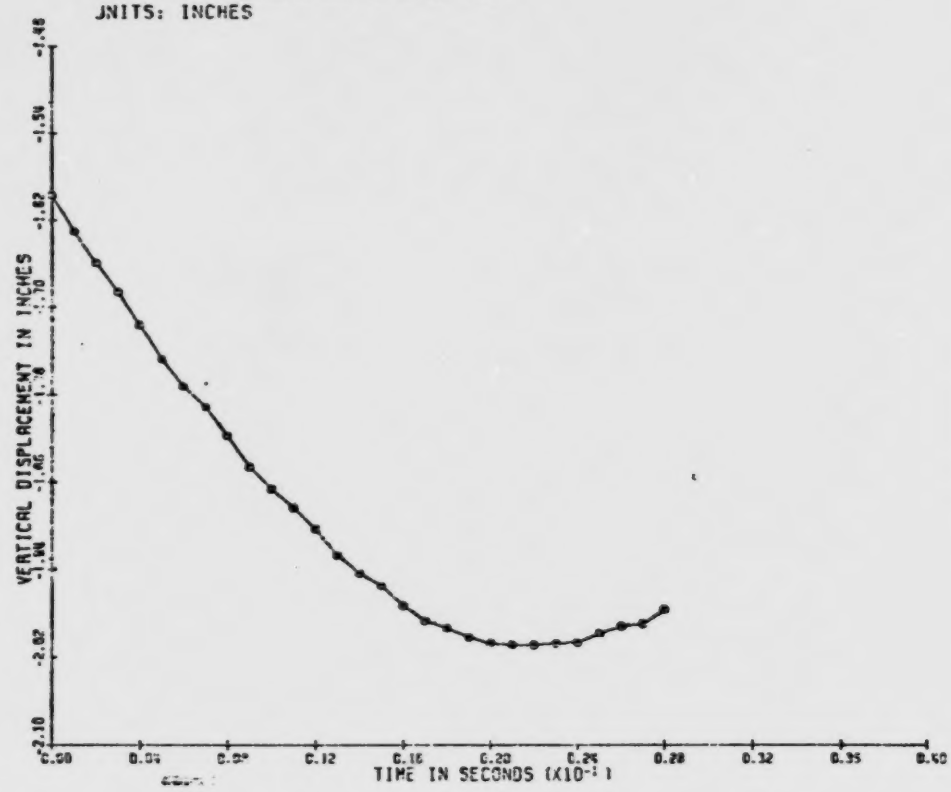

VERTICAL VELOCITY OF NODE 137
UNITS: FEET PER SECOND

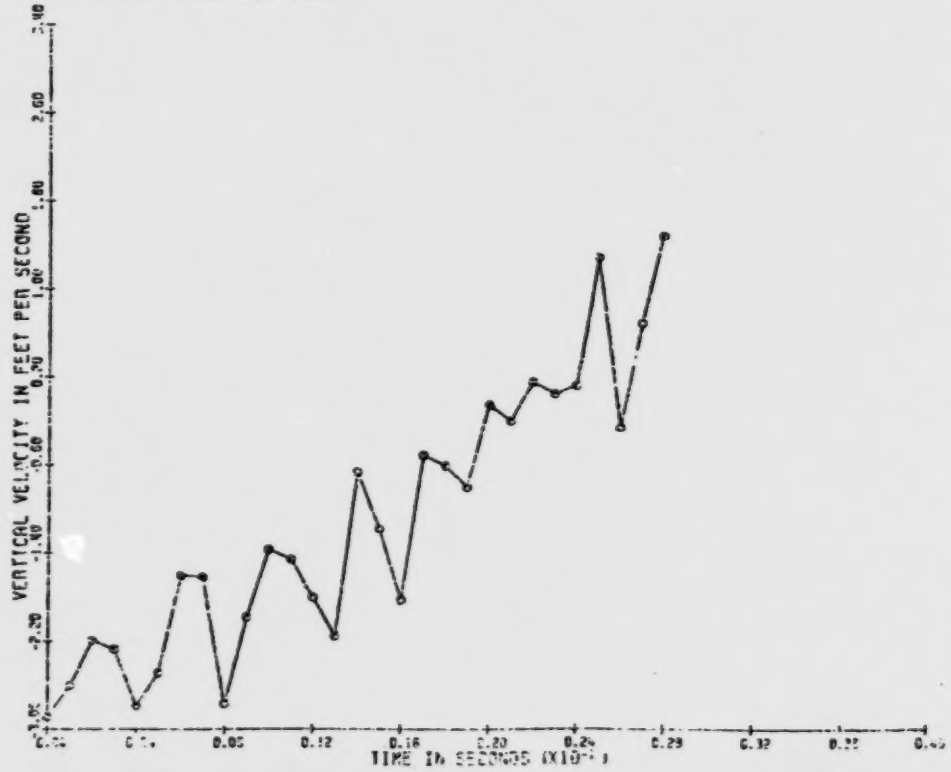

STRAINS OF NODE 78

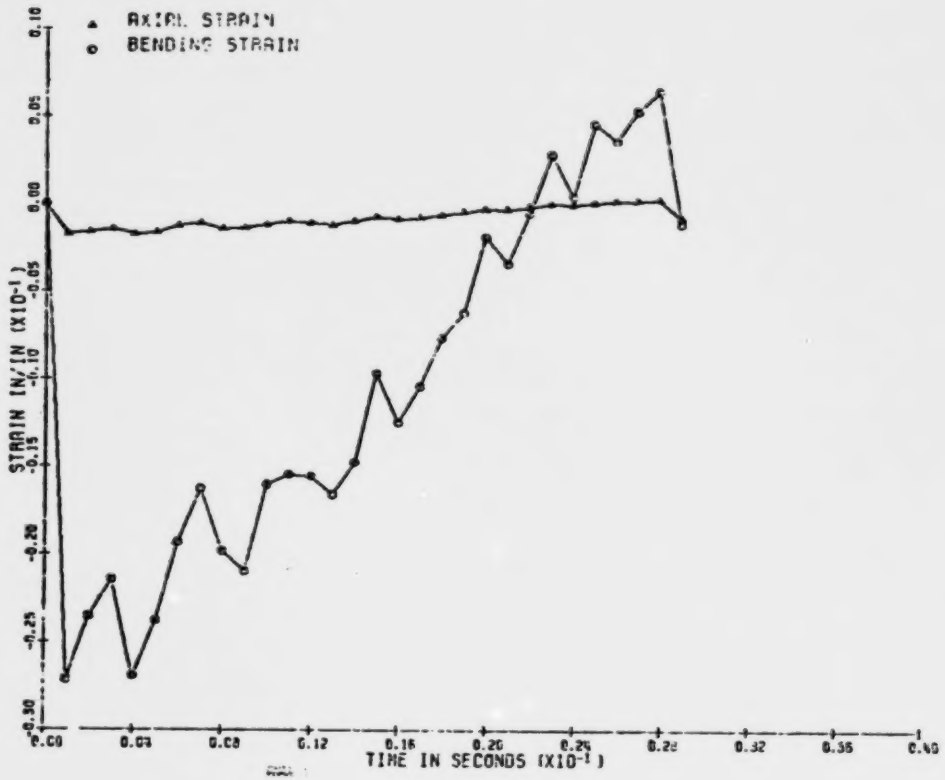

STRAINS OF NODE 80

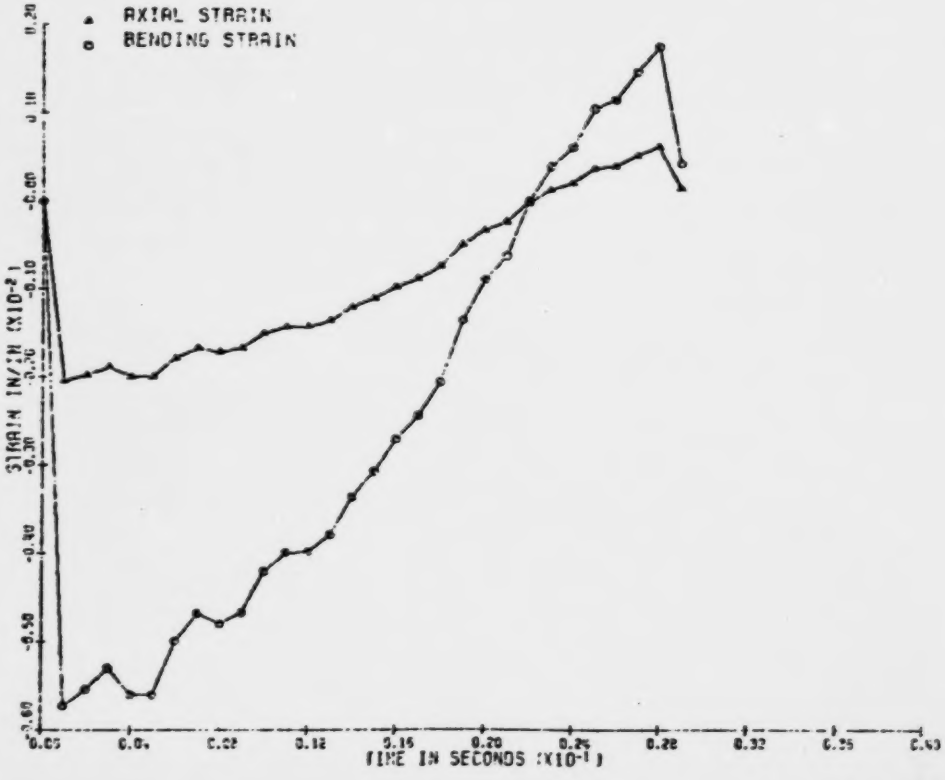

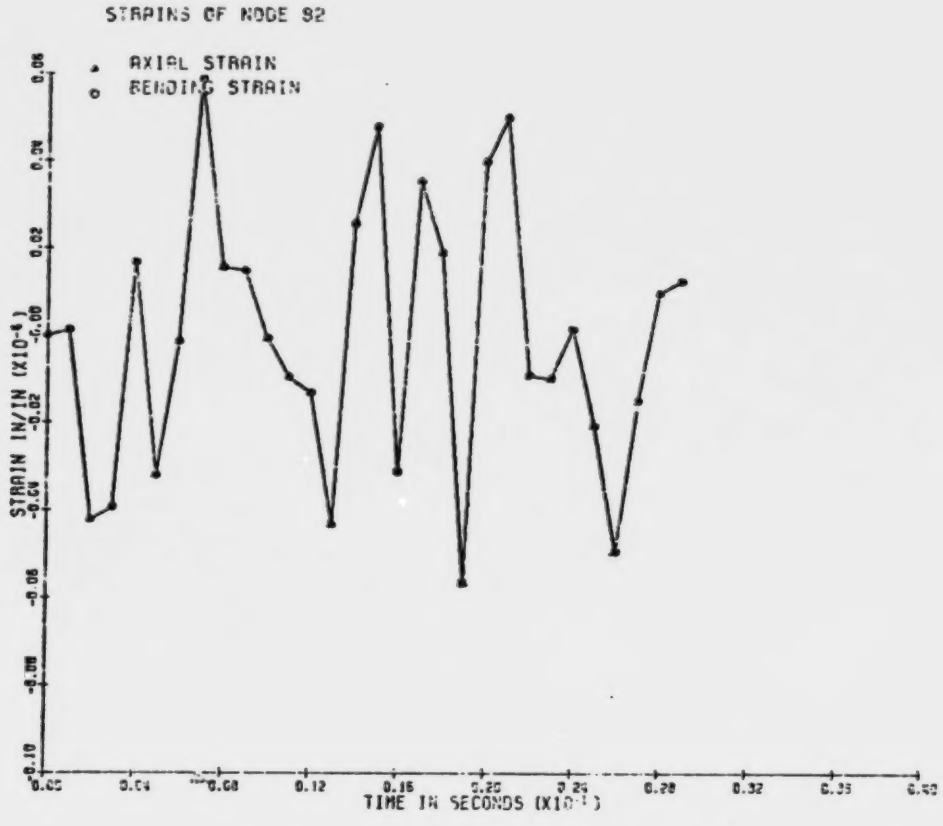
STRAINS OF NODE 82
AXIAL STRAIN
BENDING STRAIN
STRAIN IN/IN (X10-4)
TIME IN SECONDS (X10-1)

INITIAL IMPACT CONDITIONS AT T = C.O$_{sec}$
WING LOAD SIMULATION: 527 IBS
VERTICAL VELOCITY = -4.37 FT PER SECOND
HORIZONTAL VELOCITY = 0.00 FT PER SECOND
ANGLE = 0.00 DEG. PITCH RATE = 0.00 RAD/SECOND

TIME IS 0.0000 SECONDS
TIME STEP = 0.00100 SECONDS

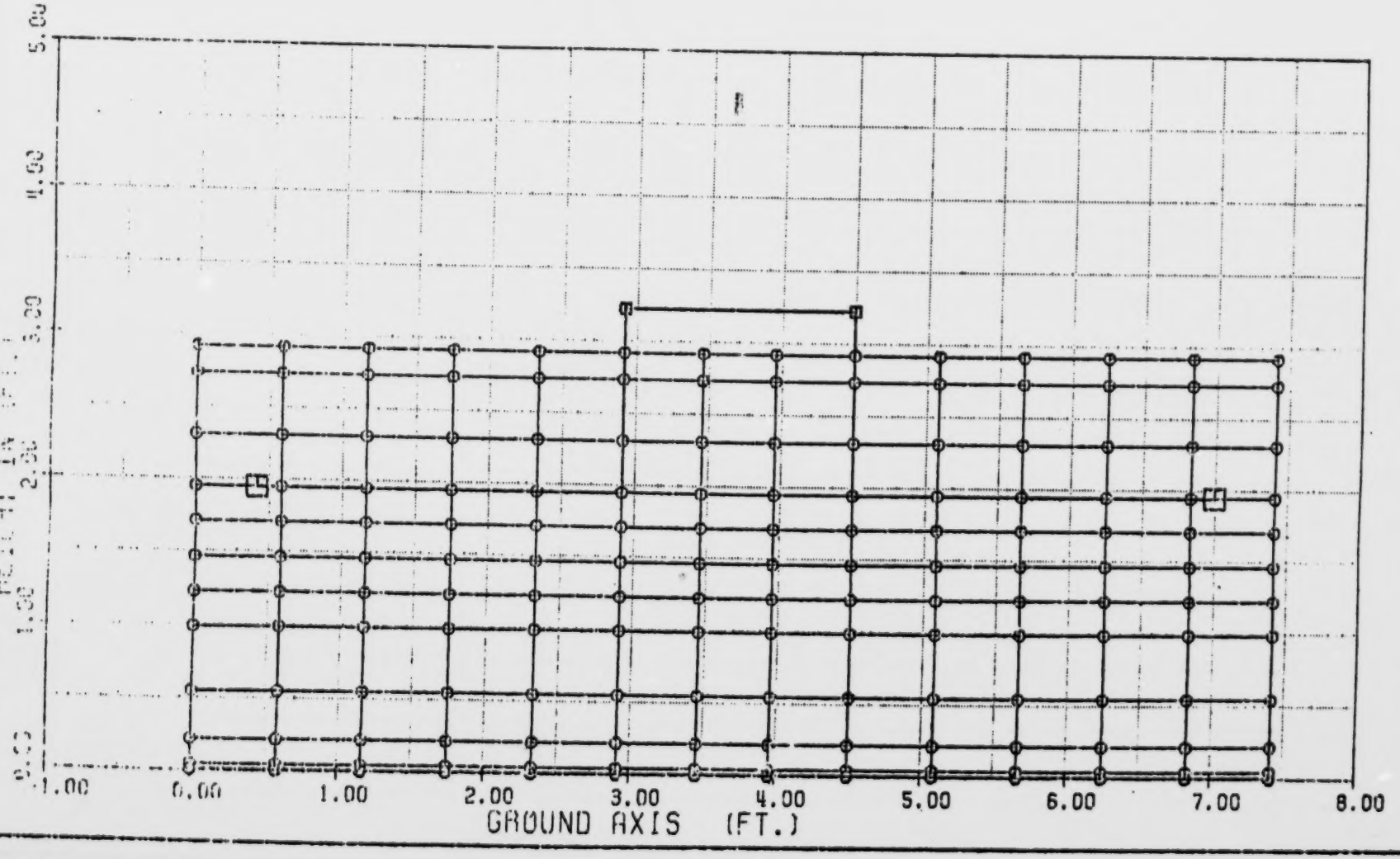

INITIAL IMPACT CONDITIONS AT T = 0.0000
WING LOAD SIMULATION: 527 LBS
VERTICAL VELOCITY = -4.37 FT PER SECOND
HORIZONTAL VELOCITY = 0.00 FT PER SECOND
ANGLE = 0.00 DEG. PITCH RATE = 0.00 RAD/SECOND

TIME IS 0.0110 SECONDS
TIME STEP = 0.00100 SECONDS

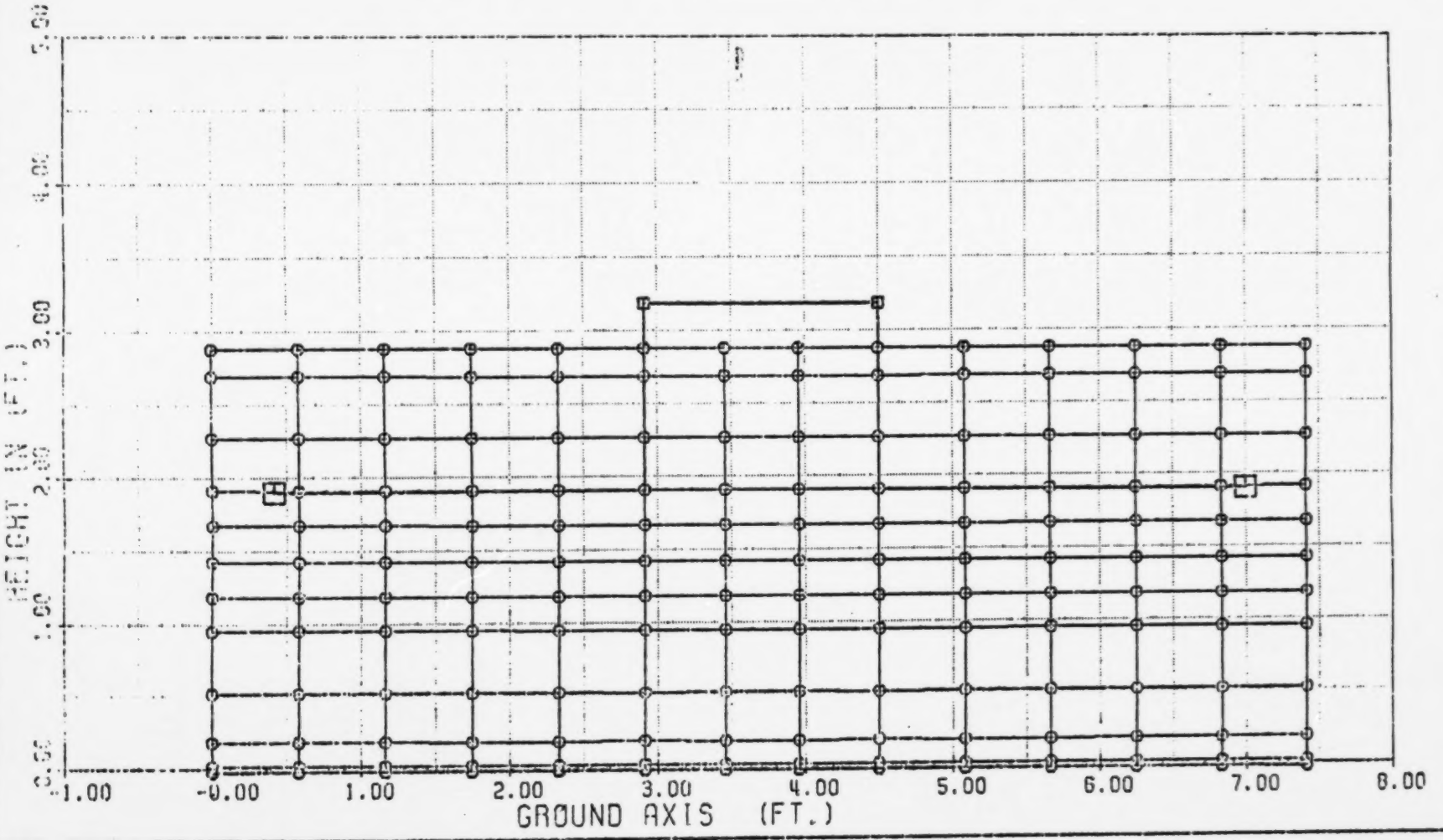

INITIAL IMPACT CONDITIONS AT T = 0.0000
WING LOAD SIMULATION: 537 IBS
VERTICAL VELOCITY = -4.37 FT PER SECOND
HORIZONTAL VELOCITY = 0.00 FT PER SECOND
ANGLE = 0.00 DEG. PITCH RATE = 0.00 RAD/SECOND

TIME IS 0.0211 SECONDS
TIME STEP = 0.00012 SECONDS

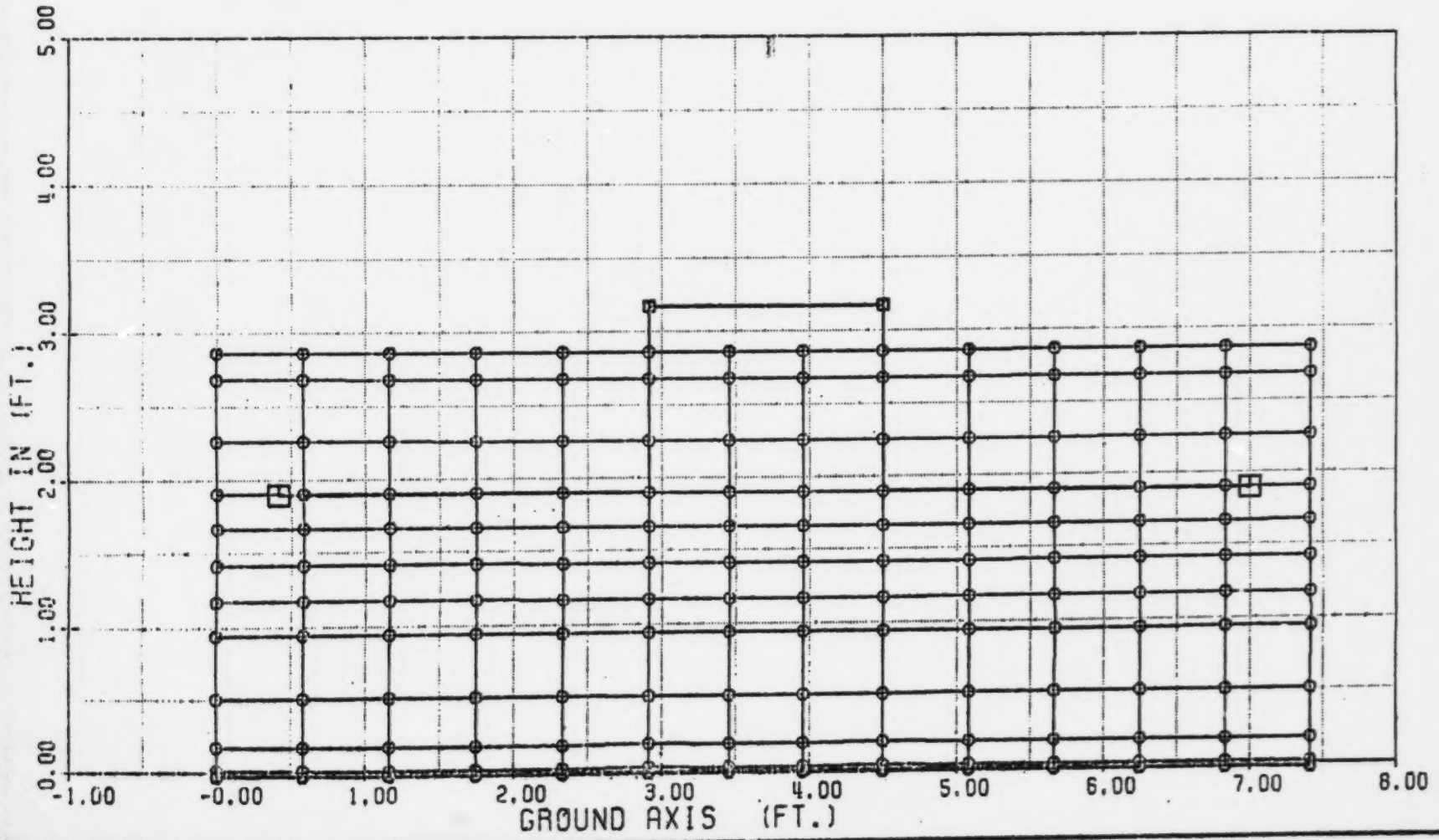

INITIAL IMPACT CONDITIONS AT T = 0.0000

WING LOAD SIMULATION: 527 LBS

VERTICAL VELOCITY = -4.37 FT PER SECOND

HORIZONTAL VELOCITY = 0.00 FT PER SECOND

ANGLE = 0.00 DEG. PITCH RATE = 0.00 RAD/SECOND

TIME IS 0.0225 SECONDS

TIME STEP = 0.00012 SECONDS

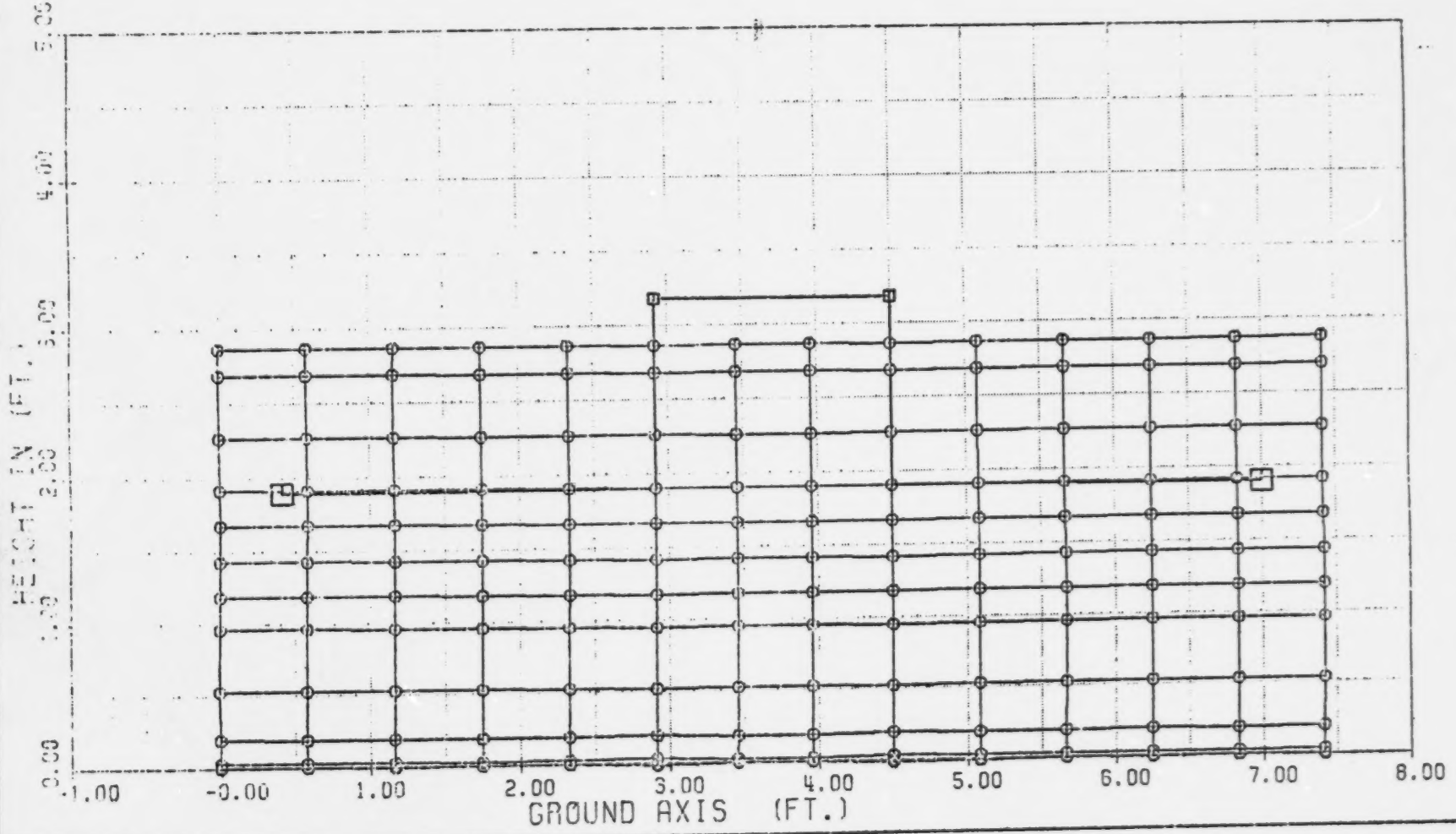

INITIAL IMPACT CONDITIONS AT T = 0.0
WING LOAD SIMULATION: 537 IBS
VERTICAL VELOCITY = -4.37 FT PER SECOND
HORIZONTAL VELOCITY = 0.00 FT PER SECOND
ANGLE = 0.00 DEG. PITCH RATE = 0.00 RAD/SECOND

TIME IS 0.0239 SECONDS
TIME STEP = 0.00012 SECONDS

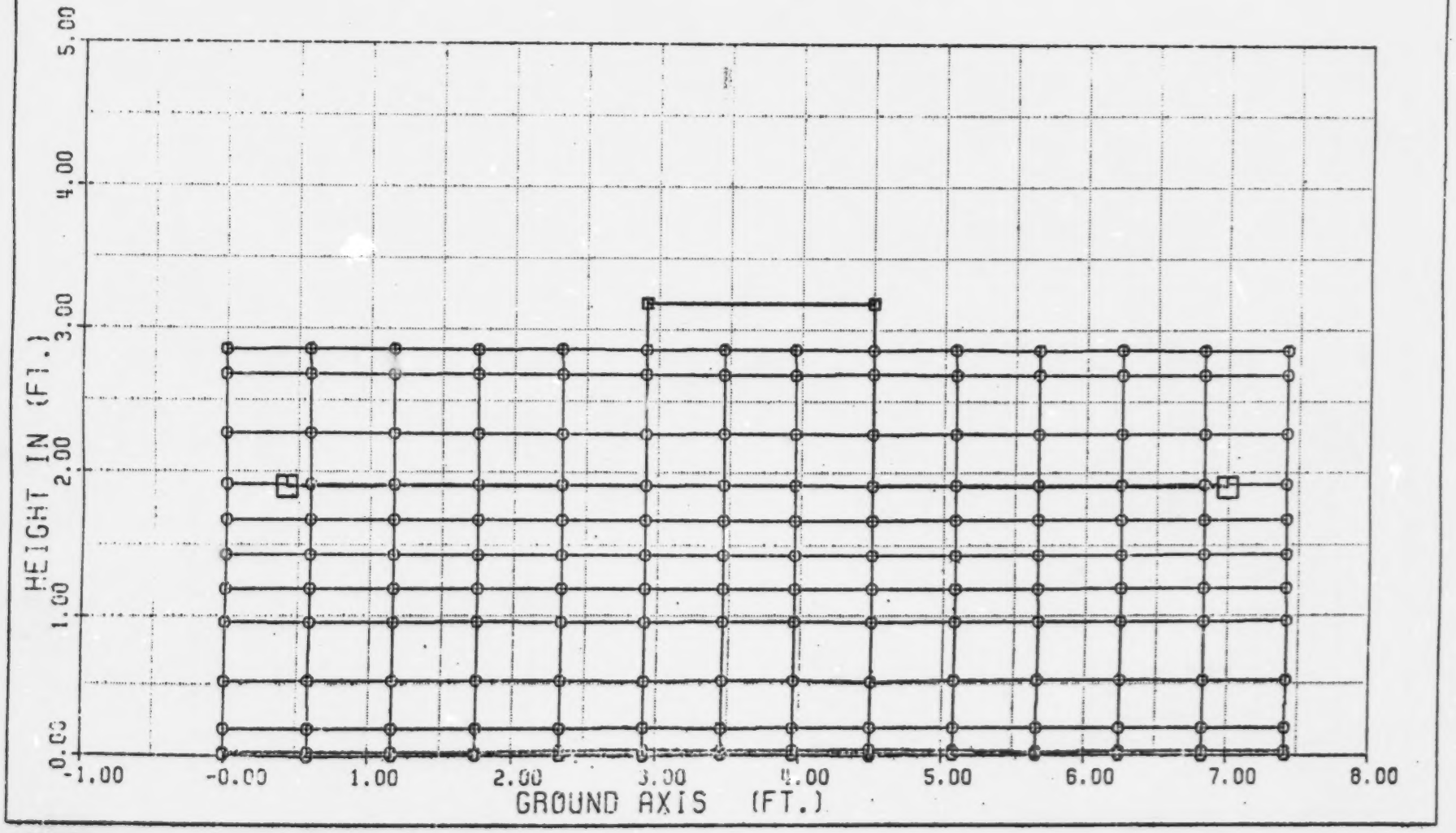

INITIAL IMPACT CONDITIONS AT T = 0.0 msec
WING LOAD SIMULATION: 527 LBS
VERTICAL VELOCITY = -4.37 FT PER SECOND
HORIZONTAL VELOCITY = 0.00 FT PER SECOND
ANGLE = 0.00 DEG. PITCH RATE = 0.00 RAD/SECOND

TIME IS 0.0252 SECONDS
TIME STEP = 0.00012 SECONDS

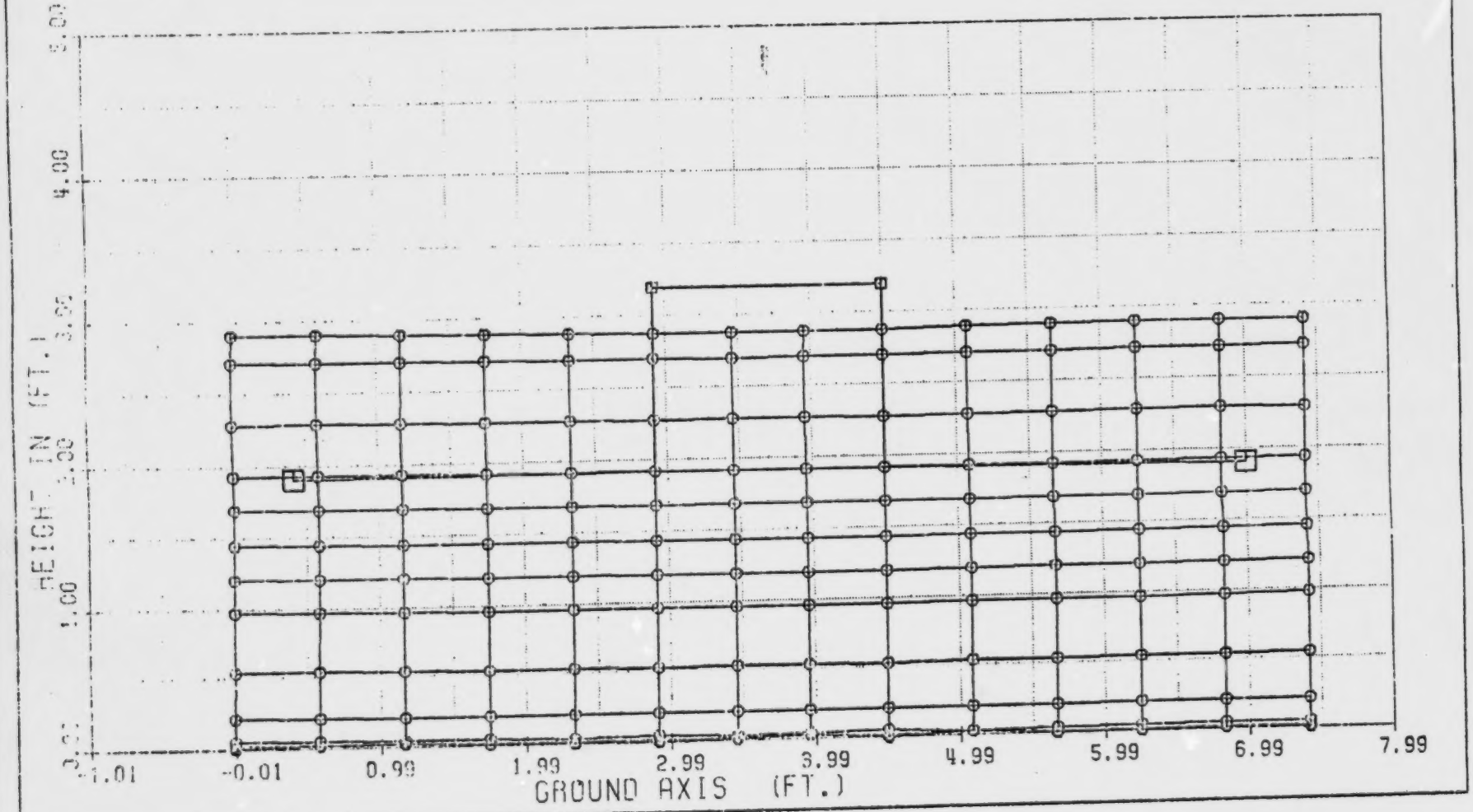

VERTICAL ACCELERATION OF NODE 211
UNITS: (G)

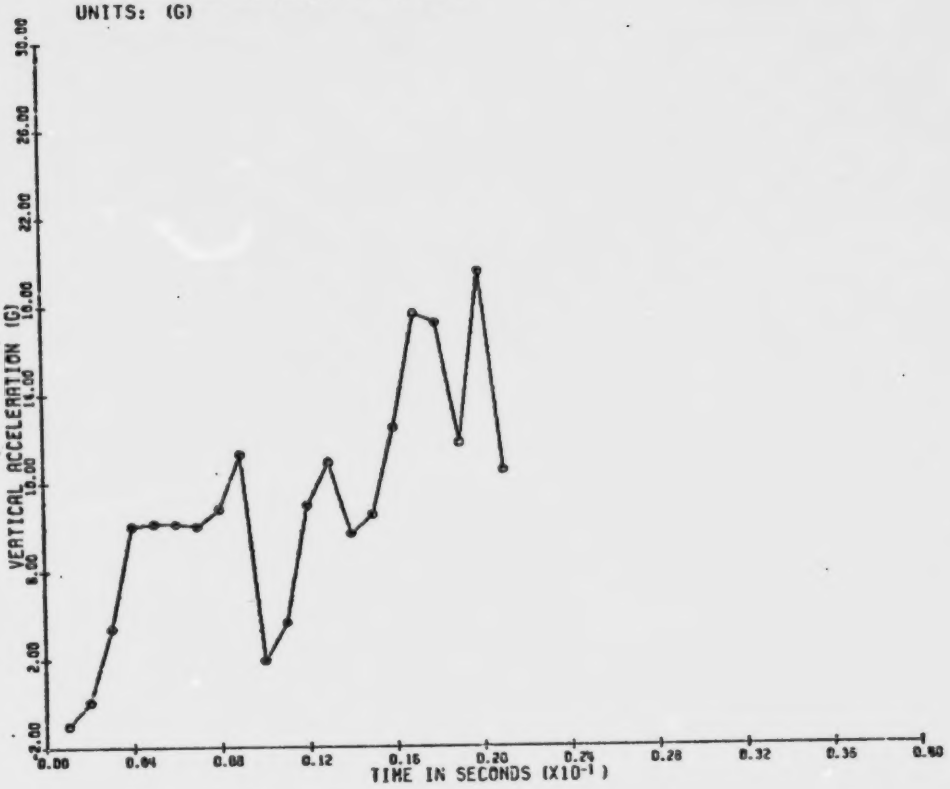

VERTICAL ACCELERATION OF NODE 214
UNITS: (G)

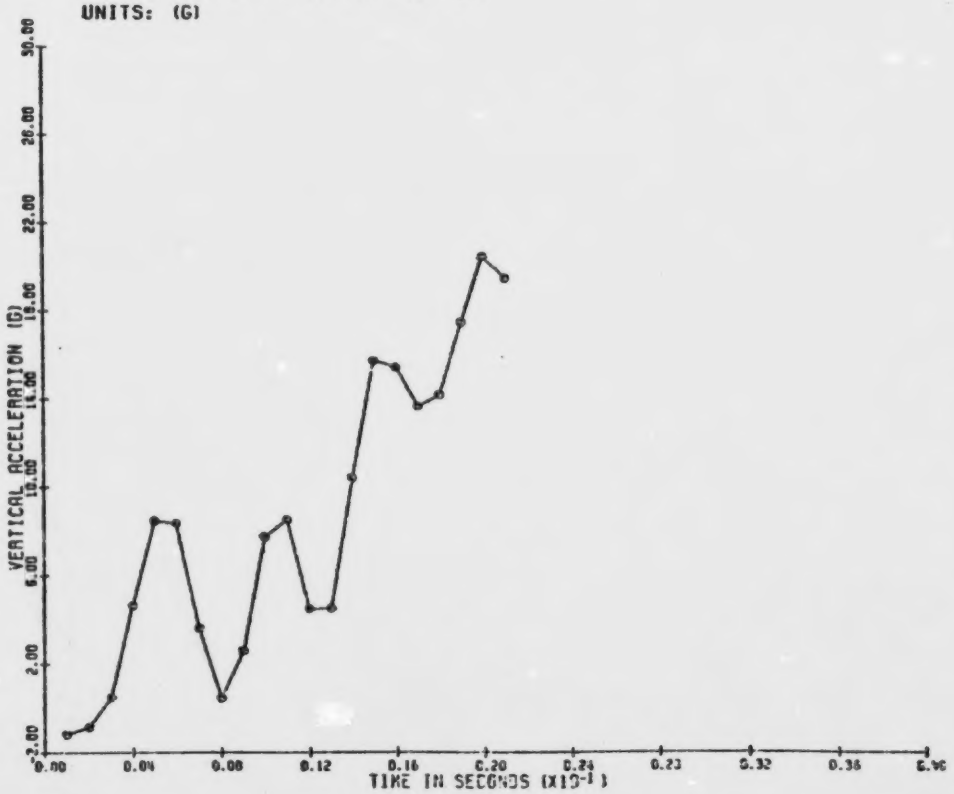

VERTICAL ACCELERATION OF NODE 61
UNITS: (G)

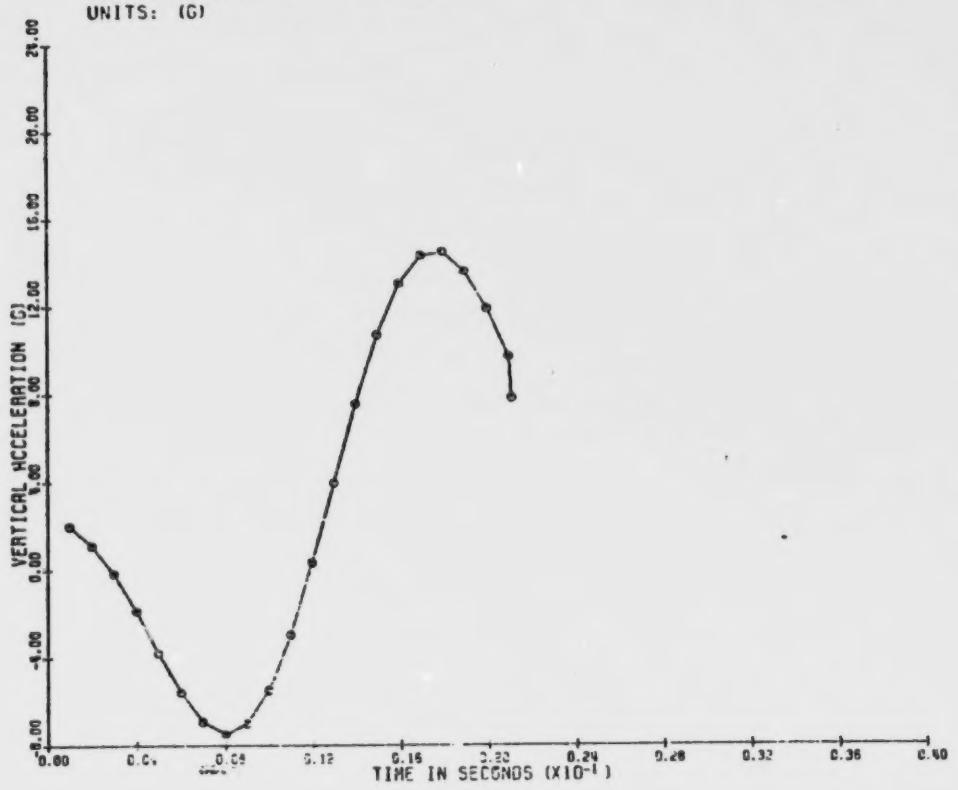

VERTICAL ACCELERATION OF NODE 137
UNITS: (G)

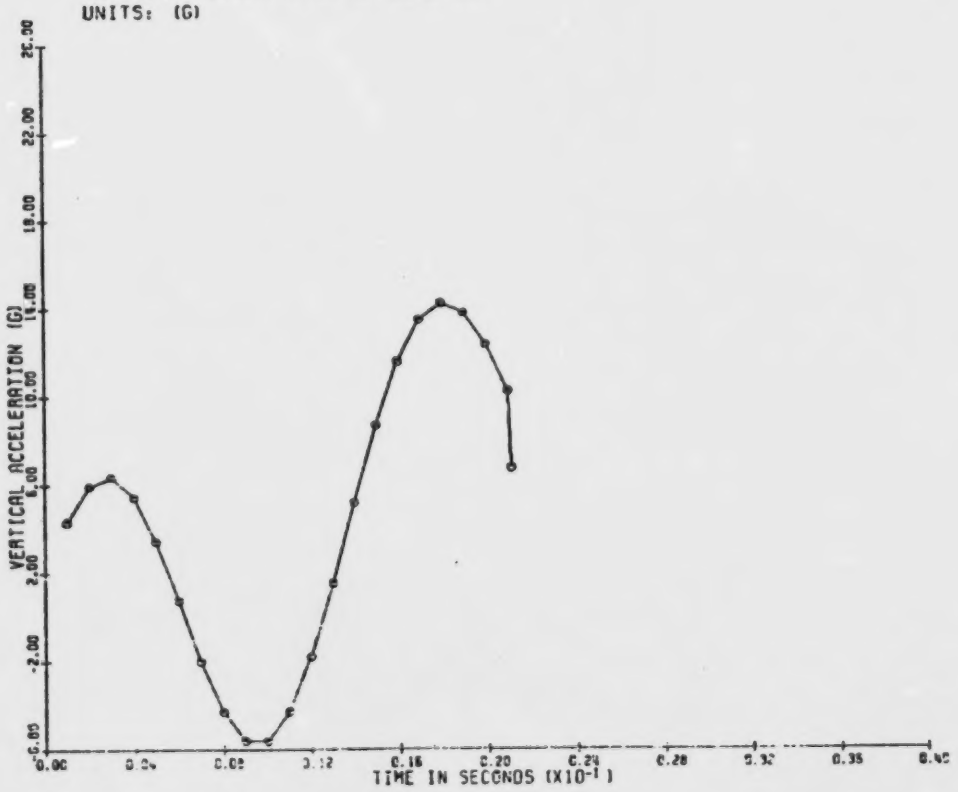

VERTICAL ACCELERATION OF NODE 136
UNITS: (G)

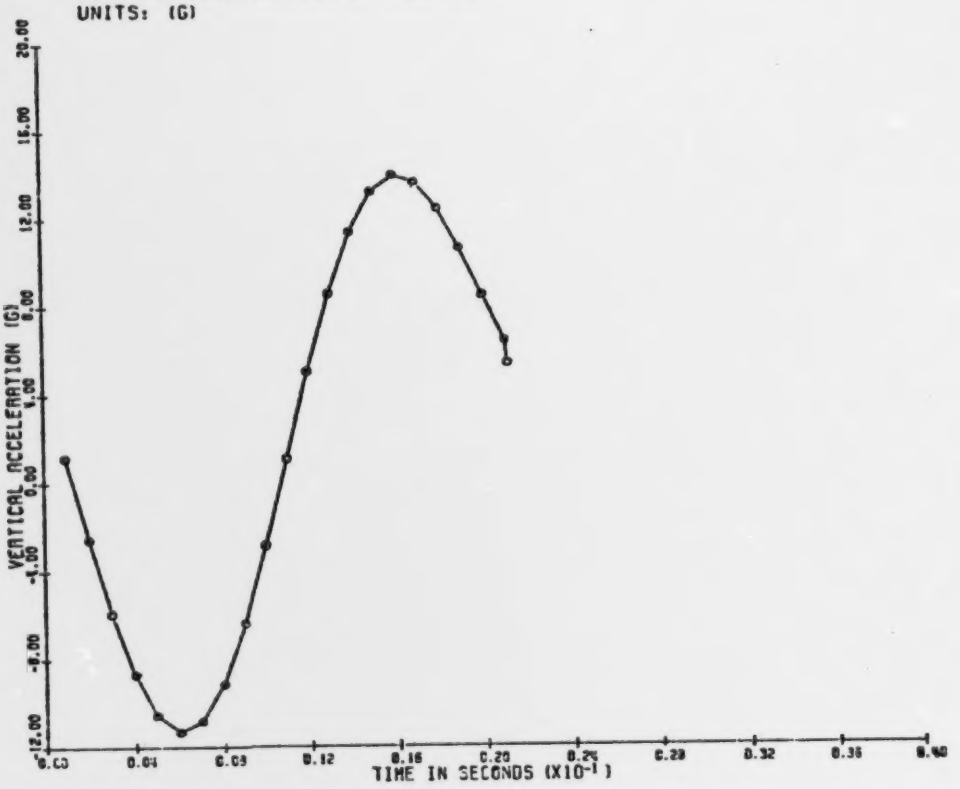

VERTICAL ACCELERATION OF NODE 82
UNITS: (G)

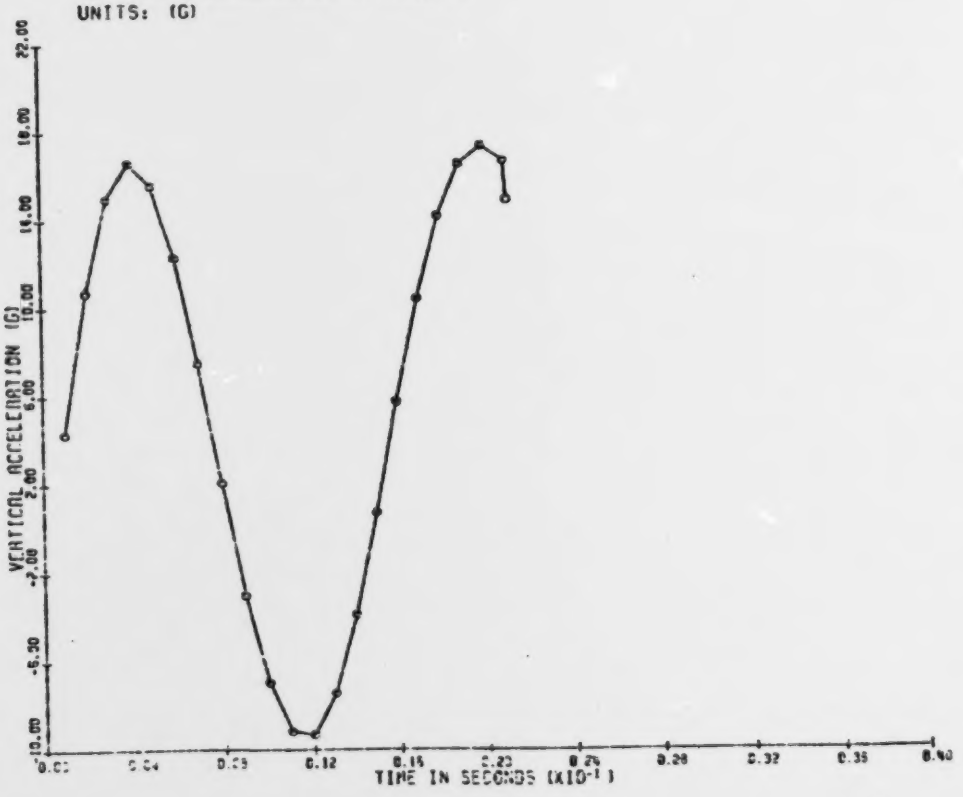

VERTICAL DISPLACEMENT OF NODE 211
UNITS: INCHES

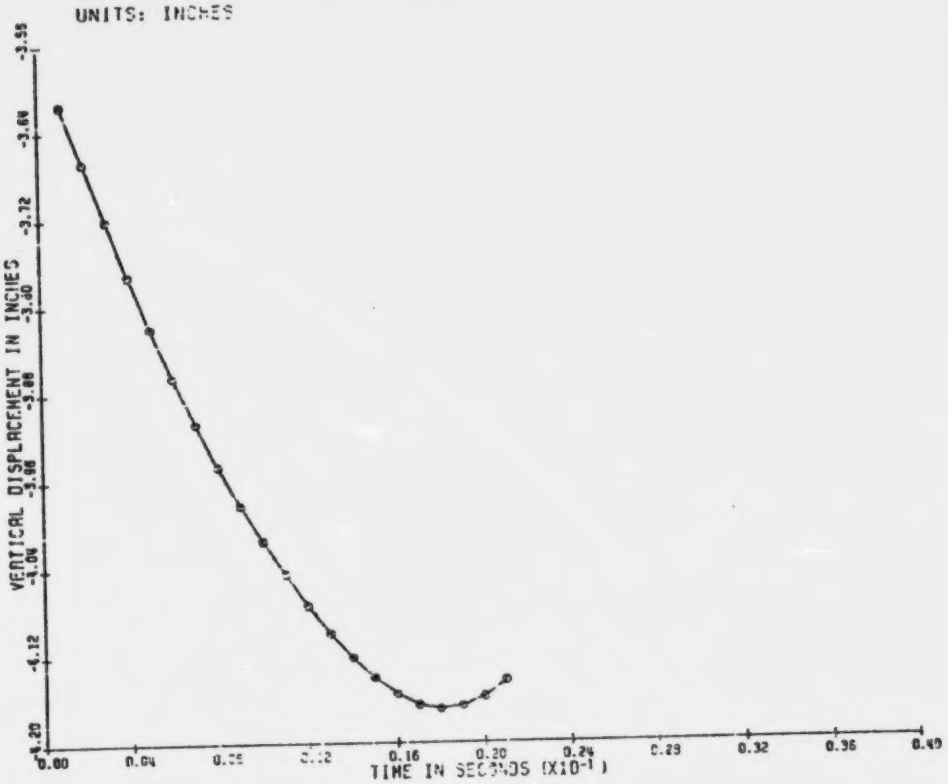

VERTICAL VELOCITY OF NODE 211
UNITS: FEET PER SECOND

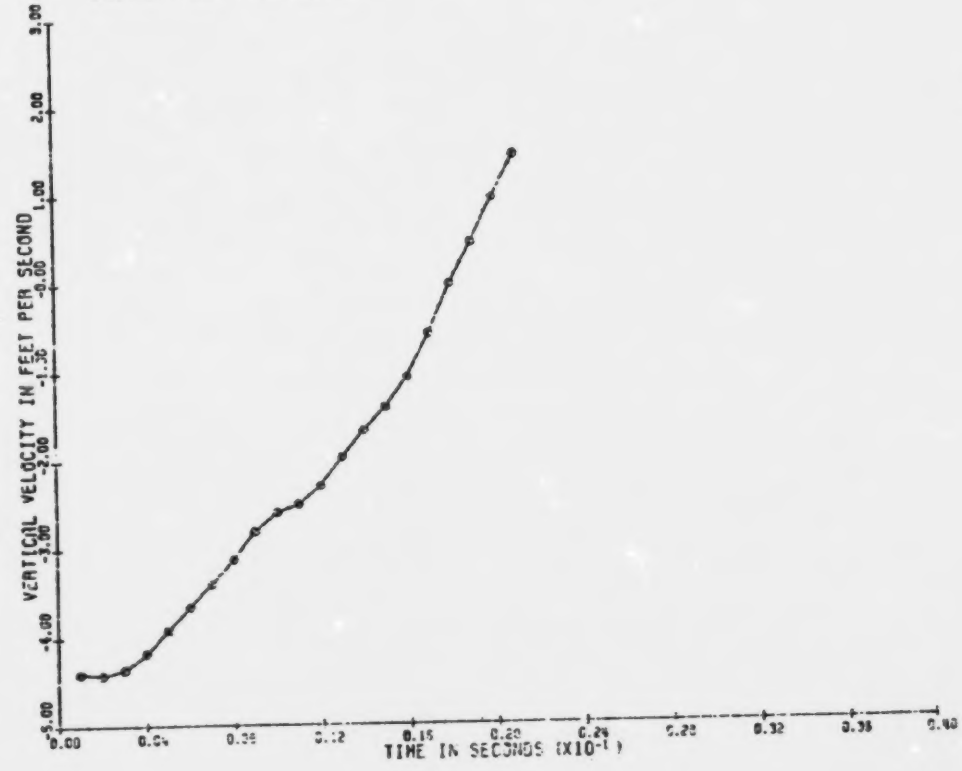

VERTICAL DISPLACEMENT OF NODE 214
UNITS: INCHES

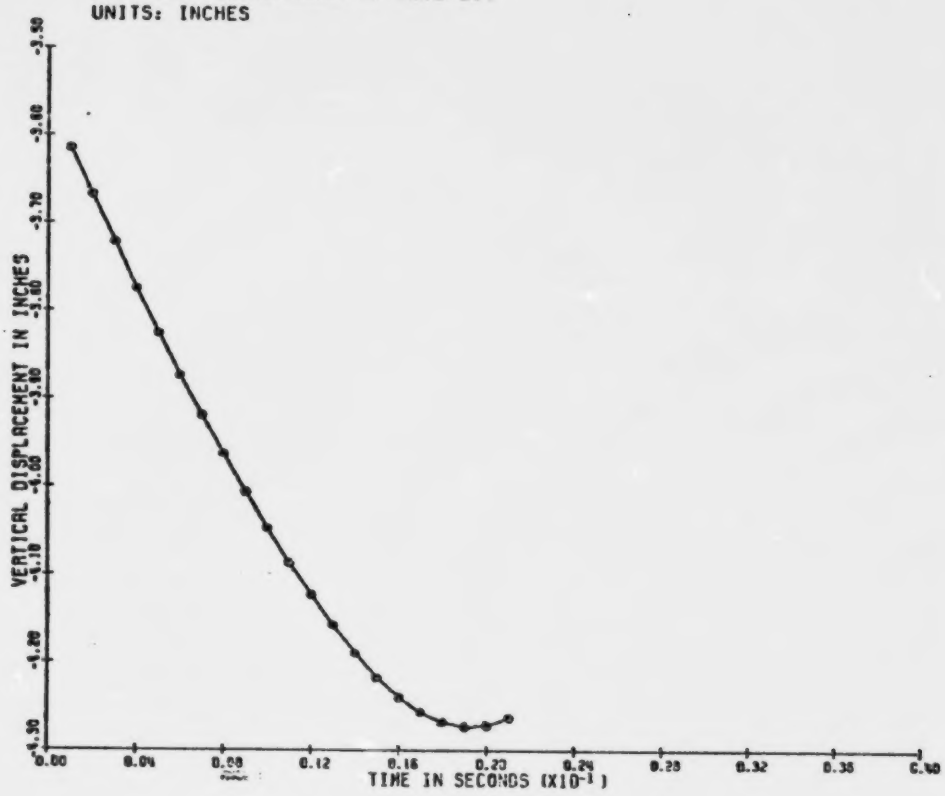

VERTICAL VELOCITY OF NODE 214
UNITS: FEET PER SECOND

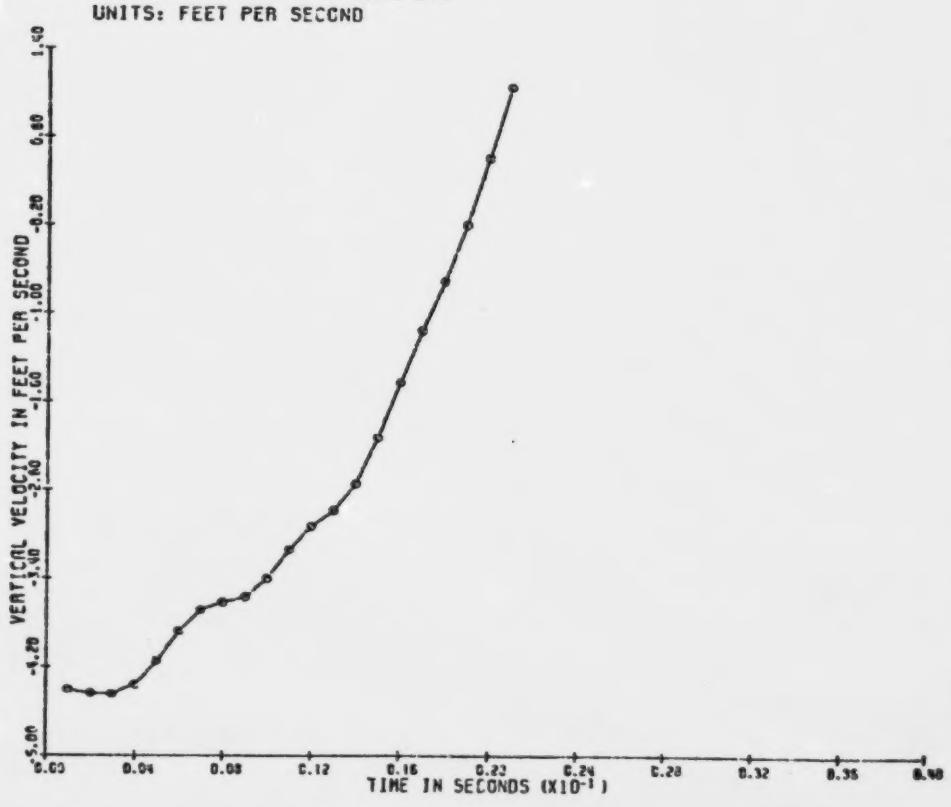

VERTICAL DISPLACEMENT OF NODE 61
UNITS: INCHES

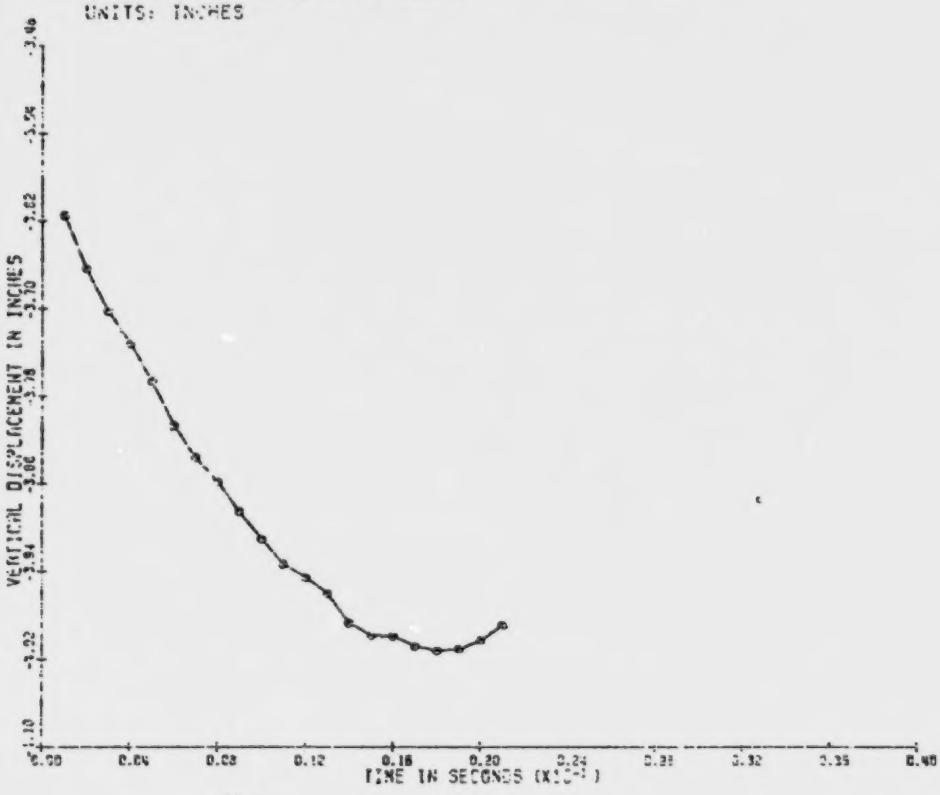

VERTICAL VELOCITY OF NODE 61
UNITS: FEET PER SECOND

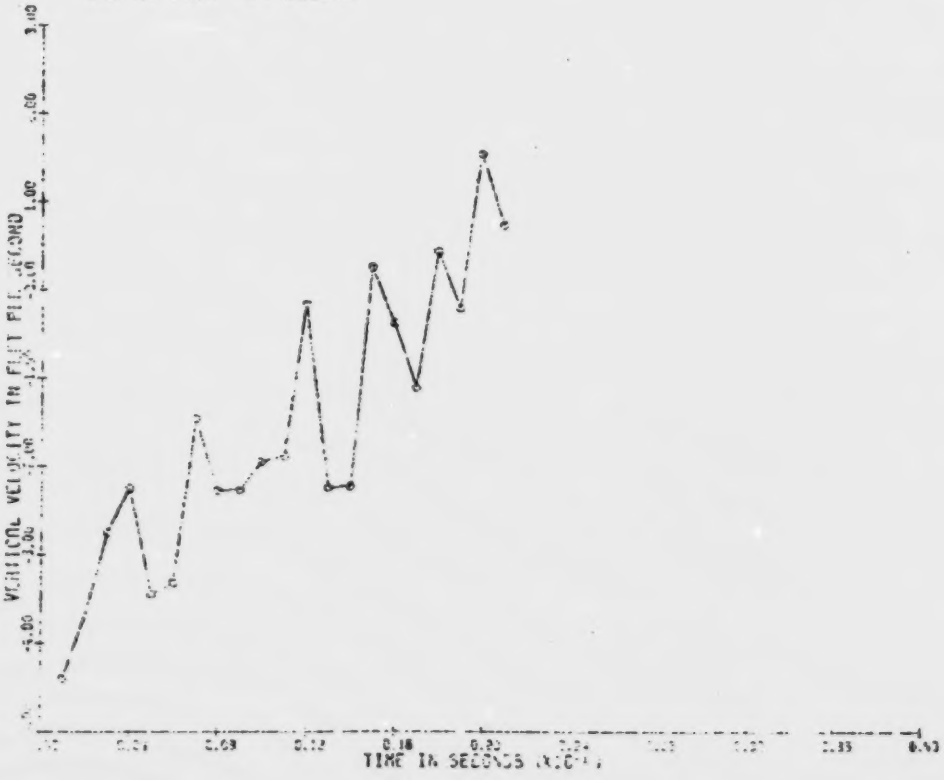

VERTICAL DISPLACEMENT OF NODE 136
UNITS: INCHES

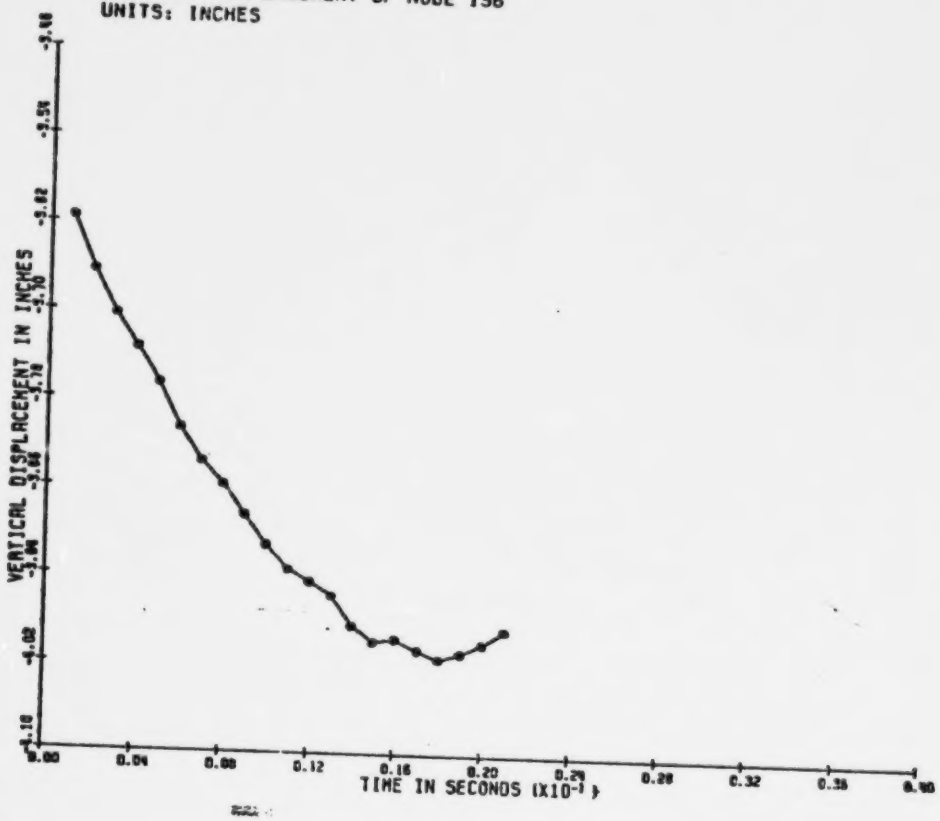

VERTICAL VELOCITY OF NODE 136
UNITS: FEET PER SECOND

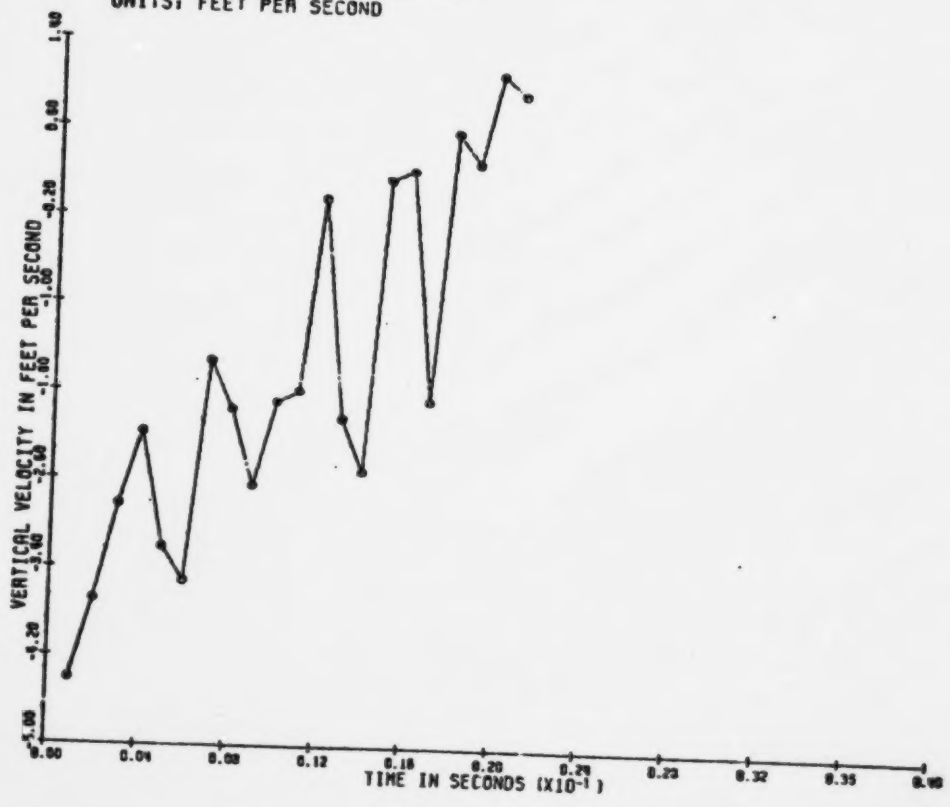

VERTICAL DISPLACEMENT OF NODE 137
UNITS: INCHES

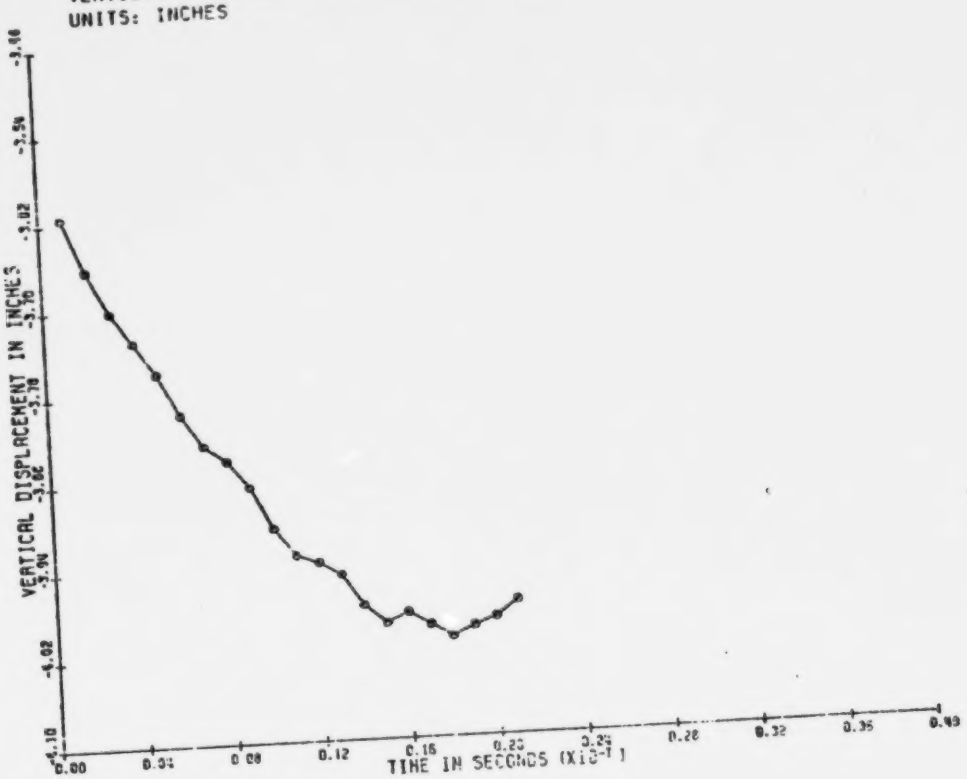

VERTICAL VELOCITY OF NODE 137
UNITS: FEET PER SECOND

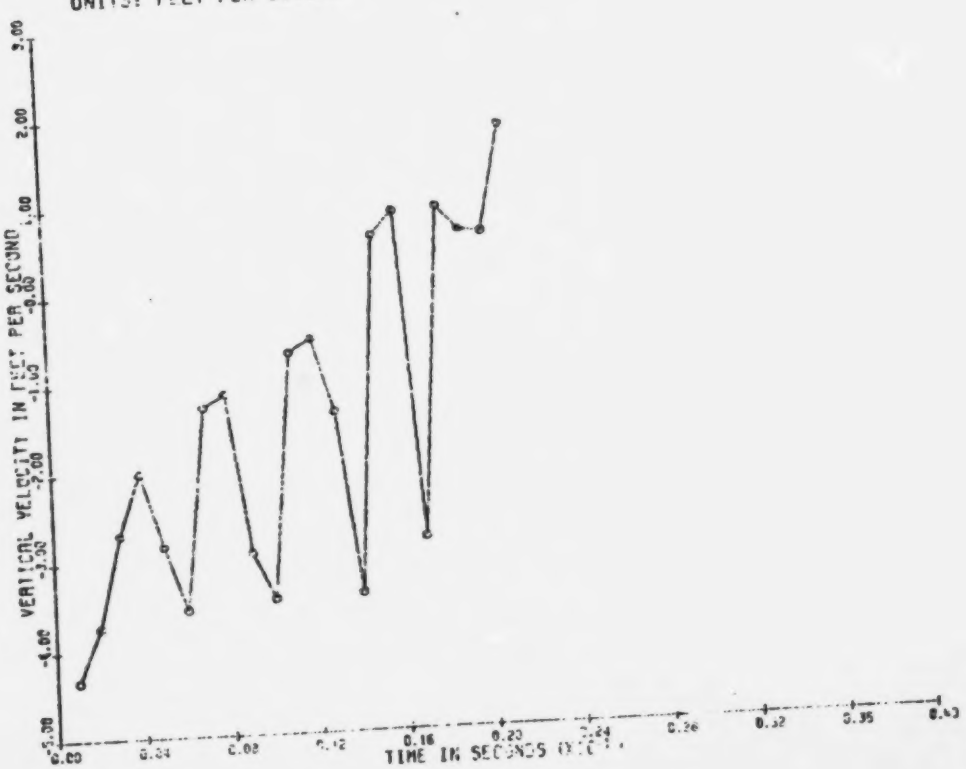

STRAINS OF NODE 78

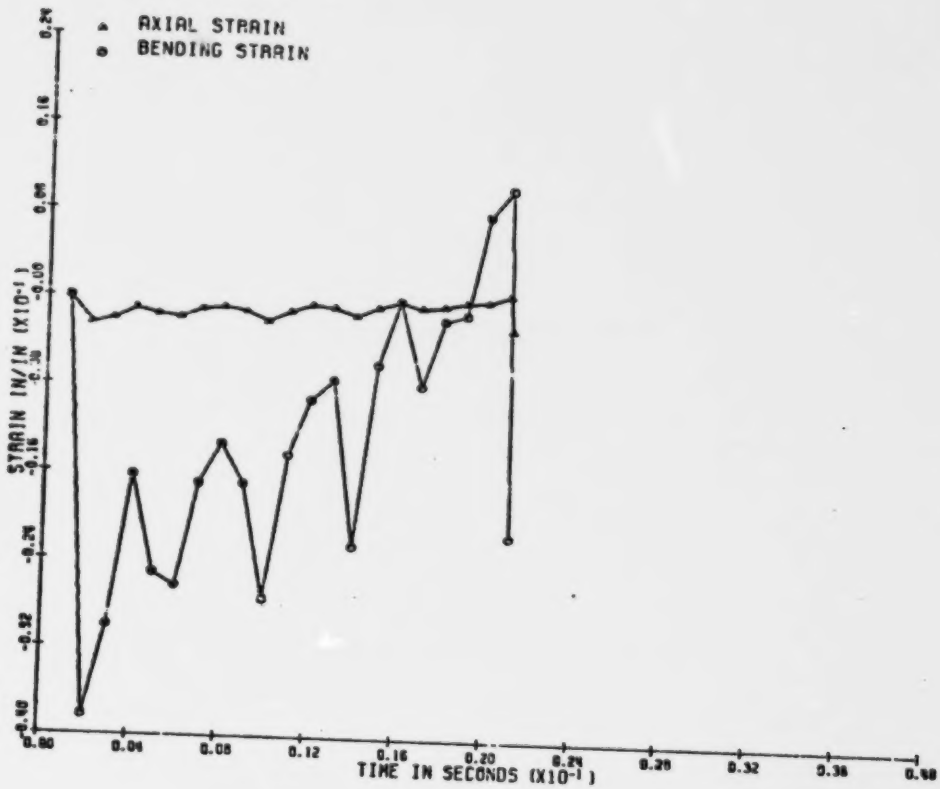

STRAINS OF NODE 80

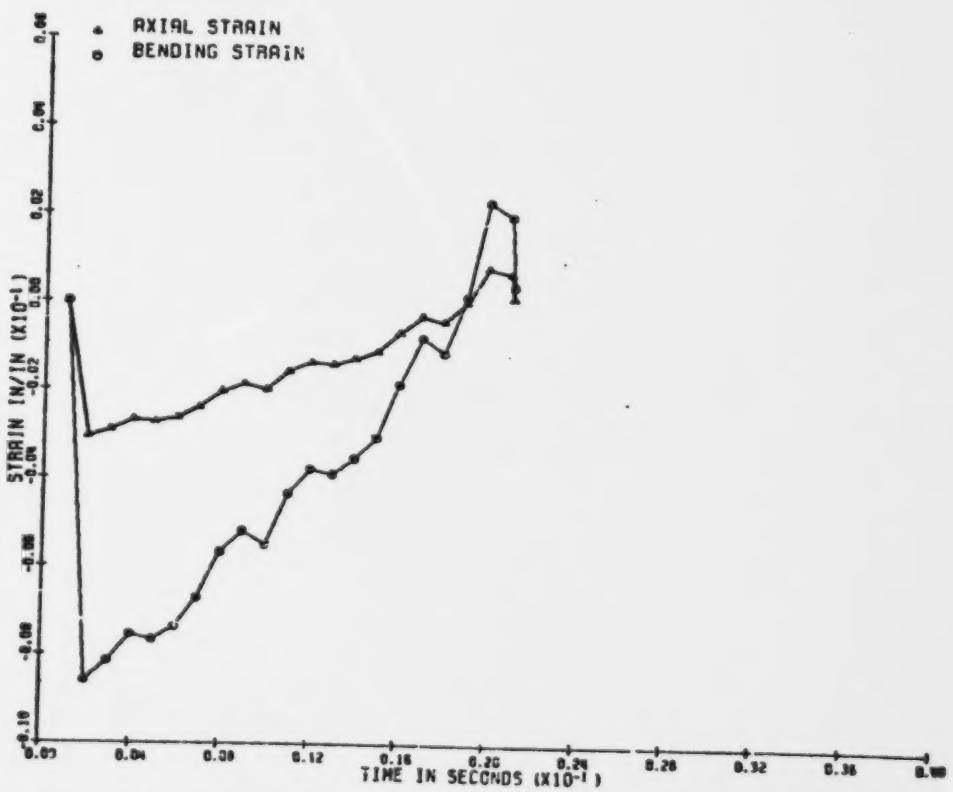

APPENDIX C

PREDICTED OBLIQUE ANGLE

IMPACT RESPONSE BASED ON

LMFE ANALYSIS

CASE 1: V_o = 34.7 in/sec

α = 1.92°

Wing Load = 537 lbs.

CASE 2: V_o = 26.0 in/sec

α = 3.00°

Wing Load = 537 lbs.

DISPLACEMENTS, ACCELERATIONS

STRAINS AND GRAPHICS

INITIAL IMPACT CONDITIONS AT TIME = 0
WING LOAD = 537 LBS
ANGLE = -1.92 DEG
VERTICAL VELOCITY = 34.70 IN/SEC
HORIZONTAL VELOCITY = 0.00 IN/SEC
PITCH RATE = 0.00 RAD/SEC
LOWEST HEIGHT = 0.00 IN
ΔT = 0.00008 SEC
COEF. RESTITUTION = 0.70
COEF. FRICTION = 0.20

TIME RELEASE = 0.00000 SEC
TIME IMPACT = 0.00000 SEC
ANGLE = -1.92 DEG
VERTICAL VELOCITY = 34.70 IN/SEC
HORIZONTAL VELOCITY = 0.00 IN/SEC
PITCH RATE = 0.00 RAD/SEC
LOWEST HEIGHT = 0.00 IN

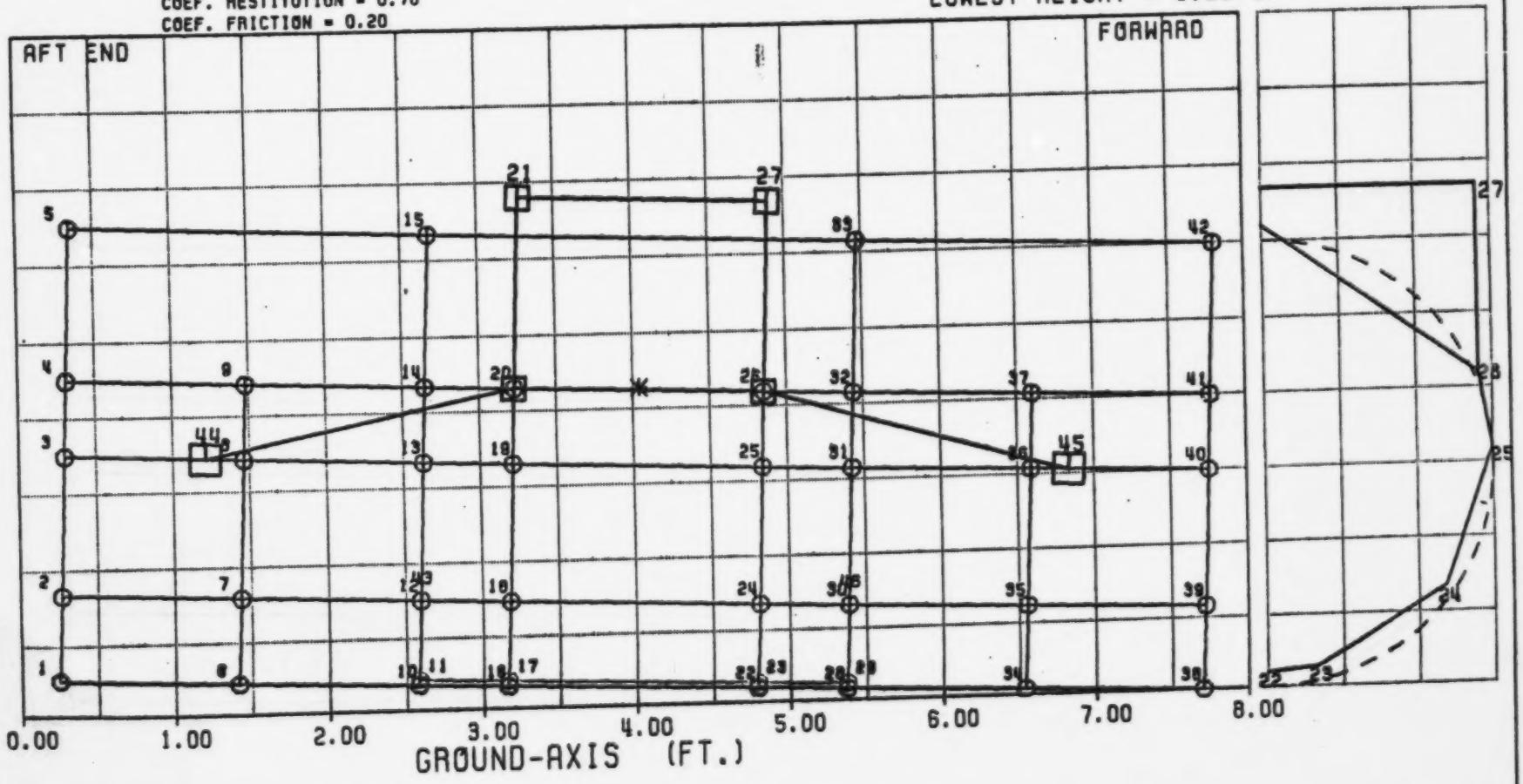

ELASTIC/BUCKLING MODEL FIG.

INITIAL IMPACT CONDITIONS AT TIME = 0
WING LOAD = 537 LBS
ANGLE = -1.82 DEG
VERTICAL VELOCITY = 34.70 IN/SEC
HORIZONTAL VELOCITY = 0.00 IN/SEC
PITCH RATE = 0.00 RAD/SEC
LOWEST HEIGHT = 0.00 IN
ΔT = 0.00008 SEC
COEF. RESTITUTION = 0.70
COEF. FRICTION = 0.20

TIME RELEASE = 0.02700 SEC
TIME IMPACT = 0.02700 SEC
ANGLE = -1.81 DEG
VERTICAL VELOCITY = -38.66 IN/SEC
HORIZONTAL VELOCITY = -5.85 IN/SEC
PITCH RATE = 0.17 RAD/SEC
LOWEST HEIGHT = -0.03 IN

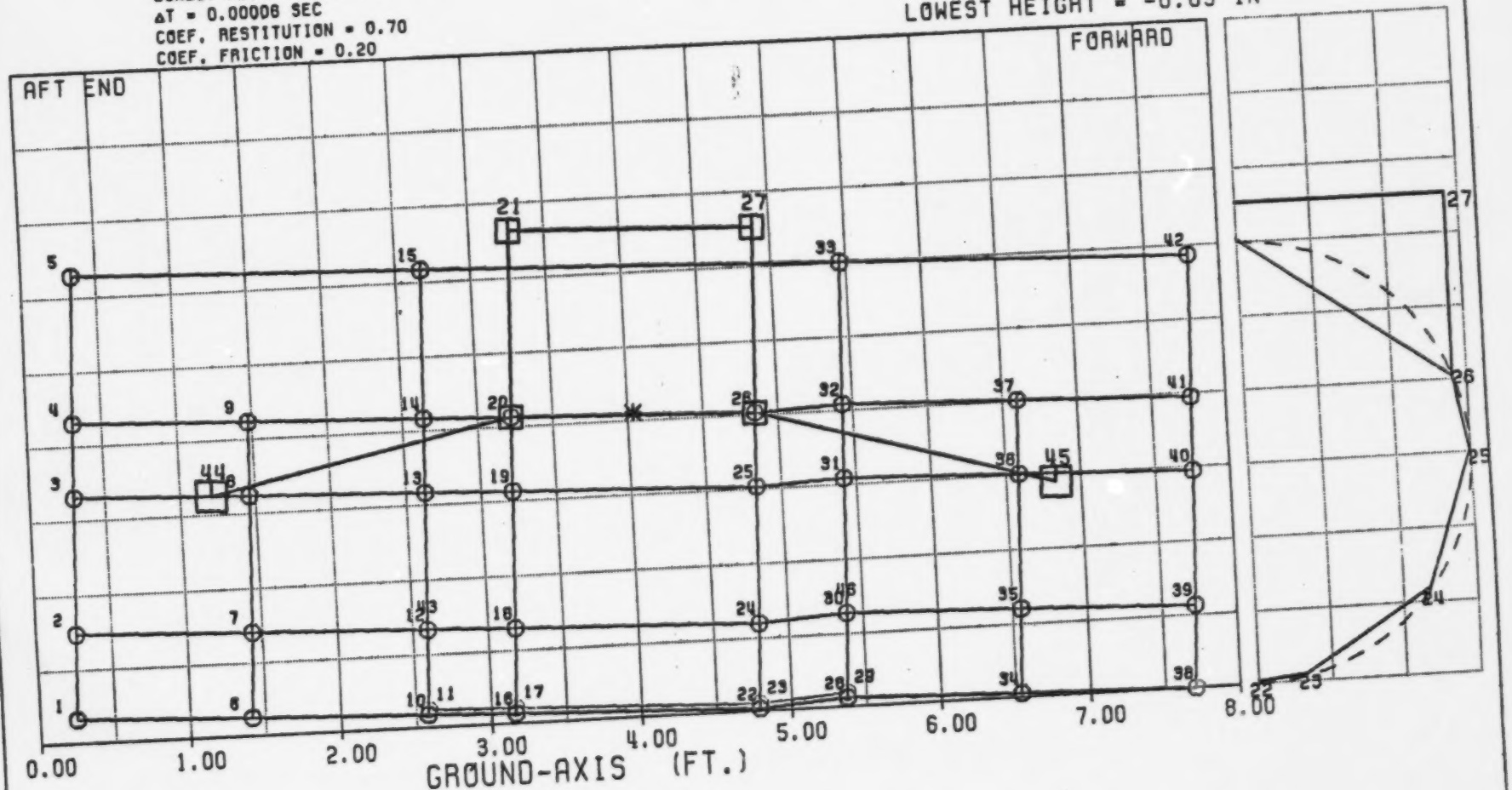

ELASTIC/BUCKLING MODEL

FIG:

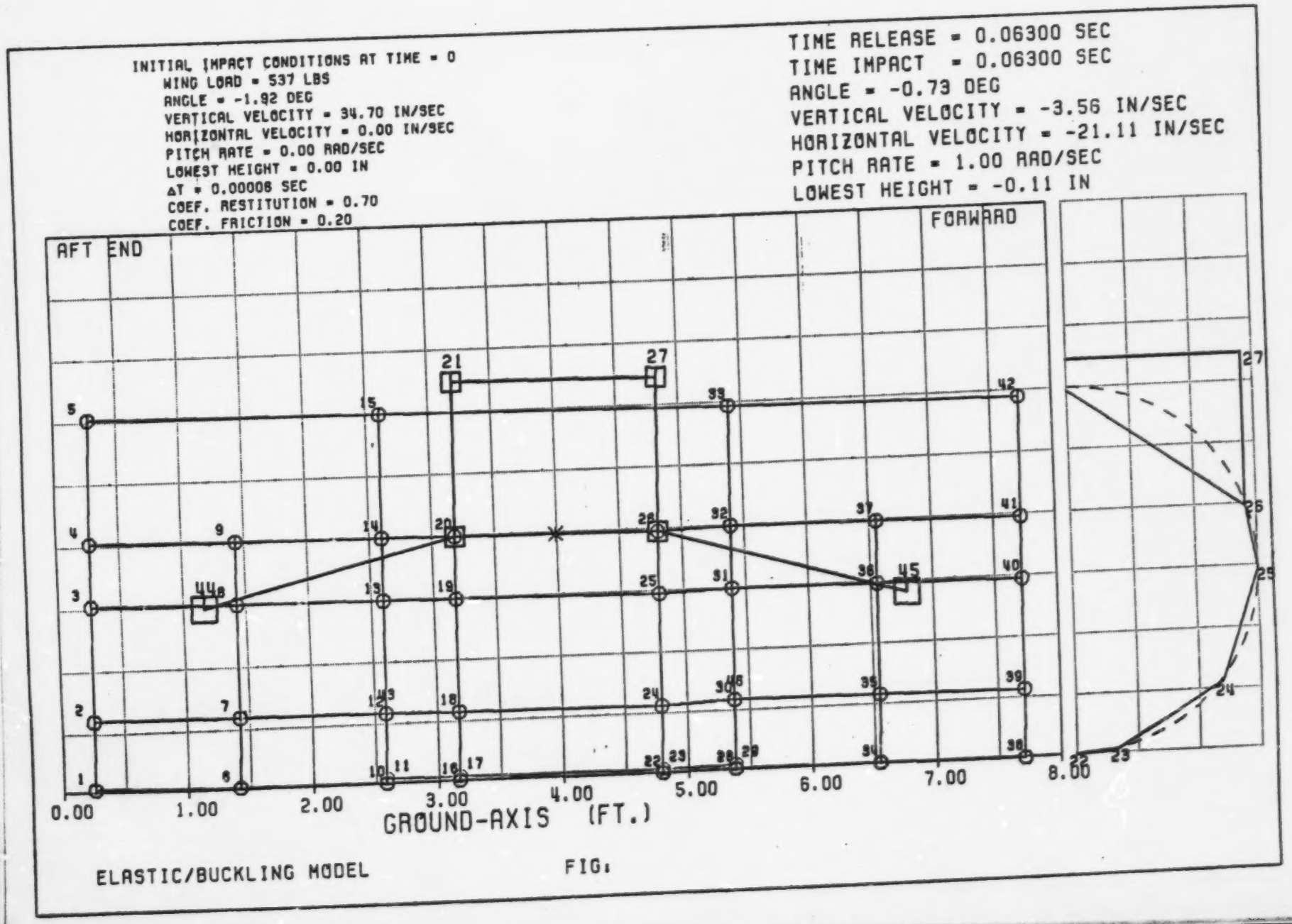

ELASTIC/BUCKLING MODEL

FIG.

INITIAL IMPACT CONDITIONS AT TIME = 0
WING LOAD = 537 LBS
ANGLE = -1.92 DEG
VERTICAL VELOCITY = 34.70 IN/SEC
HORIZONTAL VELOCITY = 0.00 IN/SEC
PITCH RATE = 0.00 RAD/SEC
LOWEST HEIGHT = 0.00 IN
ΔT = 0.00006 SEC
COEF. RESTITUTION = 0.70
COEF. FRICTION = 0.20

TIME RELEASE = 0.11700 SEC
TIME IMPACT = 0.11700 SEC
ANGLE = 1.43 DEG
VERTICAL VELOCITY = 27.72 IN/SEC
HORIZONTAL VELOCITY = -14.50 IN/SEC
PITCH RATE = 0.04 RAD/SEC
LOWEST HEIGHT = -0.07 IN

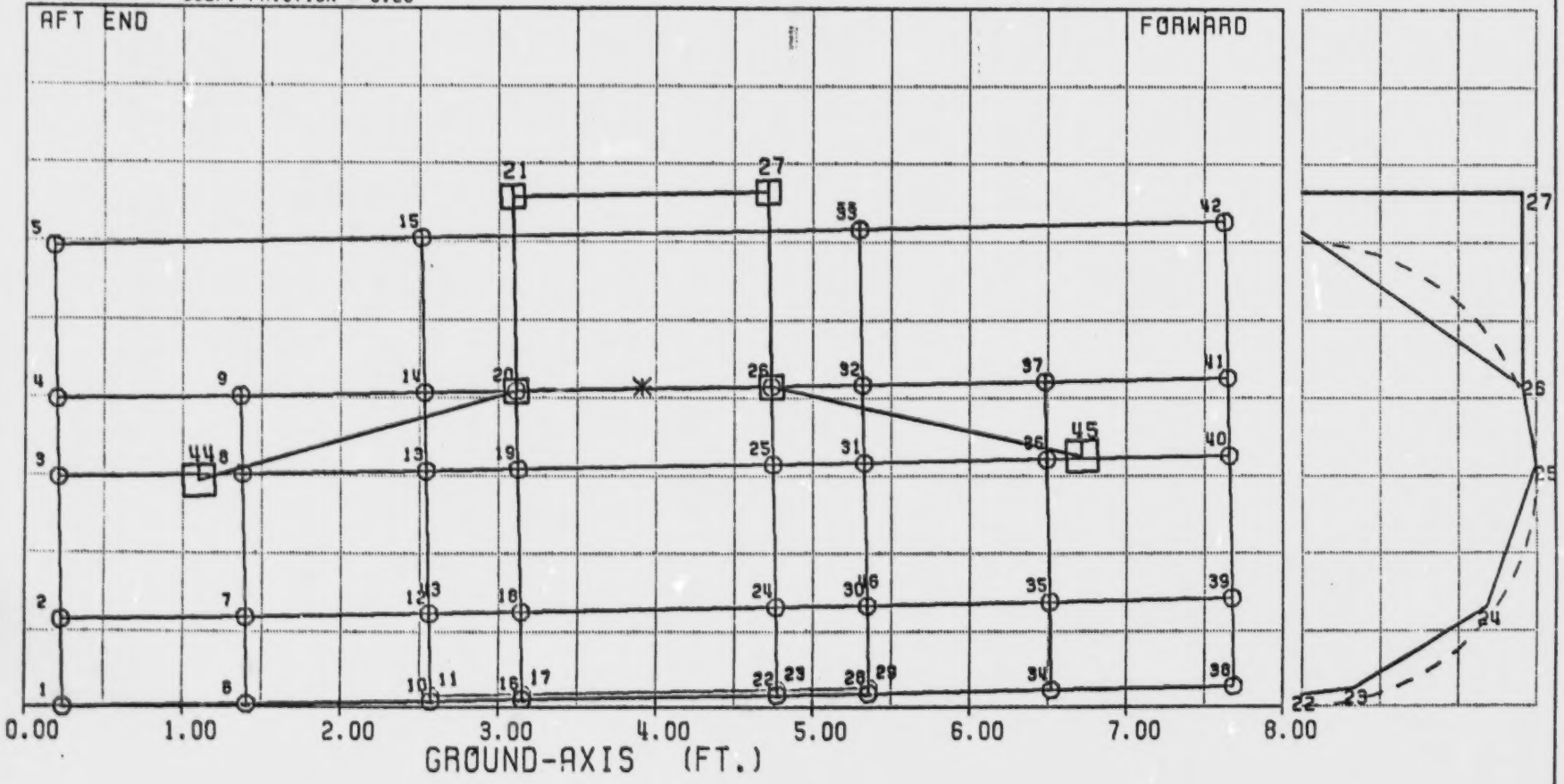

ELASTIC/BUCKLING MODEL

FIG:

INITIAL IMPACT CONDITIONS AT TIME = 0
WING LOAD = 537 LBS
ANGLE = -1.92 DEG
VERTICAL VELOCITY = 34.70 IN/SEC
HORIZONTAL VELOCITY = 0.00 IN/SEC
PITCH RATE = 0.00 RAD/SEC
LOWEST HEIGHT = 0.00 IN
ΔT = 0.00006 SEC
COEF. RESTITUTION = 0.70
COEF. FRICTION = 0.20

TIME RELEASE = 0.16062 SEC
TIME IMPACT = 0.16062 SEC
ANGLE = 1.70 DEG
VERTICAL VELOCITY = 11.44 IN/SEC
HORIZONTAL VELOCITY = -10.43 IN/SEC
PITCH RATE = 0.13 RAD/SEC
LOWEST HEIGHT = 0.31 IN

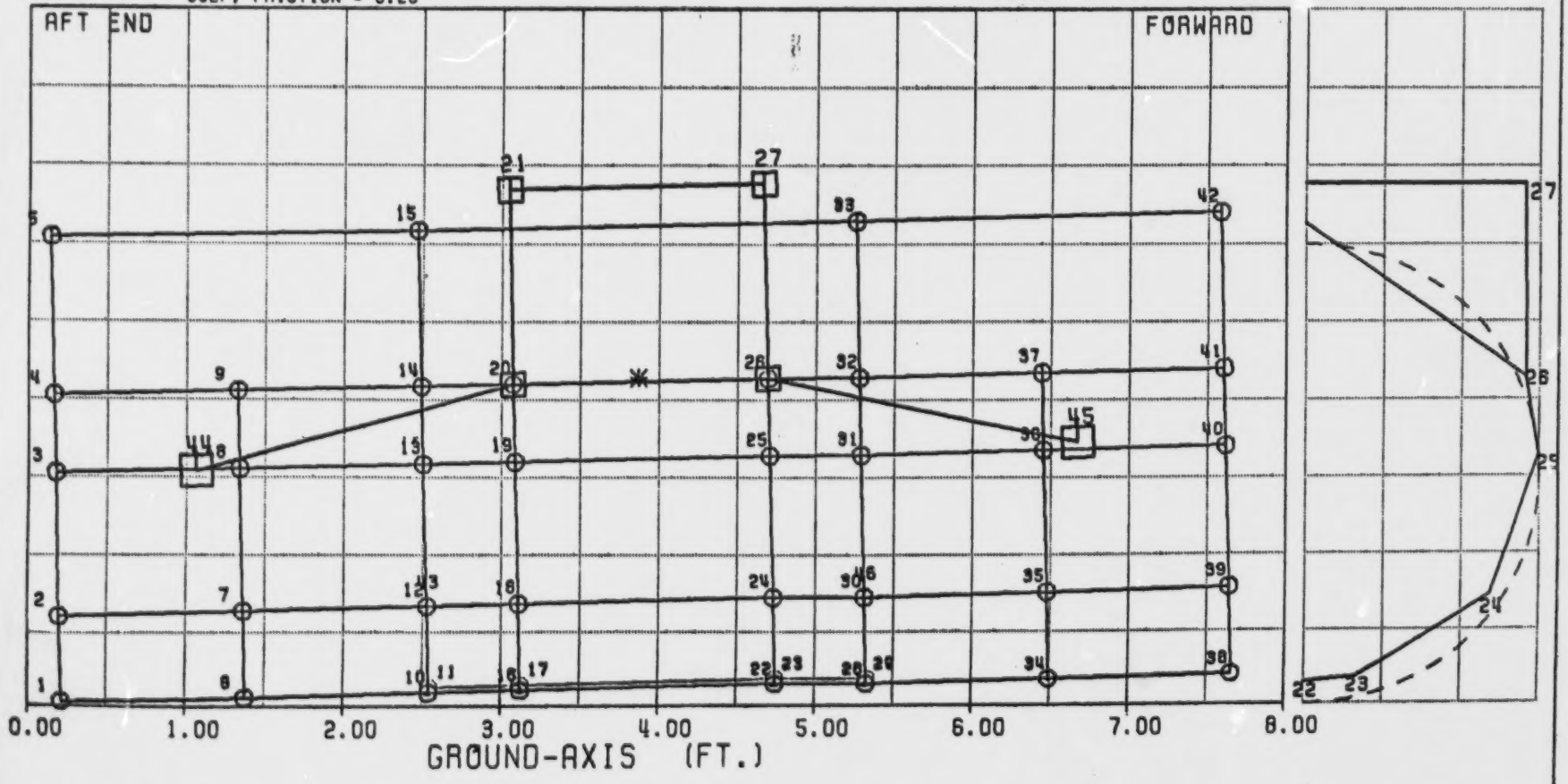

ELASTIC/BUCKLING MODEL

FIG.

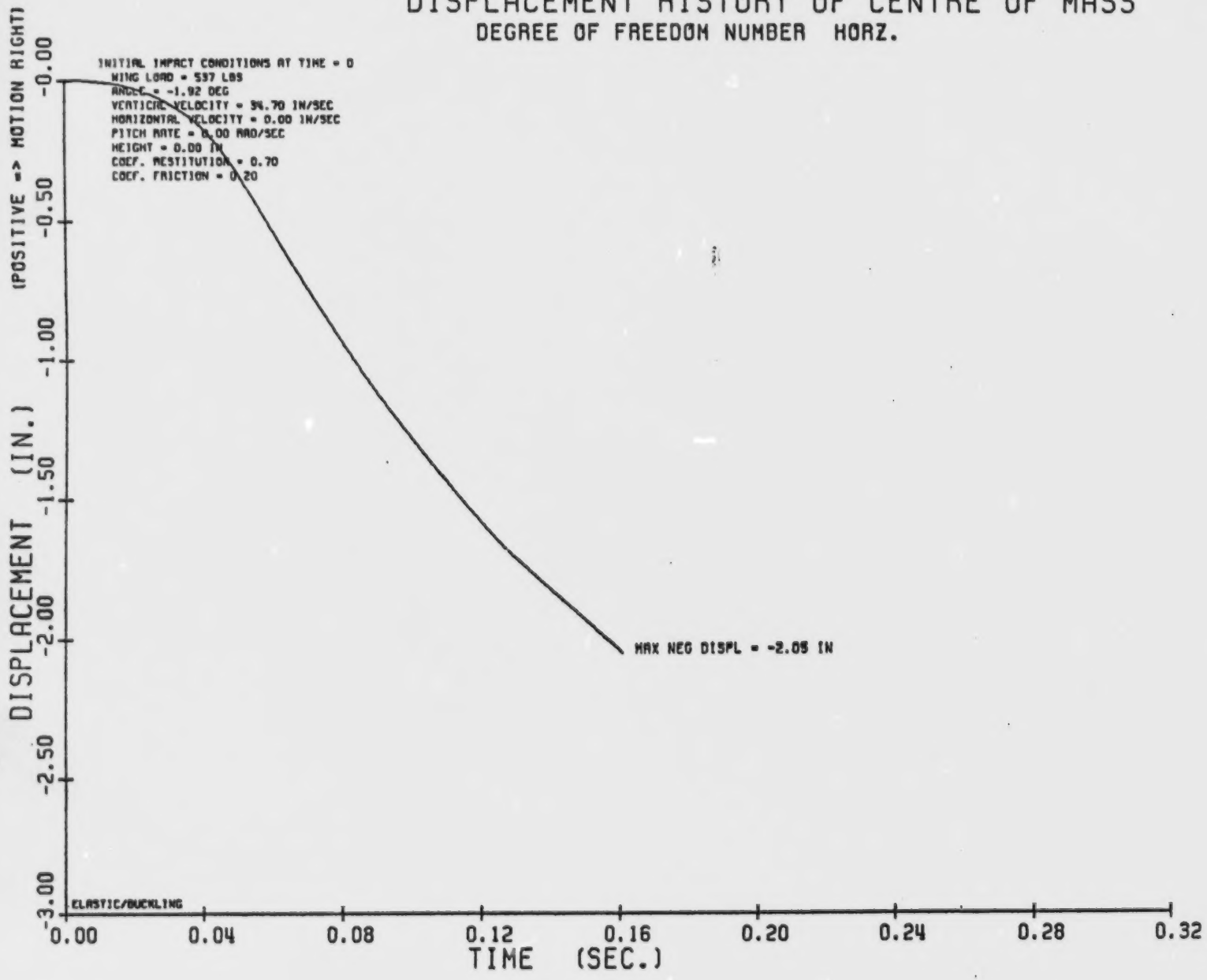
DISPLACEMENT HISTORY OF CENTRE OF MASS
DEGREE OF FREEDOM NUMBER HORZ.
INITIAL IMPACT CONDITIONS AT TIME = 0
WING LOAD = 537 LBS
ANGLE = -1.92 DEG
VERTICAL VELOCITY = 96.70 IN/SEC
HORIZONTAL VELOCITY = 0.00 IN/SEC
PITCH RATE = 0.00 RAD/SEC
HEIGHT = 0.00 IN
COEF. RESTITUTION = 0.70
COEF. FRICTION = 0.20
MAX NEG DISPL = -2.05 IN
ELASTIC/BUCKLING
DISPLACEMENT (IN.)
(POSITIVE => MOTION RIGHT)
-0.00
-0.50
-1.00
-1.50
-2.00
-2.50
-3.00
0.00
0.04
0.08
0.12
0.16
0.20
0.24
0.28
0.32
TIME (SEC.)

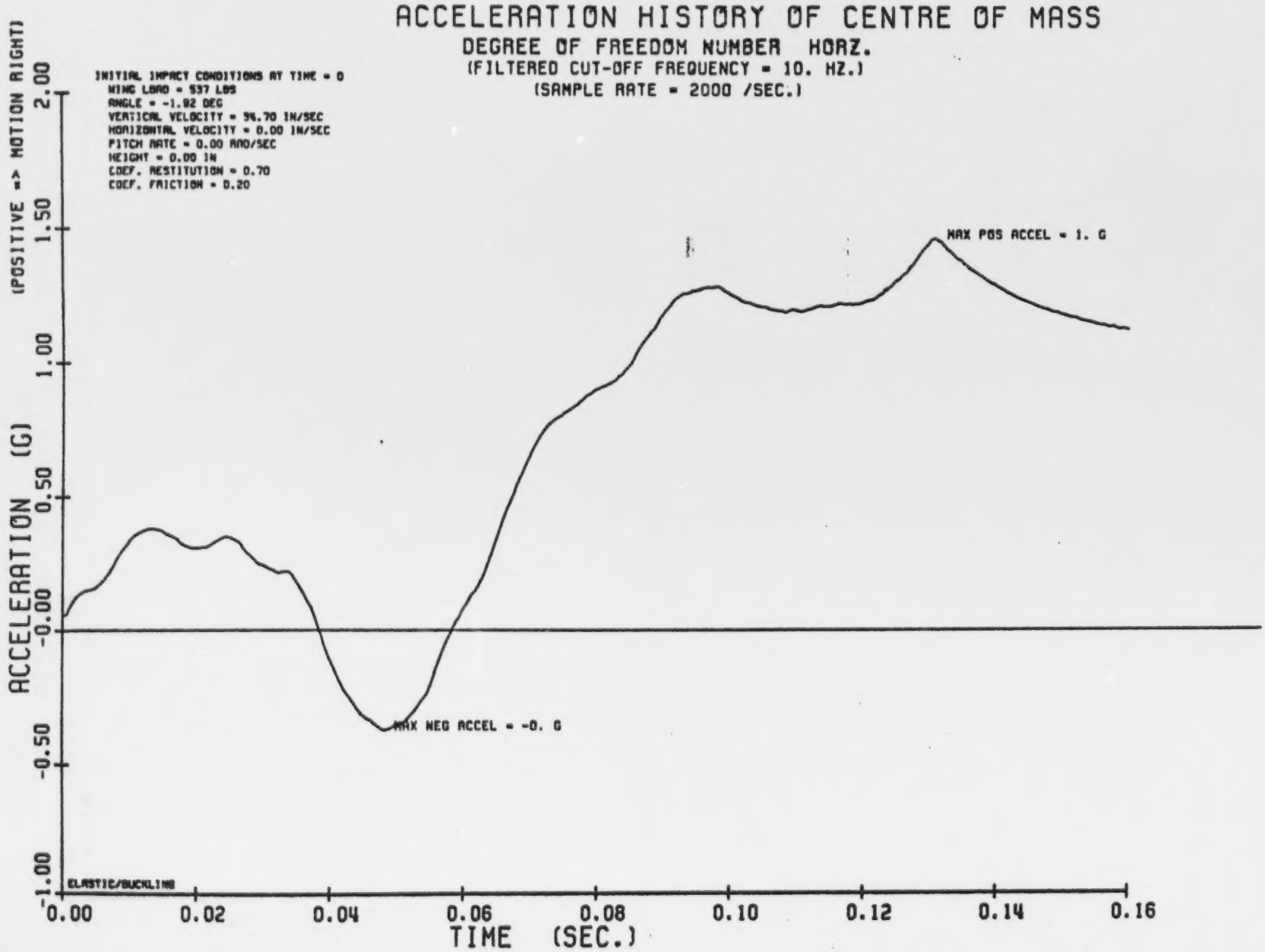
ACCELERATION HISTORY OF CENTRE OF MASS
DEGREE OF FREEDOM NUMBER HORZ.
(FILTERED CUT-OFF FREQUENCY = 10. HZ.)
(SAMPLE RATE = 2000 /SEC.)
INITIAL IMPACT CONDITIONS AT TIME = 0
WING LOAD = 537 LBS
ANGLE = -1.92 DEG
VERTICAL VELOCITY = 96.70 IN/SEC
HORIZONTAL VELOCITY = 0.00 IN/SEC
PITCH RATE = 0.00 RAD/SEC
HEIGHT = 0.00 IN
COEF. RESTITUTION = 0.70
COEF. FRICTION = 0.20
MAX POS ACCEL = 1. G
MAX NEG ACCEL = -0. G
ELASTIC/BUCKLING
ACCELERATION (G)
(POSITIVE => MOTION RIGHT)
2.00
1.50
1.00
0.50
-0.00
-0.50
-1.00
0.00
0.02
0.04
0.06
0.08
0.10
0.12
0.14
0.16
TIME (SEC.)

ACCELERATION HISTORY OF CENTRE OF MASS

DEGREE OF FREEDOM NUMBER ANGULAR PITCH

(FILTERED CUT-OFF FREQUENCY = 10. HZ.)

(SAMPLE RATE = 2000 /SEC.)

INITIAL IMPACT CONDITIONS AT TIME = 0
WING LOAD = 537 LBS
ANGLE = -1.82 DEG
VERTICAL VELOCITY = 94.70 IN/SEC
HORIZONTAL VELOCITY = 0.00 IN/SEC
PITCH RATE = 0.00 RAD/SEC
HEIGHT = 0.00 IN
COEF. RESTITUTION = 0.70
COEF. FRICTION = 0.20

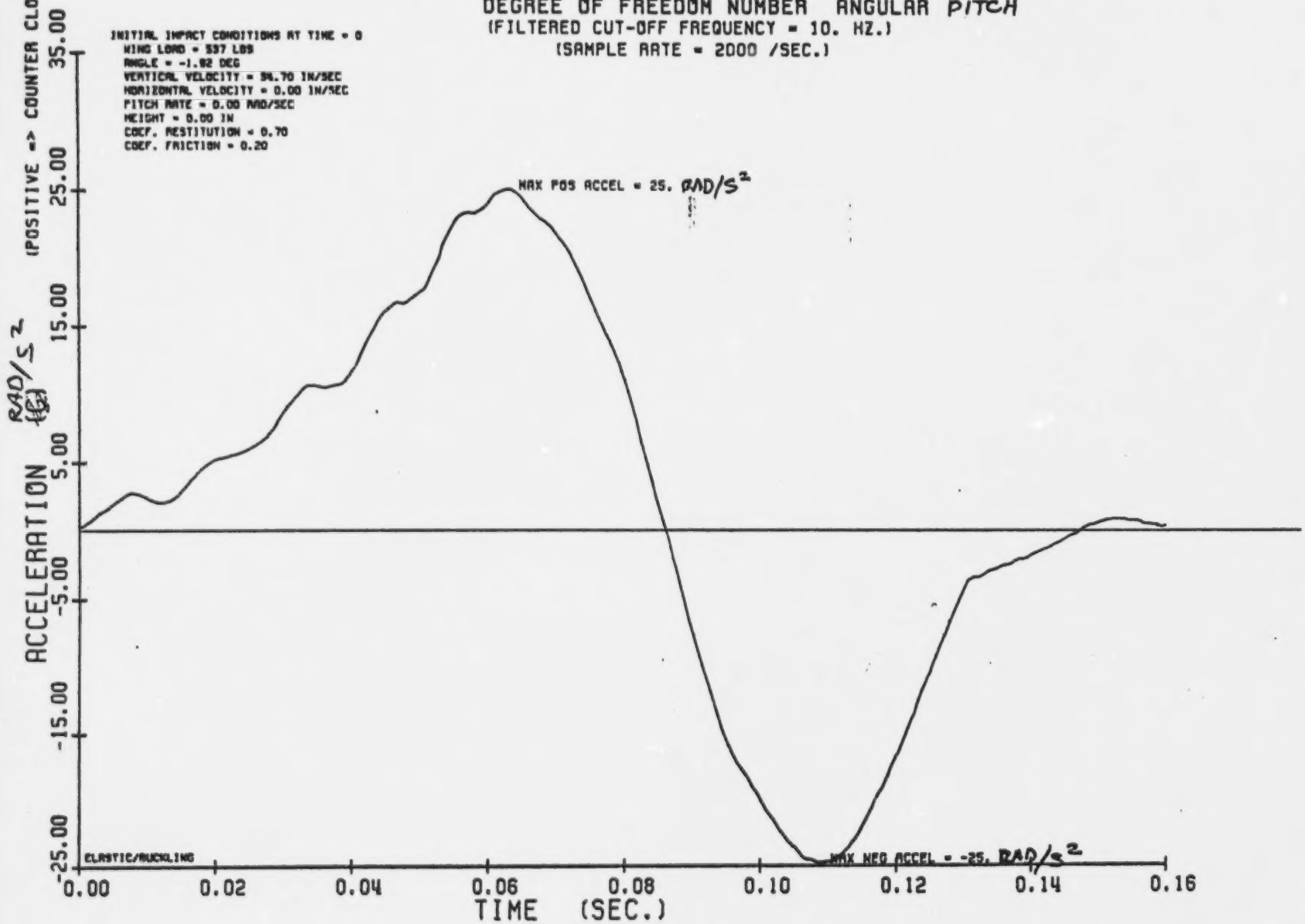

DISPLACEMENT HISTORY OF MASS 12

DEGREE OF FREEDOM NUMBER 23 VERT.

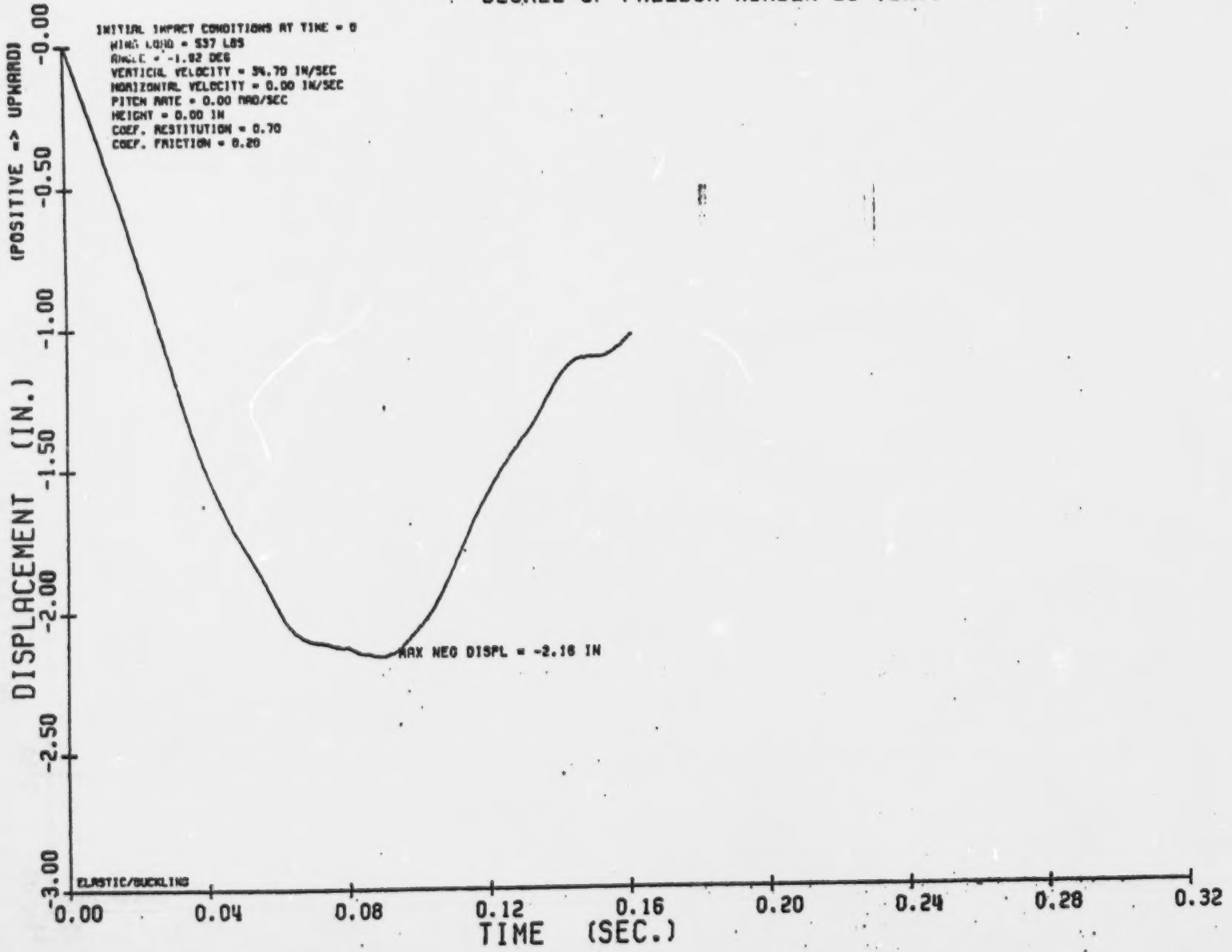

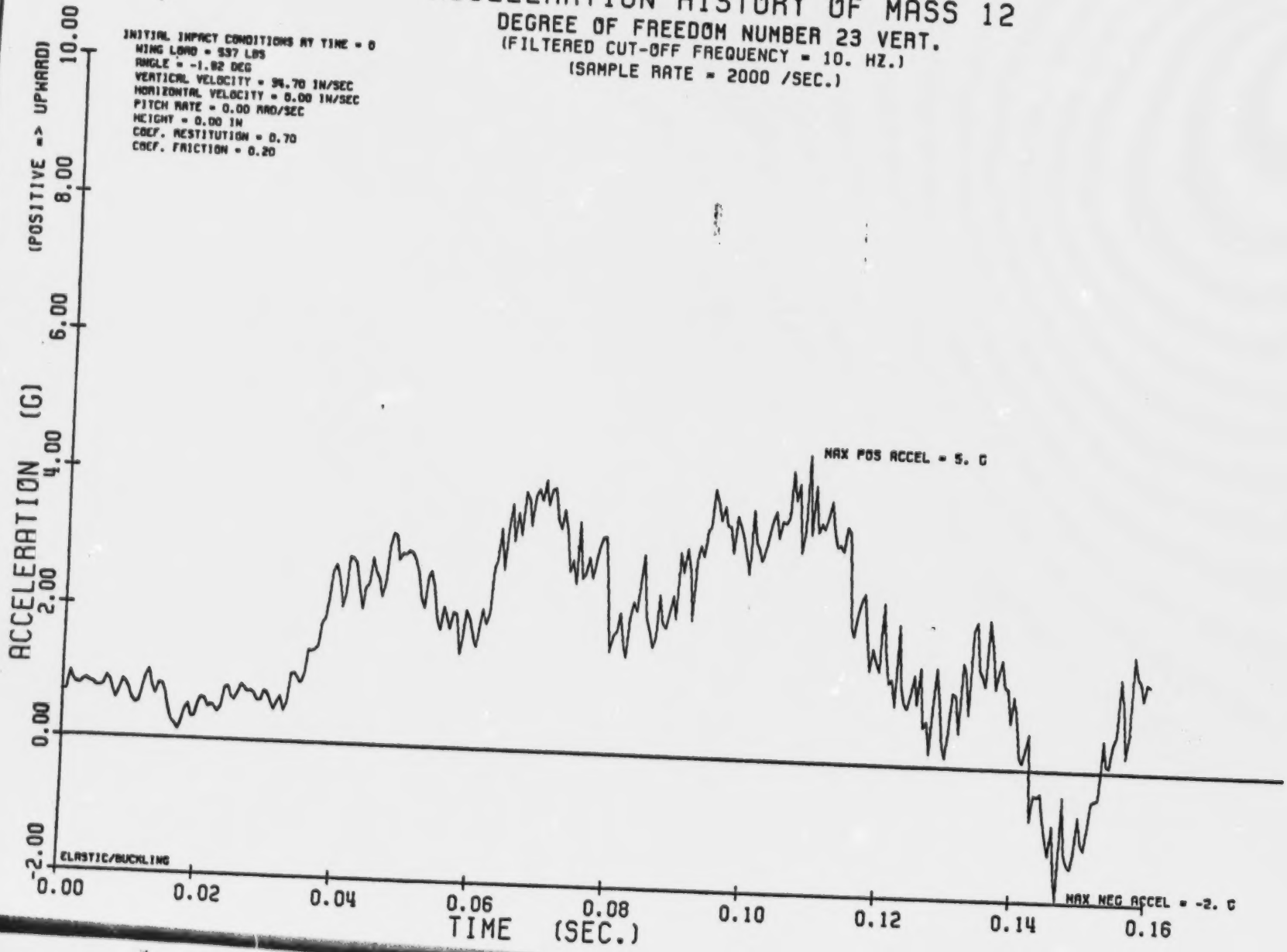
ACCELERATION HISTORY OF MASS 12
DEGREE OF FREEDOM NUMBER 23 VERT.
(FILTERED CUT-OFF FREQUENCY = 10. HZ.)
(SAMPLE RATE = 2000 /SEC.)
INITIAL IMPACT CONDITIONS AT TIME = 0
WING LOAD = 537 LBS
ANGLE = -1.82 DEG
VERTICAL VELOCITY = 96.70 IN/SEC
HORIZONTAL VELOCITY = 0.00 IN/SEC
PITCH RATE = 0.00 RAD/SEC
HEIGHT = 0.00 IN
COEF. RESTITUTION = 0.70
COEF. FRICTION = 0.20
ACCELERATION (G)
(POSITIVE => UPWARD)
10.00
8.00
6.00
4.00
2.00
0.00
-2.00
MAX POS ACCEL = 5. G
MAX NEG ACCEL = -2. G
ELASTIC/BUCKLING
0.00
0.02
0.04
0.06
0.08
0.10
0.12
0.14
0.16
TIME (SEC.)

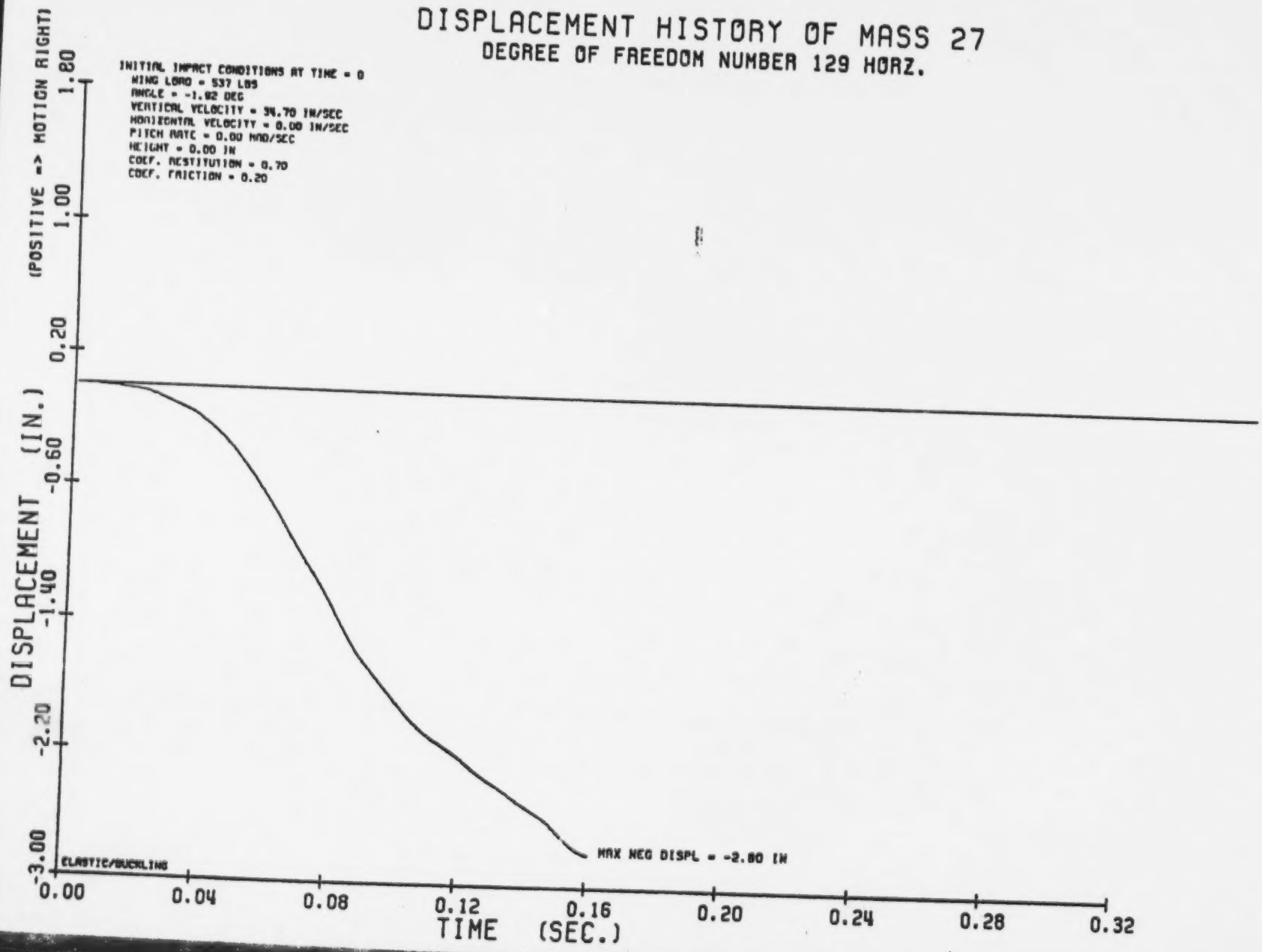
DISPLACEMENT HISTORY OF MASS 27
DEGREE OF FREEDOM NUMBER 129 HORZ.
INITIAL IMPACT CONDITIONS AT TIME = 0
WING LOAD = 537 LBS
ANGLE = -1.82 DEG
VERTICAL VELOCITY = 36.70 IN/SEC
HORIZONTAL VELOCITY = 0.00 IN/SEC
PITCH RATE = 0.00 RAD/SEC
HEIGHT = 0.00 IN
COEF. RESTITUTION = 0.70
COEF. FRICTION = 0.20
(POSITIVE => MOTION RIGHT)
DISPLACEMENT (IN.)
1.80
1.00
0.20
-0.60
-1.40
-2.20
-3.00
ELASTIC/BUCKLING
MAX NEG DISPL = -2.80 IN
0.00
0.04
0.08
0.12
0.16
0.20
0.24
0.28
0.32
TIME (SEC.)

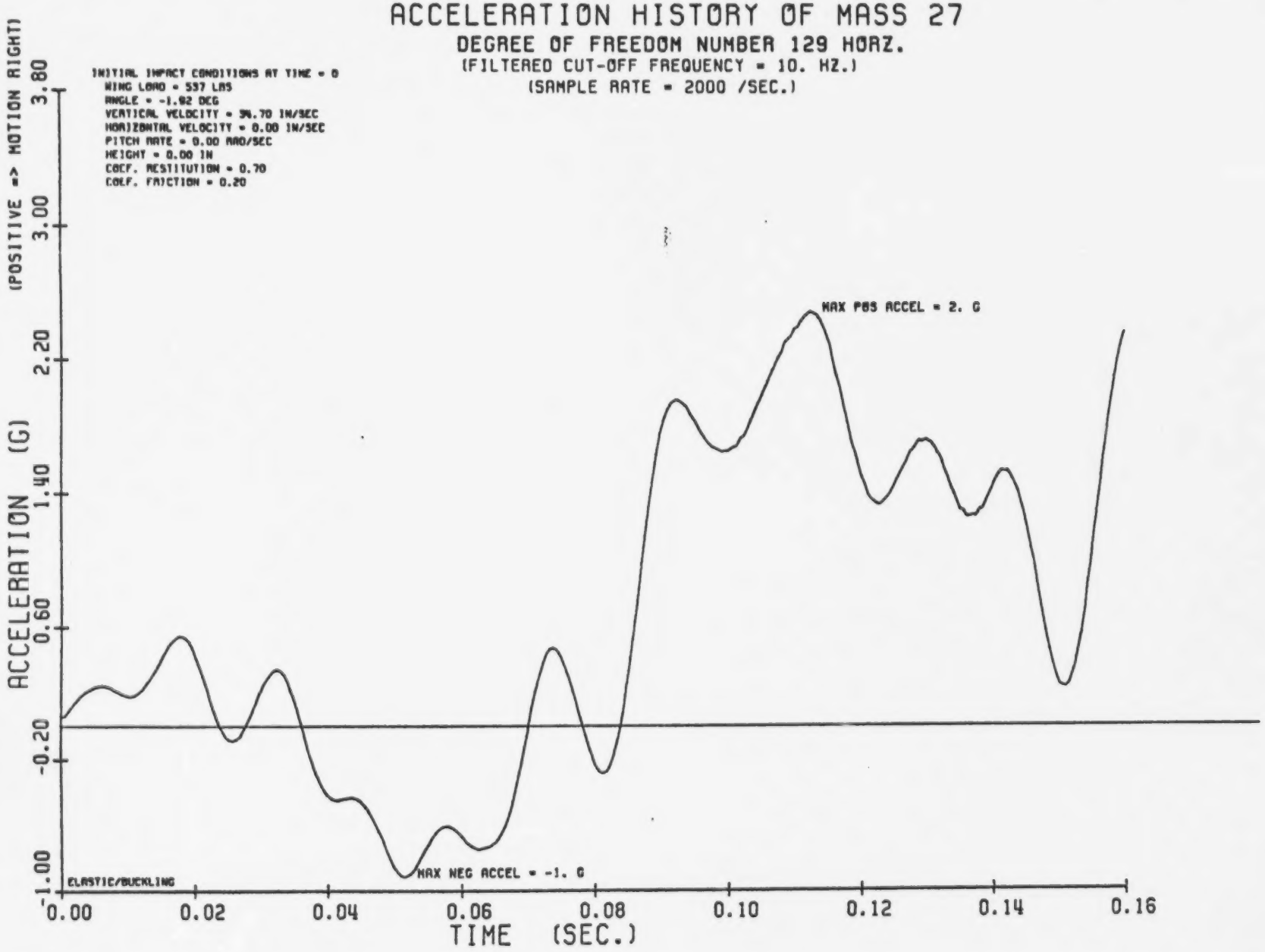
ACCELERATION HISTORY OF MASS 27
DEGREE OF FREEDOM NUMBER 129 HORZ.
(FILTERED CUT-OFF FREQUENCY = 10. HZ.)
(SAMPLE RATE = 2000 /SEC.)
INITIAL IMPACT CONDITIONS AT TIME = 0
WING LOAD = 537 LBS
ANGLE = -1.92 DEG
VERTICAL VELOCITY = 96.70 IN/SEC
HORIZONTAL VELOCITY = 0.00 IN/SEC
PITCH RATE = 0.00 RAD/SEC
HEIGHT = 0.00 IN
COEF. RESTITUTION = 0.70
COEF. FRICTION = 0.20
MAX POS ACCEL = 2. G
MAX NEG ACCEL = -1. G
ELASTIC/BUCKLING
ACCELERATION (G)
(POSITIVE => MOTION RIGHT)
3.80
3.00
2.20
1.40
0.60
-0.20
-1.00
0.00
0.02
0.04
0.06
0.08
0.10
0.12
0.14
0.16
TIME (SEC.)

DISPLACEMENT HISTORY OF MASS 27

DEGREE OF FREEDOM NUMBER 130 VERT.

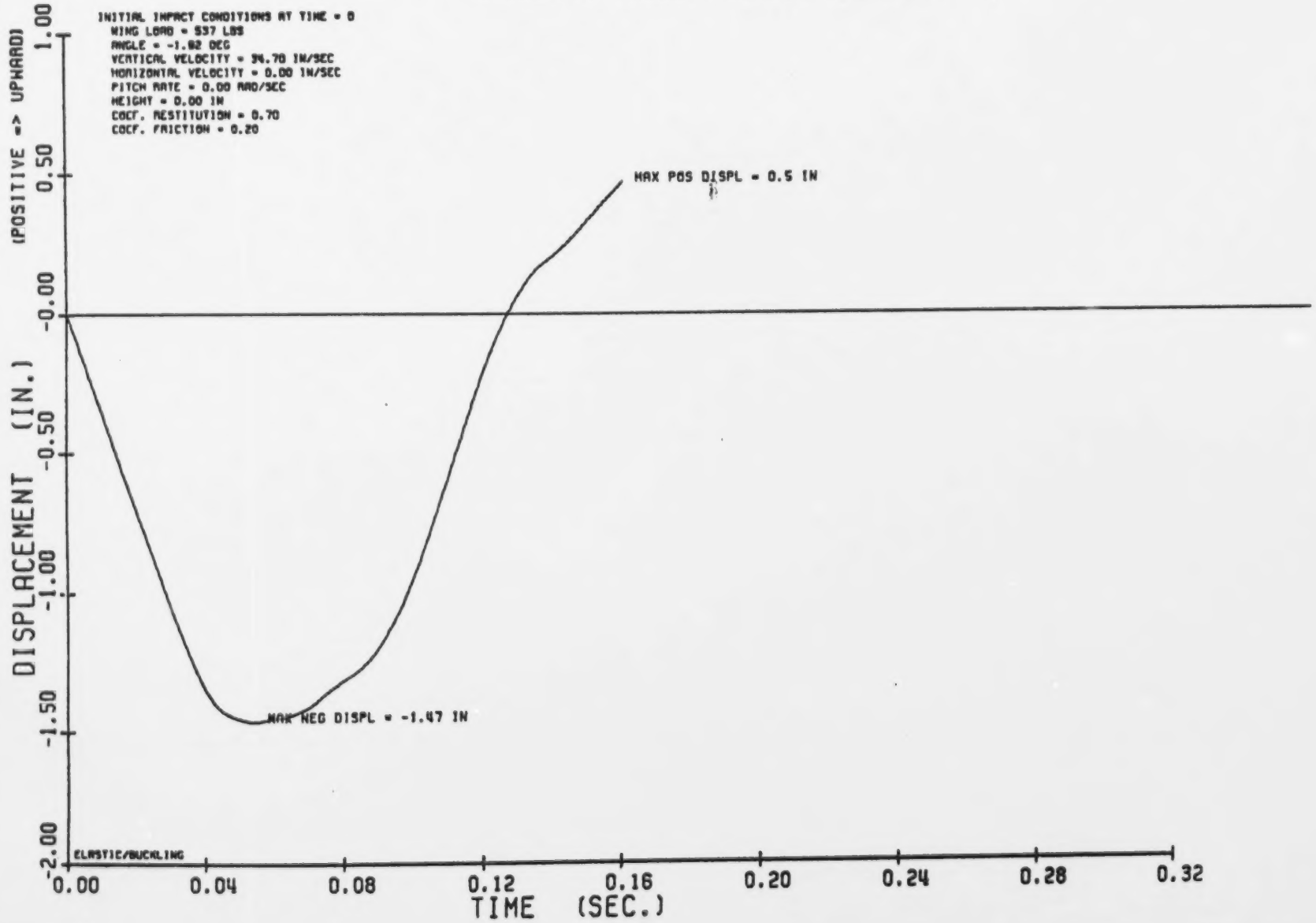

ACCELERATION HISTORY OF MASS 27

DEGREE OF FREEDOM NUMBER 130 VERT.

(FILTERED CUT-OFF FREQUENCY = 10. HZ.)

(SAMPLE RATE = 2000 /SEC.)

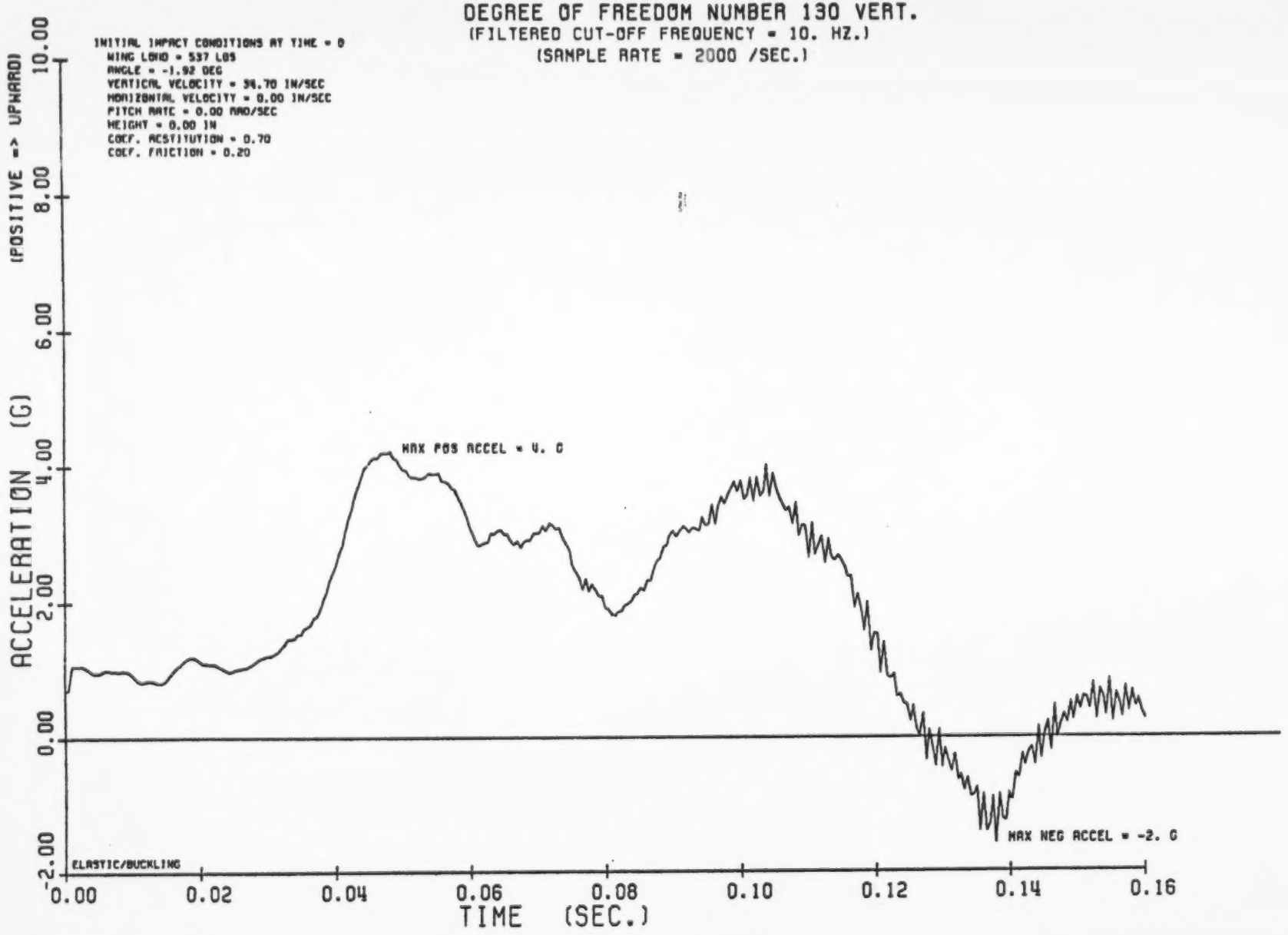

DISPLACEMENT HISTORY OF MASS 44

DEGREE OF FREEDOM NUMBER 142 VERT.

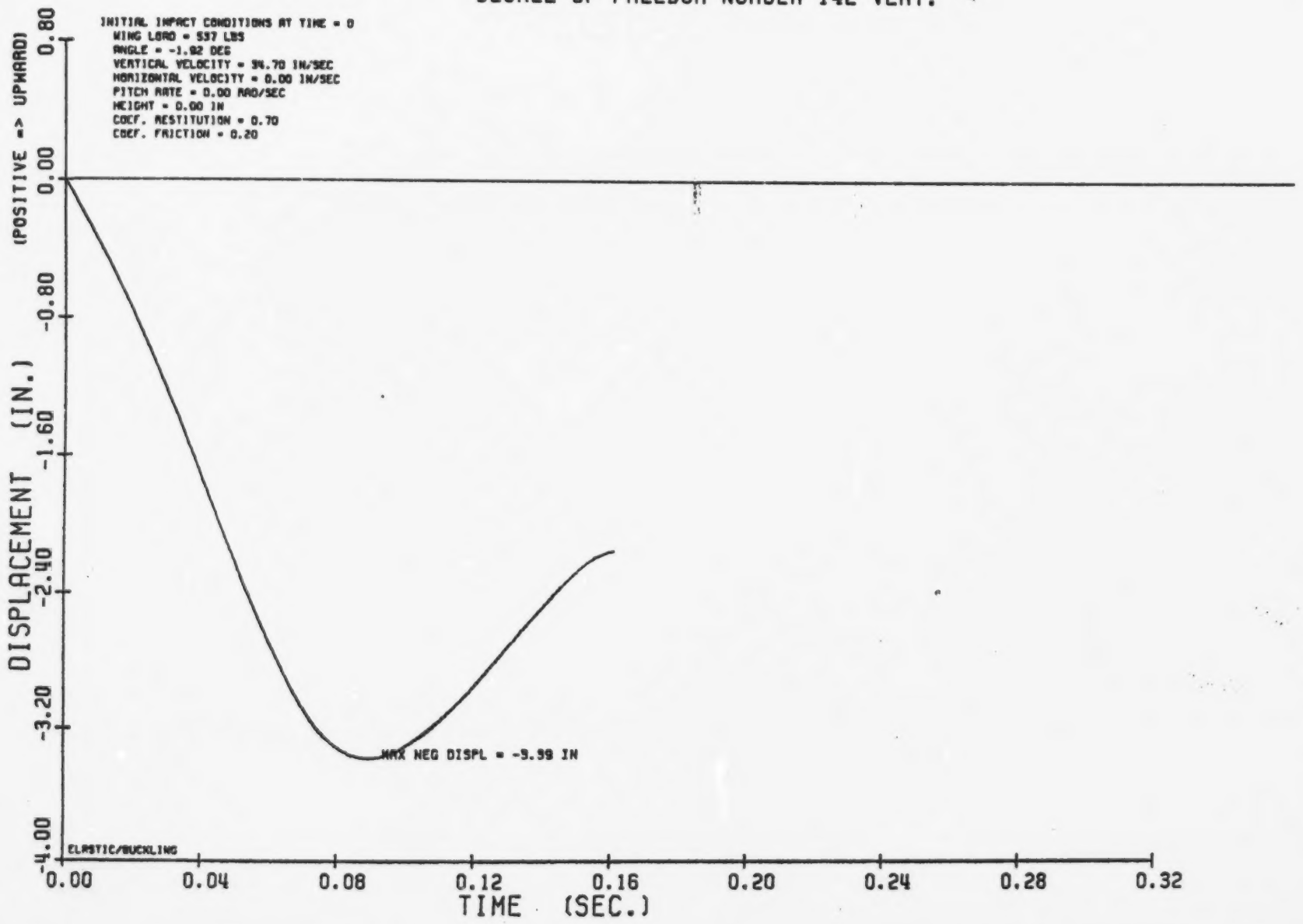

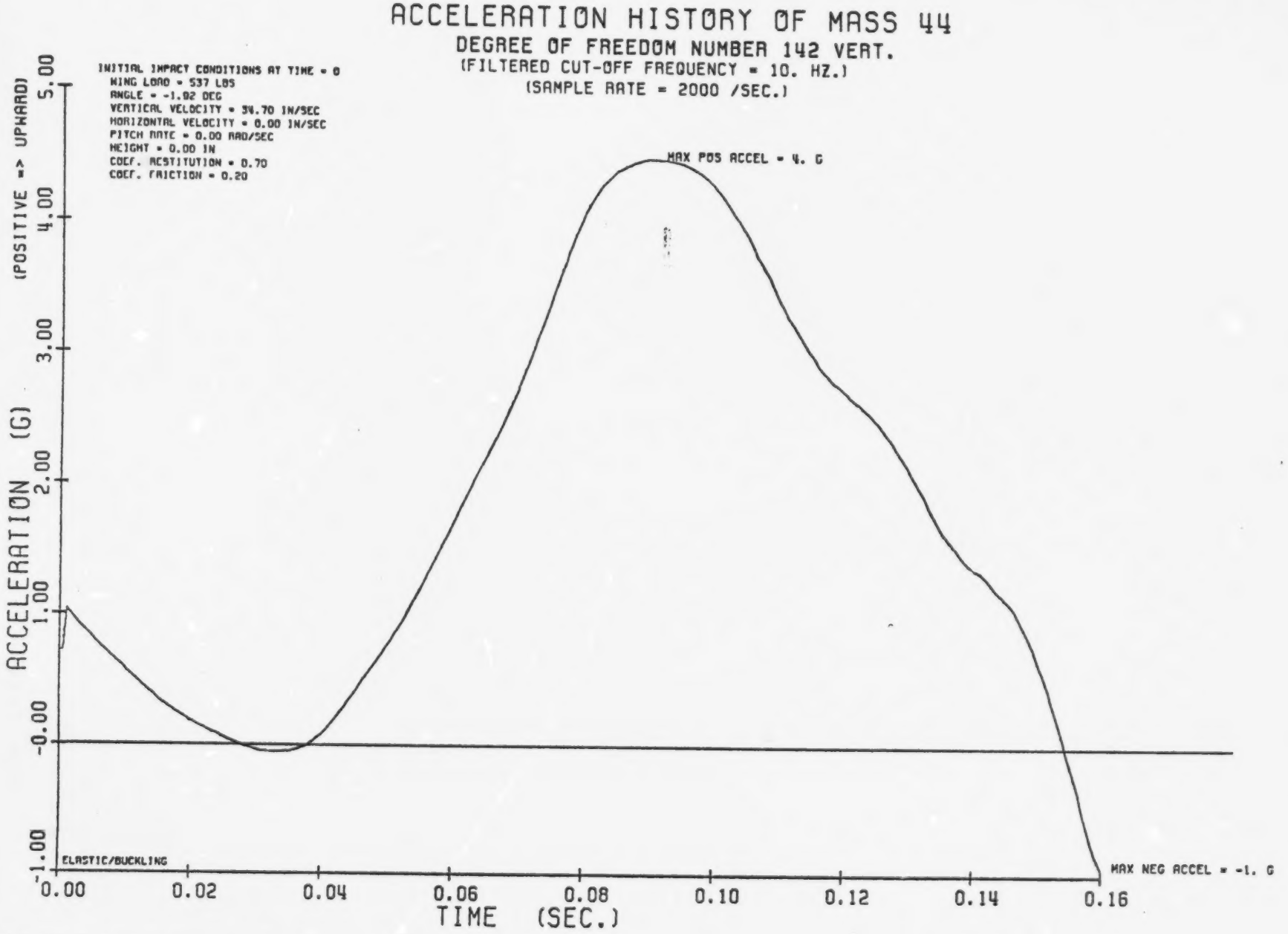
ACCELERATION HISTORY OF MASS 44
DEGREE OF FREEDOM NUMBER 142 VERT.
(FILTERED CUT-OFF FREQUENCY = 10. HZ.)
(SAMPLE RATE = 2000 /SEC.)
INITIAL IMPACT CONDITIONS AT TIME = 0
WING LOAD = 537 LBS
ANGLE = -1.02 DEG
VERTICAL VELOCITY = 34.70 IN/SEC
HORIZONTAL VELOCITY = 0.00 IN/SEC
PITCH RATE = 0.00 RAD/SEC
HEIGHT = 0.00 IN
COEF. RESTITUTION = 0.70
COEF. FRICTION = 0.20
MAX POS ACCEL = 4. G
MAX NEG ACCEL = -1. G
ELASTIC/BUCKLING
ACCELERATION (G) (POSITIVE => UPWARD)
5.00
4.00
3.00
2.00
1.00
-0.00
-1.00
0.00
0.02
0.04
0.06
0.08
0.10
0.12
0.14
0.16
TIME (SEC.)

STRAIN HISTORY OF BEAM 31

(LOWER (OUTER) SURFACE STRAIN)

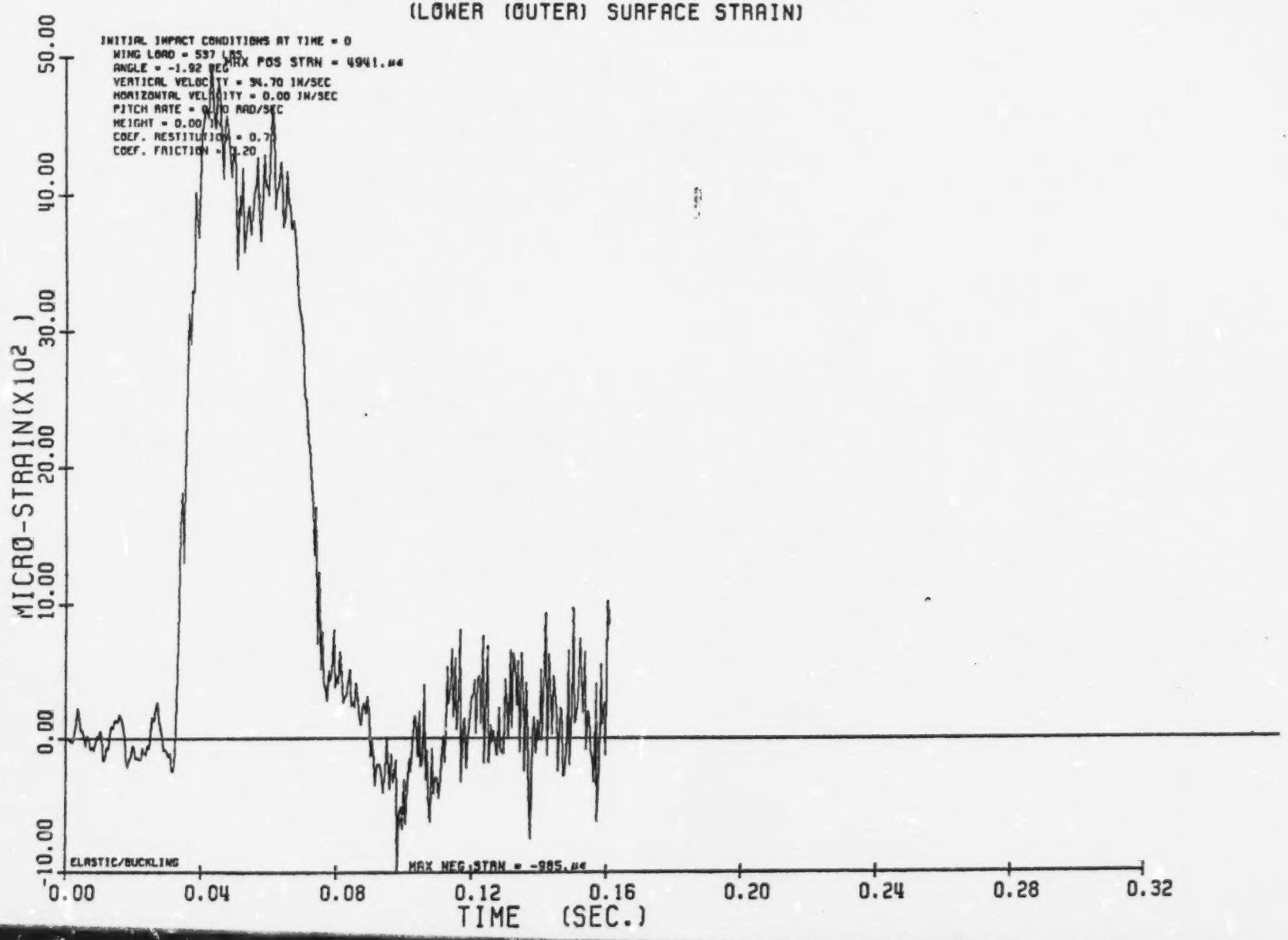

STRAIN HISTORY OF BEAM 31
(UPPER (INNER) SURFACE STRAIN)

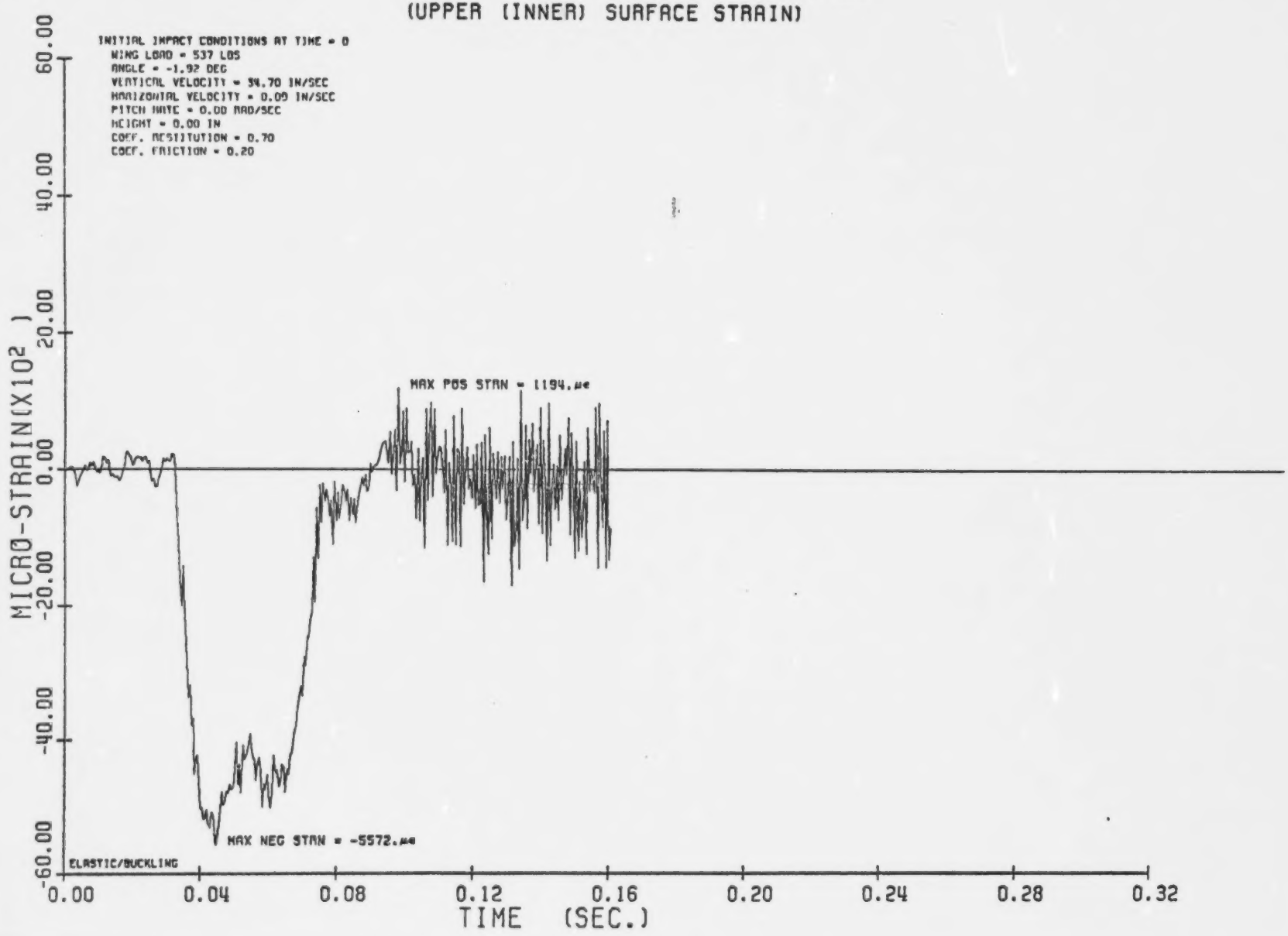

APPENDIX D

PREDICTED 'FREE-FLIGHT' IMPACT RESPONSE BASED ON LMFE ANALYSIS

Horizontal Velocity = 259 in/sec

Vertical Impact Velocity = 34.59 in/sec

$\alpha_o = 3^o$, $\alpha_{o_{impact}} = 10.62^o$

$\dot{\alpha}_o = 1.43$ rad/sec at impact

Wing Load = 537 lbs.

DISPLACEMENTS, ACCELERATIONS STRAINS AND GRAPHICS FOR FREE-FLIGHT PHASE (PRIOR TO IMPACT) AND POST-IMPACT PHASE

JOB:CC340230 HASPJOB02276 PRIORITY 4 JOB 1848
DATE:13/09/81 TIME:13:37 (PLOTST EXECUTION)

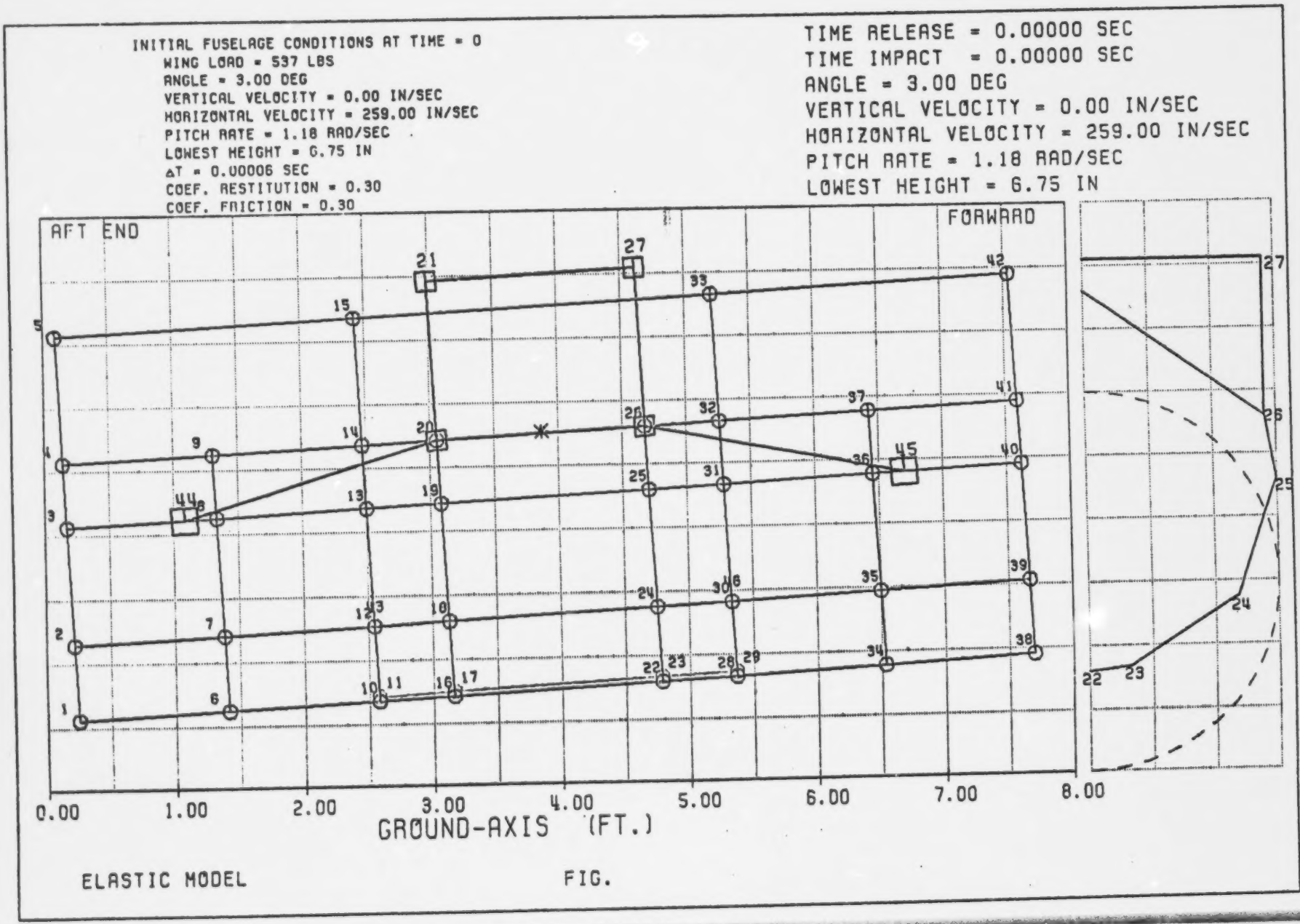

ELASTIC MODEL FIG.

INITIAL FUSELAGE CONDITIONS AT TIME = 0
WING LOAD = 537 LBS
ANGLE = 3.00 DEG
VERTICAL VELOCITY = 0.00 IN/SEC
HORIZONTAL VELOCITY = 259.00 IN/SEC
PITCH RATE = 1.18 RAD/SEC
LOWEST HEIGHT = 6.75 IN
ΔT = 0.00006 SEC
COEF. RESTITUTION = 0.30
COEF. FRICTION = 0.30

TIME RELEASE = 0.02700 SEC
TIME IMPACT = 0.00000 SEC
ANGLE = 4.80 DEG
VERTICAL VELOCITY = -9.92 IN/SEC
HORIZONTAL VELOCITY = 257.36 IN/SEC
PITCH RATE = 1.19 RAD/SEC
LOWEST HEIGHT = 5.37 IN

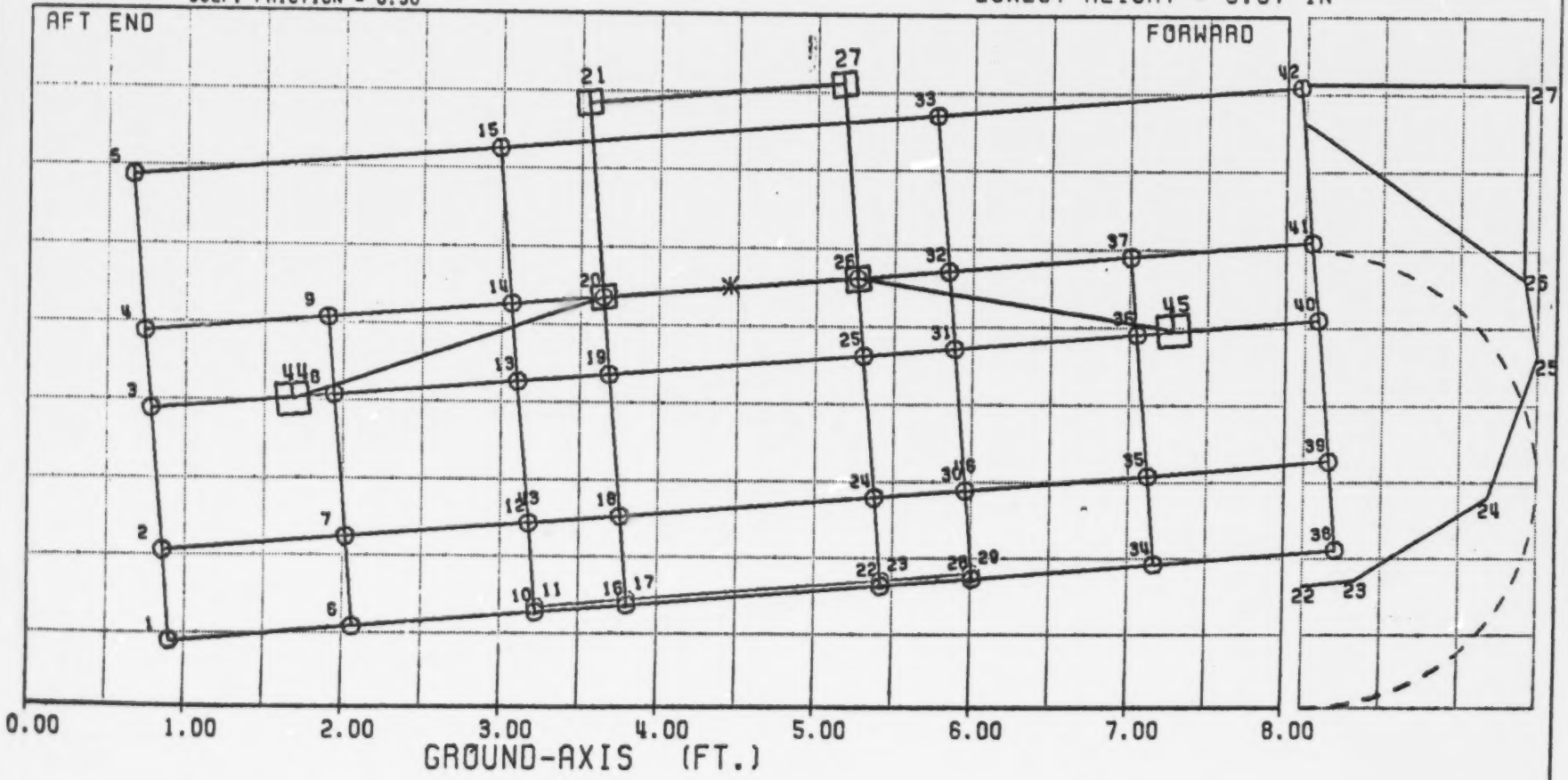

ELASTIC MODEL

FIG.

INITIAL FUSELAGE CONDITIONS AT TIME = 0
WING LOAD = 537 LBS
ANGLE = 3.00 DEG
VERTICAL VELOCITY = 0.00 IN/SEC
HORIZONTAL VELOCITY = 259.00 IN/SEC
PITCH RATE = 1.18 RAD/SEC
LOWEST HEIGHT = 6.75 IN
ΔT = 0.00006 SEC
COEF. RESTITUTION = 0.30
COEF. FRICTION = 0.30

TIME RELEASE = 0.05400 SEC
TIME IMPACT = 0.00000 SEC
ANGLE = 6.65 DEG
VERTICAL VELOCITY = -18.56 IN/SEC
HORIZONTAL VELOCITY = 252.28 IN/SEC
PITCH RATE = 1.23 RAD/SEC
LOWEST HEIGHT = 3.78 IN

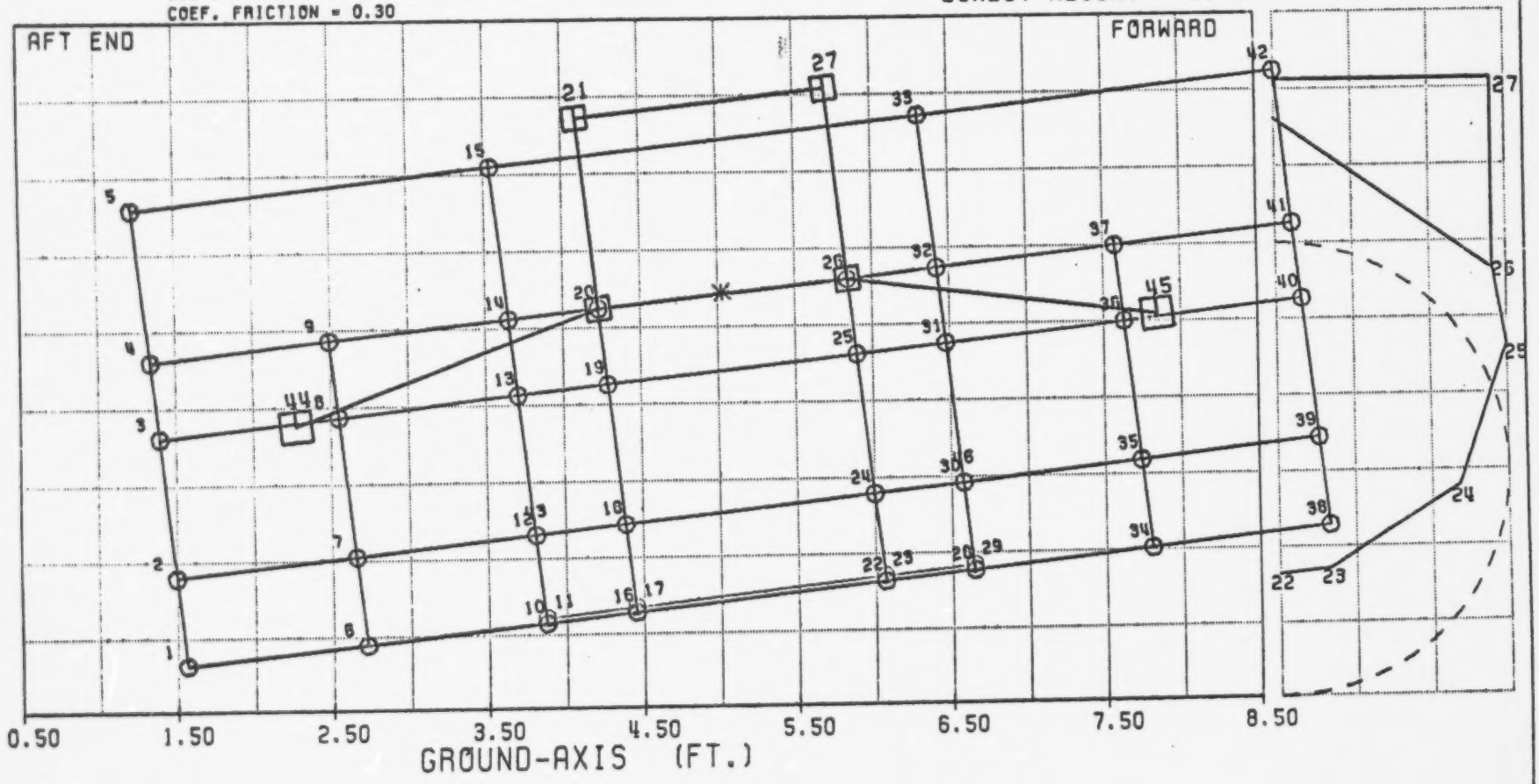

ELASTIC MODEL

FIG.

INITIAL FUSELAGE CONDITIONS AT TIME = 0
WING LOAD = 537 LBS
ANGLE = 3.00 DEG
VERTICAL VELOCITY = 0.00 IN/SEC
HORIZONTAL VELOCITY = 259.00 IN/SEC
PITCH RATE = 1.18 RAD/SEC
LOWEST HEIGHT = 6.75 IN
ΔT = 0.00006 SEC
COEF. RESTITUTION = 0.30
COEF. FRICTION = 0.30

TIME RELEASE = 0.08100 SEC
TIME IMPACT = 0.00000 SEC
ANGLE = 8.62 DEG
VERTICAL VELOCITY = -26.96 IN/SEC
HORIZONTAL VELOCITY = 244.14 IN/SEC
PITCH RATE = 1.32 RAD/SEC
LOWEST HEIGHT = 1.95 IN

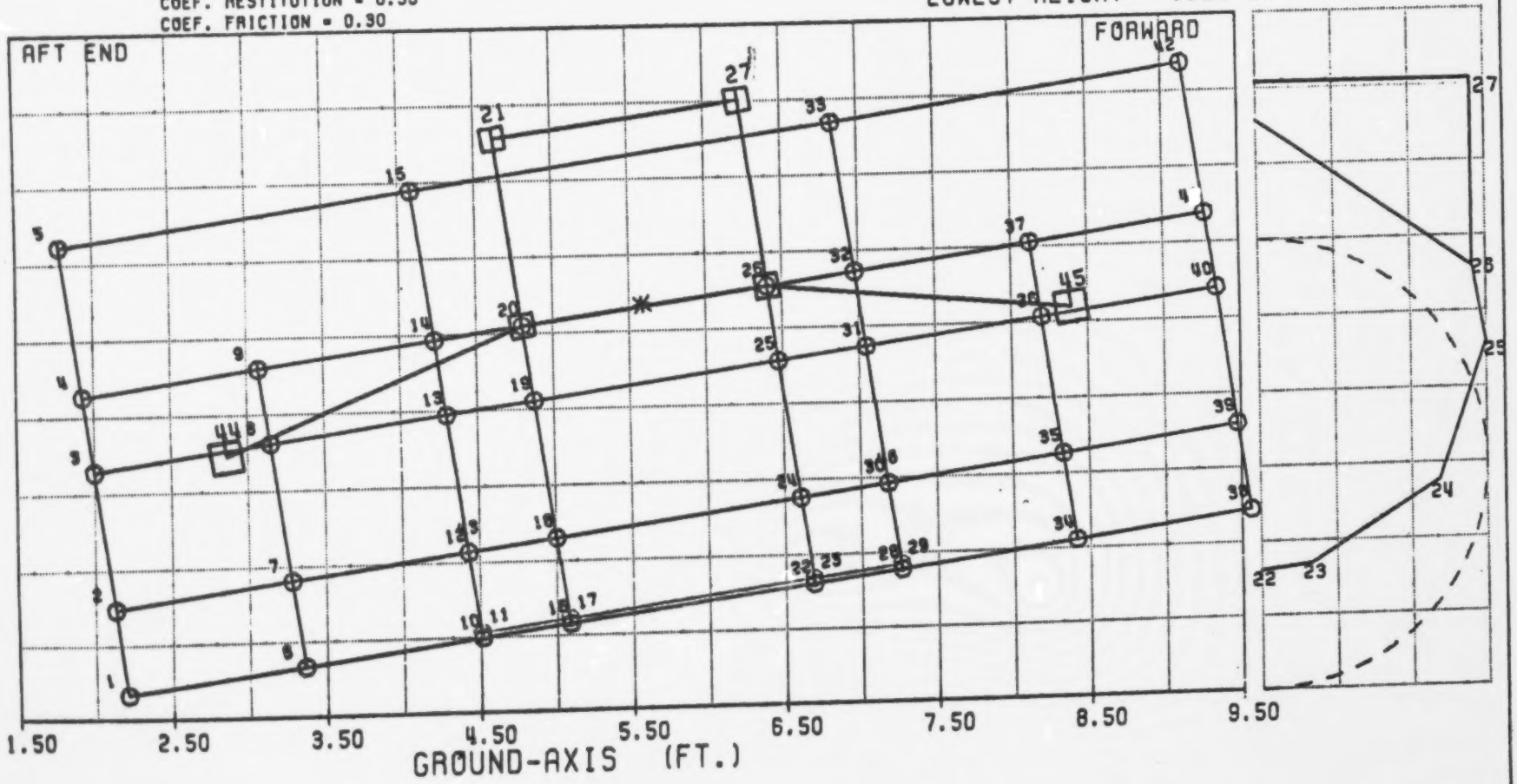

ELASTIC MODEL

FIG.

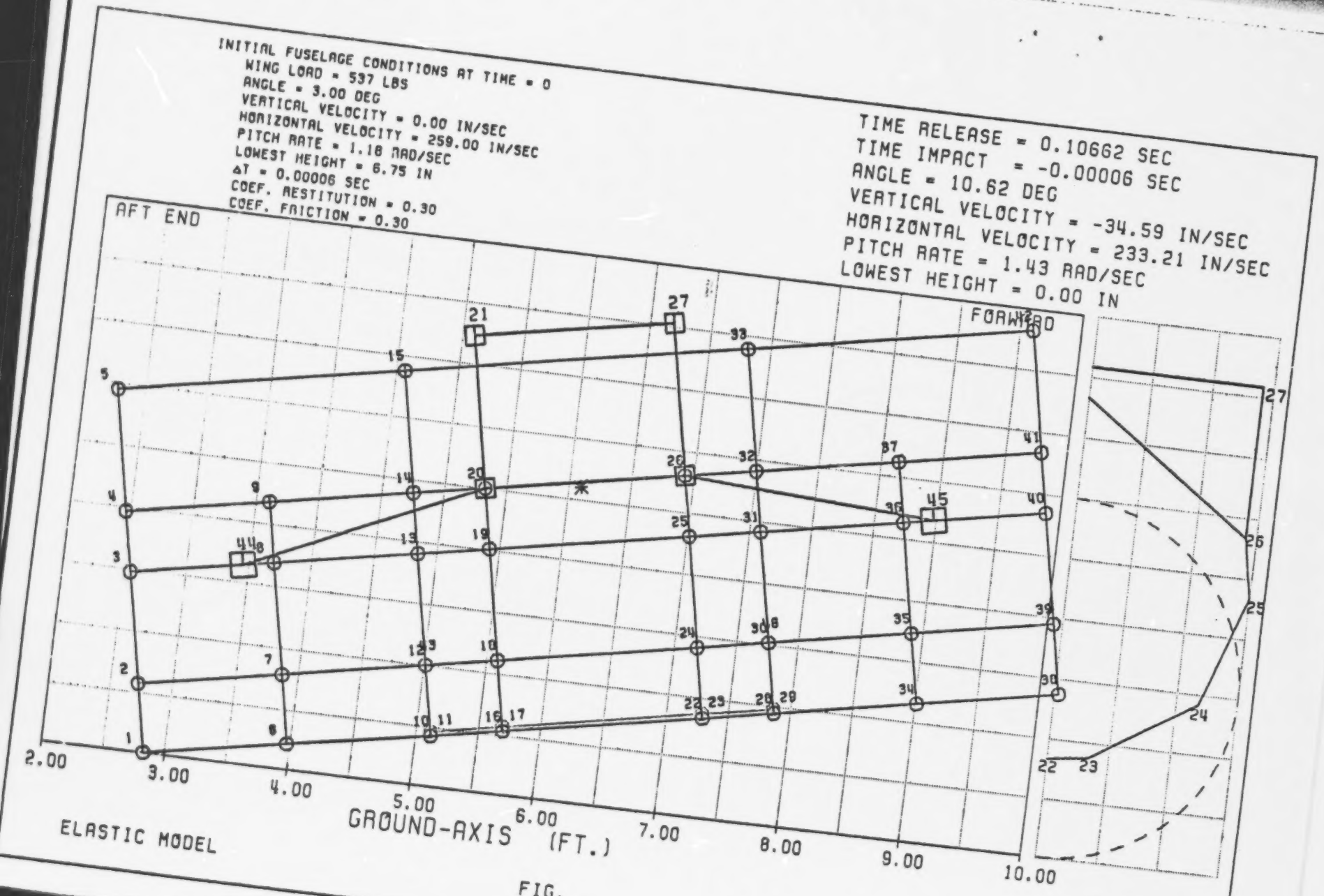
INITIAL FUSELAGE CONDITIONS AT TIME = 0
WING LOAD = 537 LBS
ANGLE = 3.00 DEG
VERTICAL VELOCITY = 0.00 IN/SEC
HORIZONTAL VELOCITY = 259.00 IN/SEC
PITCH RATE = 1.18 RAD/SEC
LOWEST HEIGHT = 6.75 IN
ΔT = 0.00006 SEC
COEF. RESTITUTION = 0.30
COEF. FRICTION = 0.30
TIME RELEASE = 0.10662 SEC
TIME IMPACT = -0.00006 SEC
ANGLE = 10.62 DEG
VERTICAL VELOCITY = -34.59 IN/SEC
HORIZONTAL VELOCITY = 233.21 IN/SEC
PITCH RATE = 1.43 RAD/SEC
LOWEST HEIGHT = 0.00 IN
AFT END
FORWARD
2.00
3.00
4.00
5.00
6.00
7.00
8.00
9.00
10.00
GROUND-AXIS (FT.)
ELASTIC MODEL

FIG.

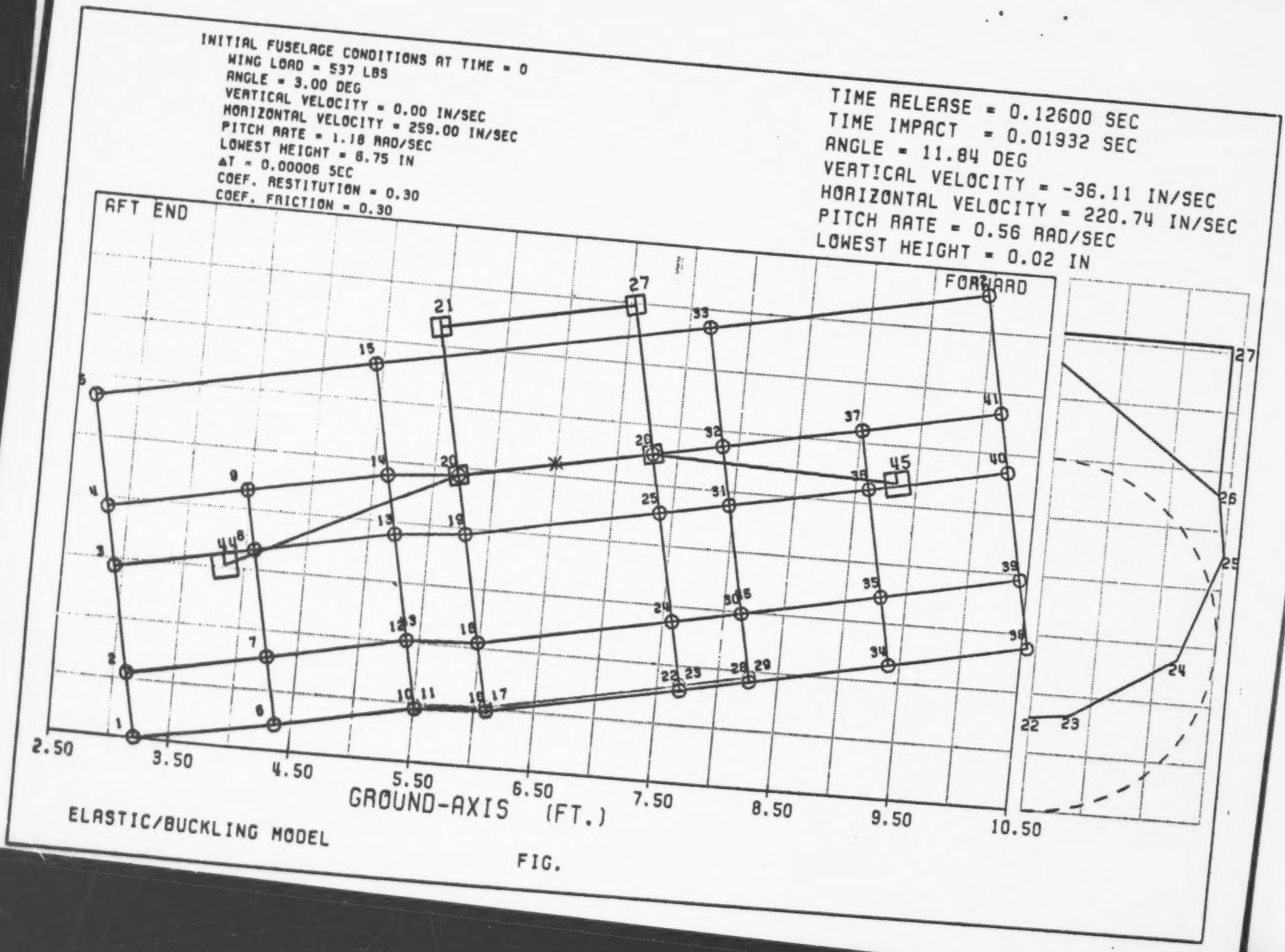

ELASTIC/BUCKLING MODEL

FIG.

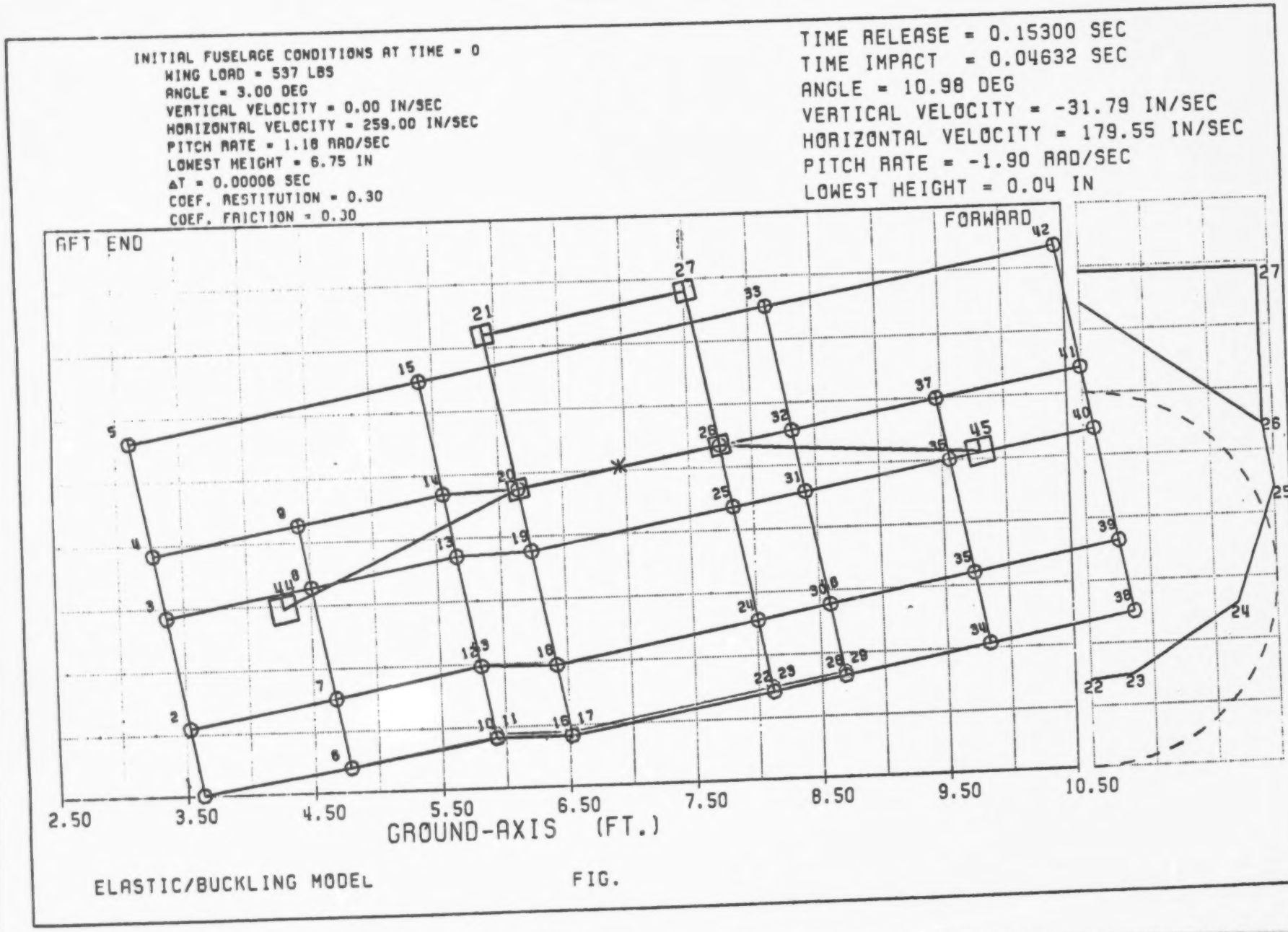

ELASTIC/BUCKLING MODEL

FIG.

INITIAL FUSELAGE CONDITIONS AT TIME = 0
WING LOAD = 537 LBS
ANGLE = 3.00 DEG
VERTICAL VELOCITY = 0.00 IN/SEC
HORIZONTAL VELOCITY = 259.00 IN/SEC
PITCH RATE = 1.18 RAD/SEC
LOWEST HEIGHT = 6.75 IN
ΔT = 0.00006 SEC
COEF. RESTITUTION = 0.30
COEF. FRICTION = 0.30

TIME RELEASE = 0.18900 SEC
TIME IMPACT = 0.08232 SEC
ANGLE = 5.13 DEG
VERTICAL VELOCITY = -34.08 IN/SEC
HORIZONTAL VELOCITY = 154.62 IN/SEC
PITCH RATE = -3.19 RAD/SEC
LOWEST HEIGHT = 0.75 IN

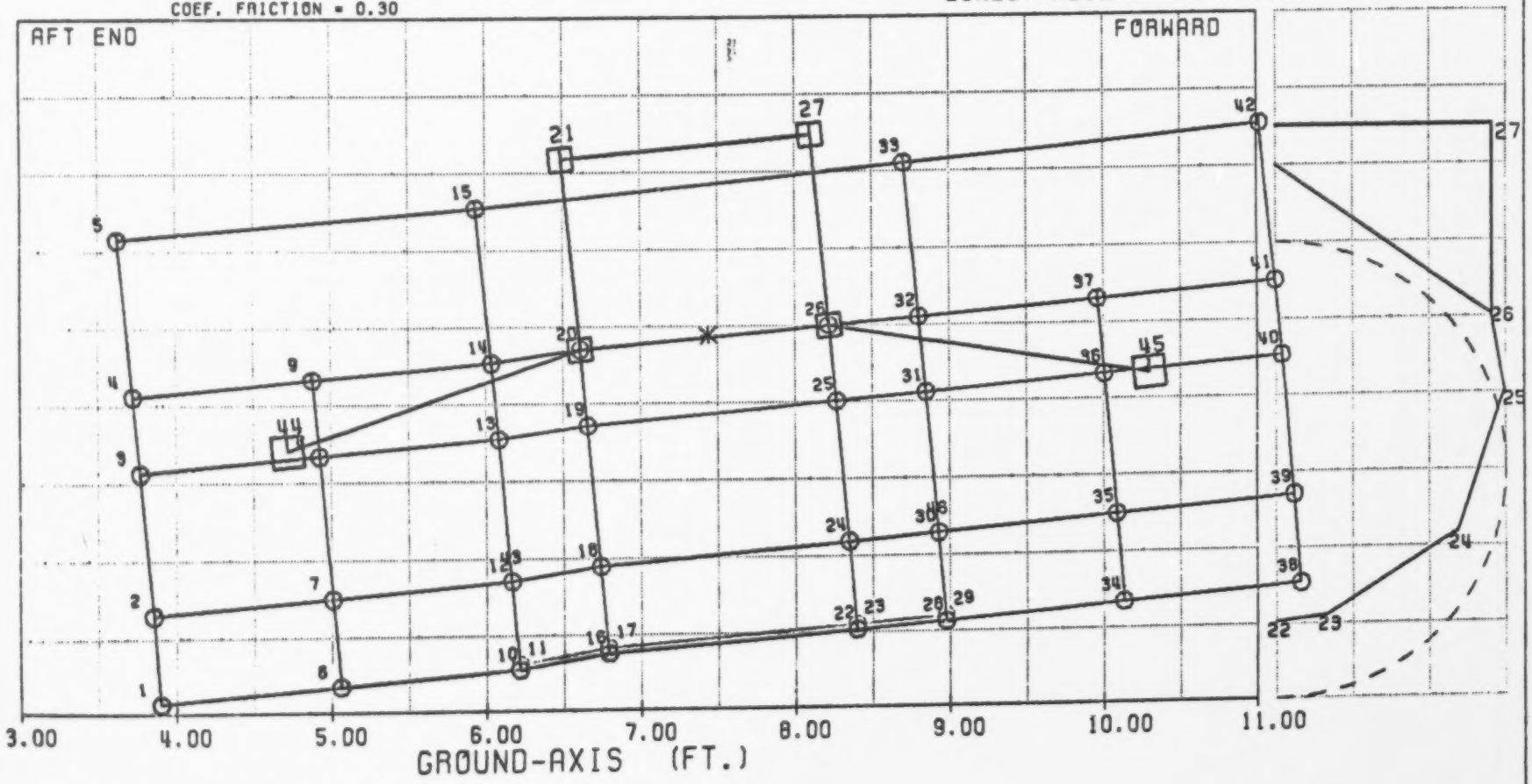

ELASTIC/BUCKLING MODEL FIG.

INITIAL FUSELAGE CONDITIONS AT TIME = 0
WING LOAD = 537 LBS
ANGLE = 3.00 DEG
VERTICAL VELOCITY = 0.00 IN/SEC
HORIZONTAL VELOCITY = 259.00 IN/SEC
PITCH RATE = 1.18 RAD/SEC
LOWEST HEIGHT = 6.75 IN
ΔT = 0.00006 SEC
COEF. RESTITUTION = 0.30
COEF. FRICTION = 0.30

TIME RELEASE = 0.21600 SEC
TIME IMPACT = 0.10932 SEC
ANGLE = 0.28 DEG
VERTICAL VELOCITY = -42.22 IN/SEC
HORIZONTAL VELOCITY = 145.47 IN/SEC
PITCH RATE = -3.15 RAD/SEC
LOWEST HEIGHT = 3.87 IN

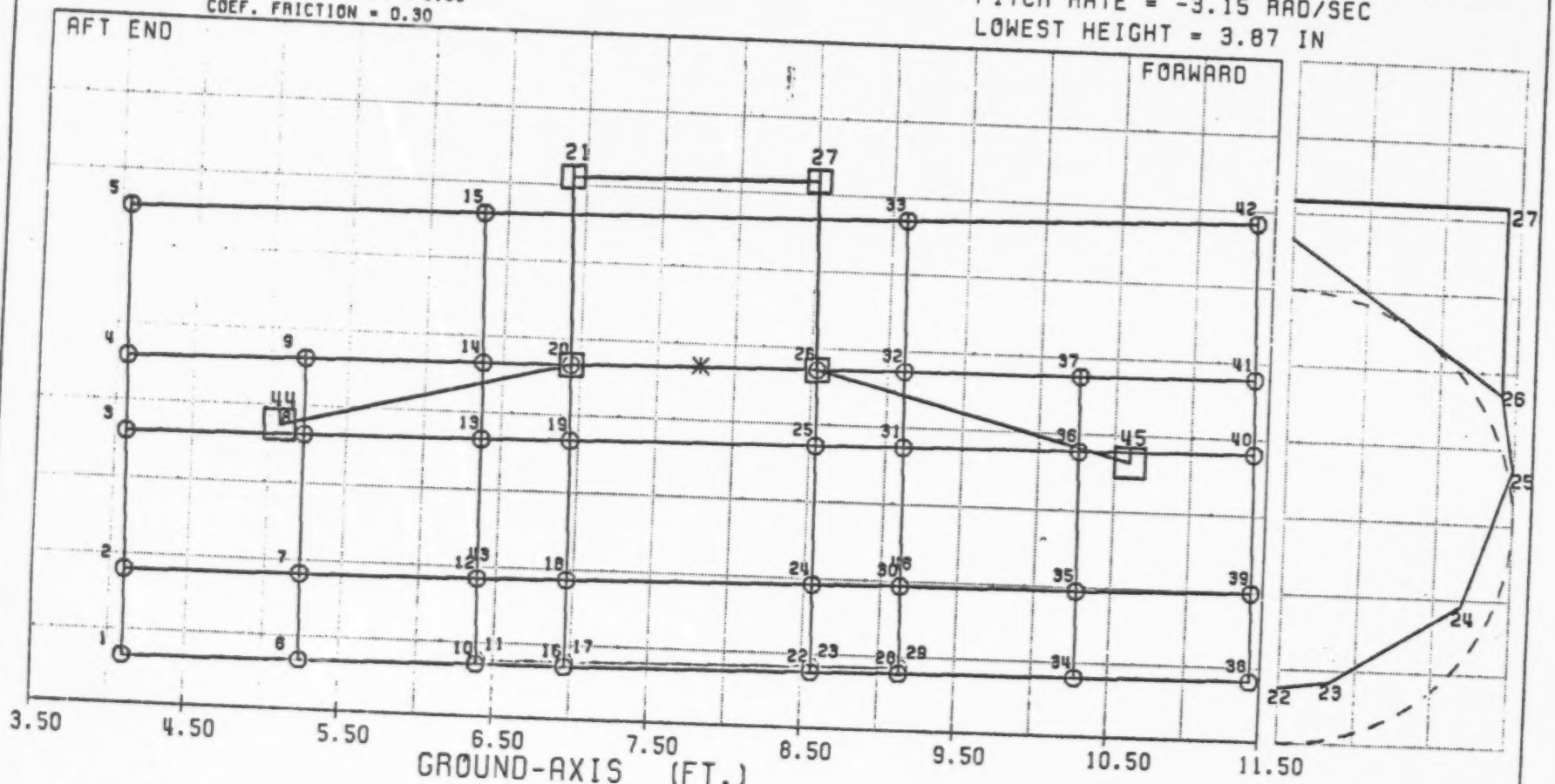

ELASTIC/BUCKLING MODEL

FIG.

INITIAL FUSELAGE CONDITIONS AT TIME = 0
WING LOAD = 537 LBS
ANGLE = 3.00 DEG
VERTICAL VELOCITY = 0.00 IN/SEC
HORIZONTAL VELOCITY = 259.00 IN/SEC
PITCH RATE = 1.18 RAD/SEC
LOWEST HEIGHT = 6.75 IN
AT = 0.00006 SEC
COEF. RESTITUTION = 0.30
COEF. FRICTION = 0.30

TIME RELEASE = 0.24300 SEC
TIME IMPACT = 0.13632 SEC
ANGLE = -4.51 DEG
VERTICAL VELOCITY = -48.57 IN/SEC
HORIZONTAL VELOCITY = 134.53 IN/SEC
PITCH RATE = -2.96 RAD/SEC
LOWEST HEIGHT = 1.13 IN

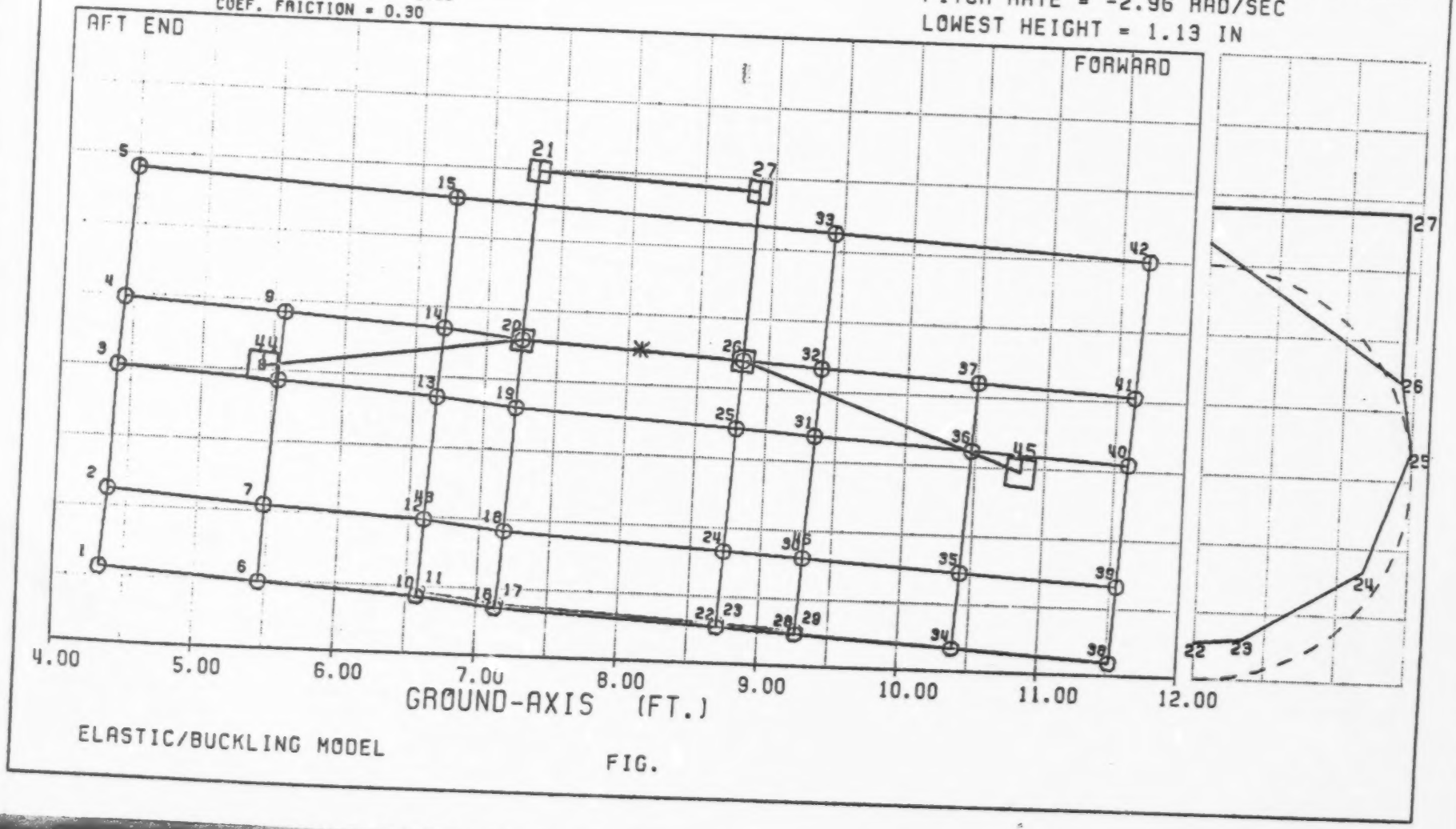

ELASTIC/BUCKLING MODEL

FIG.

JOB:CC340230 HASPJOB08096 PRIORITY 4 JOB 1982
DATE:15/09/81 TIME:17:46 (PLOTST EXECUTION)

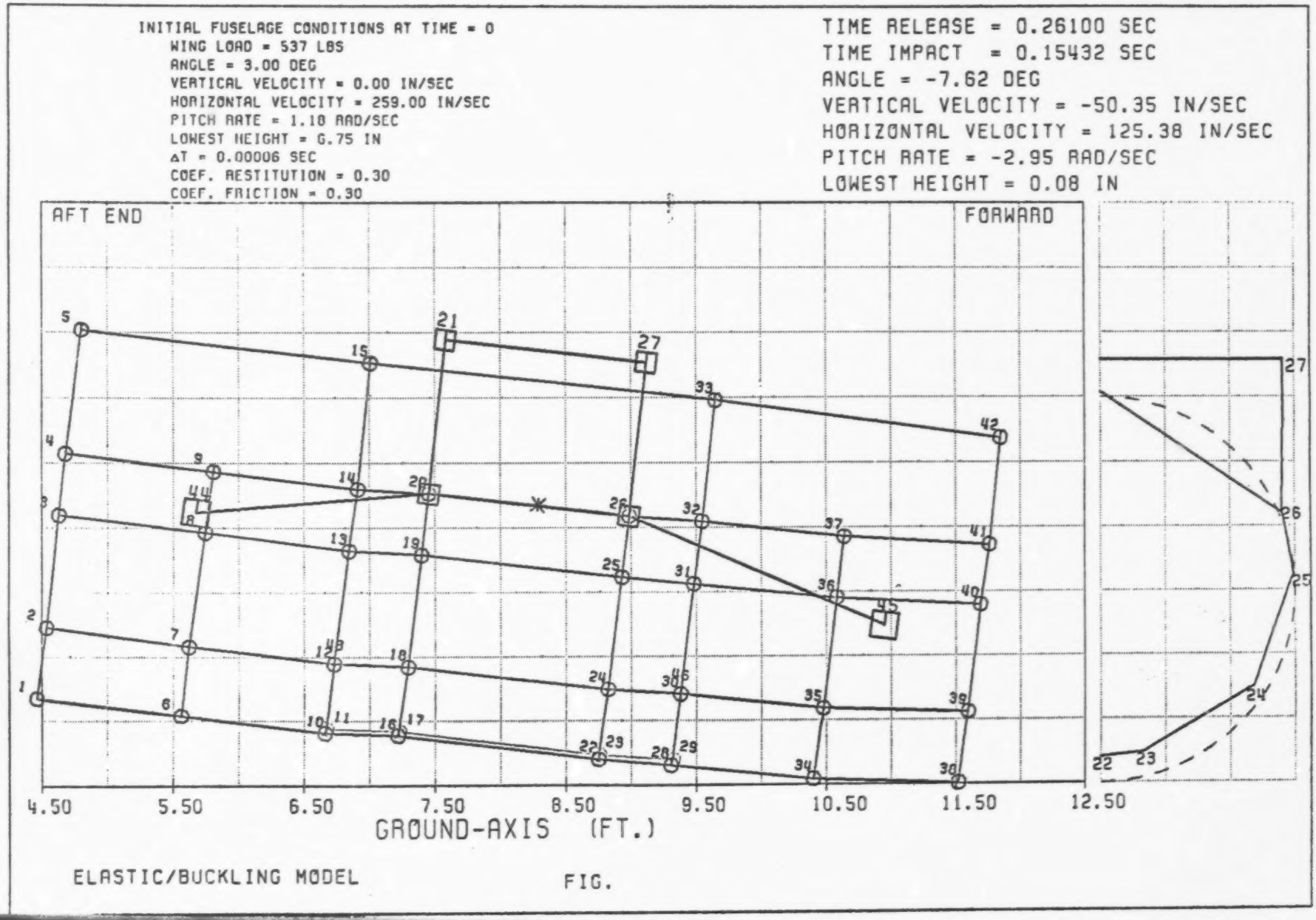

ELASTIC/BUCKLING MODEL FIG.

INITIAL FUSELAGE CONDITIONS AT TIME = 0
WING LOAD = 537 LBS
ANGLE = 3.00 DEG
VERTICAL VELOCITY = 0.00 IN/SEC
HORIZONTAL VELOCITY = 259.00 IN/SEC
PITCH RATE = 1.18 RAD/SEC
LOWEST HEIGHT = 6.75 IN
ΔT = 0.00006 SEC
COEF. RESTITUTION = 0.30
COEF. FRICTION = 0.30

TIME RELEASE = 0.28800 SEC
TIME IMPACT = 0.18132 SEC
ANGLE = -12.00 DEG
VERTICAL VELOCITY = -38.91 IN/SEC
HORIZONTAL VELOCITY = 102.49 IN/SEC
PITCH RATE = -2.69 RAD/SEC
LOWEST HEIGHT = -0.00 IN

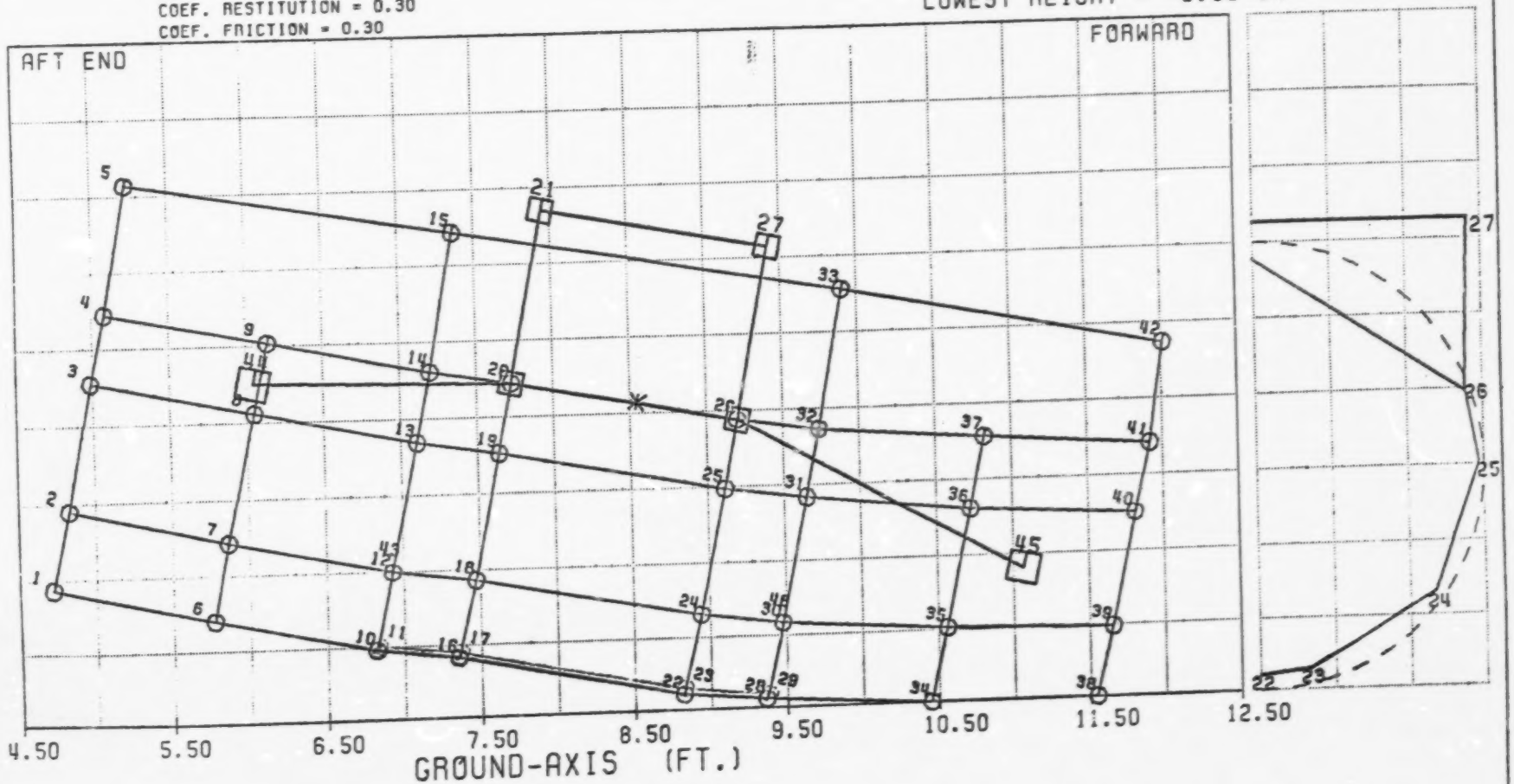

ELASTIC/BUCKLING MODEL FIG.

INITIAL FUSELAGE CONDITIONS AT TIME = 0
WING LOAD = 537 LBS
ANGLE = 3.00 DEG
VERTICAL VELOCITY = 0.00 IN/SEC
HORIZONTAL VELOCITY = 259.00 IN/SEC
PITCH RATE = 1.18 RAD/SEC
LOWEST HEIGHT = 6.75 IN
ΔT = 0.00006 SEC
COEF. RESTITUTION = 0.30
COEF. FRICTION = 0.30

TIME RELEASE = 0.31500 SEC
TIME IMPACT = 0.20832 SEC
ANGLE = -15.70 DEG
VERTICAL VELOCITY = -10.68 IN/SEC
HORIZONTAL VELOCITY = 76.55 IN/SEC
PITCH RATE = -2.38 RAD/SEC
LOWEST HEIGHT = -0.11 IN

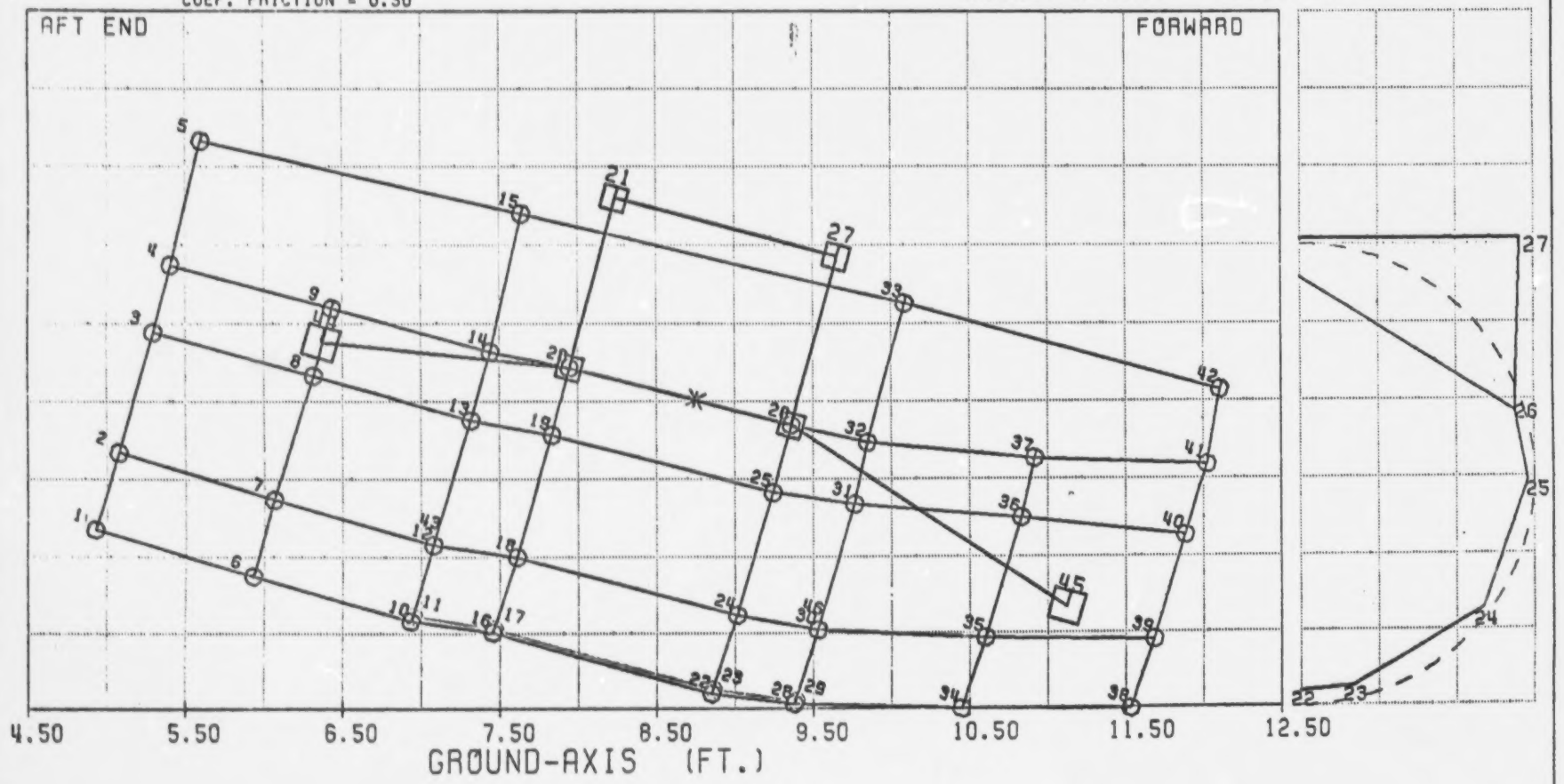

ELASTIC/BUCKLING MODEL

FIG.

INITIAL FUSELAGE CONDITIONS AT TIME = 0
WING LOAD = 537 LBS
ANGLE = 3.00 DEG
VERTICAL VELOCITY = 0.00 IN/SEC
HORIZONTAL VELOCITY = 259.00 IN/SEC
PITCH RATE = 1.18 RAD/SEC
LOWEST HEIGHT = 6.75 IN
ΔT = 0.00006 SEC
COEF. RESTITUTION = 0.30
COEF. FRICTION = 0.30

TIME RELEASE = 0.36900 SEC
TIME IMPACT = 0.26232 SEC
ANGLE = -20.03 DEG
VERTICAL VELOCITY = 63.32 IN/SEC
HORIZONTAL VELOCITY = 26.45 IN/SEC
PITCH RATE = -0.18 RAD/SEC
LOWEST HEIGHT = -0.56 IN

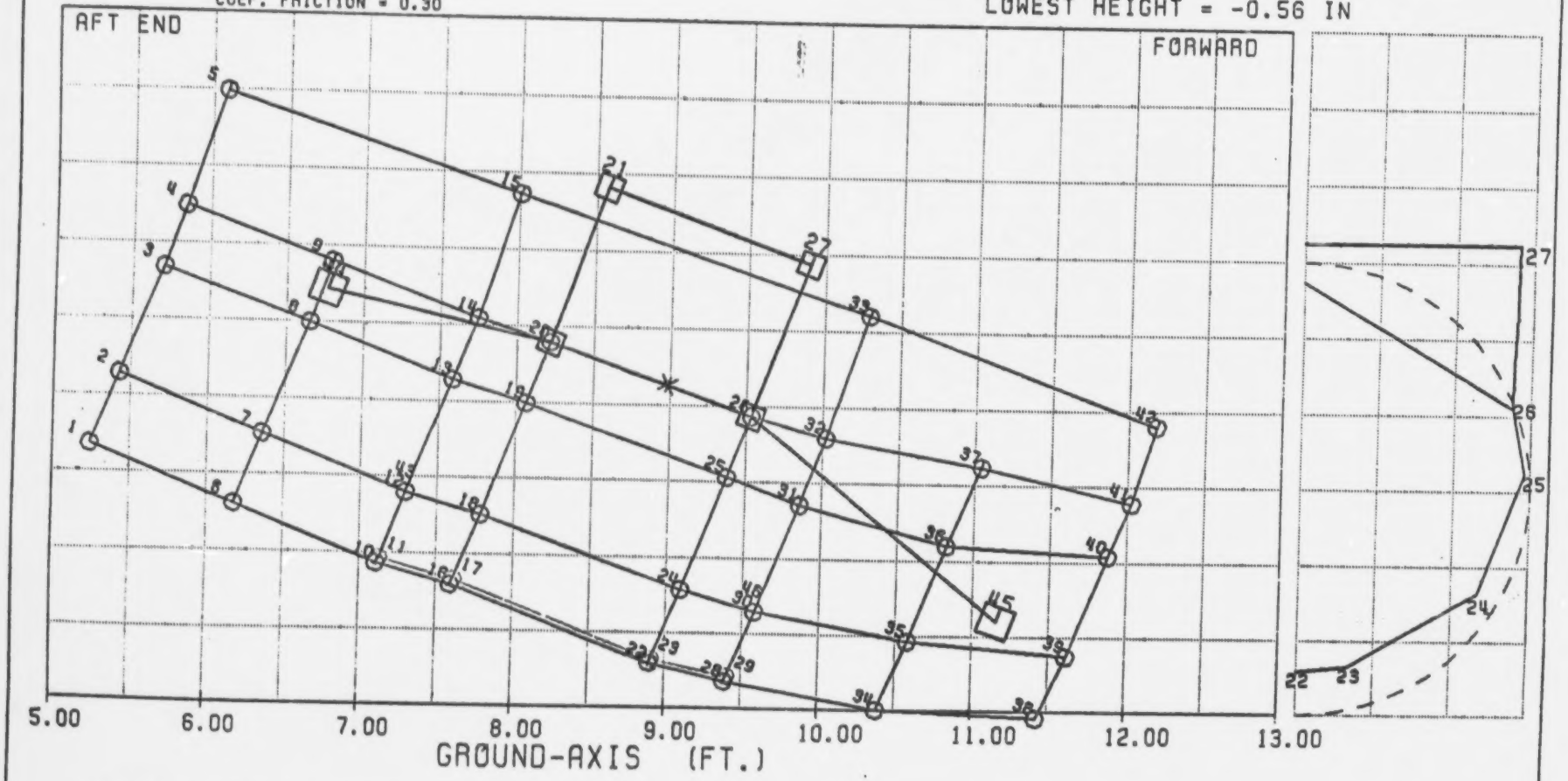

ELASTIC/BUCKLING MODEL

FIG.

INITIAL FUSELAGE CONDITIONS AT TIME = 0
WING LOAD = 537 LBS
ANGLE = 3.00 DEG
VERTICAL VELOCITY = 0.00 IN/SEC
HORIZONTAL VELOCITY = 259.00 IN/SEC
PITCH RATE = 1.18 RAD/SEC
LOWEST HEIGHT = 6.75 IN
ΔT = 0.00006 SEC
COEF. RESTITUTION = 0.30
COEF. FRICTION = 0.30

TIME RELEASE = 0.34200 SEC
TIME IMPACT = 0.23532 SEC
ANGLE = -18.42 DEG
VERTICAL VELOCITY = 27.47 IN/SEC
HORIZONTAL VELOCITY = 51.63 IN/SEC
PITCH RATE = -0.97 RAD/SEC
LOWEST HEIGHT = -0.31 IN

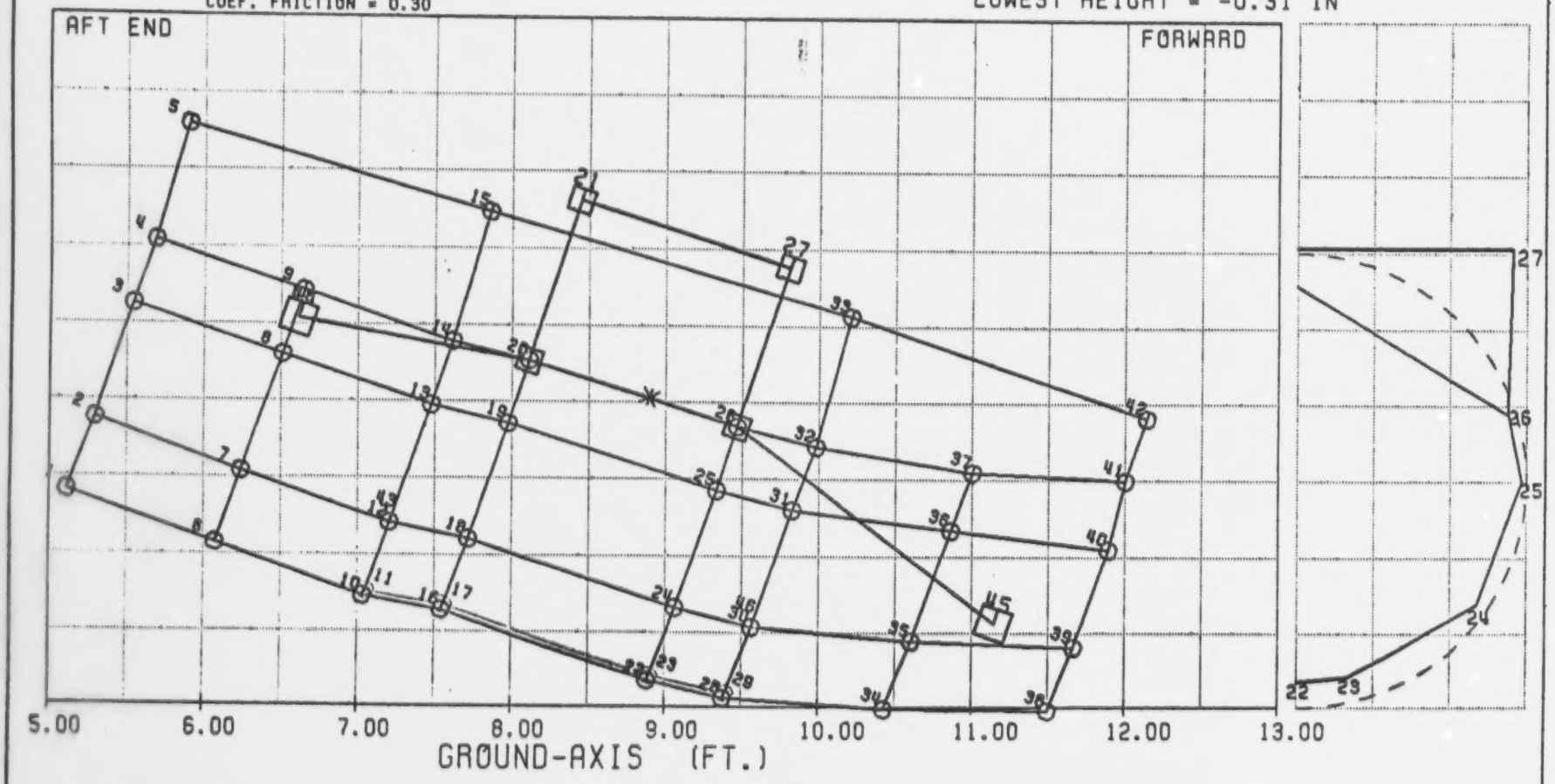

ELASTIC/BUCKLING MODEL

FIG.

INITIAL FUSELAGE CONDITIONS AT TIME = 0
WING LOAD = 537 LBS
ANGLE = 3.00 DEG
VERTICAL VELOCITY = 0.00 IN/SEC
HORIZONTAL VELOCITY = 259.00 IN/SEC
PITCH RATE = 1.18 RAD/SEC
LOWEST HEIGHT = 6.75 IN
ΔT = 0.00006 SEC
COEF. RESTITUTION = 0.30
COEF. FRICTION = 0.30

TIME RELEASE = 0.39600 SEC
TIME IMPACT = 0.28932 SEC
ANGLE = -21.35 DEG
VERTICAL VELOCITY = 89.77 IN/SEC
HORIZONTAL VELOCITY = -2.80 IN/SEC
PITCH RATE = -0.60 RAD/SEC
LOWEST HEIGHT = -0.69 IN

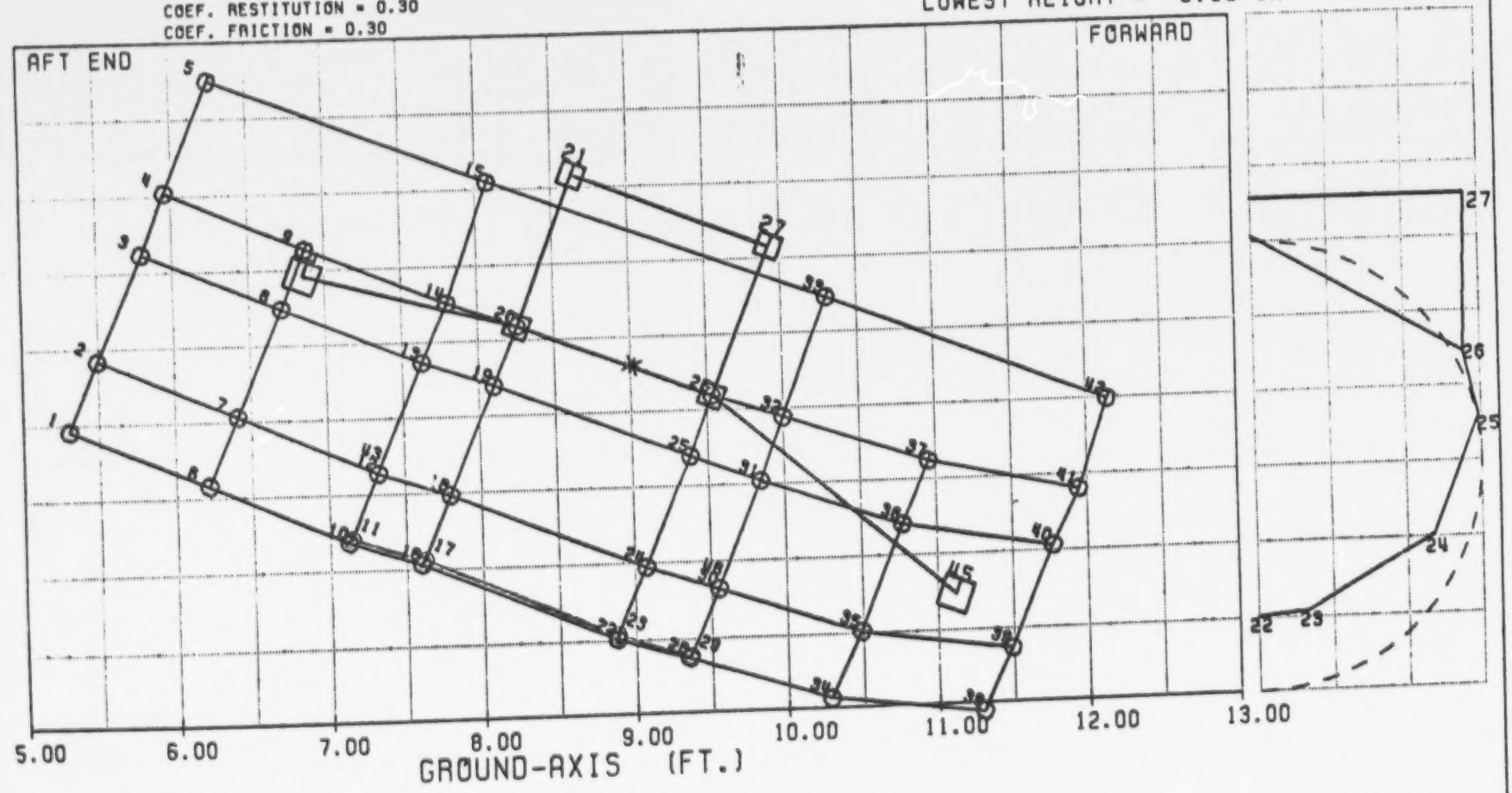

ELASTIC/BUCKLING MODEL FIG.

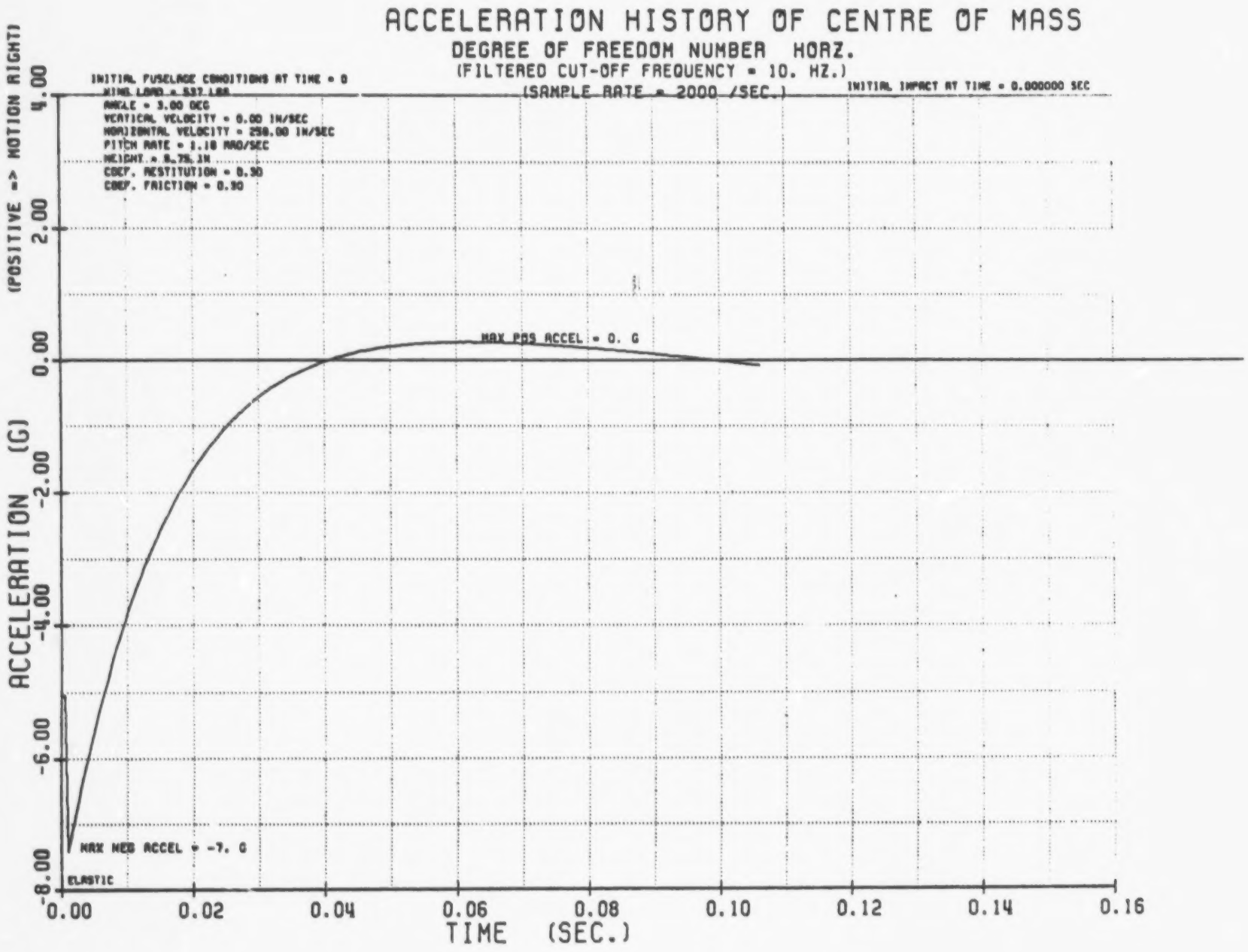
ACCELERATION HISTORY OF CENTRE OF MASS
DEGREE OF FREEDOM NUMBER HORZ.
(FILTERED CUT-OFF FREQUENCY = 10. HZ.)
(SAMPLE RATE = 2000 /SEC.)
INITIAL IMPACT AT TIME = 0.000000 SEC
INITIAL FUSELAGE CONDITIONS AT TIME = 0
ANGLE = 3.00 DEG
VERTICAL VELOCITY = 0.00 IN/SEC
HORIZONTAL VELOCITY = 250.00 IN/SEC
PITCH RATE = 1.18 RAD/SEC
COEF. RESTITUTION = 0.30
COEF. FRICTION = 0.30
MAX POS ACCEL = 0. G
MAX NEG ACCEL = -7. G
ELASTIC
ACCELERATION (G)
(POSITIVE => MOTION RIGHT)
4.00
2.00
0.00
-2.00
-4.00
-6.00
-8.00
0.00
0.02
0.04
0.06
0.08
0.10
0.12
0.14
0.16
TIME (SEC.)

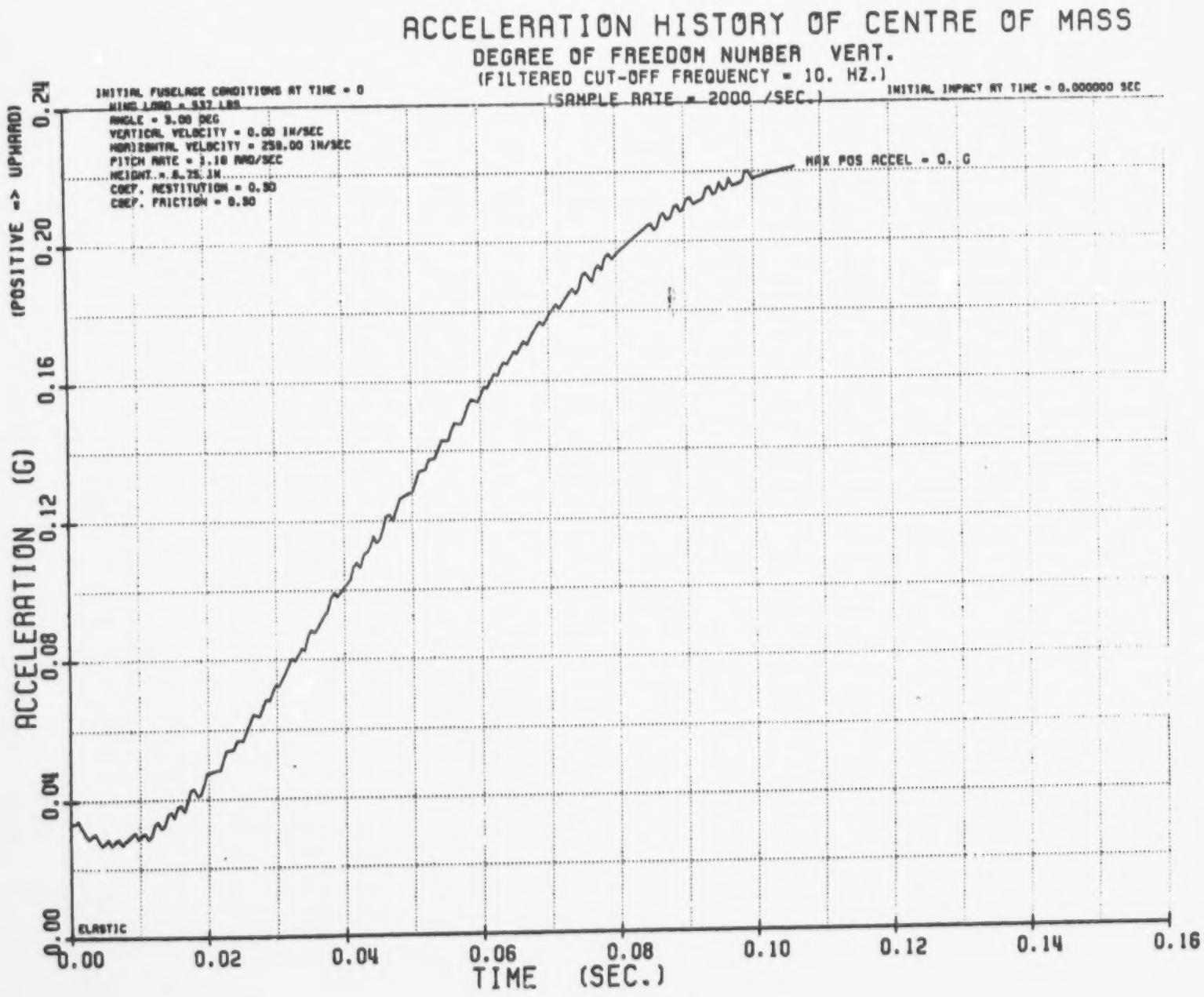
ACCELERATION HISTORY OF CENTRE OF MASS
DEGREE OF FREEDOM NUMBER VERT.
(FILTERED CUT-OFF FREQUENCY = 10. HZ.)
(SAMPLE RATE = 2000 /SEC.)
INITIAL FUSELAGE CONDITIONS AT TIME = 0
WING LOAD = 537 LBS
ANGLE = 3.00 DEG
VERTICAL VELOCITY = 0.00 IN/SEC
HORIZONTAL VELOCITY = 250.00 IN/SEC
PITCH RATE = 3.18 RAD/SEC
HEIGHT = 8.25 IN
COEF. RESTITUTION = 0.90
COEF. FRICTION = 0.90
INITIAL IMPACT AT TIME = 0.000000 SEC
MAX POS ACCEL = 0. G
ELASTIC
ACCELERATION (G)
(POSITIVE => UPWARD)
0.00
0.04
0.08
0.12
0.16
0.20
0.24
0.00
0.02
0.04
0.06
0.08
0.10
0.12
0.14
0.16
TIME (SEC.)

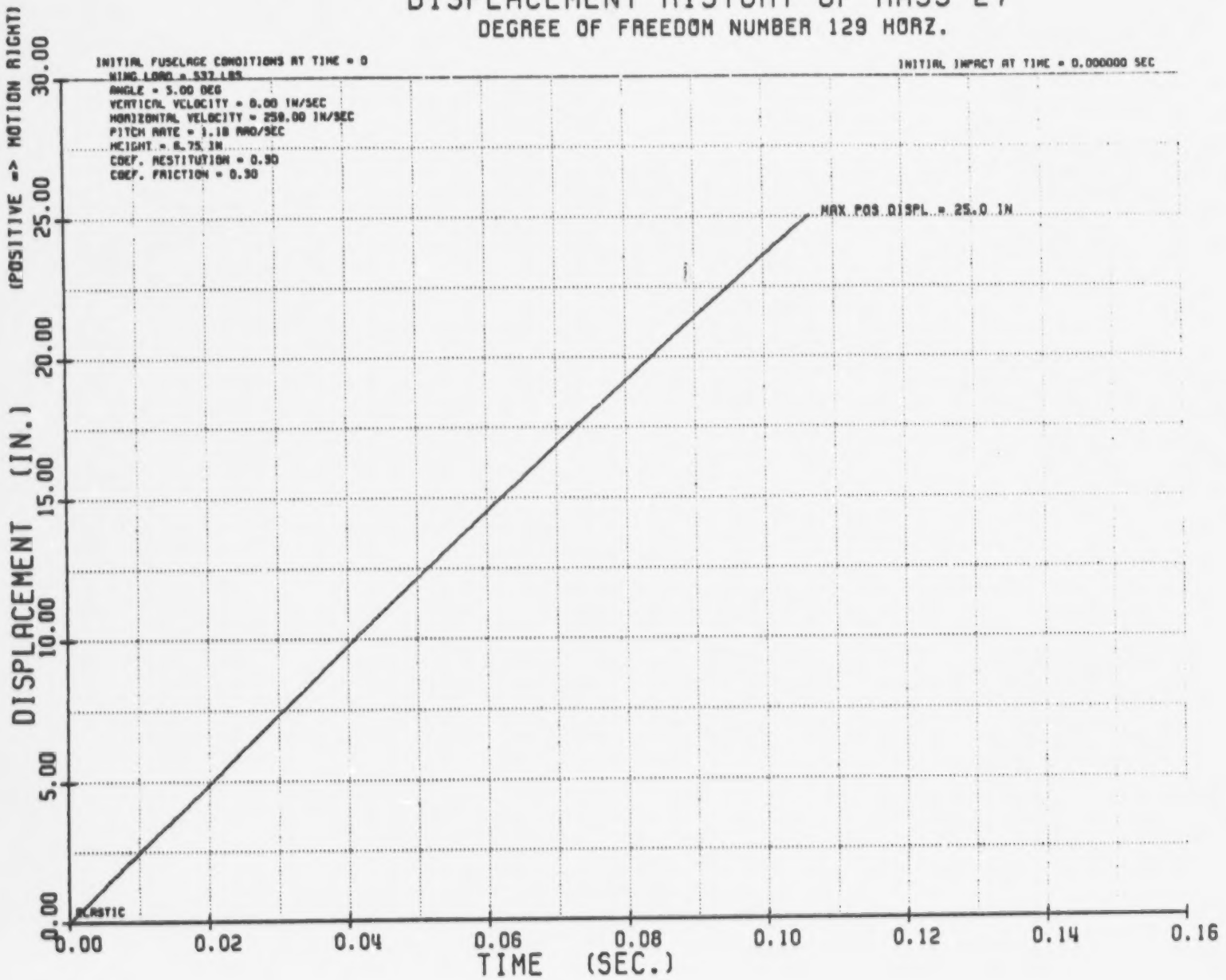
DISPLACEMENT HISTORY OF MASS 27
DEGREE OF FREEDOM NUMBER 129 HORZ.
INITIAL FUSELAGE CONDITIONS AT TIME = 0
WING LOAD = 532 LBS
ANGLE = 5.00 DEG
VERTICAL VELOCITY = 0.00 IN/SEC
HORIZONTAL VELOCITY = 250.00 IN/SEC
PITCH RATE = 1.18 RAD/SEC
HEIGHT = 6.75 IN
COEF. RESTITUTION = 0.30
COEF. FRICTION = 0.30
INITIAL IMPACT AT TIME = 0.000000 SEC
MAX POS DISPL. = 25.0 IN
KRSTIC
DISPLACEMENT (IN.)
(POSITIVE => MOTION RIGHT)
0.00
5.00
10.00
15.00
20.00
25.00
30.00
0.00
0.02
0.04
0.06
0.08
0.10
0.12
0.14
0.16
TIME (SEC.)

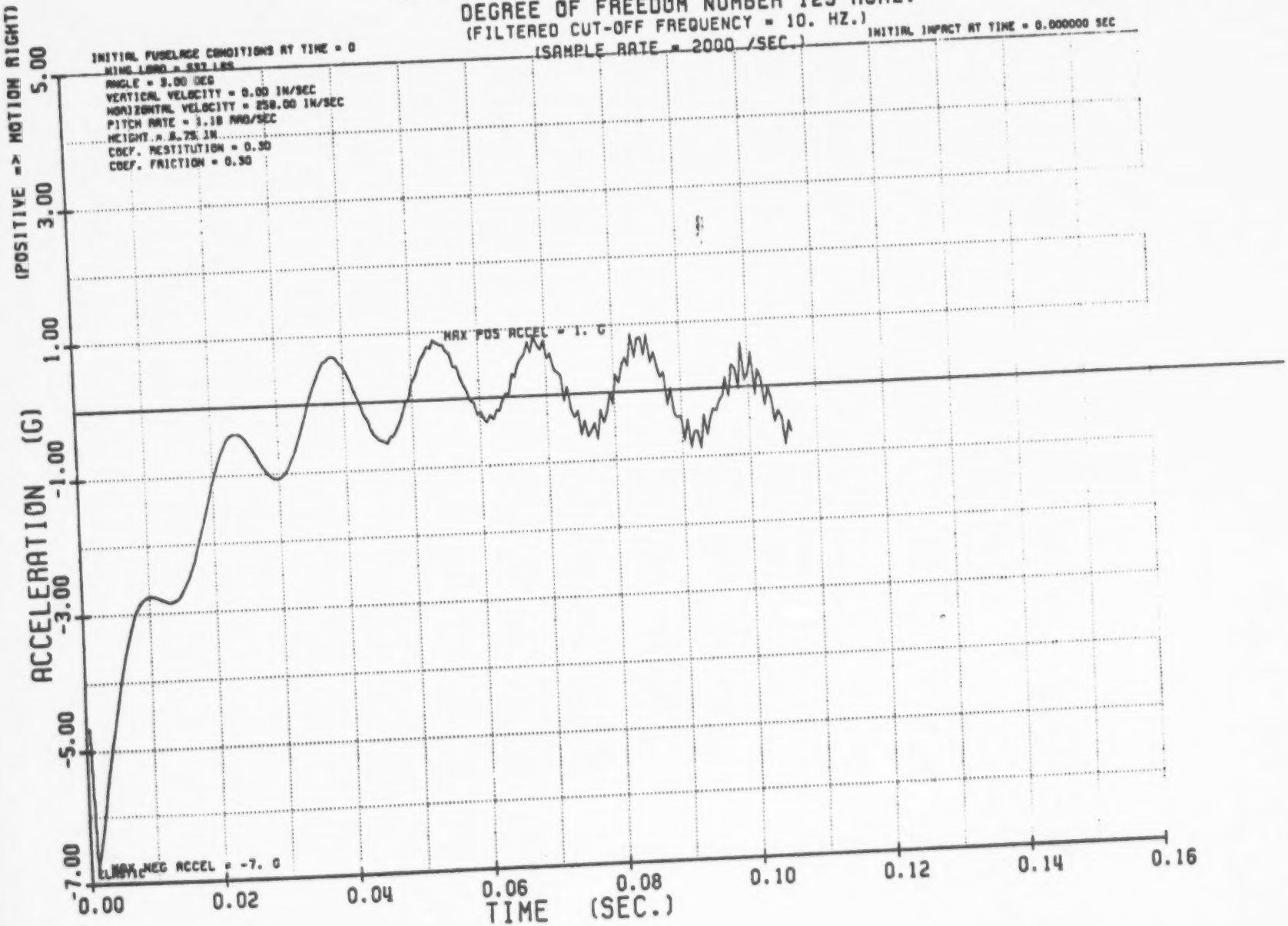
ACCELERATION HISTORY OF MASS 27
DEGREE OF FREEDOM NUMBER 129 HORZ.
(FILTERED CUT-OFF FREQUENCY = 10. HZ.)
(SAMPLE RATE = 2000 /SEC.)
INITIAL IMPACT AT TIME = 0.000000 SEC
INITIAL FUSELAGE CONDITIONS AT TIME = 0
WING LOAD = 537 LBS
ANGLE = 3.00 DEG
VERTICAL VELOCITY = 0.00 IN/SEC
HORIZONTAL VELOCITY = 258.00 IN/SEC
PITCH RATE = 3.18 RAD/SEC
HEIGHT = 8.75 IN
COEF. RESTITUTION = 0.50
COEF. FRICTION = 0.50
MAX POS ACCEL = 1. G
MAX NEG ACCEL = -7. G
(POSITIVE => MOTION RIGHT)
ACCELERATION (G)
5.00
3.00
1.00
-1.00
-3.00
-5.00
-7.00
0.00
0.02
0.04
0.06
0.08
0.10
0.12
0.14
0.16
TIME (SEC.)

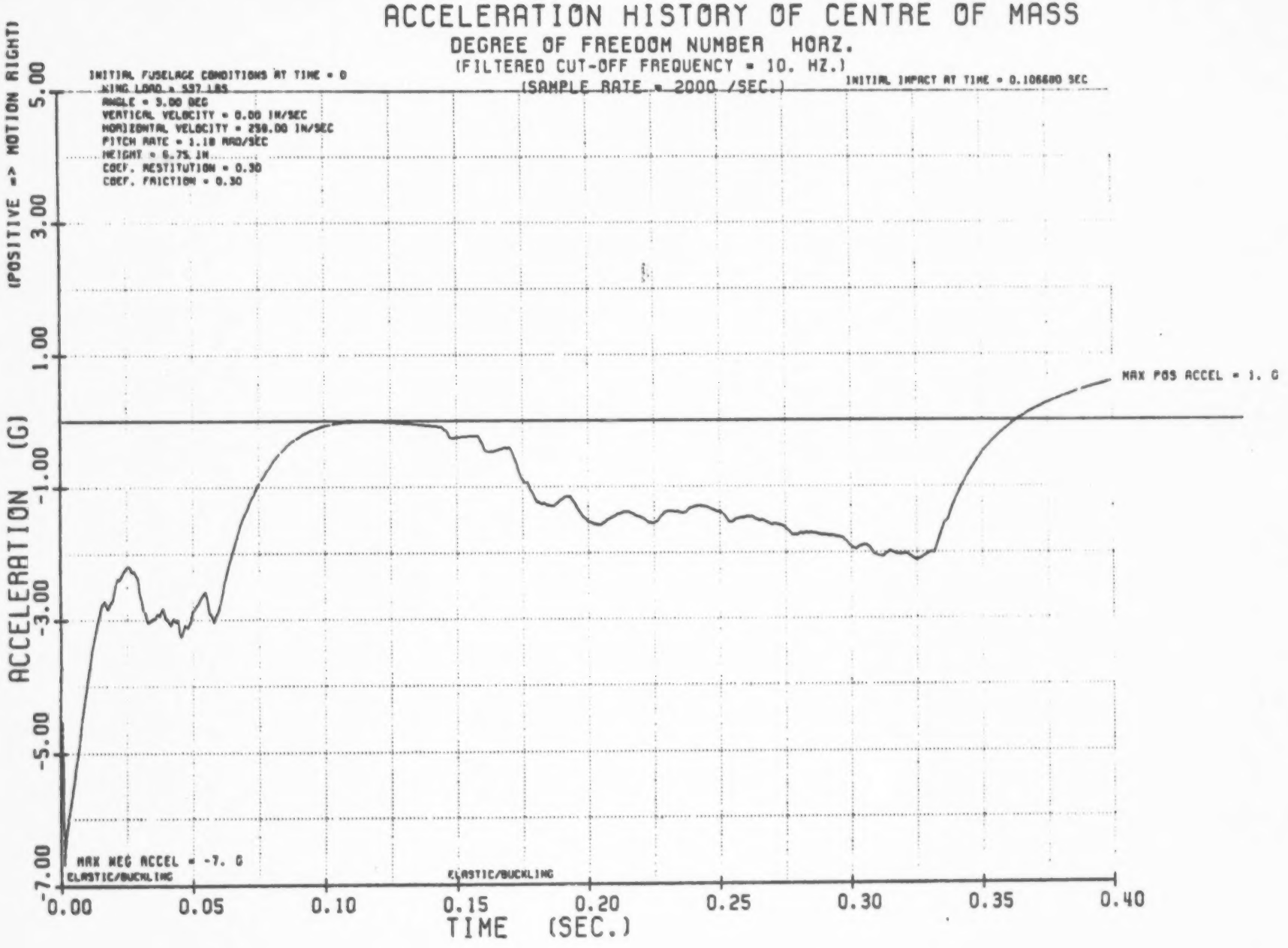
ACCELERATION HISTORY OF CENTRE OF MASS
DEGREE OF FREEDOM NUMBER HORZ.
(FILTERED CUT-OFF FREQUENCY = 10. HZ.)
(SAMPLE RATE = 2000 /SEC.)
INITIAL FUSELAGE CONDITIONS AT TIME = 0
WING LOAD = 537 LBS
ANGLE = 5.00 DEG
VERTICAL VELOCITY = 0.00 IN/SEC
HORIZONTAL VELOCITY = 250.00 IN/SEC
PITCH RATE = 1.18 RAD/SEC
HEIGHT = 6.75 IN
COEF. RESTITUTION = 0.30
COEF. FRICTION = 0.30
INITIAL IMPACT AT TIME = 0.106800 SEC
MAX POS ACCEL = 1. G
MAX NEG ACCEL = -7. G
ELASTIC/BUCKLING
ELASTIC/BUCKLING
ACCELERATION (G)
(POSITIVE => MOTION RIGHT)
5.00
3.00
1.00
-1.00
-3.00
-5.00
-7.00
0.00
0.05
0.10
0.15
0.20
0.25
0.30
0.35
0.40
TIME (SEC.)

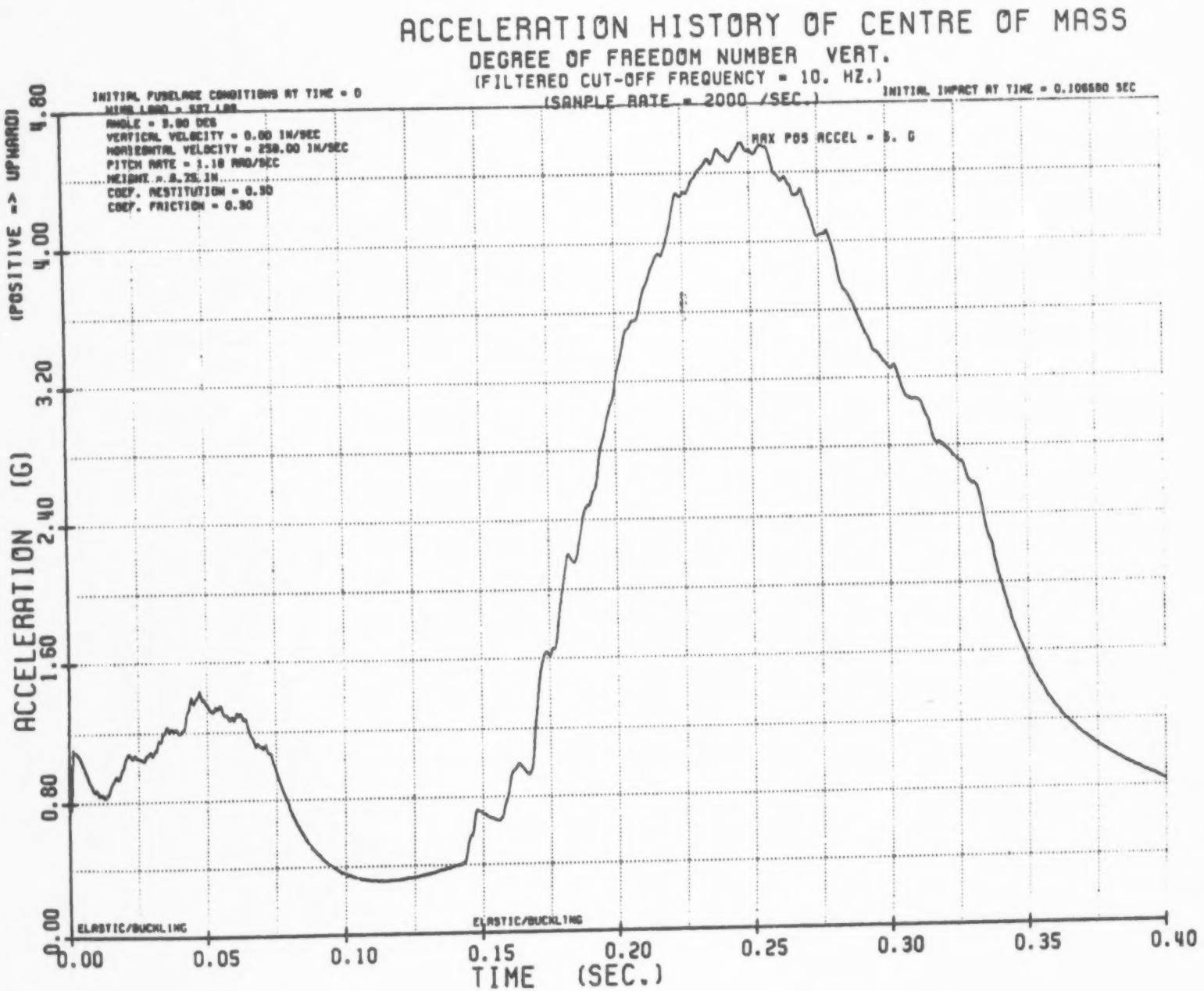
ACCELERATION HISTORY OF CENTRE OF MASS
DEGREE OF FREEDOM NUMBER VERT.
(FILTERED CUT-OFF FREQUENCY = 10. HZ.)
(SAMPLE RATE = 2000 /SEC.)
INITIAL FUSELAGE CONDITIONS AT TIME = 0
ANGLE = 3.00 DEG
VERTICAL VELOCITY = 0.00 IN/SEC
HORIZONTAL VELOCITY = 258.00 IN/SEC
PITCH RATE = 1.18 RAD/SEC
COEF. RESTITUTION = 0.50
COEF. FRICTION = 0.30
INITIAL IMPACT AT TIME = 0.106800 SEC
MAX POS ACCEL = 5. G
ACCELERATION (G)
(POSITIVE => UPWARD)
4.80
4.00
3.20
2.40
1.60
0.80
0.00
ELASTIC/BUCKLING
ELASTIC/BUCKLING
0.00
0.05
0.10
0.15
0.20
0.25
0.30
0.35
0.40
TIME (SEC.)

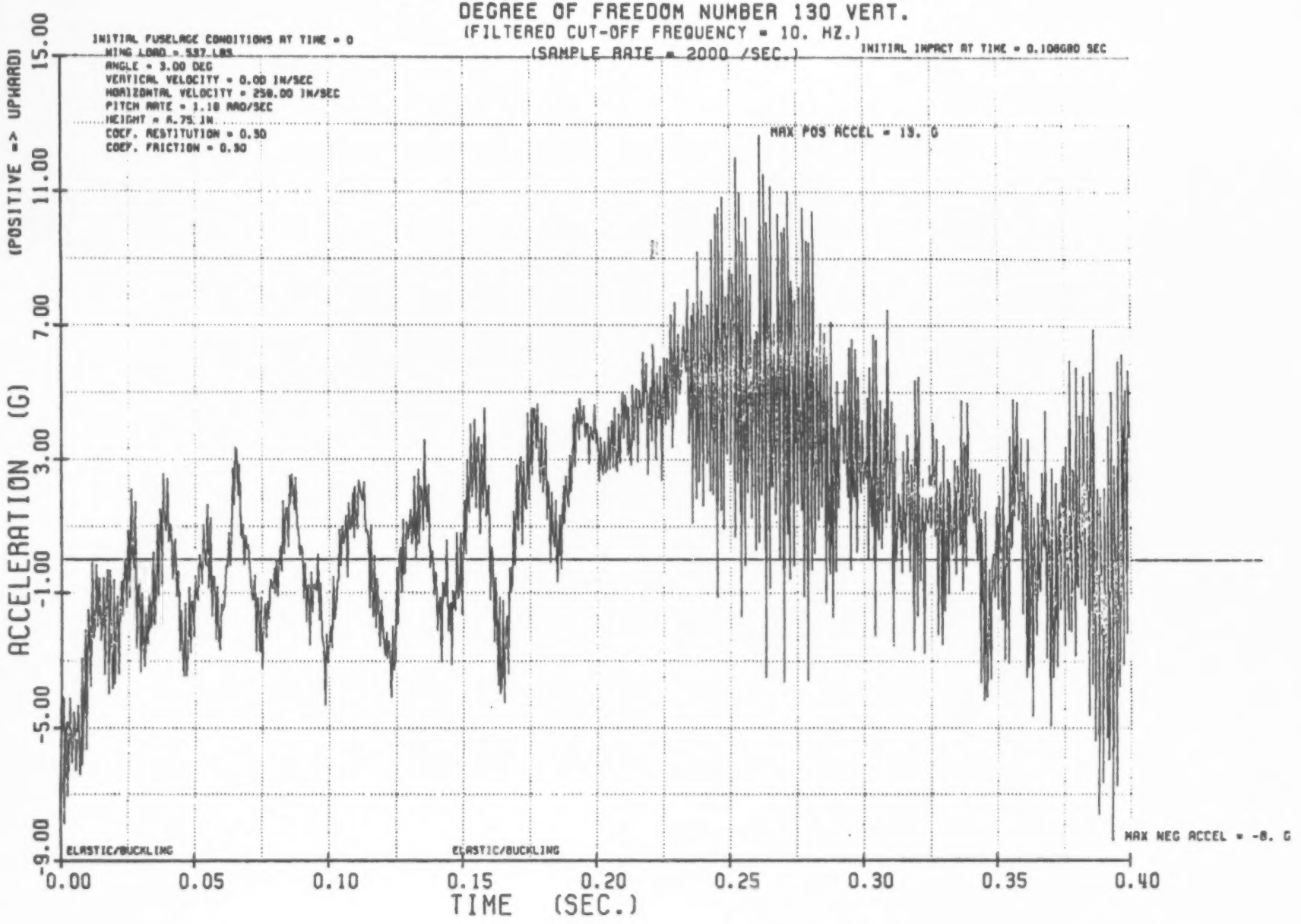
ACCELERATION HISTORY OF MASS 27
DEGREE OF FREEDOM NUMBER 130 VERT.
(FILTERED CUT-OFF FREQUENCY = 10. HZ.)
(SAMPLE RATE = 2000 /SEC.)
INITIAL FUSELAGE CONDITIONS AT TIME = 0
WING LOAD = 537 LBS
ANGLE = 3.00 DEG
VERTICAL VELOCITY = 0.00 IN/SEC
HORIZONTAL VELOCITY = 250.00 IN/SEC
PITCH RATE = 1.18 RAD/SEC
HEIGHT = 8.75 IN
COEF. RESTITUTION = 0.50
COEF. FRICTION = 0.50
INITIAL IMPACT AT TIME = 0.108680 SEC
MAX POS ACCEL = 13. G
MAX NEG ACCEL = -8. G
ELASTIC/BUCKLING
ELASTIC/BUCKLING
ACCELERATION (G) (POSITIVE => UPWARD)
15.00
11.00
7.00
3.00
-1.00
-5.00
-9.00
0.00
0.05
0.10
0.15
0.20
0.25
0.30
0.35
0.40
TIME (SEC.)

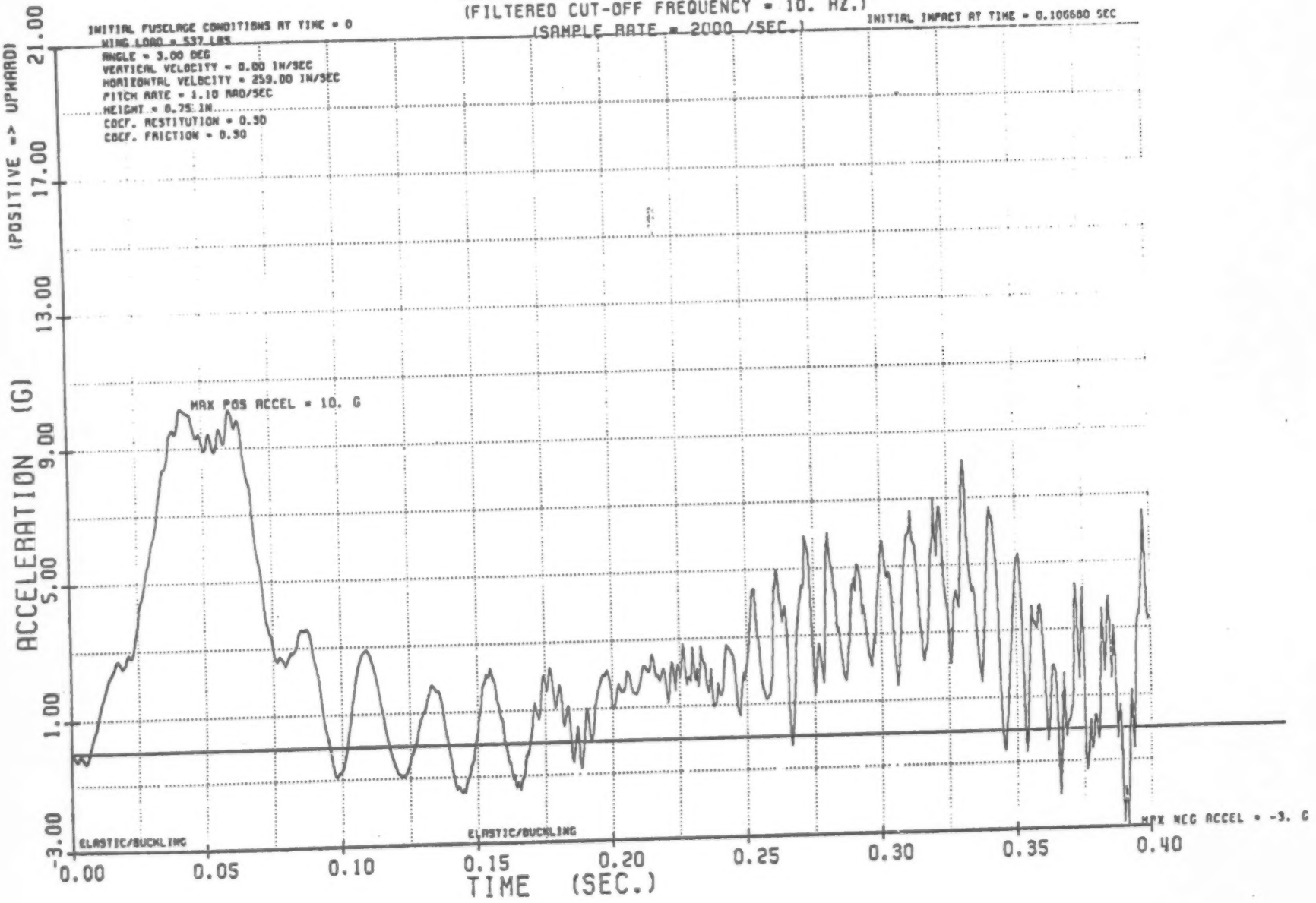
ACCELERATION HISTORY OF MASS 44
DEGREE OF FREEDOM NUMBER 142 VERT.
(FILTERED CUT-OFF FREQUENCY = 10. HZ.)
(SAMPLE RATE = 2000 /SEC.)
INITIAL FUSELAGE CONDITIONS AT TIME = 0
WING LOAD = 537 LBS
ANGLE = 3.00 DEG
VERTICAL VELOCITY = 0.00 IN/SEC
HORIZONTAL VELOCITY = 259.00 IN/SEC
PITCH RATE = 1.10 RAD/SEC
HEIGHT = 0.75 IN
COEF. RESTITUTION = 0.30
COEF. FRICTION = 0.90
INITIAL IMPACT AT TIME = 0.106680 SEC
MAX POS ACCEL = 10. G
MAX NEG ACCEL = -3. G
ELASTIC/BUCKLING
ELASTIC/BUCKLING
ACCELERATION (G)
(POSITIVE => UPWARD)
21.00
17.00
13.00
9.00
5.00
1.00
-3.00
0.00
0.05
0.10
0.15
0.20
0.25
0.30
0.35
0.40
TIME (SEC.)

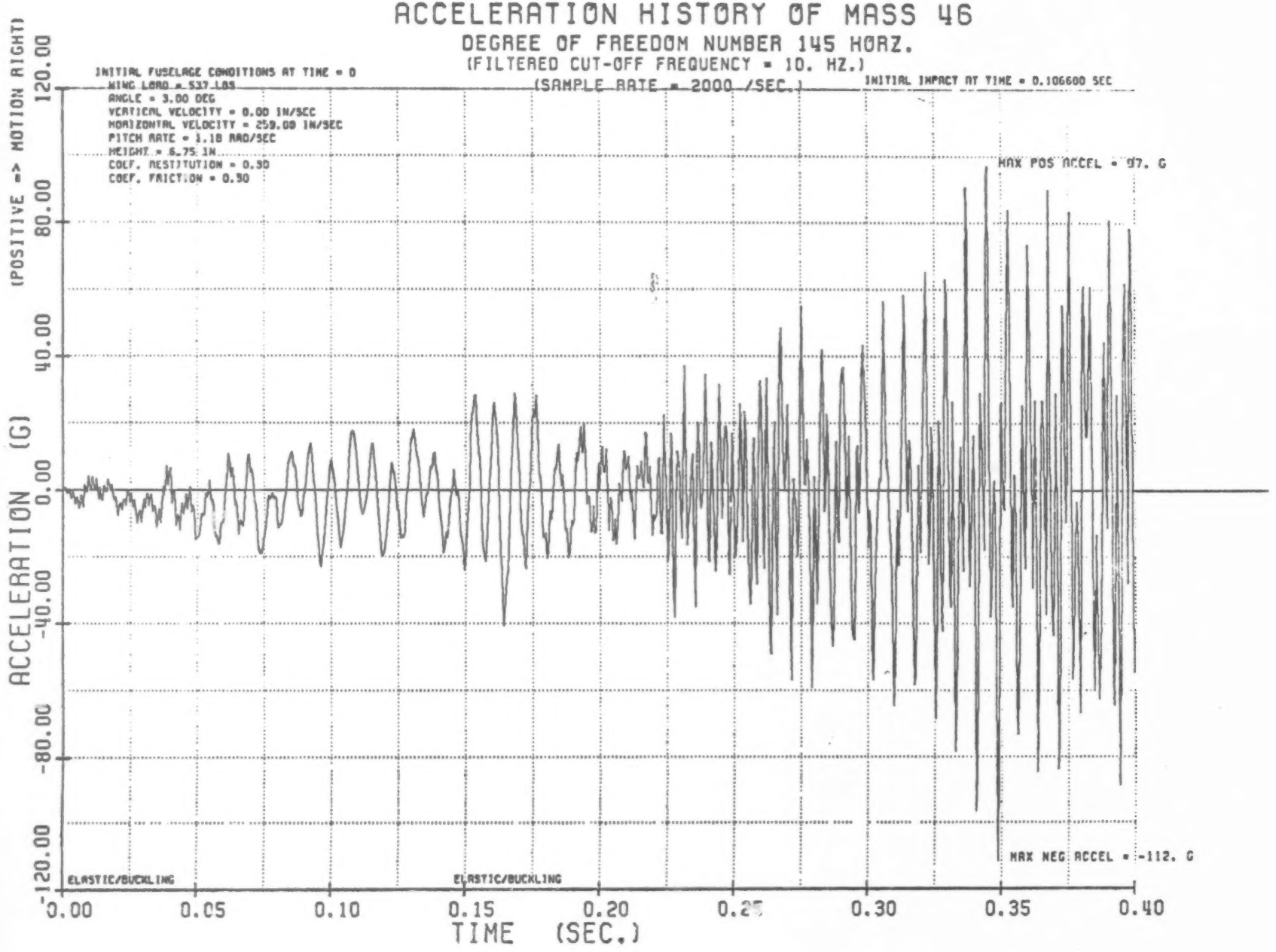
ACCELERATION HISTORY OF MASS 46
DEGREE OF FREEDOM NUMBER 145 HORZ.
(FILTERED CUT-OFF FREQUENCY = 10. HZ.)
(SAMPLE RATE = 2000 /SEC.)
INITIAL FUSELAGE CONDITIONS AT TIME = 0
WING LOAD = 537 LBS
ANGLE = 3.00 DEG
VERTICAL VELOCITY = 0.00 IN/SEC
HORIZONTAL VELOCITY = 259.00 IN/SEC
PITCH RATE = 1.18 RAD/SEC
HEIGHT = 6.75 IN
COEF. RESTITUTION = 0.90
COEF. FRICTION = 0.90
INITIAL IMPACT AT TIME = 0.106600 SEC
MAX POS ACCEL = 97. G
MAX NEG ACCEL = -112. G
ELASTIC/BUCKLING
ELASTIC/BUCKLING
ACCELERATION (G) (POSITIVE => MOTION RIGHT)
120.00
80.00
40.00
0.00
-40.00
-80.00
-120.00
0.00
0.05
0.10
0.15
0.20
0.25
0.30
0.35
0.40
TIME (SEC.)

POOR

QUALITY

ORIGINAL